AN INVESTIGATION INTO THE MECHANISM OF LONG-CHAIN FATTY ACID UPTAKE BY PANCREATIC β-CELLS

by

CHRISTINA CLAVELO-FARROW

A thesis submitted to the University of Birmingham for the degree of
MASTER OF SCIENCE BY RESEARCH

Institute of Metabolism and Systems Research
College of Medical and Dental Sciences
University of Birmingham
September 2022

Abstract

Background and aims: Pancreatic β-cell dysfunction and death is the central aspect during the development of type 2 diabetes (T2D). Although T2D is a major public health concern worldwide, the underlying cause of the disease is not yet fully established. Obesity is a primary risk factor for T2D, however, the relationship between the two conditions remains unclear. One feature observed in both obesity and T2D is an elevated concentration of free fatty acids (FFA) in the blood. It is widely believed that FFA can exert different effects in pancreatic β-cells depending on their degree of saturation, such that long-chain saturated fatty acids (LC-SFA) are toxic, whereas monounsaturated fatty acids (LC-MUFA) are not and may even offer protection against the toxic effects of LC-SFAs. However, the mechanism of long-chain free fatty acid (LC-FFA) uptake into pancreatic β-cells, where they seemingly exert these effects, is poorly understood. Identifying the mechanism of uptake is important to produce therapeutics to regulate their entry, thereby preventing the lipotoxic effects of LC-SFAs and possibly slowing the development of obesity induced T2D.

Methods: Evidence for candidate LC-FFA transport proteins in mammalian cells was investigated using a scoping review. The gene expression of candidate membrane-associated LC-FFA transport proteins in β-cells was studied using bioinformatic analysis of pre-published bulk RNA-sequencing data. Experimental studies used the human-derived EndoC-βH1 and rat-derived INS-1 832/13 pancreatic β-cell lines. LC-FFAs were conjugated to bovine serum albumin (BSA) and acute uptake was examined using a fluorescent intracellular pH indicator, pHrodo Green AM, and confocal microscopy. Inhibition of dynamin was achieved using Dyngo-4a. Membrane fluidity was determined using the fluorescent probe 2-Dimethylamino-6-lauroylnaphthalene (Laurdan) and confocal microscopy.

Results: The results of the scoping review revealed that cluster of differentiation 36 (CD36) and fatty acid transport proteins (FATP) have the most evidence to support a role in facilitating LC-FFA uptake in a range of human cell types. A bioinformatic analysis showed that long-chain acyl-CoA synthetase (ACSL) 1, ACSL3, ACSL4, FATP4, TBC1 domain family member (TBC1D) 1 and TBC1D4 are the most highly expressed candidate LC-FFA transporters in both ex-vivo human pancreatic islets and human-derived EndoC-βH1 cells. In both human-derived EndoC-βH1 cells and rat-derived INS-1 832/13 cells, the uptake of the LC-SFA, C16:0, was saturable, and inhibited in EndoC-βH1 cells in the presence of a dynamin inhibitor, indicating a protein-mediated process. BSA, the vehicle control, was also taken up into INS-1 832/13 and EndoC-βH1 cells in a manner similar to C16:0. Exposing EndoC-βH1 cells to a combination of 375μM C16:0 and 125μM C18:1 or 125μM C16:0 and 375μM C18:1 increased the lipid order of the plasma membrane. Exposure of EndoC-βH1 cells to 250μM C16:0 and 250μM C18:1, however, did not influence membrane order. The acute uptake of C16:0 into EndoC-βH1 cells was different for cells exposed to BSA alone vs. cells cultured in 250μM C16:0 and 250μM C18:1. Moreover, uptake of BSA into EndoC-βH1 cells was different to the uptake of C16:0 when cells were exposed to varying ratios of LC-SFA:LC-MUFA. BSA uptake was inhibited in EndoC-βH1 cells, but C16:0 uptake was promoted when cells were cultured in 1% BSA.

Conclusion: The mechanism of LC-FFA uptake into human β-cells appears to involve protein-mediated transport, although the exact mechanism of uptake is still unclear. Future work should aim to investigate the function of candidate LC-FFA transporters in pancreatic β-cells.

Acknowledgements

I would like to thank the people have helped me throughout this project:

- To my principal supervisor, Dr Patricia Thomas, without whom the completion of this thesis would not have been possible. Thank you for believing in my potential and for your dedicated support and guidance throughout the entirety of this project, I could not have asked for a better supervisor. I would like to extend my thanks to Dr Meurig Gallagher, who has also been an extremely helpful supervisor, particularly in the computational aspects of this thesis. Further, thank you to Dr Gabriela Da Silva Xavier for your valuable comments on this work.
- To my parents, and my aunt, whose love and support have driven all my academic achievements to date. Thank you for your continuous encouragement.
- To my housemate, Amy Churchlow, who has been an incredibly kind and supportive friend this year. Moreover, I would like to thank my best friend, Daniel Lee, for being so entertaining and for motivating me throughout this process.
- Finally, to all my teachers and lecturers during my time in education who have encouraged me to pursue a career in science. I hope that someday I will be an inspiration to others, as you have inspired me.

Contents

List of figures

Chapter 1. General introduction

Chapter 2. Identification of candidate transport proteins involved in long-chain fatty acid uptake in mammalian cells: a scoping review

Chapter 3. Using bulk RNA-sequencing data to explore expression profiles of candidate LC-FFA transport proteins in mammalian cells

Chapter 4. Using experimental techniques to investigate long-chain fatty acid transport in the rat INS-1 832/13 and the human EndoC-βH1 cell lines

Appendix B. Supplementary Figures

List of tables

Abbreviations

ACS	Acyl-CoA synthetase
ACSL	Long-chain acyl-CoA synthetases
ADP	Adenosine diphosphate
AM	Acetoxymethyl
ATP	Adenosine triphosphate
BMI	Body mass index
BSA	Bovine serum albumin fraction V
CAV	Caveolin
cDNA	Complementary DNA
CD36	Cluster of differentiation 36
CPT	Carnitine palmitoyl transferase
DMSO	Dimethyl sulfoxide
DNL	De novo lipogenesis
dsRNA	Double stranded RNA
ER	Endoplasmic reticulum
EtOH	Ethanol
FABP	Fatty acid binding protein

FATP	Fatty acid transport protein
FFA	Non-esterified “free” fatty acids
FFAR	Free fatty acid receptor
GLP-1	Glucagon-like peptide 1
GLUT	Glucose transporter
GOF	Gain-of-function
GP	Generalised polarisation
GSIS	Glucose stimulated insulin secretion
GUV	Giant unilamellar vesicle
GWAS	Genome-wide association studies
HDL	High-density lipoproteins
HSL	Hormone sensitive lipase
H_0	Null hypothesis
IL-6	Interleukin 6
K_{ATP} channel	ATP-sensitive K^+ channel
L_β	Solid gel
LC-FFA	Long-chain free fatty acids
LCIM	Live cell imaging media

LC-SFA	Long-chain saturated fatty acids
LC-MUFA	Long-chain monounsaturated fatty acids
L_d	Liquid disordered
LDL	Low-density lipoproteins
LFC	Log2 fold change
L_o	Liquid ordered
LOF	Loss-of-function
LPL	Lipoprotein lipase
LUV	Large unilamellar vesicle
miRNA	microRNAs
NGS	Next-generation sequencing
PBS	Phosphate buffered saline
PCR	Polymerase chain reaction
PFA	Paraformaldehyde
PRISMA	Preferred Reporting Items for Systematic Reviews and Meta-Analyses
ROI	Region of interest
ROS	Reactive oxygen species
RNAi	RNA interference

RNA-seq	RNA-sequencing
scRNA-seq	Single-cell RNA-sequencing
spRNA-seq	Spatial RNA-sequencing
SGLT	Sodium-glucose cotransporter
shRNA	Short hairpin RNAs
siRNA	Small interfering RNAs
SSO	Sulfo-N-succinimidyl oleate
SUV	Small unilamellar vesicle
TBC1D1	TBC1 Domain Family Member 1
TBC1D4	TBC1 Domain Family Member 4
TGN	Trans-Golgi network
TNFα	Tumour necrosis factor α
TNF-R	Tumour necrosis factor receptors
TPM	Transcripts per million
T2D	Type 2 diabetes
VC	Vehicle control
VGCC	Voltage-gated calcium channels
VLDL	Very-low-density lipoprotein

Chapter 1

General Introduction

1.1 Type 2 diabetes mellitus

Diabetes is a chronic disease that affects over 537 million people worldwide (1). The main forms of diabetes mellitus are type 1 and type 2 diabetes. However, there are also less prevalent forms including hyperglycaemia in pregnancy (such as gestational diabetes) and diabetes with a specific, possibly genetic aetiology (such as maturity onset diabetes of the young). The most prevalent form of diabetes is type 2 diabetes (T2D), which accounts for approximately 90% of diabetes cases worldwide (2).

Until recently, T2D was known as adult-onset or non-insulin-dependent diabetes due to its manifestation in adults (>40 years old), however, it is becoming increasingly apparent in younger people and children (<40 years old) (2). T2D is characterised by the World Health Organisation as raised blood glucose concentration, due to the ineffective use of insulin by the body (insulin resistance) (3, 4). Insulin resistance refers to impaired sensitivity to insulin action in target tissues, such as adipose tissue (5), skeletal muscle (6) and the liver (5). As a result, blood glucose concentrations increase, resulting in hyperglycaemia, which is compensated for by an increased secretion of insulin by pancreatic β-cells (7). The key event resulting in the development of T2D is pancreatic β-cell failure, where β-cells fail to deliver an adequate amount of insulin to counteract insulin resistance, which can result in β-cell dysfunction and death (7). It has also been suggested that pancreatic β-cells do not die in T2D, but lose their identity (i.e., β-cells lose their ability to express the full complement of β-cell genes or express genes that are abnormal to a mature, healthy β-cell) as reviewed by Swisa et al. (7). However, the phenomenon of β-cell identity loss (also known as dedifferentiation), is not yet fully understood.

Maintaining blood glucose concentration as close to the normal range (3.9-5.6mmol/L for normal fasting glucose levels (8)) as possible reduces the risk of developing microvascular complications of T2D (e.g., retinopathy, nephropathy and neuropathy) and macrovascular damage (e.g.,

cerebrovascular insults, myocardial infarction and complications associated with peripheral vascular disease, including the diabetic foot syndrome) (9). At diagnosis of T2D, initial interventions focus on lifestyle modifications, especially nutritional interventions, increased physical activity and adequate rest (10). Remarkably, Lean et al. (11) have recently reported that individuals with obesity and T2D have an 86% chance of remission if weight loss of 15kg or more is achieved within six years of diagnosis. However, if hyperglycaemia cannot be controlled with the implementation of lifestyle interventions, drug therapy may be prescribed, such as the biguanide, metformin, which acts to counter insulin resistance (12). Other drugs may also be prescribed, such as sulfonylureas, which exert their function by stimulating insulin secretion from pancreatic β-cells (10). If normal blood sugar levels are not restored with lifestyle interventions and other medications, individuals with T2D may eventually require insulin therapy (13). Despite the progress in understanding the mode of action of these existing therapies, current treatments typically treat the complications of T2D (i.e., hyperglycaemia) and there are insufficient drugs on the market that preserve the function and viability of β-cells. This is largely due to the incomplete understanding of the mechanisms underpinning the death of β-cells in the development of T2D. Hence, further investigation into the pathogenesis of T2D is essential for the development of a more effective approach to manage this disorder.

1.2 Type 2 diabetes and obesity

The risk that an individual develops T2D is dependent on a combination of genetic and environmental risk factors (14), including age, low socioeconomic status, ethnicity, family history, certain unhealthy lifestyle behaviours and metabolic syndrome (including obesity) (as recently reviewed by Kyrou et al.(15)). A recent review by Bellary et al. (16) reports that adults who are ≥65 years old display the highest T2D prevalence among any age group, accounting for nearly half of all individuals with T2D. Moreover, a systematic review and meta-analysis by Agardh et al. (17) found that low socioeconomic status (which is primarily assessed based on income, occupation, and educational level (15)) is

associated with increased T2D incidence, particularly in high-income countries. Ethnicity seemingly constitutes a further non-modifiable risk factor for T2D; for example, several studies (18, 19, 20, 21) in Europe have determined that T2D prevalence is greater in ethnic minority groups when compared to their white European counterparts. These ethnic-related differences are thought to be attributed to disparities in socioeconomic status, lifestyle, a genetic predisposition to T2D, as well as increased susceptibility for cardio-metabolic complications related to body composition, central fat distribution and obesity (as reviewed by Kyrou et al. (15)).

Genome-wide association studies (GWAS) have confirmed that T2D is a polygenic disease, which means that multiple genes are associated with an increased risk of T2D (22). While the complete genetic architecture of T2D is not yet fully understood, a large number of genes are thought to be associated with this disease; a recent meta-analysis of GWAS by Xue et al. (23) has identified 139 common and 4 rare variants associated with T2D. A large number of candidate genes have been reported to be associated with T2D, including transcription factor 7 like 2 (TCF7L2), potassium voltage-gated channel subfamily Q member 1 (KCNQ1) and potassium inwardly rectifying channel subfamily J member 11 (KCNJ11) (as reviewed by Ali, O. (24)). Further, a population-based study by Tillil, H. and Köbberling, J. (25) has observed a 40% increase in risk of developing T2D for individuals who have one parent with T2D and almost a 70% increase if both parents have the condition, suggesting that there is an element of heritability associated with the risk of developing T2D. Individuals with genes associated with T2D may never develop the condition, however, genes can be activated by several environmental factors, including an unhealthy diet and sedentary behaviour, which can lead to obesity (14, 26). For example, Neuenschwander et al. (27) have recently shown, using a meta-analyses of prospective observational studies, that a high intake or red and processed meat, as well as excess sugar, is associated with the incidence of T2D. Being overweight or obese is thought to be the largest risk factor for T2D; Public Health England have reported that

90% of adults aged between 16-54 with T2D are overweight or obese (28). The likelihood and severity of T2D are closely associated with body mass index (BMI); Abdullah et al. (28) report that there is a three times greater risk of developing T2D for individuals who are overweight and a sevenfold increase in risk for individuals with obesity. Between 1975 and 2016, the worldwide prevalence of obesity increased nearly threefold (29), and this is only expected to rise, as the World Obesity Federation predict that 1 in 5 women and 1 in 7 men, globally, will be living with obesity by 2030 (30). This rise in prevalence of obesity in adults has been accompanied by, and is expected to be accompanied by, an increased prevalence of T2D according to Public Health England (31), highlighting a strong correlation between obesity and T2D.

The World Health Organisation defines obesity as a BMI that is greater than or equal to 30kg/m^2 (29). The major cause of obesity is an energy imbalance, where energy intake exceeds energy expenditure (i.e., more energy is consumed than the body needs) (32). This additional energy is stored as fat, which can eventually result in obesity if energy intake continues to exceed the body's requirements (33). However, whilst there is a large body of evidence (as reviewed by Kahn et al. (34) and, more recently, Kyrou et al. (15)) to suggest that obesity is an important risk factor for T2D, the exact mechanism of their association remains unclear. Moreover, the current understanding of inter-individual differences is not yet fully established, as most individuals with obesity do not develop T2D (35), and it has also been observed that 10-20% of individuals suffering with T2D are individuals without obesity (36).

1.3 Adipose tissue dysfunction and ectopic fat storage in T2D

A large body of evidence suggests that adipose tissue dysfunction and ectopic fat storage is a key factor in the pathogenesis of T2D (as reviewed by Snel et al. (37)). Adipose tissue is the major site for fat storage (in the form of triglycerides) in the body, whereas ectopic fat storage involves the storage of triglyceride droplets in non-adipose tissues (e.g., the liver, heart, skeletal muscle, and

pancreas) (37, 38). The accumulation of ectopic fat occurs when the body has exceeded its capacity to store fat in subcutaneous adipose tissue (39). In lean individuals, Heilbronn et al. (40) suggest that ectopic fat storage is likely due to the failure of adipose cells to proliferate (to store excess FFAs), or the impaired capacity of organs/tissues to increase fat oxidation to compensate for excessive exposure to FFA.

Adipose tissue is not only a fat-storage organ; it also functions as an endocrine organ, to secrete of large range of bioactive compounds including cytokines (e.g., tumour necrosis factor α (TNFα) and interleukin 6 (IL-6)), hormones (e.g., leptin and resistin), and lipids (e.g., non-esterified "free" fatty acids (FFAs) and lipoprotein lipase (LPL)) (41). However, in obesity, there is an increase in the size and quantity of adipocytes, resulting in the disturbed secretion of these compounds (42). Individuals with obesity have been reported to have raised serum levels of pro-inflammatory cytokines, especially TNFα and IL-6, alongside a reduction in adiponectin (an anti-inflammatory hormone) (Figure 1.1) (42). Dysregulated secretion of these inflammatory mediators is thought to contribute to β-cell dysfunction and death, ultimately leading to T2D (43). Additionally, the increased secretion of FFAs from adipocytes, particularly the long-chain saturated fatty acid (LC-SFA) palmitate, has been shown to activate inflammatory mediators (e.g., IL-6, IL-8 and chemokine (C-C motif) ligand 2 (CCL2)) in pancreatic islets, which further promote β-cell dysfunction (44).

Ectopic fat storage is also correlated with the development of T2D (37). Levelt et al. (45) have shown that individuals with obesity and T2D have increased ectopic fat deposition when compared to lean individuals without T2D. Further, Lee et al. (46) have shown that excess fat accumulation in rat pancreatic islets precedes the development of T2D, due to the dysfunction and death of β-cells. Moreover, in individuals with T2D, β-cell function appears to be restored following the reduction of ectopic fat in the pancreas (47). Intriguingly, this association appears to be independent of BMI, as an increase in ectopic fat storage has also been linked to an increased risk of developing T2D in lean

individuals (48). Taken together, this evidence suggests that ectopic fat accumulation, especially in the pancreas, could be a key factor leading to the development of T2D.

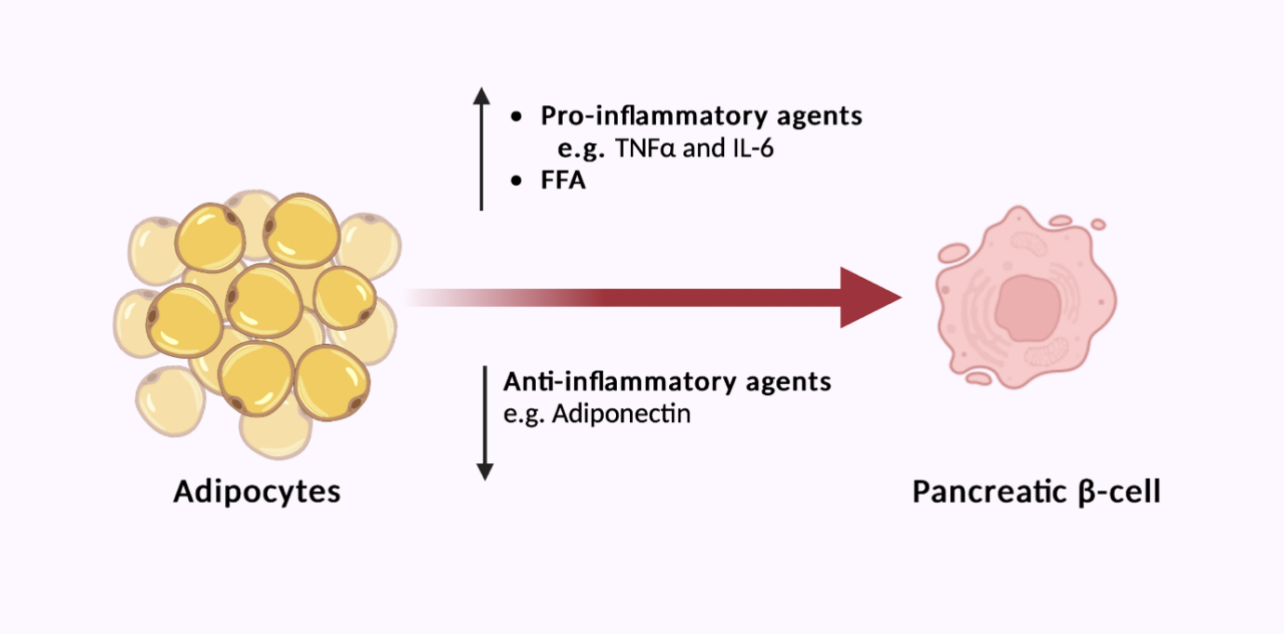

Figure 1.1 Dysfunctional secretion of bioactive compounds from adipocytes contributing to β-cell dysfunction and death. TNFα: tumour necrosis factor α; IL-6: interleukin 6; FFA: non-esterified "free" fatty acids. Created in Biorender.com.

1.4 Fatty acids

Fatty acids found in the body are either consumed or synthesised endogenously, via de novo lipogenesis (DNL) in adipose tissue and the liver, where excess carbohydrates are converted to fatty acids (49). Fatty acids are a heterogenous group of compounds that are classified according to their structure (i.e., carbon chain length and number of double bonds) (Figure 1.2) (50). These compounds are used by cells for various functions, including as an energy source, as constituents of the cell membrane, for energy storage (as triglycerides and cholesteryl esters), and as precursors for several cell signalling molecules including diacylglycerols, endocannabinoids, and ceramides (as reviewed by Calder et al. (51)). To reach target cells to exert these functions, fatty acids are transported in the

bloodstream as constituents of more complex lipids (e.g., triglycerides, which are esters composed of glycerol and three fatty acids) or as FFAs (51). Most FFAs circulating in the bloodstream are bound to serum albumin (a protein that is produced in the liver), although a small proportion of the total circulating FFAs are not bound to albumin (i.e., $<10^{-5}$ of the total FFAs in humans) (52). Changes in the ratio and concentrations of circulating fatty acids reportedly plays a significant role in the development and progression of T2D (53). These changes are collectively known as dyslipidaemia, which can be characterised as an elevation in triglycerides and FFAs, increased low-density lipoproteins (LDL), along with reduced high-density lipoproteins (HDL), which can result in elevated FFAs (54). However, an increase in total plasma FFA concentrations is seemingly the most important factor (when compared to altered triglyceride or lipoprotein levels) associated with the development of insulin resistance and the pathophysiology of T2D (55).

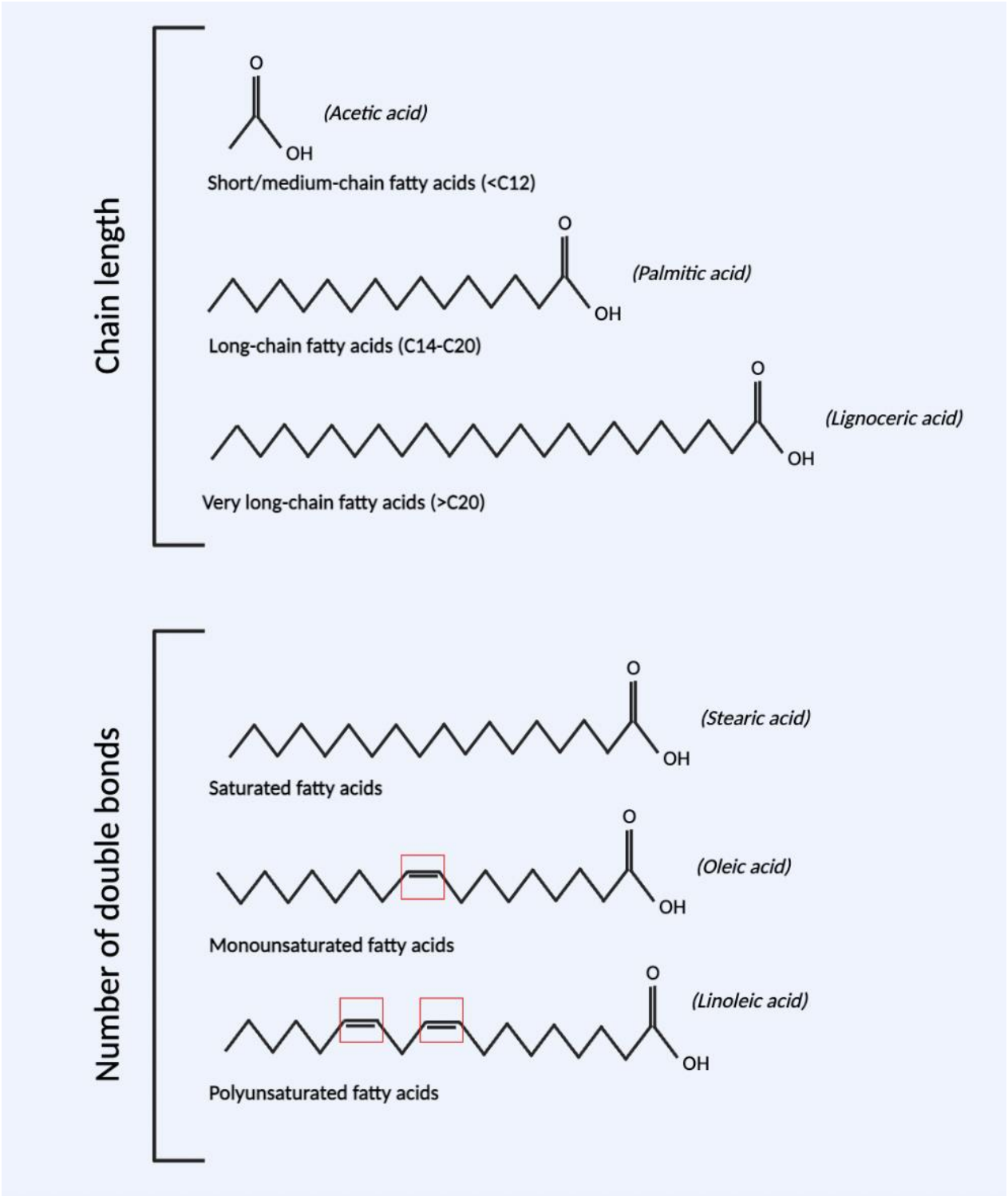

Figure 1.2 Classification of fatty acids. Fatty acids are classified according to their carbon chain length (56, 57), or arranged into three broad categories with respect to their number of carbon-carbon double bonds (illustrated with a red box): monounsaturated (one double bond), polyunsaturated (two or more double bonds) and saturated (no double bonds) (58). Literature differs in its classification of the FFAs, but for the purpose of this thesis, the chosen classification is that short and medium chain fatty acids have ≤C14:0, whereas long-chain free fatty acids (LC-FFA) have >C14:0 (59). Created in Biorender.com.

1.4.1 Free fatty acids in the plasma

Most FFAs in the plasma are hydrolysed and released from adipocyte triglyceride stores (60). In healthy individuals, lipidomic analysis of the human plasma (61) has shown that it contains approximately 214 nmol/ml of FFAs (measured after overnight fasting), which is tightly regulated to uphold the metabolic demands of the body (55). On the other hand, in individuals with obesity and T2D, there appears to be an increase (nearly three-fold) in the total concentration of plasma FFAs (62). Increased levels of FFAs in the plasma, in obesity induced T2D, have been reported to be attributed to a reduced FFA clearance, reduced ability to regulate lipolysis in adipose tissue and/or elevated adipose tissue mass, leading to the release of extra FFA (63, 64). Elevated plasma FFA can also be due to an overproduction and release of FFA into the circulation from triglyceride-rich lipoproteins (liver-derived very-low-density lipoprotein (VLDL) and intestine-derived chylomicrons), which involves the hydrolysis of triglycerides by lipoprotein lipase to liberate FFA (as reviewed by Lewis et al. (65)). However, the exact mechanisms by which plasma FFA concentrations are altered is yet to be fully established.

A recent lipidomic analysis of FFAs in the plasma, using liquid chromatography high resolution mass spectrometry (LC-HRMS), has enabled the identification of 74 different FFAs in the plasma of healthy individuals (66). Quehenberger et al. (61) report that three of these FFAs make up the majority (78%) of the composition of total FFAs within the plasma of healthy lean individuals: oleic acid (C18:1), palmitic acid (C16:0) and stearic acid (C18:0). However, the ratio of these FFAs is seemingly altered in individuals with obesity, such that the concentration of the long-chain monounsaturated fatty acid (LC-MUFA) C18:1 is decreased, whereas the LC-SFAs, C16:0 and C18:0 are increased (67). C16:0 is the most prevalent LC-SFA found within the human body and can be provided by the diet or synthesised endogenously, as described by Carta et al. (68). The tissue content of C16:0 seems to be tightly regulated; Song et al. (69) have shown that altered intake of C16:0 in the

diet does not significantly influence tissue concentration. This has been reported to be attributed to its crucial physiological role in multiple biological functions (68), such as its contribution to the physical properties of the plasma membrane (i.e., membrane fluidity) and its involvement in the post translational modification of proteins (i.e., palmitoylation) (70). Under normal physiological conditions, the accumulation of C16:0 in the cell is prevented by its increased desaturation to palmitoleic acid (C16:1) and/or its conversion to C18:0 and subsequent desaturation to C18:1 (68). However, an excess production of C16:0 by DNL has been observed in individuals with hyperglycaemia (a complication associated with T2D) and has been reported to promote a metabolic dysregulation and systemic inflammatory response, leading to dyslipidaemia, resistance to insulin and impaired fat deposition and distribution (68, 71).

1.4.2 Free fatty acids and insulin resistance

Insulin resistance is thought to be the main contributor to the pathogenesis of T2D (72). The main factors that promote the development of insulin resistance include a chronic overconsumption of calories (73), an increased circulation of FFAs (74), and age (75). The key role for insulin in the healthy tissues (e.g., adipose, liver and muscle) is to regulate the storage, mobilisation and utilisation of glucose and free fatty acids, to maintain physiologically desirable levels of these nutrients (65, 76, 77). However, in insulin resistance, there is a diminished responsiveness of target cells to circulating insulin (78).

Insulin resistance is reported to result in dyslipidaemia (abnormal levels of fats in the blood) and the excessive secretion of FFA into the body's circulation (79). Under normal physiological conditions, insulin stimulates the activity of lipoprotein lipase (LPL) (80), an enzyme which mediates the clearance of circulating triglyceride-rich lipoproteins (81), and inhibits hormone sensitive lipase (HSL), an enzyme which hydrolyses intracellular triglyceride stores to FFA and glycerol in adipocytes, thereby reducing the quantity and release of FFA into the circulation (82). A reduced

insulin effect in individuals with insulin resistance, however, results in the reduced clearance of triglycerides and increased flux of FFA into the circulation, which can cause dyslipidaemia (83). In essence, insulin resistance can increase the concentration of circulating fatty acids which, consequently, can worsen insulin resistance.

1.5 Pancreatic β-cells

Pancreatic β-cells are found in the endocrine tissue of the pancreas, within aggregates of functionally distinct cells termed the 'islets of Langerhans' (84). Figure 1.3 illustrates the cells comprising the islets of Langerhans (henceforth known as 'islets'). Different cells comprising the pancreatic islet secrete various hormones, which are essential for the regulation of blood glucose.

The primary role of pancreatic β-cells is to secrete the hormone insulin in response to glucose and fatty acids, to regulate blood glucose concentrations by inducing glucose storage in the liver, muscles, and adipose tissue (85, 86). In humans, glucose-stimulated insulin secretion (GSIS) is usually stimulated when blood glucose concentrations reach approximately 4.4 mM to 6.6 mM (87).

The key role of α-cells, on the other hand, is to secrete the hormone glucagon in response to hypoglycaemia (blood sugar level <3.9mM) (88, 89). Glucagon then acts as a signal to mobilise glucose from the liver, thereby restoring blood glucose levels to a normal range (90). Intriguingly, recent studies in mice (91, 92, 93) and human (92, 93) models have shown that proglucagon-derived peptides, such as glucagon and glucagon-like peptide 1 (GLP-1), which are secreted from α-cells, contribute to GSIS via paracrine actions.

Another key component of the pancreatic islet are δ-cells, which secrete somatostatin in response to several stimuli, including acetylcholine, glutamate, urocortin 3, ghrelin and high glucose levels (94). The main role of somatostatin is to inhibit both insulin and glucagon secretion via paracrine signalling, to maintain glucose homeostasis, as demonstrated in several investigations (95, 96)

ε-cells, which secrete the “hunger hormone”, ghrelin, are also located in the pancreatic islet (97). The key role of ghrelin is to stimulate appetite (97), however, this hormone has also been suggested to contribute to an increase in blood glucose levels by suppressing the release of insulin from pancreatic β-cells (97).

The main function of γ-cells is to secrete the hormone pancreatic polypeptide, which has a key role in satiety (98). However, this hormone is also involved in regulating hepatic glucose levels, by increasing insulin sensitivity of the liver to reduce hepatic glucose production (98). Interestingly, Khan et al. (99) have also demonstrated that pancreatic polypeptide inhibits insulin secretion from human and rodent β-cells.

Ultimately, each cell comprising the pancreatic islet has a distinct role in the maintenance of glucose homeostasis. Further, paracrine signalling between different cells in the pancreatic islet is seemingly important for the regulation of insulin secretion from β-cells.

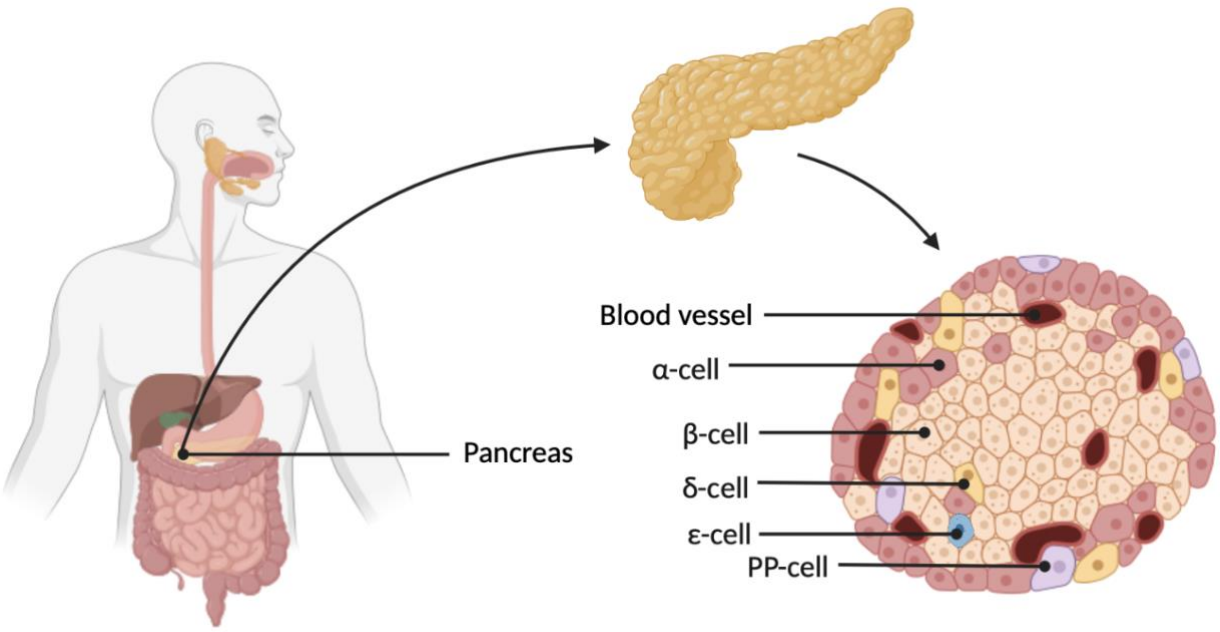

Figure 1.3 Cell types located in the islets of Langerhans in the pancreas. The cells comprising the islets of Langerhans secrete different hormones, which are important for blood glucose control: α-cells (glucagon), β-cells (insulin), δ-cells (somatostatin), ε-cells (ghrelin) and γ (or PP)-cells (pancreatic polypeptide) (84). Created in Biorender.com.

1.5.1 Insulin secretion

The principal physiological stimulus for insulin secretion is an elevated concentration of circulating glucose that is observed in the post-prandial state (after a meal) (100, 101). At present, the complete mechanisms of insulin secretion are unclear, although it is thought to occur via K_{ATP}-dependent (also known as 'triggering') and K_{ATP}-independent (also known as 'amplifying') pathways (101).

The triggering pathway is the canonical pathway of GSIS (Figure 1.4). In β-cells, there is an influx of glucose through glucose transporter type 1 (GLUT1) and type 2 (GLUT2) transporters (mainly GLUT2 in rodents) in the plasma membrane, then its metabolic breakdown and oxidation to yield adenosine triphosphate (ATP) at the expense of adenosine diphosphate (ADP), resulting in a change in the ATP:ADP ratio in the cell (102, 103). An elevation in the ratio of ATP to ADP results in the

closure of ATP-sensitive K^+ (K_{ATP}) channels, leading to depolarisation of the membrane and consequent opening of voltage-gated calcium channels (VGCC) (102). The increase in calcium concentration that follows the opening of VGCCs then triggers the release of insulin granules via exocytosis (102).

The precise mechanisms of the amplification pathway remain elusive at present. Within this pathway, the metabolism of glucose generates further signals, in addition to the signals sent by the K_{ATP}-dependent pathway, which enhance the number of insulin vesicles secreted from the cell (as described by Kalwat, M.A. and Cobb, M.H. (103)). These signals do not involve K_{ATP} channels (103). Further detail on the current proposed mechanisms involved in this pathway is beyond the scope of this thesis; a more extensive review has been published by Kalwat, M.A. and Cobb, M.H. (103).

Insulin secretion is not only triggered by glucose, but it is also stimulated in response to FFA. It is thought that FFA can support insulin secretion by augmenting GSIS (104) or through their oxidation (105). Evidence suggests FFA induce insulin secretion via membrane receptor activation (106) or via their metabolites (fatty acyl-coenzyme A molecules) (107) (Figure 1.4). However, like glucose, the mechanisms whereby FFA stimulate insulin secretion remain to be fully elucidated (108).

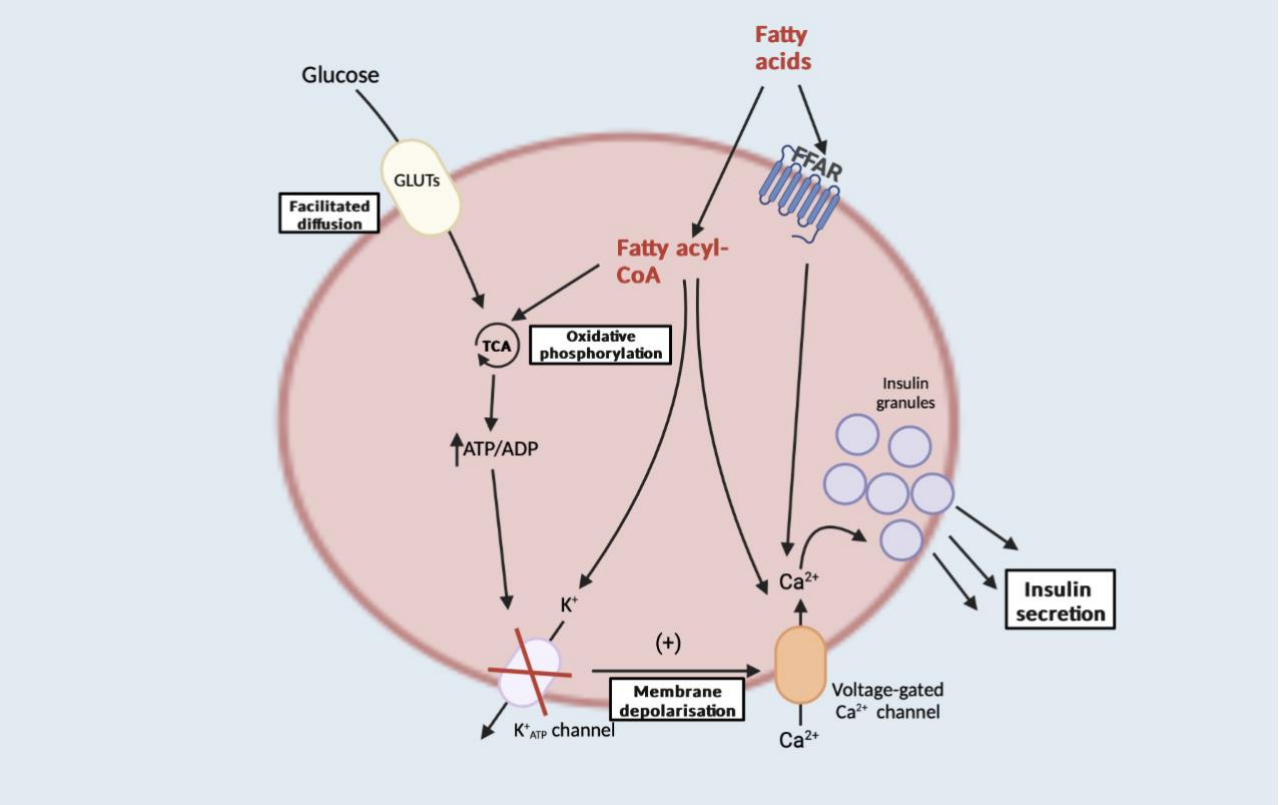

Figure 1.4 Overview of the K_{ATP}-dependent pathway of glucose-stimulated insulin secretion (GSIS) and its potentiation via fatty acids. Glucose metabolism is the primary signal for insulin secretion *(100, 101)*. Fatty acids augment GSIS by directly modulating ion channels via its metabolites (fatty acyl-CoA) *(109)*, or by increasing the ATP/ADP ratio via the oxidative phosphorylation of fatty acyl-CoA *(105)*. Moreover, binding of FFA to G protein-coupled receptors (e.g., FFAR1), generates lipid signalling molecules such as IP3 and DAG which contribute to an increase in intracellular Ca^{2+} and, thus, an increase in insulin secretion *(110)*. FFA: free fatty acid; FFAR1: free fatty acid receptor 1; GLUT: glucose transporter; ATP: adenosine triphosphate; ADP: adenosine diphosphate; TCA: tricarboxylic acid cycle; K^+_{ATP} channel: ATP-sensitive K^+ channel; IP3: inositol-3-phosphate; DAG: diacylglycerol. Created in Biorender.com.

1.6 The plasma membrane as a cellular organelle

The plasma membrane is a key constituent of the cell for the maintenance of its structure and function (111). The major component of the plasma membrane are phospholipids, which are composed of two fatty acyl chains (the hydrophobic region) and a phosphate headgroup (the hydrophilic region) (112). These phospholipids are packed together in a parallel fashion, in two layers, to form the phospholipid bilayer (112). The structure of the membrane was first proposed by Singer and Nicolson (113); these researchers suggested that membranes are composed of globular molecules (proteins) that are

partially embedded in a fluid phospholipid matrix, termed the “fluid mosaic model”. In more recent years, however, evidence has indicated that specialised membrane domains (e.g., lipid rafts), as well as extracellular matrix structures and the membrane-associated cytoskeleton, are important components of the membrane when describing its structure, fluidity, and function (114) (Figure 1.5).

The main functions of the plasma membrane are to provide structure for the cell and to regulate the transport of molecules between the cytoplasm of the cell and its external environment (114). Components of the plasma membrane (e.g., proteins, glycoproteins and lipids) can be assembled into macromolecular complexes, which can take part in various cellular functions, including cellular recognition, ion and metabolite transport, activation of enzymes, cell adhesion, etc. (114). The alteration of these complexes, however, has been correlated with the development of numerous diseases (115). Changes in the levels of different phospholipid species in the plasma membrane, for example, have been reported in many diseases, including obesity, hypertension, schizophrenia, infectious diseases and cancer (as reviewed by Escribá et al. (115)). An altered membrane composition is thought to disrupt receptor function, as well as alter the permeability of substances through the membrane which could, in turn, impact the normal functions of the cell (116). Intriguingly, insulin resistance, the key factor leading to the development of T2D, has also been reported to alter the lipid and protein composition of the plasma membrane, thereby modifying its fluidity, structure and function (see section 1.7.1) (117).

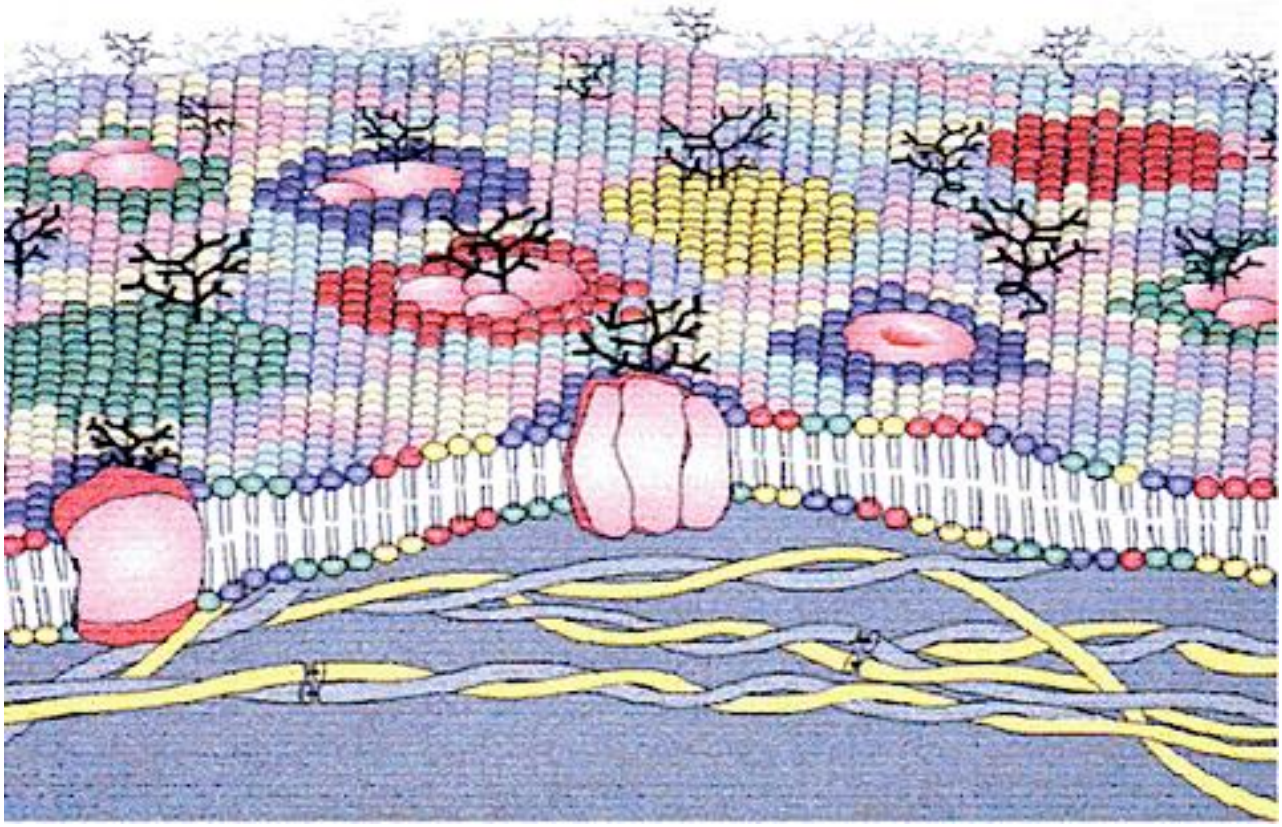

Figure 1.5 An updated version of the fluid mosaic model of the plasma membrane. Phospholipids are shown forming specialised membrane regions (e.g., lipid rafts) and domains around integral membrane proteins. Cytoskeletal structures are shown underpinning the phospholipid bilayer, which regulates the movement of proteins and lipids. Figure taken from Escribá et al. (115)

1.7 The role of long-chain saturated fatty acids in pancreatic β-cell dysfunction and death

To compensate for insulin insensitivity, pancreatic β-cells experience a period of dysfunction prior to β-cell death (118). The dysfunction of β-cells is thought to be, in part, due to an elevation of plasma FFA (118). As discussed in section 1.5.1, there is an increased demand for β-cells to produce insulin in response to hyperglycaemia (raised blood sugar levels), to restore glucose homeostasis. Pancreatic β-cells initially cope with the increased insulin demand via increasing insulin production (known as β-cell compensation), as well as their cell size (hypertrophy) and number (hyperplasia) (119). Interestingly, these adaptive responses are reported to be augmented by acute elevations of FFA levels, especially of the LC-SFA C16:0 (120). For example, various in-vitro studies in rodent (120,

121) and human islets (120, 122) have shown that the acute exposure of β-cells to C16:0 facilitates GSIS. Chronic increases in plasma FFA, however, have been shown to result in disturbances in lipid homeostasis, which can ultimately result in a reduction in β-cell function and viability (118).

It is widely believed that increased levels of FFAs promote pancreatic β-cell dysfunction and death via a process termed lipotoxicity (38, 123), subsequently resulting in the development of T2D (118). Figure 1.6 illustrates several mechanisms that have been proposed to be involved in β-cell lipotoxicity, however, the mechanisms of β-cell lipotoxicity are yet to be fully established. The induction of lipotoxicity depends on the plasma FFA concentration, extent of exposure to the FFA, and intriguingly, the composition of the FFA (i.e., carbon chain length and the degree of saturation) (118). There is a consensus that LC-SFAs, such as C16:0 and C18:0, are the most deleterious to β-cells, whereas short-chain saturated and long-chain unsaturated fatty acids are less toxic (124). This has been consistently reported in studies using rodent β-cells (125, 126, 127) as well as human pancreatic islets (128). In contrast, it has been reported that LC-MUFAs do not exert a toxic action in pancreatic β-cells and have even been shown to prevent the toxic effects of LC-SFAs (129, 130, 131). Moreover, several studies (132, 133, 134) have suggested that lipotoxicity is augmented by elevated levels of glucose (i.e., hyperglycaemia), in a process referred to as ‘glucolipotoxicity’. Individuals with T2D largely present with a combination of increased levels of FFA and glucose in the circulation (55). When glucolipotoxicity occurs, pancreatic β-cells start to fail to compensate for insulin resistance, such that insulin gene expression and secretion are reduced, and β-cell mass declines (135). Consequently, glucose and FFA levels increase, ultimately resulting in further β-cell dysfunction and death which contributes to T2D (135). There are many extensive theories surrounding the mechanisms resulting in glucolipotoxicity, however it is beyond the scope of this thesis to discuss them in detail. Rather, this thesis is largely focused on the impact of lipotoxicity

(Figure 1.6), and particularly its association with the phospholipid membrane, in pancreatic β-cells (see section 1.7.1).

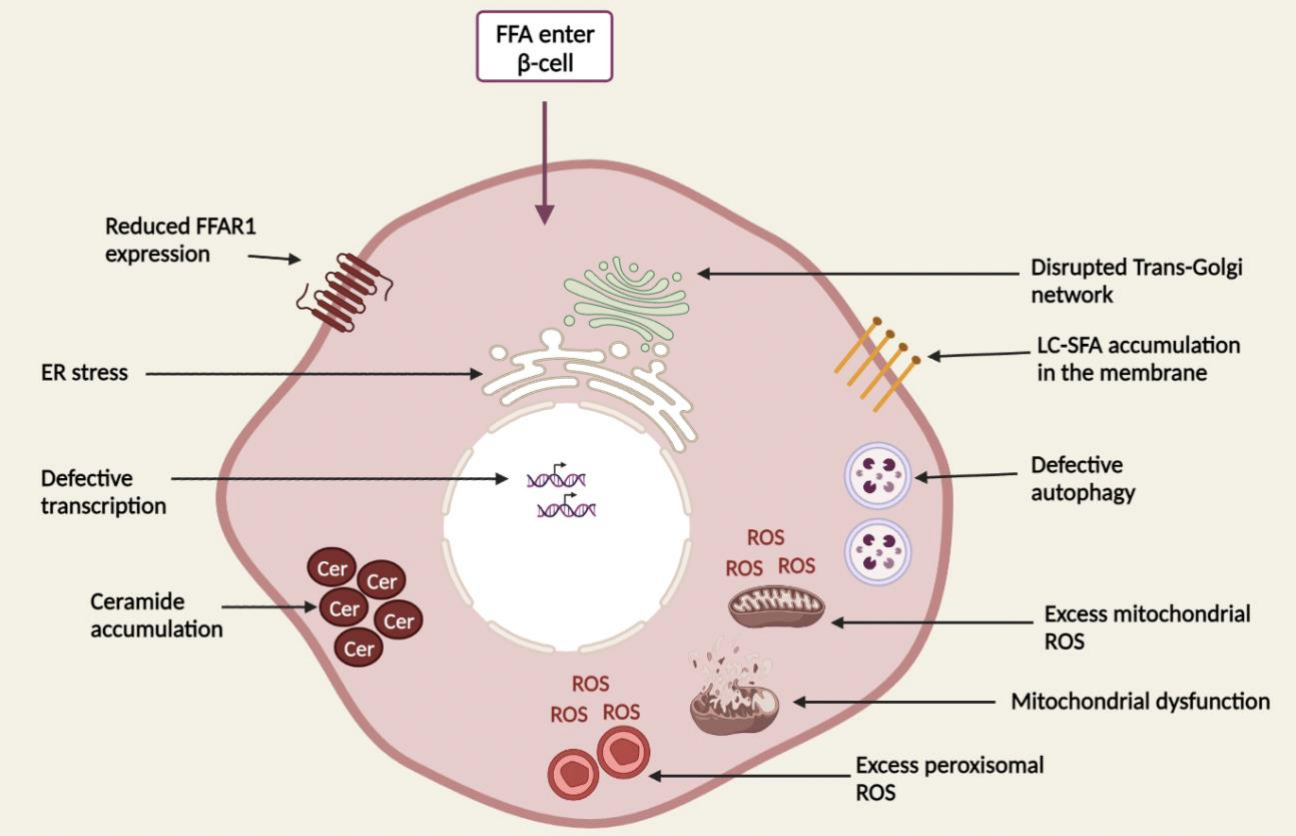

Figure 1.6 Mechanisms of lipotoxicity in pancreatic β-cells. Chronic increases in plasma FFA can prompt lipotoxicity. First, FFA enter the cell via an unknown mechanism, where they induce their toxic effects. Each of these lipotoxic effects shown in the diagram, either alone or in combination, have been reported to contribute to β-cell dysfunction and eventually cell death. Information taken from Oh et al. (118), Lenzen et al. (136), Payet et al. (137), Lytrivi et al. (138) and Weijers et al. (112). FFA: free fatty acids; FFAR1: free fatty acid receptor 1; LC-SFA: long-chain saturated fatty acids; ROS: reactive oxygen species; ER: endoplasmic reticulum. Figure adapted from Dr Patricia Thomas' teaching slides (unpublished) (139). Created in Biorender.com

1.7.1 The membrane-centric theory of lipotoxicity

As discussed in section 1.4.1, plasma concentrations of LC-SFA species are elevated, whereas LC-MUFAs are reduced in individuals with T2D. Many researchers have proposed that low membrane fluidity is an important contributor to the pathogenesis of T2D (112, 140, 141, 142), which is believed

to be attributed to a greater ratio of saturated to unsaturated fatty acyl chains of phospholipids in the membrane (112). Several mechanisms that are reported to be involved in β-cell lipotoxicity (Figure 1.6) have also been associated with a modification in the structure and/or function of the phospholipid membrane, including ceramide accumulation, oxidative stress, and disruptions to the trans-Golgi network. Alterations in the plasma membrane structure, potentially due to such mechanisms, may be a contributing factor towards the toxic effects of LC-SFA in mammalian cells. Alternatively, these factors involved in lipotoxicity might arise due to changes in the plasma membrane structure which, in turn, could alter LC-FFA uptake. There is seemingly very little research into the role of the phospholipid membrane in β-cell lipotoxicity, specifically.

1.7.1.1 Ceramide accumulation

Ceramides, which belong to the sphingolipid family, have been reported to be important mediators of β-cell lipotoxicity, ultimately resulting in β-cell dysfunction and death (143). These molecules consist of a sphingoid base and a LC-FFA chain, which are linked by an amide bond (Figure 1.7) (144). Under normal physiological conditions, sphingolipids have a role in cell signalling, as well as being structural components of cell membranes (145), however, excessive exposure of β-cells to LC-SFA (e.g., C16:0 and C18:0) has been shown to induce ceramide formation and accumulation, which may be detrimental to the cell (118). One potential mechanism for the role of ceramide accumulation in β-cell lipotoxicity, and subsequent dysfunction and death, is its effects on membrane fluidity.

De novo ceramide synthesis is reported to be associated with FFA-induced β-cell lipotoxicity (118). The LC-SFA, C16:0, is thought to be the preferential substrate for *de novo* ceramide synthesis, via the condensation of palmitoyl-CoA (the "activated" form of C16:0) with L-serine via serine palmitoyl-transferase (146). Therefore, an excess availability of C16:0 can result in the over-production of ceramide, leading to its accumulation in the cell (118). Evidence for the role of ceramide

accumulation in lipotoxicity includes that patients with T2D present with raised sphingolipid levels in plasma, adipose tissue, and muscle (147, 148, 149).

Intriguingly, it is thought that ceramide accumulation modulates the biophysical properties of lipid rafts in the plasma membrane, which can alter the function of membrane receptors which reside within these lipid rafts (150). Such receptors include certain classes of TNF receptors (TNF-R), for example TNFR1/2 and Fas, which are involved in the initiation of apoptosis via the activation of molecules called caspases (151, 152). In vitro studies using model membranes (153, 154) have shown that ceramide molecules pack tightly together with one another in the phospholipid membrane, due to their saturated fatty acyl chains (154), to form small ceramide-enriched microdomains. As a result, lipid rafts (and receptors within these lipid rafts) cluster together which, in turn, may trigger the extrinsic apoptotic pathway via a phenomenon known as proximity-induced caspase activation (150, 155). Evidence for this includes that forced clustering of Fas receptors occurs due to the extracellular addition of radioactive C16:0-ceramide, which clusters in distinct membrane domains, and that the addition of an anti-ceramide antibody (e.g., ceramide monoclonal antibody 15B4) prevents Fas-induced apoptosis (156). Further, the disruption of these lipid rafts (e.g., via cholesterol depletion) has been shown to prevent signalling via these receptors, thereby inhibiting apoptosis (157). Taken together, this evidence suggests that the tight packing of ceramides within lipid rafts may be necessary for signalling via receptors, such as TNF-R, which are involved in the induction of cell death.

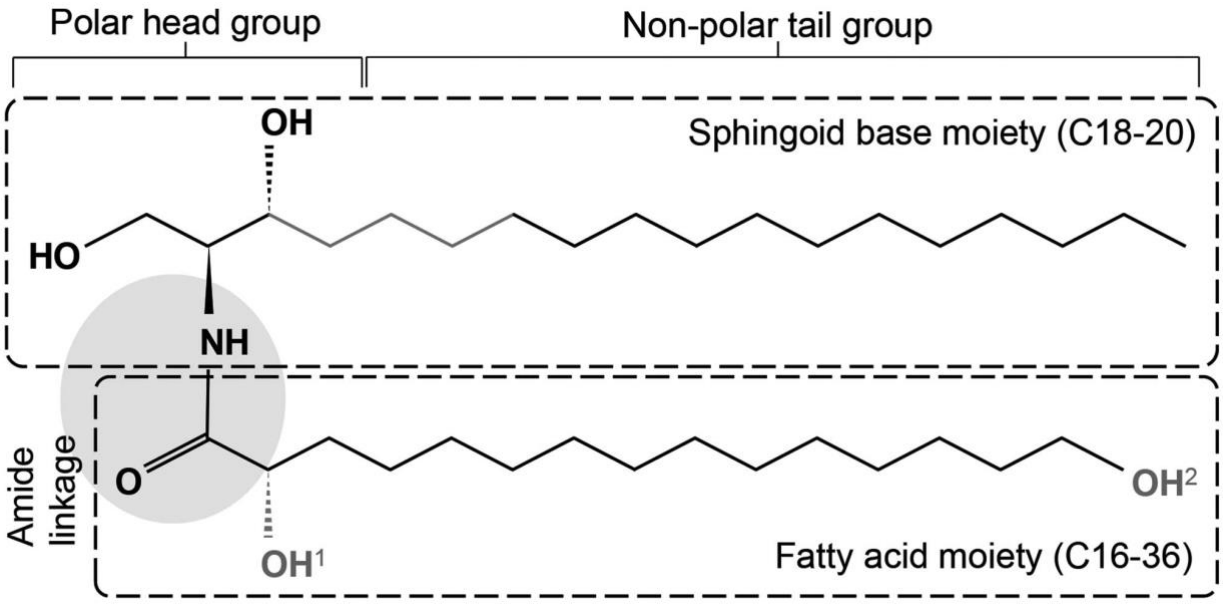

Figure 1.7 The basic chemical structure of a ceramide molecule. Figure adapted from Cha et al. (144)

1.7.1.2 Oxidative stress

One possible mechanism involved in the development of lipotoxicity is oxidative stress, which is caused by the production of reactive oxygen species (ROS), due to the oxidation of FFA in the mitochondria (158). ROS are a subgroup of free radicals, which are molecules that contain oxygen and have an uneven number of electrons (159). The uneven number of electrons of ROS makes these molecules highly reactive and highly unstable (159), resulting in their reaction with lipids, proteins, carbohydrates, and nucleic acids, causing irreversible damage or complete destruction to these molecules (158). Moreover, membrane phospholipids are reported to be primary targets for ROS-mediated damage (160).

In oxidative stress, there is an excess of ROS and insufficient reducing agents (antioxidants) to detoxify ROS (158). A marker of oxidative DNA damage, 8-hydroxy-2'-deoxyguanosine, has been reported to be increased in pancreatic islets of individuals with T2D (161), whereas levels of the

antioxidant, superoxide dismutase, are seemingly reduced (162). Pancreatic β-cells are especially vulnerable to oxidative damage, due to their low antioxidant capacity (163). For example, human pancreatic islets have been reported to express low levels of antioxidants such as catalase and glutathione peroxidase (164). Intriguingly, ROS are thought to play a vital role in glucose-stimulated insulin secretion (165), which might explain the low antioxidant levels in β-cells. However, accumulation of ROS above normal levels, due to excess levels of FFA, can cause irreparable damage within pancreatic β-cells, ultimately contributing to their dysfunction and death (165).

Interestingly, it has been shown that ROS modify the acyl chains of membrane phospholipids, via lipid peroxidation of unsaturated chains (166, 167). As a result, this may alter the secretion of insulin from pancreatic β-cells (166, 168). A recent study by Cohen et al. (168) has shown that increasing levels of C16:0 and glucose can enhance phospholipid remodelling in rodent pancreatic β-cells, involving the increased incorporation of C16:0 into phospholipids, coupled with the release of other FFAs such as arachidonic acid (AA) and linoleic acid (LA). Subsequent peroxidation of AA and LA by ROS produces 4-hydroxy-2*E*-nonenal (4-HNE), a lipid hydroperoxide which has been reported to facilitate GSIS though the activation of nuclear receptor peroxisome proliferator-activated receptor-δ (PPARδ) (166). However, at high levels C16:0 and glucose, the augmentation of insulin secretion is lost, probably due to the accumulation of cytotoxic effects within the cell (168). Taken together, this evidence suggests that the accumulation of the LC-SFA, C16:0, in the phospholipid membrane can enhance oxidative stress within the cell, which, in turn, could perhaps be a contributing factor towards the progression of β-cell dysfunction and death.

1.7.1.3 Trans-Golgi network

The trans-Golgi network (TGN) is a key secretory pathway involved in directing newly synthesised proteins towards different destinations within the cell, including the plasma membrane (169). It has been suggested that the accumulation of saturated FFA within the cell can alter the organisation of

the TGN, by reducing the number of secretory vesicles travelling to the plasma membrane (137). As a result, this process could disrupt the delivery of vital proteins, including those involved in maintaining glucose homeostasis, to the plasma membrane (137). For example, elevated C16:0 has been shown to result in downregulation of sortilin, which is a protein found within the Golgi compartment that is involved in the formation of glucose transporter type 4 (GLUT4) vesicles (170). Correspondingly, the trafficking of GLUT4 receptors to the plasma membrane in response to insulin is prevented which could, in part, account for insulin resistance in T2D (137, 170). On the contrary, LC-MUFAs (e.g., C16:1 and C18:1) seemingly do not impair GLUT4 trafficking; rather, they have been reported to restore the abundance of sortilin and reverse the effects of C16:0 (170). Taken together, this evidence suggests that the accumulation of saturated LC-FFA within the cell may prevent the translocation of proteins (e.g., GLUT4) to the plasma membrane via disruption of the trans-Golgi network, however, LC-MUFAs could counteract this disruption.

In summary, a number of mechanisms that have been reported to be involved in β-cell lipotoxicity (i.e., ceramide accumulation, oxidative stress, and modifications to the trans-Golgi network) have also been associated with an altered structure of the phospholipid membrane. It is important to consider the role of the phospholipid membrane in lipotoxicity, as a change in membrane structure has also been associated with an altered uptake of LC-FFA (as discussed further in chapter 4).

1.7.2 The protective role of monounsaturated fatty acids

As discussed in section 1.7, it is widely believed that LC-SFAs are toxic to pancreatic β-cells, whereas LC-MUFAs are better tolerated. There is a substantial amount of evidence supporting the cytotoxic effects of LC-SFAs (e.g., C16:0) however, the impact of LC-MUFAs in β-cell lipotoxicity remains unclear.

Several investigations (133, 137, 171) have shown that C18:1 exerts a lipotoxic effect in pancreatic β-cells. although most studies (126, 134, 172, 173, 174) have reported that LC-MUFAs play a protective role in β-cells, to inhibit the cytotoxic effects of LC-FFAs. Mechanisms for the protective role of LC-MUFAs include; 1) peroxisome proliferator-activated receptor (PPAR) activation, which might promote the sequestration, and thus the cytotoxic effects, of LC-SFAs (173), 2) inhibition of caspase 3 activity, a protein which is involved in the apoptotic pathway (175), and 3) directing LC-SFAs towards storage as triglycerides, which has been shown to be positively correlated with cell survival (176). Moreover, LC-MUFA could exert a cytoprotective effect by restoring the structure and/or function of the phospholipid membrane. As discussed in section 1.7.1, modifications to membrane composition and fluidity are thought to be brought about by LC-SFAs. On the other hand, unsaturated fatty acid chains could have a role in stabilising the lipid membrane, by preventing such modifications (177), which could potentially protect against the cytotoxic effects of LC-SFAs. Collectively, this evidence implies that LC-MUFAs have a role in protecting cells from lipotoxicity-induced β-cell dysfunction and death, however, more research is required to elucidate the mechanisms involved in mediating this cytoprotection.

1.8 Theories for long-chain saturated fatty acid uptake

The mechanism of LC-FFA uptake into pancreatic β-cells is poorly understood at present. Therefore, it is important to characterise the mechanism of LC-FFA uptake into pancreatic β-cells to enable the production of therapeutics which regulate their entry, to slow or possibly prevent the progression of T2D.

As discussed above, LC-FFAs are important components of many cellular processes. As such, it is vital that they must travel from the extracellular fluid, cross the phospholipid bilayer of the cell, and enter the cytoplasm (178). Currently, the molecular mechanism of LC-FFA uptake remains a topic of a debate, however the main models suggested in literature include simple passive diffusion (i.e., the

movement of the molecule down its concentration gradient without the assistance of proteins), or protein-mediated transport, which includes facilitated diffusion and active transport (e.g., endocytosis) (Figure 1.8) (179). Facilitated diffusion involves either channel or carrier proteins to facilitate the diffusion of substances across the membrane (180). Carrier proteins undergo a conformational change when presented with the substrate, which then opens a channel for the substrate to cross the membrane (180). On the other hand, channel proteins form pores in the membrane to enable the translocation of the substrate across the membrane (180). Both channel and carrier proteins do not use an energy source (180, 181). However, in active transport, substrates move across the plasma membrane against their concentration gradient using free energy from either a direct source of chemical energy (primary active transport), usually from ATP, or a concentration gradient of a second substrate (secondary active transport) (182). Endocytosis involves the internalisation of plasma membrane lipids, integral membrane proteins and extracellular fluid into the cell, to produce internal membranes (183). In this way, substrates may be delivered into the cell, enclosed within these internal membranes (183). Overall, the method by which LC-FFAs transport across the plasma membrane of the cell (i.e., via passive diffusion or protein-mediated transport) is still unclear, particularly in pancreatic β-cells. However, there are several compelling arguments for each model.

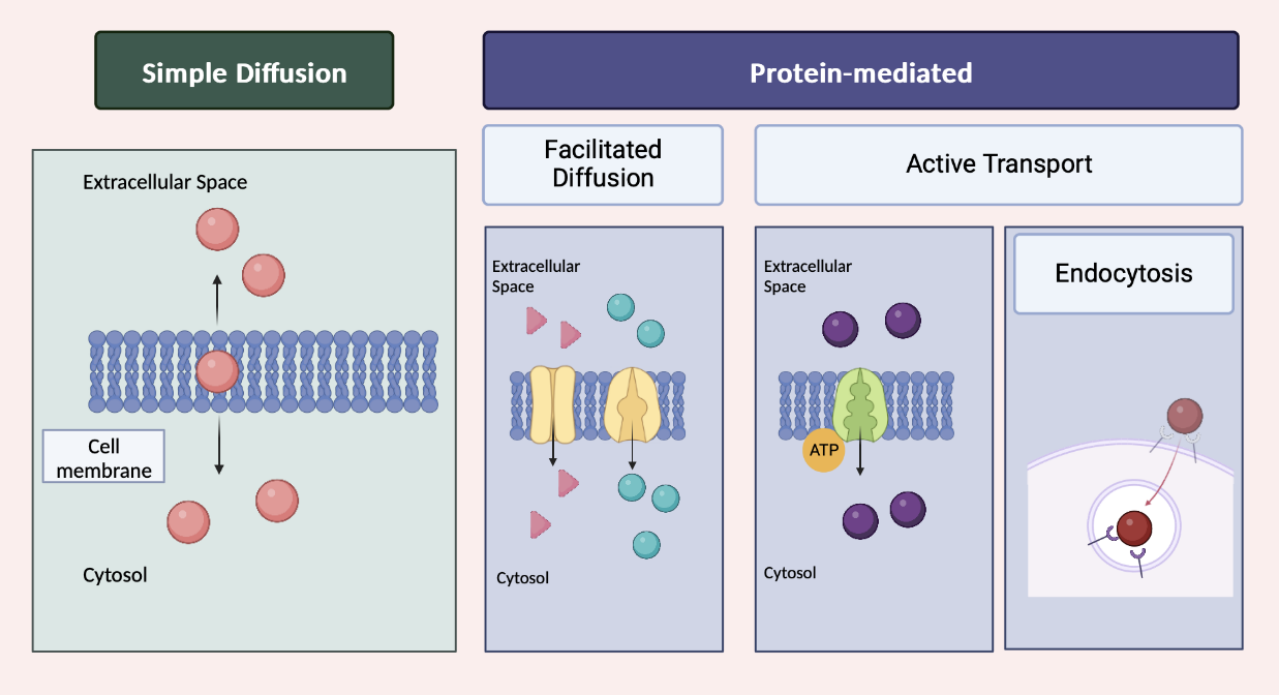

Figure 1.8 Theories of long-chain fatty acid uptake include simple diffusion and protein-mediated transport. Created in BioRender.com.

1.8.1 Passive diffusion of LC-FFAs

The premise of the passive diffusion model is that LC-FFAs can cross the membrane without the assistance of proteins (184). One argument for this theory is that passive diffusion should be the preferred mechanism of transport into cells, rather than protein-mediated transport, to meet their high metabolic demand (185). Evidence supporting the role of passive diffusion in LC-FFA uptake includes 1) physics-based modelling (186), 2) the ionisation properties of LC-FFAs (187), 3) LC-FFAs can translocate the membrane of small and large unilamellar vesicles (SUVs and LUVs respectively) (185), and 3) the flip-flop model of passive diffusion (188), and 4) the vectorial acylation hypothesis (179).

Physics-based modelling seemingly supports the theory of passive diffusion of LC-FFAs. According to the Meyer-Overton rule, a physics-based model, the addition of methylene groups (a carbon with two hydrogens), to carboxylic acids (e.g., fatty acids) should increase their solubility in lipids,

therefore enhancing diffusion through the lipid bilayer (189). Therefore, in keeping with the Meyer-Overton rule, it should be expected that LC-FFAs can traverse the plasma membrane using simple passive diffusion. However, the more recent work of Grime et al. (190), which used quantitative visualisation of passive diffusion, reported a contradictory phenomenon; hydrophilic substances, rather than lipophilic substances, display the highest membrane permeability. It is important to note that the Meyer-Overton rule was established over 120 years ago and does not account for transport mediated by membrane proteins, channels, or pumps, as these were not known at the time (189).

The ionisation properties of LC-FFAs in the plasma membrane implies that a protein transporter should not be required for transport (191). Kamp, F. and Hamilton, J.A. (187) examined LC-FFA uptake in SUV and LUV, which are simple model membranes containing a single lipid bilayer, and that are devoid of proteins. In this study, the researchers reported that in the phospholipid bilayer of SUVs and LUVs, a high population of LC-FFAs (~50%) exist in their un-ionised form (that is, that the LC-FFA does not have an electric charge) at pH 7.4 (Figure 1.9) (187, 191). This is physiologically relevant in human cells, including in pancreatic β-cells, where intracellular pH is generally between 7.0 and 7.4 (192, 193). In another study, observations by Kamp et al. (194) have then determined that the un-ionised LC-FFAs are able to rapidly diffuse ($t_{1/2}$ (half-life) < 1 second) across the membrane, down its concentration gradient, without the use of a protein transporter in SUVs and LUVs.

The ionisation properties of LC-FFA aid the understanding of the flip-flop model of passive diffusion (Figure 1.9), which several researchers (188, 195, 196, 197, 198) believe explains the trans-bilayer movement of LC-FFAs. In this model, it is thought that LC-FFA insert into the plasma membrane with their tail aligned with the fatty acyl chains of phospholipids, resulting in equal numbers of un-ionised and ionised LC-FFA in the membrane (188). This ionisation property enables the translocation of uncharged LC-FFA via passive diffusion through the hydrocarbon core (‘flip’) (188).

Then, at the inner sheet of the phospholipid bilayer, a small number of LC-FFA molecules can desorb into the cytoplasm, where they release H^+ (188). As a result, the passive movement of LC-FFA across the plasma membrane could create new pH gradients or modify those that are already present (187). This pH gradient might drive flip-flop of LC-FFAs across the membrane as demonstrated by Pohl et al. (195). Using artificial phospholipid membranes, these researchers (195) found that the transport of LC-FFAs, including stearic acid and linoleic acid, is increased when pH is lower in the extracellular compartment compared to the intracellular compartment, suggesting that a pH gradient could be necessary for LC-FFA transport via passive diffusion. The notion that a pH gradient across the membrane drives LC-FFA flip-flop is also supported by studies using isolated rat adipocytes (196) and cardiomyocytes (197), as well as human embryonic kidney cells (198).

Further evidence supporting the role of passive diffusion in LC-FFA uptake is the vectorial acylation hypothesis, which suggests that transport and activation of LC-FFAs are functionally coupled to one another (179). In this model, it has been proposed by several studies (179, 199, 200) that LC-FFAs are trapped inside the cell by the esterification of LC-FFAs with coenzyme A by long-chain acyl-CoA synthetases (ACSLs). This process is thought to contain LC-FFAs within the cell, as LC-FFA are converted to long-chain fatty acyl-CoA thioesters, which cannot translocate the plasma membrane (201). As such, an intracellular concentration gradient of LC-FFAs is created to drive their uptake into the cell. These acyl-CoA synthetases may be localised to internal membranes, particularly at the ER (179), or at the plasma membrane (202). Evidence supporting the vectorial acylation hypothesis of LC-FFA uptake includes that inhibition and overexpression of ACSL enzymes results in corresponding changes to LC-FFA uptake (179, 199, 200). It is important to note, however, that while most evidence supports the role of vectorial acylation in the passive diffusion of LC-FFAs, it has also been reported that vectorial acylation could be functionally coupled to LC-FFA transport by proposed LC-FFA transport proteins (202).

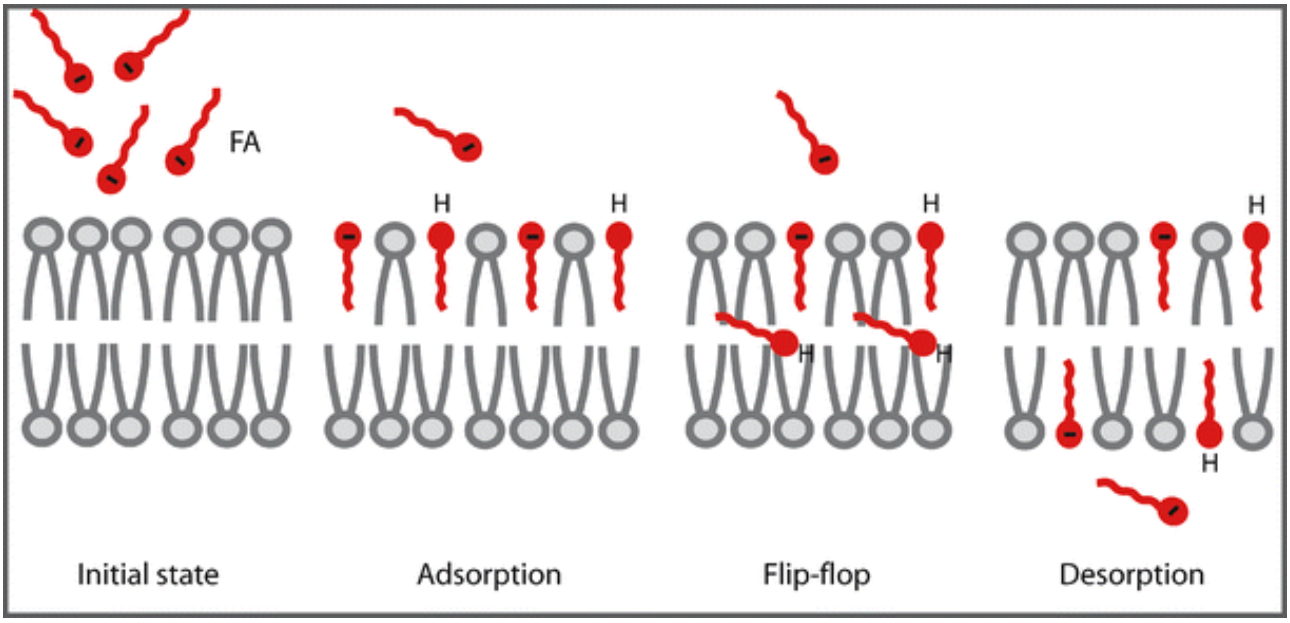

Figure 1.9 The flip-flop model of passive diffusion. LC-FFA bind to the outer surface of the phospholipid bilayer (188). Once ionisation equilibrium is reached (50% of ionised and un-ionised LC-FFA at pH 7.4.), the un-ionised LC-FFA 'flip' to the inner sheet of the membrane and subsequently desorb into the intracellular compartment (187, 188). LC-FFA: long-chain 'free' fatty acid; FA: fatty acid. Figure taken from Hamilton, J.A. and Brunaldi, K. (188).

1.8.2 Protein-mediated transport of LC-FFAs

There is evidence to suggest a role for proteins in the uptake of LC-FFAs across the plasma membrane into mammalian cells. One intriguing theory to support the use of proteins in LC-FFA transport is that, given the important roles of LC-FFA in the human body (outlined in section 1.4), their intracellular concentrations should be carefully regulated (203). Thus, proteins might provide this rigorous control that is required (203). It is widely accepted that the transport of glucose, another major fuel substrate, is governed by proteins at the cell membrane (204), including GLUTs (205) and sodium-glucose cotransporters (SGLTs) (206) with the isoforms within these families being specific to tissue type. Like glucose, it is feasible that proteins could be involved in facilitating the transport of LC-FFA into cells.

1.8.2.1 Facilitated diffusion or active transport?

Some researchers (204, 207) argue that LC-FFAs are transported across the plasma membrane into the cell via facilitated diffusion, which involves the spontaneous passive trans-bilayer movement of LC-FFAs from the extracellular space into the cytosol of the cell with the use of specific transmembrane proteins (181). Evidence for the use of a facilitated transport mechanism for LC-FFAs is largely due to the theory that it would be beneficial for highly metabolically active cells, that utilise high levels of LC-FFAs, to have a high affinity mechanism to recruit FFA from the extracellular milieu for use in the cell (204). The use of protein transporters for LC-FFA uptake would be particularly useful to ensure LC-FFA uptake occurs when concentrations are low, and to limit uptake when extracellular concentrations are high (208). Such evidence supporting the role of facilitated diffusion/active transport in LC-FFA uptake includes 1) mathematical models (185), 2) LC-FFA require proteins to transport across the mitochondrial membrane (209) and 3) loss- and gain-of-function studies (210).

Mathematical models have also shown support for the theory of facilitated diffusion of LC-FFAs. Interestingly, a recent study by Barta et al. (185) suggests, using mathematical models, that LC-FFAs require not one or the other, but a combination of both passive and facilitated diffusion mechanisms to meet the energy requirements of the cell (185). This mathematical model implies that the passive diffusion of LC-FFAs must be assisted by supplementary mechanisms, potentially via membrane proteins that interact with receptors for albumin (receptors) or catalyse the flip-flop of LC-FFAs (fatty acid transporters) (185). However, it is possible that flip-flop is an energy-mediated process, rather than a passive, as flippase enzymes involved in the flip-flop process are thought to be ATP-dependent (211). As such, recent literature generally does not specify whether the transport of LC-FFAs involves a facilitated or active transport mechanism, but rather solely focuses on investigating protein involvement.

It is well understood that LC-FFA require a proteins to translocate the mitochondrial membrane for subsequent β-oxidation, whereas medium-chain FFA can enter via simple diffusion (212, 213). In the cell, LC-FFAs are converted to long-chain fatty acyl-CoAs (the activated form of LC-FFA), which require a carnitine shuttle to cross the mitochondrial membrane (214). This involves the esterification of LC-FFAs with carnitine in the cytoplasm to produce acylcarnitines, which is catalysed by carnitine palmitoyltransferase (CPT) 1 (213). The acylcarnitines are then transported into the mitochondrion via carnitine acylcarnitine translocase (CACT) and are subsequently reconverted to fatty acyl-CoAs by CPT2, where they can then be used for subsequent β-oxidation for energy production (213). There are differences between the mitochondrial membrane and the plasma membrane, however. For example, Sjöstrand, F. S. (215) discovered that the plasma membrane is thicker (approximately 90-100 Å) in comparison to the mitochondrial membrane (approximately 50-60Å). Further, Schenkel L.C. and Bakovic M. (216) report that the phospholipid composition is different in the mitochondrial membrane when compared to the plasma membrane. Despite these differences, this evidence raises the question: if LC-FFAs require the assistance of proteins for transport into the mitochondria, should it be expected that they require transport proteins to translocate across the plasma membrane?

There are a multitude of loss- and gain-of-function studies that further support the role of facilitated diffusion/active transport in the uptake of LC-FFAs, however, there appear to be inconsistencies in the results of such studies. The proteins that have been previously suggested to facilitate LC-FFA uptake, as well as discrepancies in the literature, are explored in greater detail in chapter 2.

1.8.2.2 Endocytosis

There is evidence to suggest a role for endocytosis in LC-FFA uptake into mammalian cells. Endocytosis is an essential mechanism of transport for materials, particularly large molecules or those that cannot easily penetrate the plasma membrane, into cells (183). Clathrin-mediated endocytosis is the best characterised mechanism for the trafficking of molecules from the cell surface to the cell

interior (217), however there are also clathrin-independent mechanisms for endocytosis, including caveolae-mediated endocytosis (218). Caveolae are flask-shaped structures, produced by the assembly of integral membrane proteins, named caveolins, which bind directly to cholesterol within the membrane (82). Both clathrin- and caveolae-mediated endocytosis depend on the function of a GTPase called dynamin (218).

Intriguingly, caveolae-mediated endocytosis, specifically, has been implicated in the transport of LC-FFAs into mammalian cells. A recent study by Hao et al. (219) suggests a mechanism by which LC-FFAs are internalised to the cell via a caveolae-dependent process mediated by cluster of differentiation 36 (CD36), a proposed LC-FFA transport protein. In support of this, Daquinag et al. (220) recently suggested a mechanism whereby lipolysis triggers caveolae-mediated endocytosis of CD36 from the plasma membrane into lipid droplets. This mechanism is thought to be like that of the membrane-associated transporter of glucose, named GLUT4, which has been reported to be continuously recycled between intracellular stores and the plasma membrane, with its internalisation mediated by endocytosis (217). Moreover, the inhibition of caveolin-1 (CAV1) in hepatocytes has been reported to reduce the uptake of C18:1 (221). On the other hand, Pohl et al. (222) propose that caveolae are not involved in the uptake of LC-FFA, as these investigators did not observe any effect on the uptake of C18:1 following the expression of a dominant-negative mutant of dynamin in adipocytes. As there is little evidence to support or refute a role for caveolae-mediated endocytosis, it is important that researchers examine this mechanism in future studies. Seemingly, no studies have examined the role of endocytosis in LC-FFA uptake into pancreatic β-cells, specifically.

1.9 Summary

In general, literature supports a role for LC-SFAs (e.g., C16:0) in the induction of β-cell dysfunction and death, whereas LC-MUFAs are seemingly less toxic or exert a protective effect against LC-SFAs. Further, an elevation in the plasma levels of LC-SFAs, which is associated with T2D, has also been

reported to reduce membrane fluidity, which might affect the structure, and thus function, of the phospholipid membrane, thereby potentially altering the uptake of LC-FFA. The mechanism by which LC-FFAs traverse the plasma membrane and enter pancreatic β-cells, however, is yet to be determined. Subsequently, the work of this thesis proposes to investigate the potential mechanisms of LC-FFA uptake by identifying candidate LC-FFA transport proteins in β-cells, as well as investigating the role of passive diffusion and protein-mediated transport by manipulating the composition of the phospholipid membrane of β-cells. Ultimately, these investigations will provide a means to develop therapeutic interventions to regulate the entry of LC-FFAs into pancreatic β-cells, to reduce the toxic effects of LC-SFAs and potentially slow/prevent the progression of T2D.

1.10 Thesis aims and objectives

The overall aim of this thesis was to explore the mechanisms of LC-FFA uptake in pancreatic β-cells. Thus, the objectives of this study were:

1. To identify candidate transporters for LC-FFAs with the most evidence to support uptake in mammalian cells.
2. To determine which of these candidate LC-FFA transport proteins are expressed in human pancreatic β-cells.
3. To investigate the role of endocytosis in LC-FFA transport across the plasma membrane of human β-cells.
4. To investigate the role of the lipid phase of the plasma membrane in LC-FFA uptake in human pancreatic β-cells.

Chapter 2

Identification of candidate transport proteins involved in long-chain fatty acid uptake in mammalian cells: a scoping review

2.1 Introduction

To date, there exists nearly 30 years of conflicting research regarding the mechanism by which LC-FFAs translocate the plasma membrane of cells. This ongoing search for such mechanisms was first sparked by the well-characterised entry of glucose into cells, requires proteins to traverse the plasma membrane (223). Additional evidence includes that loss-of-function (LOF) and gain-of-function (GOF) studies support a role for candidate LC-FFA transporters (as discussed in greater detail below). In the period that this theory has been investigated, a wealth of literature has been published to elucidate the function of candidate LC-FFA transport proteins. However, there appear to be inconsistencies in these publications regarding which proteins are involved in LC-FFA uptake. These inconsistencies could be due to several different factors, including experimental techniques used in LOF/GOF studies, different cell types and mammalian models to study uptake. Therefore, in this chapter we have constructed a scoping review to generate an overview of this conflicting research and to identify the proteins that have the most evidence to support a role in LC-FFA transport.

2.1.1 Candidate transport proteins

2.1.2 Loss and gain of function to study LC-FFA uptake

To identify proteins which might be involved in LC-FFA transport across the membrane (i.e., candidate LC-FFA transport proteins), nearly 30 years' worth of LOF and GOF studies have been conducted.

2.1.2.1 Loss of function

LOF methods are those targeting DNA, RNA, or proteins to suppress function (224), then examining the effect of this on a dependent variable. In the context of the publications explored in this scoping review; this involves suppressing the function of candidate transport proteins to examine how this impacts LC-FFA uptake. Several different techniques may be used to achieve this (Figure 2.1), including knockout methods (e.g., CRISPR-based gene editing or homologous recombination), or a

knockdown approach (e.g., RNA interference (RNAi), chemical inhibition, morpholinos or hypomorphic mutations), as reviewed by Housden et al. (224). The principal difference between these two types of approach is that knockout methods target the gene to completely abolish its function, while knockdown methods target the DNA, RNA, or protein to reduce the abundance of functional protein (224). Seemingly, the most common LOF techniques used to suppress the function of candidate LC-FFA transport proteins are knockout, chemical inhibition and knockdown using RNAi (Figure 2.1).

To study the function of candidate LC-FFA transport proteins, many investigators use knockout methods, e.g., the generation of mice that are deficient for the protein of interest. For example, Febbraio et al. (225) generated CD36 null mice, to study the role of CD36 in LC-FFA uptake, using targeted homologous recombination. This involved generating a DNA construct containing a null mutation for CD36 which replaces one allele of the wild type gene (225). Then, this was followed by selective breeding to generate mice homozygous for the null mutation ($CD36^{-/-}$), resulting in the production of a non-functioning protein (225). In other studies, Hao et al. (219) used CD36 and CAV1 null mice to investigate the function of these proteins in LC-FFA transport and Newberry et al. (226) investigated the function of a protein named fatty acid binding protein 1 (FABP1) in LC-FFA uptake using FABP1 null mice. In summary, gene knockout using mice with a null mutation for a specific gene have been used to study the role of various proteins, including CD36, CAV1 and FABP1, in LC-FFA transport.

Numerous publications (184, 222, 227, 228, 229) have used chemical inhibition to examine the role of candidate LC-FFA transport proteins. Chemical inhibition involves the selective binding of a compound to a protein of interest, which prevents binding to other ligands, thereby suppressing gene function (222). For example, many studies (222, 228, 230) have reported sulfo-N-succinimidyl oleate (SSO) to selectively bind to CD36, thereby competitively inhibiting LC-FFA transport across the

plasma membrane. Several publications (231, 232, 233) have also used chemical inhibitors to target members of the FABP family. For instance, Stremmel, W. (233) studied the function of FABP8 in LC-FFA uptake using a monospecific antibody to inhibit expression of the protein. In another study, Zhou et al. (227) used a monospecific antibody to study the role of FABP1 in LC-FFA uptake. In summary, chemical inhibition is a popular technique used to study the function of candidate LC-FFA transporters, including CD36 and several members of the FABP family.

Experimental RNAi has also been implemented in studies investigating candidate LC-FFA transporters. This technique involves the introduction of double stranded RNA (dsRNA) into the cytoplasm of the cell, where it binds to messenger RNA (mRNA) with a homologous sequence, resulting in the degradation of this mRNA and reduced protein production (234). The main substrates involved in regulating this process are microRNAs (miRNA), synthetic small interfering RNAs (siRNA) and short hairpin RNAs (shRNA) (Figure 2.1) (235). Each of these substrates are non-coding RNAs, but there are subtle differences between them, such as their origin, number of strands, structure, and specificity (236, 237). Many investigations (238, 239, 240, 241) have used siRNA or shRNA to study the function of candidate LC-FFA transport proteins, such as the work of Benninghoff et al. (238), where the researchers used siRNAs to inhibit the expression of proteins, such as CD36 and FATP4 in murine myocytes, to study their role in LC-FFA uptake. Moreover, this study reported both CD36 and FATP4 to increase LC-FFA uptake using this method. In another publication, Lobo et al. (240) used shRNAs to inhibit the expression of CD36 and ACSL1 in murine adipocytes, to examine the role of these proteins in LC-FFA uptake. Altogether, experimental RNAi appears to be a popular technique to study the role of proteins in LC-FFA transport.

2.1.2.2 Gain of function

GOF techniques involve targeting DNA, RNA or proteins to change their function or expression pattern (242). In the context of identifying candidate LC-FFA transport proteins, this involves

overexpression (increasing the expression) of the protein to examine its effect on LC-FFA transport (243) (Figure 2.1). To achieve overexpression, exogenous nucleic acids (DNA or RNA), which code for a specific protein, are delivered into the cell using a vector that is designed for gene delivery (244). Promoter and enhancer sequences, which are also delivered into the cell, then control expression of the gene in order to achieve overexpression (245).

There are two main mechanisms for gene delivery to achieve overexpression: viral (246) and non-viral (Figure 2.1) (247). Several studies have used non-viral delivery systems to induce overexpression of candidate transport proteins to study LC-FFA uptake, including lipid-based transfection (where a lipid complex is used to deliver nucleic acids into the cell) (248, 249, 250, 251), and electrotransfection (where cells are exposed to an electric field, which enables entry of the nucleic acid) (252, 253). On the other hand, other studies have used viral delivery systems to achieve overexpression of candidate LC-FFA transport proteins, such as retroviral expression vectors (243, 254, 255), adenoviral vectors (256) and lentiviral vectors (257). Overall, there are a range of different viral and non-viral systems used to deliver the desired gene into the cell for overexpression. Moreover, several of these gene delivery techniques have been used in experimental studies to study the role of candidate LC-FFA transport proteins.

2.1.2.3 Limitations of loss of function and gain of function techniques

It is vital to address which experimental conditions were used to study the role of candidate transport proteins in LC-FFA uptake, because each method has limitations. First, while knockout models are a valuable research tool, using techniques such as homologous recombination can result in the death of transgenic animals, or gene expression may not be completely inhibited (224). The use of chemical inhibition also presents problems. For example, a recent report has questioned the specificity of the chemical inhibitor SSO; Jay et al. (184) argue that SSO is not a specific inhibitor for CD36, suggesting that it modifies several plasma membrane localised proteins along with CD36. Naturally, this may

impact the reliability of studies using SSO to study the effects of CD36. Further, this raises concerns as to whether other chemical inhibitors are truly specific to their target protein, as off-target effects might influence LC-FFA uptake. Knockdown approaches using RNAi are generally thought to be extremely sequence-specific, however there is a risk that incomplete gene inhibition might occur, as well as the possibility of off-target effects (258). Finally, the use of overexpression to study protein function has several drawbacks. For example, researchers have reported this technique to be harmful to the cell (259), likely due to the exhaustion of cellular resources to produce and transport proteins, which could impact observations of LC-FFA uptake. In addition, different studies might overexpress a particular protein to a different degree (260), which could result in a change in observation (i.e., one study might increase the expression of a candidate LC-FFA transporter more than in another study, resulting in different outcomes).

Overall, each experimental technique comes with its own advantages and disadvantages. Therefore, it is important that the experimental technique used is considered when interpreting the results of a LOF/GOF study examining the role of candidate LC-FFA transporters. As such, it is vital that a wide range of techniques are used to investigate the role of candidate LC-FFA transport proteins to maximise rigour and enhance the likelihood of identifying transport proteins which facilitate LC-FFA uptake in-vivo. Thus, we chose to investigate the experimental technique used within the studies collected in this scoping review.

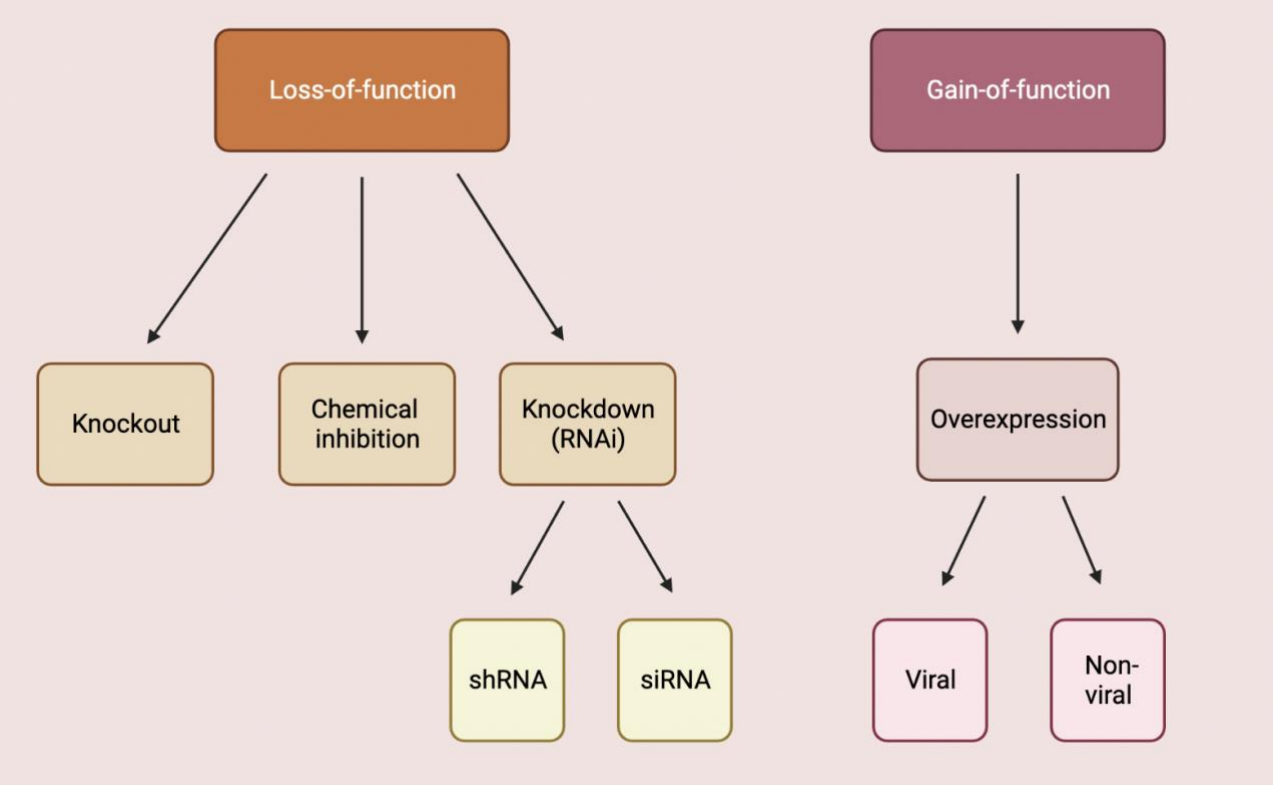

Figure 2.1 The most common experimental techniques used to study candidate LC-FFA transport proteins. Loss-of-function techniques (left) include knockout, chemical inhibition or knockdown using RNAi of the target protein. Frequently used substrates for RNAi include shRNA and siRNA. Gain-of-function techniques (right) involve overexpression of the protein using viral or non-viral delivery systems. RNAi: RNA interference; shRNA: short hairpin RNA; siRNA: small interfering RNA. Created in Biorender.com.

2.1.3 Cell types used to study LC-FFA uptake

Within the vast array of LOF and GOF studies used to study LC-FFA uptake, several cell types have been utilised. Seemingly, most studies use adipocytes, (184, 202, 225) cardiomyocytes (228, 229, 261) and myocytes (238, 256, 262) to examine the role of candidate transport proteins in LC-FFA uptake. This is unsurprising, as these cell types are highly metabolically active and play important roles in lipid homeostasis (222, 262, 263). For example, LC-FFAs are the major oxidative fuel used for contractile activity in cardiac muscle and during rest and mild-intensity exercise in skeletal muscle (262, 263), while adipocytes are the main site for lipid storage and mobilisation (222). Conversely, very little is known about LC-FFA transport into pancreatic β-cells. Due to the diversity in the

structure and function of different cell types in the body (264, 265, 266), we cannot assume that LC-FFA transport is the same in pancreatic β-cells as it is in other cell types. For instance, the processing and utilisation of LC-FFA is distinct to tissue type; in adipocytes, LC-FFA are converted to triglycerides (222), while in myocytes and cardiomyocytes (262, 263, 267), LC-FFA are primarily oxidised to produce ATP (the energy currency of the cell). In hepatocytes, the central organ for fatty acid metabolism (268), LC-FFAs are stored in small quantities as triglycerides, oxidised to produce ATP or secreted into the plasma as triglyceride-enriched VLDL. Moreover, LC-FFA can be utilised in hepatocytes as a substrate to produce ketone bodies (an alternative energy source when glucose is not readily available) (269). Thus, as the processing and utilisation of LC-FFA is unique to each cell type, it is important to delineate whether the mechanism of LC-FFA uptake is also distinct to each cell type. In addition, it is widely believed that glucose uses two types of transporters (SGLTs and GLUTs), with isoforms being specific to cell type (206), so it is vital to explore whether candidate transport proteins for LC-FFAs also have cell type specificity. Therefore, we wished to investigate whether candidate LC-FFA transport proteins have a role in LC-FFA uptake in different cell types, according to the literature identified in this scoping review.

2.1.4 Mammalian models used to study LC-FFA uptake

Studies investigating the role of candidate LC-FFA transport proteins have employed a range of mammalian model systems, both in-vitro and in-vivo. Using live humans would be the preferred method to study LC-FFA uptake as this would provide the most accurate indication of the physiological process, but this is difficult due to the ethical implications. First, it is unlikely that permission would be granted to take a biopsy from healthy human pancreatic tissue to study LC-FFA uptake (270). Second, a pancreatic biopsy is an incredibly invasive procedure that can result in pancreatitis, which would be an unacceptable risk to inflict upon healthy volunteers (271, 272). Instead, most research investigating the function and dysfunction of pancreatic β-cells uses rodent β-

cells, human islets, and post-mortem tissue. However, rodent β-cells have several differences when compared to human β-cells, including glucose transporters (273), expression of genes for insulin (rodent β-cells have two genes, whereas human β-cells have one) (274) and islet composition (275). This raises doubts as to whether rodent β-cells are an appropriate model to study T2D. Moreover, human islets contain several cell types including α-cells, β-cells, δ-cells, ε-cells and γ (or PP)-cells (84), which means this model is unsuitable for studying β-cells specifically. These are several limitations for conducting experiments in pancreatic tissue, however, other tissue types will share similar, or have their own, limitations. For example, post-mortem tissue (of any tissue type) is of variable quality and can only offer insight into one point in time (276), so it is not possible to observe LC-FFA uptake in real time using this method. Nevertheless, the use of rodent models, pancreatic islets and post-mortem tissue have still resulted in significant advances in the understanding of obesity and T2D.

Great care should be taken when selecting mammalian models to study the function of candidate transport proteins, in order to obtain the most accurate representation of human biology. This is because there are notable interspecies differences; for example, observations seen in animal models are not always replicated in humans (277). A study conducted by Mishima et al. (277) found that changes in the expression levels of human trophoblastic fatty acid transport protein 2 (FATP2) and FATP4, when cultured in hypoxic conditions compared to normal conditions, are different to that detected in murine placental FATP2 and FATP4. This study reports that in humans, hypoxia enhances FATP2 and reduces FATP4 expression, but that there is no change in the levels of these proteins in mice (277). In addition, Thomas et al. (278) recently demonstrated that there is a difference in the way that pancreatic β-cells route LC-SFA in rodent vs. human cells. Taken together, this evidence raises doubts as to whether rodent models provide an accurate representation of certain cellular

functions in humans. Thus, in this scoping review, we aimed to investigate whether the mammalian model used to examine the role of candidate LC-FFA proteins impacts the study outcome.

2.1.5 Aim and objectives

At present, the method of transport of LC-FFAs, especially into pancreatic β-cells, remains unclear. Chapter 1 describes the theories of LC-FFA uptake, including simple passive diffusion and protein-mediated processes, but this chapter focuses on the protein-mediated theory of LC-FFA transport. Firstly, as nearly 30 years' worth of research have investigated the role of candidate LC-FFA transport proteins, we aimed to consolidate which proteins have the most evidence to support a role, prior to any bioinformatic analysis or experimental work. To achieve this, a scoping review was conducted, which was an ideal method to map all the available evidence to date regarding LC-FFA candidate transport proteins and to identify key gaps in the literature (279). As so little is known about uptake into pancreatic β-cells, studies investigating the uptake of LC-FFAs into any mammalian tissue type were included in this review.

Aim: To investigate the evidence for candidate LC-FFA transport proteins in mammalian cells.

Objectives:

1. Conduct a scoping review based on PRISMA guidelines (279). Briefly, this work involved:
    a. Identifying candidate LC-FFA transport proteins
    b. Categorising candidate LC-FFA transport proteins according to cell type
    c. Determining if the experimental technique used to examine the candidate LC-FFA transport proteins influences observations

In this way, we wished to 1) construct an overview of nearly 30 years of conflicting research examining the role of candidate LC-FFA transport proteins, and 2) identify candidate transport proteins for LC-FFAs in pancreatic β cells, using previously published literature. From the identified

proteins, those studied in more than one publication would be carried forward for bioinformatic analysis (chapter 3).

2.2 Method

This scoping review was carried out in collaboration with Dr Patricia Thomas, in accordance with the Preferred Reporting Items for Systematic Reviews and Meta-Analyses (PRISMA) extension for scoping reviews (279).

2.2.1 Data sources and searches

Using a defined set of keywords (Table 2.1) we searched three databases: PubMed, Web of Science and Google Scholar. The data search was completed on the 23/11/2021. No further papers were retrieved after this date. Searches were carried out using a combination of three key phrases as listed by row in Table 1, using Boolean operators. For example, “Fatty acids” AND “Cells” AND “Candidate transport proteins”. Once searches were completed by row, additional searches were carried out involving random combinations of phrases, taking one from each column (Phrase 1, Phrase 2, and Phrase 3). Duplicated papers and studies which were not original research were then withdrawn.

Table 2.1 Key words used to retrieve publications

Phrase 1	**Phrase 2**	**Phrase 3**
Fatty acids	Cells	Candidate transport proteins
Fats	Beta cells	Transport proteins
Long-chain saturated fatty acids	Pancreatic beta cells	Transmembrane proteins
Fatty acids	Adipocytes	Fatty acid transport proteins
LC-SFA	Hepatocytes	Fatty acid uptake
FFA	Myocytes	Fatty acid transport
LCFA		

2.2.2 Study selection

First, we assessed the titles of all papers against the inclusion and exclusion criteria (Table 2.2). Publications were eligible for abstract review if they met all the inclusion criteria and did not include ≥1 of the exclusion criteria.

Table 2.2 Inclusion/exclusion criteria

	Inclusion Criteria	**Exclusion Criteria**
Publication type	- Peer-reviewed journal articles - Reported in English	- Secondary research (e.g., reviews) - Conference abstracts/proceedings - Articles not translated into English
Data type	- Experimental data	- Computational data (e.g., data generated from mathematical models)
Model systems	- Mammalian cells	- Non-mammalian cells - Artificial membranes
Treatment	- LC-FFA - Mediators of LC-FFA candidate transport protein expression and activity	- Short-chain fatty acids - Medium-chain fatty acids - Lipids other than LC-FFA (e.g., cholesterol) - Lipoproteins

		- Free fatty acids (not conjugated to albumin) - Compounds other than LC-FFA or those mediating the expression or activity of LC-FFA candidate transport proteins
Indications	- Healthy cells - Healthy individuals	- Disease conditions (e.g., cancer, cardiomyopathy, cardiovascular disease)
Outcome	- Protein-mediated LC-FFA transport at the plasma membrane	- Protein-mediated LC-FFA transport not at the plasma membrane (e.g., mitochondrial membrane) - Passive diffusion - Flip-flop mechanism (non-protein mediated)

Studies were then screened based on their abstract and included for further analysis if they met the inclusion criteria and excluded if they met any of the exclusion criteria (Table 2.2). The remaining studies were then screened based on their full text to establish the final publications included for review.

2.2.3 Data extraction

A data extraction matrix was produced to arrange key information from each publication (Appendix A – Supplementary Table 1). This data included the study reference (author name and year of publication), cell type used, model organism, candidate transport protein(s), experimental conditions (i.e., chemical inhibition, knockout, knockdown, overexpression, or case control studies), the LC-FFA transported and whether the protein facilitated LC-FFA transport or not. Subsequent data visualisation was conducted using RStudio (v4.1.1) in-house scripts.

2.3 Results

Overall, the screened literature supports a role for candidate transport proteins in LC-FFA uptake, with a total of 43 out of 45 final publications reporting that one or more proteins are involved. In total, 1588 publications were retrieved (Figure 2.2). Then, after the removal of duplicates and research that was not deemed original research (e.g., reviews etc.), 706 studies remained. To produce a reliable database, the titles, abstracts, and full text of these papers were examined sequentially against the inclusion and exclusion criteria. After screening, a total of 45 studies were included in a final database for review.

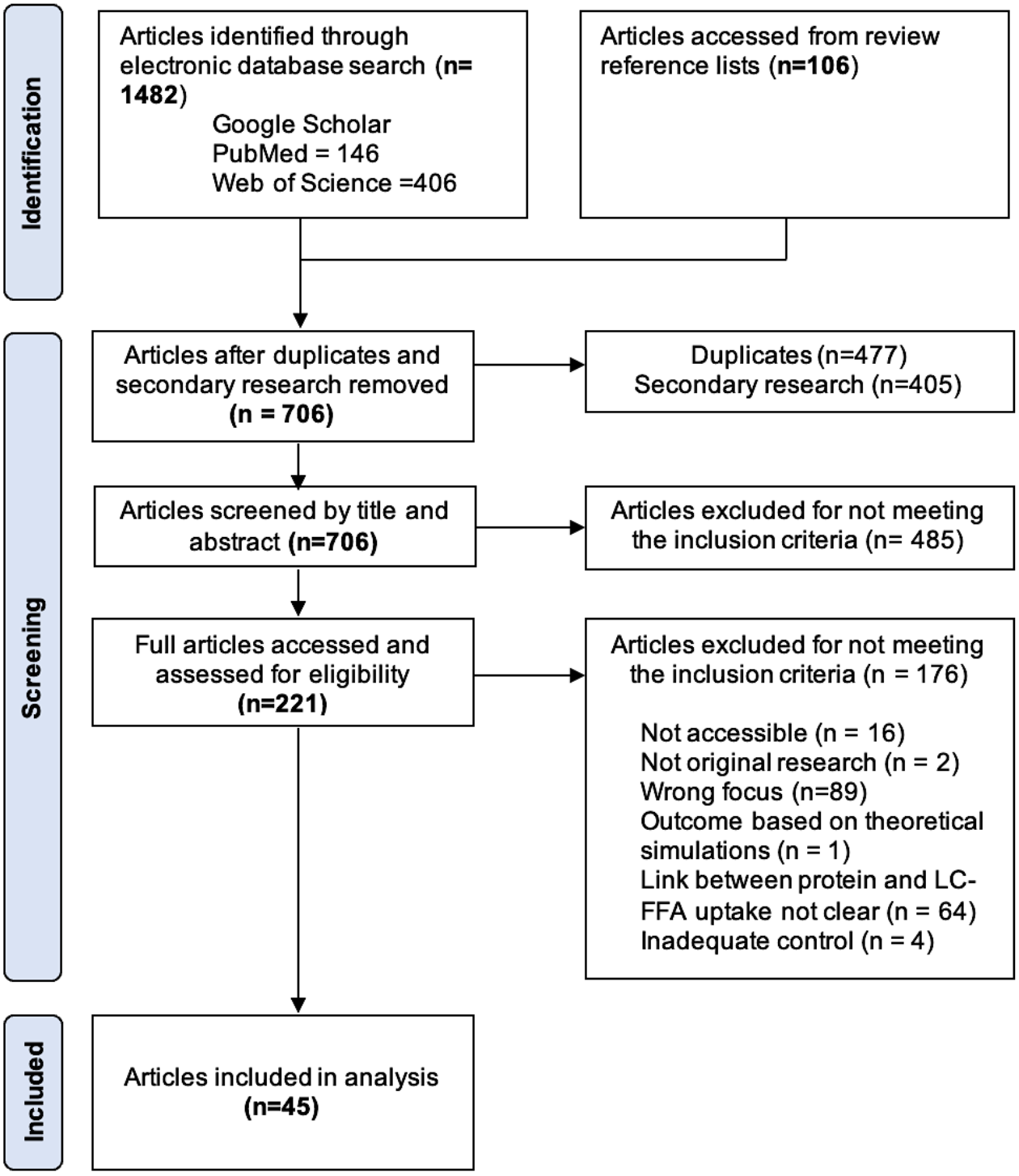

Figure 2.2 PRISMA flow diagram of the study selection process. Included and excluded publications are outlined, together with reasons for exclusion.

2.3.1 Overview of candidate LC-FFA transport proteins identified

Here, we have identified 23 candidate LC-FFA transport proteins within the 45 publications retrieved for review (Figure 2.3). The most studied protein was CD36 (in 27 different publications). From the literature, 22 of the total 23 proteins studied were reported to play a role in LC-FFA uptake in mammalian cells. However, many of these proteins were studied in very few publications (i.e., less than 2). Overall, we conclude that CD36 and the FATP family have the most evidence in literature to defend their role in LC-FFA transport in numerous cell types.

It is out of the scope of this thesis to discuss all the candidate LC-FFA transport proteins identified. Thus, candidate transport proteins were grouped into protein families, and only those that were found to be studied in >1 publication will be discussed henceforth in this thesis: the FATP, FABP, CAV and ACSL families, CD36, TBC1 Domain Family Member 1 (TBC1D1) and 4 (TBC1D4). It was decided here that additional research should be conducted (to obtain more robust results) if observations were reported in ≤2 publications, in accordance with the work of other published scoping reviews (280, 281). Previous publications offer a more detailed report on the role of the Rab family (238), TM4SF5 (282), PHB (257), ANX2 (257), DHHC4 and DHHC5 (283) in LC-FFA transport.

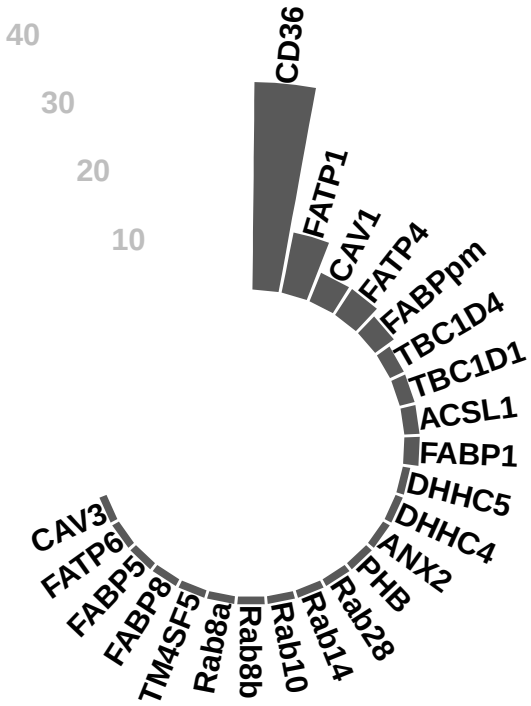

Figure 2.3 Overview of candidate LC-FFA transport proteins identified in the literature. The Y axis represents the number of publications retrieved in this scoping review that investigated the role of each candidate LC-FFA transport protein (x axis).

2.3.2 Cell type used to study candidate transport proteins

Next, we explored whether the outcome of the study (i.e., whether the candidate transport protein facilitated LC-FFA transport or not) was influenced by the cell type used (Figure 2.4). A wealth of evidence was found to support a role for CD36 in facilitating the uptake of LC-FFA in multiple cell types, especially in adipocytes (219, 222, 225, 240, 257, 283, 284), cardiomyocytes (228, 229, 261, 284, 285, 286), myocytes (238, 256, 284, 287, 288) and giant sarcolemmal vesicles (232, 286, 289), where the protein was found to aid transport in ≥3 separate publications for each cell type. We also discovered a considerable number of studies to support the role of the FATP family of proteins in LC-FFA transport in adipocytes (202, 239, 243, 290, 291) and myocytes (238, 256, 291) (≥3 different publications for each cell type validated this role). The CAV family of proteins were found to facilitate LC-FFA transport in adipocytes, where 2 separate publications (203, 219) validated this role. The TBC1D1 and TBC1D4 proteins were only studied in two publications, with each using a different cell type (Adipose-derived mesenchymal stem cells (241) and myocytes (238)). Further, these two studies had differing results; Mikłosz et al. (241) reported that TBC1D1 has no role in facilitating LC-FFA transport, but that TBC1D4 is a negative regulator of LC-FFA uptake (knockdown of the protein increased uptake), while Benninghoff et al. (238) suggested both TBC1D1 and TBC1D4 to be negative regulators of LC-FFA uptake. Thus, the evidence is inconclusive regarding the role of TBC1D1 and TBC1D4 proteins in LC-FFA transport. Moreover, the ACSL family were only studied in one cell type, with contrasting results; Gargiulo et al. (202) supported its role in LC-FFA transport while Lobo et al. (240) did not. Therefore, there is insufficient evidence to support a role for the ACSL proteins in LC-FFA transport.

Overall, we conclude that CD36 and the FATP family have the most evidence in literature to defend their role in LC-FFA transport in numerous cell types. However, additional research is needed to decipher whether candidate transport proteins have a different role in different cell types.

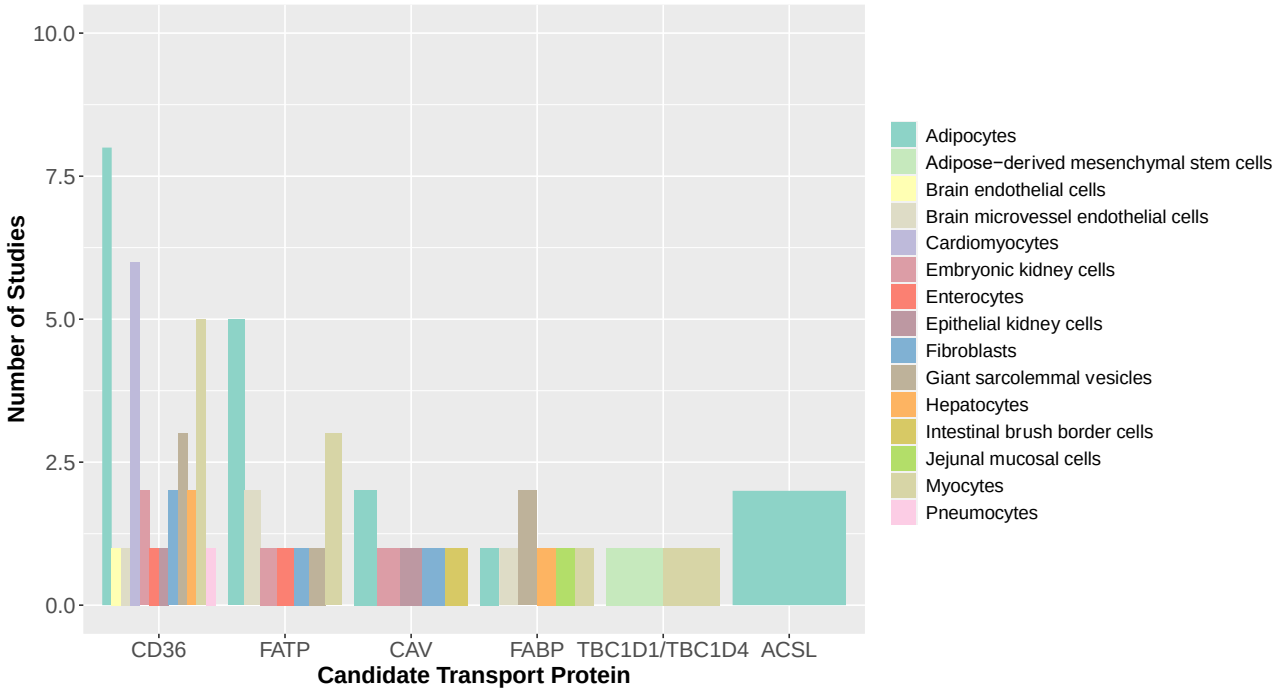

Figure 2.4 Mammalian cell types used to study the effect of each candidate transport protein family. The number of studies using each cell type is summarised for each candidate transport protein family.

2.3.3 LOF and GOF techniques used to study candidate transport protein

To establish whether the experimental condition used to study the function of our candidate transport proteins in LC-FFA uptake influences observations, we identified the number of studies using each technique (Table 2.3) and the outcome of those studies. We establish here that studies supporting the involvement of CD36 in LC-FFA transport remains true regardless of the experimental conditions used, including chemical inhibition of CD36 (222, 228, 229, 232, 257, 285, 286, 287, 288, 289, 292, 293, 294), knockout (219, 225, 261, 286), silencing using RNAi (siRNA/shRNA) (238, 240, 283, 295) and overexpression (248, 249, 255, 256, 283) , as ≥4 separate publications for each method supported a role for CD36 in LC-FFA transport. Out of the total investigations examining the role of CD36, nearly half (48%) used chemical inhibition. Furthermore, one case control study (284) comparing individuals with sufficient and deficient levels of CD36 also validated the role of the

protein in LC-FFA uptake. Hames et al. (284) reported that participants with a homozygous or heterozygous null mutation (Pro90Ser) for CD36 had a significantly reduced rate of uptake of LC-FFA, particularly of C16:0, in muscle and adipose tissue compared to control volunteers. Interestingly, the rate of LC-FFA uptake was indifferent in liver tissue of individuals with deficient CD36 compared to individuals who had sufficient CD36 (284).

For the FATP family, studies reported a role for these proteins in LC-FFA uptake when using experimental conditions such as knockdown using RNAi (including siRNA and shRNA) (238, 239, 290, 295) and overexpression (202, 243, 250, 252, 256, 296), in ≥4 publications for each technique. Studies investigating the role of the CAV family used a range of experimental conditions, although each condition was investigated in <3 publications. Chemical inhibition was the preferred technique to study the role of the FABP family (72% of publications), where all 5 studies (227, 231, 232, 233, 297) reported this protein family to be involved in LC-FFA transport. However, no publications used a gain of function methodology to study the FABP family. Only one experimental technique (knockdown using siRNA) was used to study TBC1D1 and TBC1D4 (100% of publications) (238, 241), so it cannot be said that the conditions used had an impact on observations. Two different experimental conditions were used to study the ACSL family (knockdown (240) and overexpression (202)), with different outcomes for each condition used. However, as only one paper was used for each condition, we cannot conclude that this difference was influenced by the technique used.

Altogether, we deduce here that CD36 and the FATP family are supported in the literature to have a role in LC-FFA uptake, despite the use of different experimental conditions. Additional research is needed to determine whether the experimental technique used to study the role of other candidate transport proteins has an impact on observations.

Table 2.3 Experimental techniques (LOF and GOF) used to study the effect of each candidate transport protein family. The number of studies using each technique to investigate the role of each candidate LC-FFA transporter is outlined.

	Number of studies
CD36	
Chemical Inhibition	14
Knockout	4
Knockdown	4
Overexpressed	6
Clinical technique	1
FATP	
Chemical Inhibition	1
Knockout	0
Knockdown	6
Overexpressed	6
Clinical technique	0
CAV	
Chemical Inhibition	1
Knockout	2
Knockdown	2
Overexpressed	1
Clinical technique	0
FABP	
Chemical Inhibition	5
Knockout	1
Knockdown	1
Overexpressed	0
Clinical technique	0
TBC1D1 and TBC1D4	
Chemical Inhibition	0
Knockout	0
Knockdown	4
Overexpressed	0
Clinical technique	0
ACSL1	

Chemical Inhibition	0
Knockout	0
Knockdown	1
Overexpressed	1
Clinical technique	0

2.3.4 Mammalian models used to study candidate transport proteins

To establish whether each candidate LC-FFA transport protein has evidence to facilitate uptake in humans, we identified the mammalian model used in each study (Figure 2.5). In essence, we could then determine whether the research conducted to date has distorted what can be extrapolated to humans.

In the retrieved studies, CD36 had strong evidence to support its role in facilitating LC-FFA transport in 3 models, including human (256, 283, 284, 295, 298), mouse (219, 222, 225, 238, 240, 249, 257, 261, 286, 292) and rat (228, 229, 232, 285, 287, 288, 289, 293, 294) (≥4 different publications for each model concluded this protein to have a role). The FATP family was also reported to aid LC-FFA transport in human (250, 256, 295) and mouse (202, 238, 239, 243, 250, 252, 290, 291) models (in ≥3 separate publications for each model).

The literature generally supports a role for the CAV family in LC-FFA uptake in mouse models, where 3 different studies (203, 219, 299) concluded that this protein family is involved in transport. However, the CAV family was only studied in one publication (198) using a human model. Evidence supporting the role of the FABP family was largely in rat models, where 4 different publications (231, 232, 233, 297) reported that members of the FABP family facilitate uptake. Only one publication (295) studied the role of the FABP family using a human model. Of the studies investigating the role of TBC1D1 and TBC1D4, a total of 2 models were used (human (241) and mouse (238)), in only one

publication each. Similarly, the ACSL family was only investigated in mouse models, in only 2 publications (202, 240).

In summary, we determine here that CD36 and FATP are seemingly supported to have a role in LC-FFA transport in humans. Evidence supporting the role of CAV and FABP family members was largely in different mammalian models (i.e., not human), which restricts our knowledge on the function of these proteins in humans. Further research is necessary to determine whether CAV, FABP, ASCL, TBC1D1 and TBC1D4 family members have a role in LC-FFA uptake in humans, as there are limited studies (≤1) using human models to investigate LC-FFA uptake.

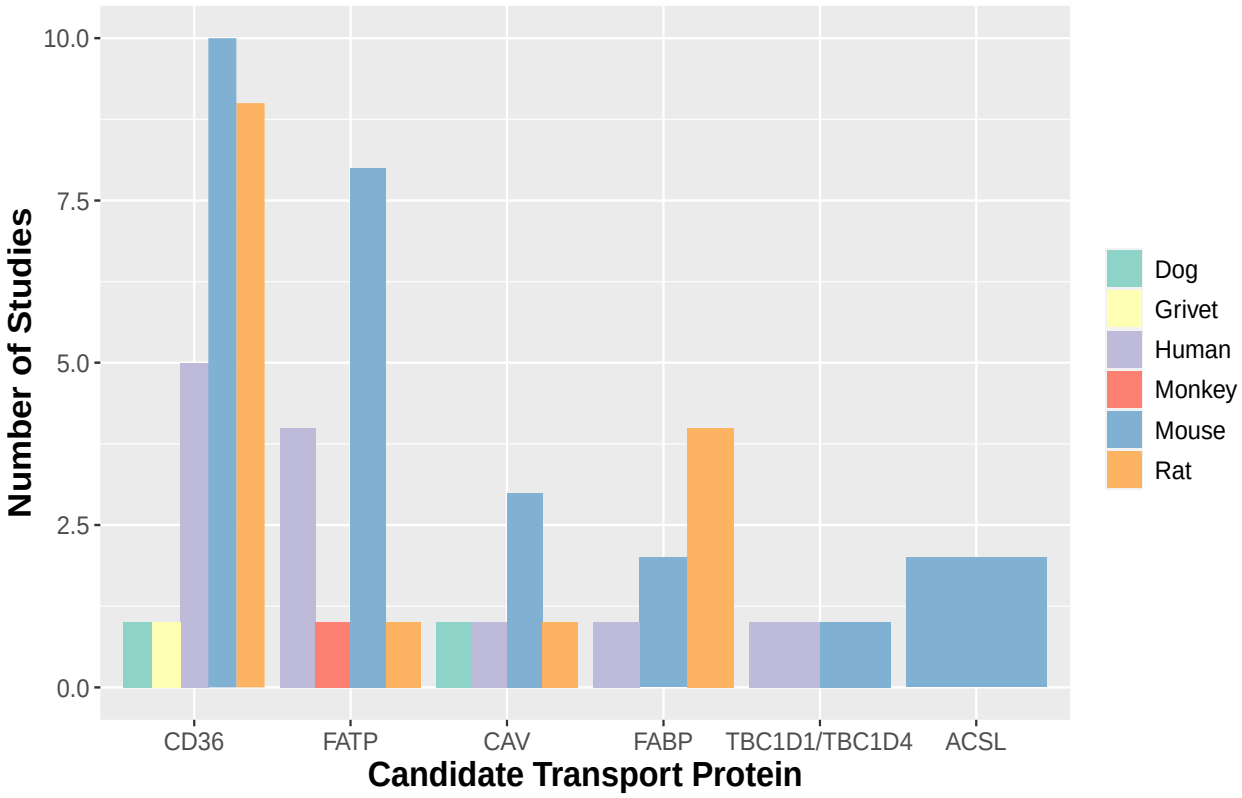

Figure 2.5 Mammalian models used to study the effect of each candidate transport protein family. The number of studies using each mammalian model is visualised for each candidate transport protein family.

2.4 Discussion

This chapter aimed to identify candidate proteins that may be involved in LC-FFA transport across the plasma membrane of pancreatic β-cells. To find such proteins, we conducted an extensive scoping review of nearly 30 years of conflicting literature surrounding this topic to date. Our results have shown that CD36 and the FATP family are the candidate transport proteins with the most evidence to support a role in LC-FFA uptake. Publications consistently reported a role for these proteins in LC-FFA uptake across a range of mammalian cell types, models (including human models) and LOF and GOF techniques, indicating that these proteins are likely to be involved in facilitating LC-FFA transport. Several other proteins were also implicated in transport, including the FABP, CAV and ACSL family members, as well as TBC1D1 and TBC1D4, but further investigation is needed to support a role for these proteins. Publications investigating these proteins simply did not have enough evidence to support their role in transport across a range of different cellular models/LOF and GOF techniques. Further, the FABP, CAV and ACSL family members, as well as TBC1D1 and TBC1D4, did not have enough evidence to support a role for LC-FFA uptake in human models. Therefore, no accurate conclusions could be made as to whether the model or technique used had an impact on the outcome of the studies investigating these candidate transport proteins. Importantly, no studies examining the role of candidate LC-FFA transport proteins in pancreatic β-cells were retrieved in this review. Future studies should investigate the role of these candidate transport proteins in LC-FFA uptake in pancreatic β-cells, to examine whether they facilitate LC-FFA transport in this cell type.

2.4.1 Potential mechanisms for CD36 in facilitating LC-FFA transport

Here, we have discovered that CD36 has the most evidence, out of all candidate LC-FFA transporters identified in this review, to support a role in facilitating LC-FFA uptake. However, the mechanism of CD36-mediated uptake is still not completely understood. Several mechanisms have been proposed, including insulin-stimulated upregulation of CD36 (300), sequestering LC-FFAs at the

plasma membrane and organising them into specific membrane domains (301), and a collaborative effort with other candidate transport proteins (222).

A recent review by Glatz et al. (300) suggested that CD36 is the main mediator of short-term regulation of FA uptake in cardiomyocytes, one of the main cellular models we have identified here to study this protein, via its constant subcellular recycling between endosomes and the sarcolemma. In this model, it is thought that the net translocation of CD36 from endosomes to the sarcolemma occurs within minutes and is triggered by the presence of insulin or muscle contraction, thereby increasing the rate of FFA uptake (300). Then, removal of the stimulus results in immediate internalisation of CD36, thereby lowering FA uptake rate (300). Interestingly, this mechanism is akin to the regulation of glucose uptake, where GLUT4 is thought to be recycled between intracellular structures and the plasma membrane (302). In an earlier review, Glatz, J.F.C. and Luiken, J.J.F.P. (301) proposed that CD36 functions by sequestering LC-FFAs in the membrane and arranging them within specific membrane domains, following its stimulated translocation to the membrane. As such, this is thought to make the LC-FFAs accessible for subsequent transport and/or enzymatic conversion by acyl-CoA synthetase (301). A study by Pohl et al. (222) agrees with this model, where it was reported that CD36 is exclusively located in plasma lipid rafts to control LC-FFA uptake. However, additional research is needed to support this model for CD36 in regulating LC-FFA uptake, especially in pancreatic β-cells.

Intriguingly, it has also been proposed that CD36 may act in concert with other candidate transport proteins to achieve LC-FFA uptake into metabolic tissues (219). One recent study by Hao et al. (219) reported that CD36 is localised in and may require caveolae for LC-FFA uptake. In the study, it was demonstrated that knockout of CAV1 abolishes CD36-dependent LC-FFA uptake in murine adipocytes (219). This is unsurprising in adipocytes, as caveolae are extremely abundant in this cell type, comprising roughly one third of the plasma membrane (219, 303). In addition, Vistisen et al.

(304) found CD36 to colocalise with a different isoform of the caveolin family, CAV3, in human skeletal muscle, which further supports this model of CD36-mediated uptake. Hao et al. (219) suggested that this collaborative effort of CD36 and caveolae in FFA uptake involves endocytosis, in which FAs bind to CD36 at the plasma membrane, which ultimately results in the internalisation of caveolae to enclose FAs within vesicles. These vesicles are then thought to traffic the internalised FAs to lipid droplets for storage or to the ER for esterification (219). Further investigation is necessary to delineate whether CD36 requires other proteins, particularly members of the CAV family, to carry out LC-FFA transport.

Collectively, these findings suggest that CD36 might use a different mechanism for LC-FFA transport, depending on the cell type, or a combination of mechanisms to achieve uptake. Therefore, if CD36 is involved in LC-FFA uptake in pancreatic β-cells, we cannot assume that the mechanism of transport used is the same as in other cell types.

2.4.2 Potential mechanisms for the FATP family in facilitating LC-FFA transport

Gain and loss-of-function studies have suggested that the FATP family of proteins have a role in LC-FFA uptake in a range of cell types, but their exact mechanism of action is still unclear. The main proposed theories of FATP-mediated LC-FFA transport are that these proteins 1) directly transport LC-FFA (243), 2) activate LC-FFA via intrinsic acyl-CoA synthetase (ACS) activity (305, 306), or 3) function with both transport and enzymatic activity, independently (307).

Interestingly, reports have suggested that members of the FATP family might be indirect transporters, by activating LC-FFAs via their intrinsic ACS activity (305, 306). This activity is thought to result in the esterification of LC-FFAs to produce long-chain fatty acyl-CoA thioesters (212), which can be used in metabolic processes such as β-oxidation to generate cellular energy (308), the production of complex lipids (e.g., phospholipids, triacylglycerol and cholesterol esters) (308), the modification of

proteins (309) and as ligands for transcription (310). The conversion of LC-FFA to long-chain fatty acyl-CoA thioesters, which are plasma membrane-impermeable (201), traps the LC-FFAs within the cell, which supposedly maintains a constant concentration gradient for LC-FFAs to diffuse into the cell (212). This concept is termed 'vectorial acylation' (212) (discussed in section 1.8.1). For example, a wealth of literature (311, 312, 313, 314) has proposed that the specific isoform FATP4 is located intracellularly, in subcellular compartments like the ER, rather than at the plasma membrane. Moreover, these studies (311, 312, 313, 314) have shown that the localisation of FATP4 to the ER may be sufficient to drive LC-FFA transport across the plasma membrane, supporting this vectorial acylation model of uptake.

One interesting theory is that FATP4 might require a signal to regulate its subcellular localisation (238), such that when this signal is active, the protein is not found at the plasma membrane but rather in intracellular compartments. Indeed, a recent publication by Benninghoff et al. (238) reports that the knockdown of TBC1D1 and TBC1D4 results in an increased abundance of FATP4 at the plasma membrane, indicating that RabGTPase-activating proteins (RabGAPs) may be involved in the regulation of the subcellular localisation and abundance of the protein. Further, Stahl et al. (250) reported that FATP4 is expressed at high levels in the plasma membrane of microvilli in enterocytes. This study (250) also reported chemical inhibition of FATP4 to significantly reduce LC-FFA uptake, which suggests that localisation of this protein to the plasma membrane is necessary for LC-FFA uptake. Additionally, we have identified several studies supporting the role of other isoforms of the FATP family in LC-FFA uptake, including FATP1 (202, 239, 243, 252, 256, 290, 291, 295) and FATP6 (296). Consistently, each of these studies have reported that FATP1 is localised to the plasma membrane of cells, where it aids LC-FFA transport. This further supports that localisation to the plasma membrane is required for the transport function of the FATP protein family.

Taken together, several possible outcomes can be deduced from these findings. Firstly, different isoforms of the FATP family might exert their LC-FFA transport function using different mechanisms. For instance, FATP4 might function intracellularly, using its intrinsic enzymatic activity, while FATP1 functions at the plasma membrane, using a direct transport mechanism and/or enzymatic activity. Secondly, these proteins, particularly FATP4, may require a signal to translocate to the plasma membrane (238), where they use a direct transport mechanism and/or ACS activity to transport LC-FFAs across the plasma membrane. Further investigation into the role of subtypes within the FATP family of transporters, particularly FATP2-6, in LC-FFA transport is necessary to delineate whether different isoforms carry out different transport mechanisms. Future studies should also be carried out to identify which signal (if any) is required to regulate the localisation of these proteins in the cell. For example, future studies might investigate physiological triggers that reduce the expression of TBC1D1 and TBC1D4.

2.4.3 Possible cell type specificity

We cannot assume that LC-FFA transport is the same across all cell types, given that different metabolically active mammalian cell types, such as adipocytes, hepatocytes, and pancreatic β-cells, have different roles in regulating lipid homeostasis (as discussed in section 2.1.3) (252, 315). For example, the utilisation of FFAs is different in adipocytes vs. pancreatic β-cells; adipocytes are known to be the primary site of lipid storage and mobilisation (316), whereas in unstimulated pancreatic islets, FFA are seemingly a major energy source (rather than glucose) (317). For storage, FFA are usually converted to triglycerides, whereas for use as an energy source, FFA are generally directed towards the mitochondria for β-oxidation (268). Thus, it is possible that LC-FFA transport could also be different to channel FFAs differently, to exert these different functions within different cell types. Further, cellular signals for FFA storage vs. oxidation are different, which might imply that LC-FFA transport could also be different, in response to these signals. In pancreatic β-cells, it is thought that

glucose is converted to malonyl-CoA within the cell, which inhibits CPT-1, thereby inhibiting fatty acid oxidation (105). In the absence of glucose, fatty acids (as long-chain acyl CoA) can transport into the mitochondria for oxidation (105). On the other hand, in adipocytes, storage of FFAs involves stimulation of adipocytes by insulin, which promotes glucose uptake and subsequent expression of lipogenic gene sterol regulatory element-binding protein 1 (SREBP1), which regulates the expression of genes required for triglyceride synthesis (318). These different cellular signals for FFA utilisation within the different cell types (e.g., for storage vs. oxidation) should be considered when investigating LC-FFA uptake. Of course, transport of FFAs might also be different in other cell types that utilise FFA differently, for example in the liver, where FFA can be converted to ketone bodies during fasting, which involves the transformation of FFAs to urinary acetoacetate and 3-β-hydroxybutyrate in the mitochondria (269). Taken together, as there is currently not enough evidence to support or refute that LC-FFA transport is different in individual cell types, we propose that candidate LC-FFA transport proteins should be investigated in individual cell types. In particular, future work should study the role of candidate LC-FFA transporters in cell types that have not been studied thus far, including pancreatic β-cells.

2.4.4 Isoforms of the candidate LC-FFA transport proteins

To obtain a broad overview of the candidate LC-FFA transport proteins, and to overcome time restrictions, proteins found in the literature were categorised according to their family rather than as each individual protein. Individual isoforms that were identified in the literature can be found within our data extraction matrix (Appendix A – Supplementary Table 1). However, it is important to note that many different candidate LC-FFA transporters, and many isoforms within each family, were identified in this scoping review. One reasonable suggestion for this variety in transporters is that the different candidate LC-FFA transport protein families, or their isoforms, have cell type specificity. As mentioned in section 1.8.2, transporters for glucose (GLUTs and SGLTs) have known cell type

specific isoforms that are specific to tissue type (205, 206). Moreover, there are known cell type specific isoforms for candidate LC-FFA transporters; for example, isoforms of the ACSL family have been shown to be cell-type specific (319). Further, these different transporters might be involved in the uptake of different classes of fatty acids (320), channel LC-FFAs differently within the cell (e.g., to the mitochondria for fatty acid oxidation or to the ER where they are converted to triglycerides for storage) (320, 321), and/or cooperate with one another to transport LC-FFAs across the membrane (219, 320). For example, FFAR4 (also known as GPR120) is a transmembrane fatty acid receptor that is thought to be specifically activated by unsaturated medium- and long-chain FFAs (322), which raises questions as to whether candidate LC-FFA transport proteins are also specific to different classes of fatty acids. In conclusion, further investigation is required to determine the role of different candidate transport protein isoforms.

2.4.5 Limitations

The findings from this review are restricted by several factors. Scoping reviews enable researchers to map the existing literature in a particular topic area and to identify gaps where future research should be conducted (323), however, we encountered several limitations with the use of this methodology.

Scoping reviews, by definition, do not include a quality appraisal of the included studies (324). Thus, we were unable to identify gaps in the research related to low quality. Rather, this type of review aims to categorise the existing literature by common themes and topics (324). In this case, we wished to gain an overview of all the candidate LC-FFA transport proteins identified to date, and categorise according to the cell type used, mammalian models and experimental techniques, to help identify where additional research should be carried out. Moreover, as scoping reviews only map the body of literature on a topic at a singular point in time, they are usually outdated soon after their completion (324). Therefore, this review should be updated according to published guidance (325).

2.4.6 Summary

In summary, many different LC-FFA transporters were identified, but CD36 and FATP have the most evidence to support a role in facilitating LC-FFA uptake in humans. The FABP, ACSL and CAV family members, along with TBC1D1 and TBC1D4, were also named to facilitate LC-FFA uptake, but further evidence is required to underpin their role in transport. Finally, very little is known about LC-FFA uptake in pancreatic β-cells.

Chapter 3

Using bulk RNA-sequencing data to explore expression profiles of candidate LC-FFA transport proteins in mammalian cells

3.1 Introduction

As detailed in the scoping review in chapter 2, the mechanism by which LC-FFAs traverse the plasma membrane and therefore enter pancreatic β-cells is still in question. It is essential to consider this process in pancreatic β-cells, because LC-FFAs, particularly LC-SFAs, have been implicated in the development and progression of T2D via a process termed lipotoxicity, which may result in the death and dysfunction of these cells (38, 123) (discussed in section 1.7). Therefore, understanding the mechanism of LC-FFA uptake will enable the production of therapeutics which regulate their entry. Accordingly, pancreatic β-cell viability could be preserved, thus slowing, or possibly preventing the progression of T2D. Literature supports a role for protein-mediated LC-FFA uptake, particularly via CD36 and FATP, into other metabolically active cell types, especially in adipocytes, myocytes, and cardiomyocytes (as discussed in section 2.4). However, the function of these membrane-associated LC-FFA transport proteins requires further investigation in pancreatic β-cells, specifically. Further, the identification of which isoforms of the candidate LC-FFA transporter family members are expressed in pancreatic β-cells should be explored, as there is a possibility that these isoforms may show cell-type specificity (discussed in section 2.4.5).

The lack of research into the mechanism of LC-FFA uptake in pancreatic β-cells might, in part, be due to the difficulty in finding suitable mammalian models that offer an accurate representation of human pancreatic β-cells (as outlined in section 2.1.4). Thus, in this chapter the aim was to identify an appropriate in vitro model to study LC-FFA uptake into pancreatic β-cells. Moreover, to compare the gene expression of candidate LC-FFA transporters in different metabolically active cell types to that in pancreatic β-cells, to gain insight into whether different cell types utilise a different transport mechanism (see section 2.1.3). In this way, we would identify whether the results of studies using different metabolically active cell types to study LC-FFA uptake can be applied to pancreatic β-cells. To achieve these aims, gene expression profiles were constructed in various ex-vivo mammalian cell

types, as well as two different pancreatic β-cell lines, for the candidate LC-FFA transport proteins identified in chapter 2.

3.1.1 RNA-sequencing

The central dogma of molecular biology describes the unidirectional flow of information that is stored in genes as DNA, then transcribed to RNA, and finally translated into proteins (Figure 3.1) (326). Although DNA stores genetic information, it is the transcription of genes into RNA molecules, specifically mRNA, that activates the genes (327). These mRNA molecules are produced on demand when required by the cell (327). Therefore, by investigating which mRNA transcripts are expressed in the cell, we can determine which genes are active in a particular cell type, thereby gaining a greater understanding of cellular processes.

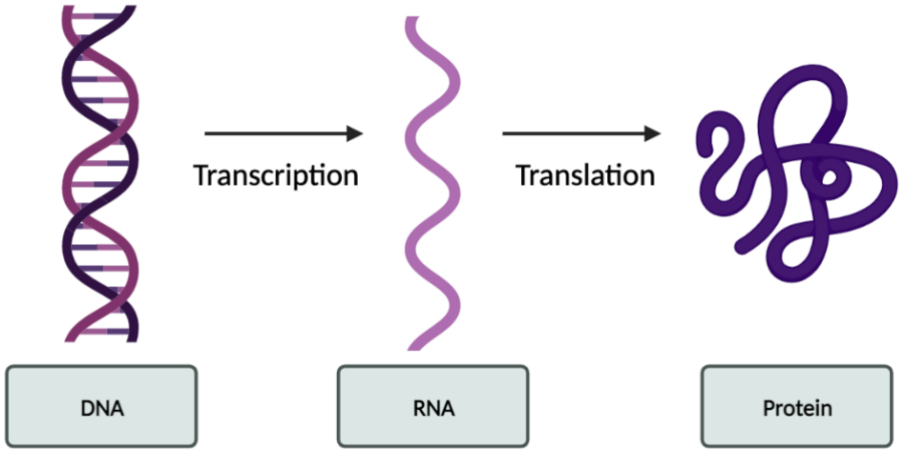

Figure 3.1 The central dogma of molecular biology. DNA is transcribed to RNA, which is translated into proteins. Created with BioRender.com.

3.1.2 Overview of RNA-sequencing

Analysing gene expression is essential to provide insight into the cellular transcriptome, which refers to the RNA molecules present within the cell. Investigating these molecules is vital to interpret the functional components of the genome, and to understand disease (328). This can be achieved using RNA-sequencing (RNA-seq), an accurate and highly reproducible method used to quantify transcriptomes (329).

Transcriptomics studies have significantly progressed over the past few decades, with the continuous evolution of more advanced technologies. In the past, transcriptomics largely relied on first-generation sequencing technologies, including the Maxam-Gilbert method (330) and the more commonly employed Sanger sequencing method (331), which both involve the sequencing of DNA. However, these techniques were time-consuming and expensive, driving the production of next-generation sequencing (NGS) technologies, which sequence nucleotides much more rapidly and at a lower cost comparatively (332). As such, RNA-seq with NGS is increasingly the preferred method for transcriptomics studies.

3.1.3 Experimental considerations for RNA-sequencing

Briefly, the RNA-seq workflow involves extracting RNA from the cell, generating complementary DNA (cDNA), constructing an RNA sequencing library (by ligation of cDNA to sequencing adapters), and sequencing using an NGS platform (333). However, it is important to consider several experimental details in RNA-seq, including the sample size, the library type (e.g., single vs. paired end sequencing, sequencing depth and fragment size), how the sample was collected and the RNA extraction protocol, and the type of RNA-seq method used (e.g., single cell vs. bulk RNA-seq). These experimental details should be considered as they may have an impact on the quality of the data.

The number of biological and technical replicates should be considered, to minimise false positives and enhance statistical power (334). As such, Schurch et al. (334) have suggested that at least 6 biological replicates should be used in RNA-seq experiments, rising to a minimum of 12 biological replicates for differential gene expression analysis. Further, McIntyre et al. (335) report that a low number of technical replicates (i.e., less than 5 reads per nucleotide) may result in variable detection of exons, and thus inconsistent estimates of gene expression.

The library type should also be accounted for when analysing RNA-seq data. In paired-end sequencing, both ends of the cDNA fragment are sequenced, whereas only one end is sequenced in single-end sequencing (336). It has been reported that paired-end and single-end reads provide reasonably vigorous gene expression estimates (337). However, while single-end sequencing is cheaper, it has been reported to increase errors in read counts and cause false positives and negatives when analysing differentially expressed genes (336). These errors are minimised when using paired-end sequencing, as it involves double the amount of sequencing compared to paired-end sequencing (336).

When analysing RNA-seq data, the RNA extraction protocol should be considered. The RNA extraction protocol should ideally involve a measurement of the RNA integrity, to ensure that the RNA is of adequate quality. RNA integrity is typically measured using an Agilent Bioanalyzer, which generates a number between 1 and 10 (10 being the sample with the highest quality, exhibiting the least degradation) (327). Romero et al. (338) suggest that an RNA integrity number (RIN) between 7.9 and 6.4 should be used as a cut-off value in the context of RNA degradation in dying tissue, whereby any sample with a RIN value below the cut-off level is excluded from further study. Subsequently, a RIN cut-off of 6.5 was used in the present study.

It is also vital to consider the RNA-seq method used within each study when analysing RNA-seq data, as discussed in section 3.1.4.

3.1.4 Types of RNA-sequencing and recent developments

The main RNA-seq techniques include classic bulk RNA-seq, single-cell RNA-seq (scRNA-seq) and spatial RNA-seq (spRNA-seq) (339). Bulk RNA-seq investigates the transcriptome of tissue sections, biopsies, or pooled cell populations (340). However, averaging pooled cell populations does not allow direct assessment of specific cell subtypes, which is vital to understand the complexity of biological systems. This limitation of bulk RNA-seq led to the development of scRNA-seq, a technique that has enabled researchers to define RNA molecules in individual cells on a genomic scale, capturing cell-to-cell variability at high resolution (341). While the current bulk and scRNA-seq methods deliver extremely detailed information in terms of tissues or cell populations, neither application captures spatial information, which removes the relationship between cellular context and gene expression (328). It is well-recognised that cellular organisation in tissues is intimately related to biological function (236), so in order to overcome this limitation, spRNA-seq was developed. This technique enables researchers to quantify RNA expression, while retaining spatial context of cells and tissues (236). All three RNA-seq techniques mentioned here are valuable in biomedical research, however, the preferred method is dependent on the study conducted and what the researcher aims to achieve.

3.1.5 RNA-sequencing in the field of diabetes and obesity research

Since its introduction nearly two decades ago (342), RNA-seq has been employed in several studies (343, 344, 345) in the field of diabetes and obesity research. For instance, Muraro et al. (345) used scRNA-seq to characterise various cell types in the human islet. In addition to the classical markers for each cell type, this study (345) revealed novel marker genes for alpha cells (such as PLCE1 and KLHL41), β cells (PFKFB2 and SIX2), delta cells (such as PRG4 and RGS2) and PP cells (such as SERTM1 and CARTPT). Moreover, Xin et al. (346) discovered 245 genes related to T2D using

scRNA-seq analysis of human islets, of which 38% had previously been reported to modulate cell growth in non-islet cells. This was an important observation, as reduced β-cell mass in patients with T2D is widely considered to be correlated with the onset and progression of the disease (347). Using bulk RNA-seq, Diedisheim et al. (343) identified changes in gene expression following the induction of β-cell dedifferentiation, including the reduced expression of many β-cell markers, such as MAFA, ZNT8, GCK and SLC2A2. Essentially, this enabled the authors to construct and validate an in vitro model of β-cell dedifferentiation. The studies mentioned here are just a small number of examples of how RNA-seq technology has revolutionised research in the field of diabetes and obesity research. Hopefully, the rapid development of such techniques will allow deeper discovery into gene expression in the context of diabetes and obesity in future studies.

3.1.6 Aim and objectives

In this chapter, the gene expression of candidate LC-FFA transport proteins identified within chapter 2 is explored using pre-published bulk RNA-seq data. The evidence gathered in the scoping review of this thesis supports a role for CD36 and the FABP, ACSL and CAV family members, along with TBC1D1 and TBC1D4, in LC-FFA uptake in mammalian cells. Therefore, it was hypothesised here that these candidate LC-FFA transport proteins would be highly expressed at the transcriptional level in pancreatic β-cells. The aims and objectives of this chapter were:

Aim: To characterise the gene expression of candidate membrane-associated LC-FFA transport proteins in human and rodent pancreatic β-cells as well as in various ex-vivo, metabolically active human cell types.

Objectives:

1. To analyse the gene expression of candidate membrane-associated LC-FFA transport proteins in pancreatic β-cells. Briefly, this work involved:

a. Characterising the gene expression of candidate LC-FFA transport proteins in the immortal human-derived EndoC-βH1 pancreatic β-cell line.
b. Comparing candidate LC-FFA transporter expression in the EndoC-βH1 cell line in relation to that of ex-vivo human islets
c. Comparing candidate LC-FFA transporter expression in pancreatic β-cells with respect to that of various other ex-vivo mammalian cell types
d. Identifying the gene expression of candidate LC-FFA transport proteins in the rodent-derived INS-1 pancreatic β-cell line

In summary, this will enable us to 1) identify whether the human-derived EndoC-βH1 cell line is a physiologically relevant model to study LC-FFA uptake in human β-cells, 2) compare candidate transport gene expression between different human tissue types and 3) obtain an overview of candidate LC-FFA transporter expression in the rodent INS-1 cell line.

3.2 Methods

3.2.1 Pre-published data for ex-vivo human tissue and the human-derived EndoC-βH1 cell line

Published counts data for human adipocytes, hepatocytes, pancreatic islets and the EndoC-βH1 cell line analysed within this study were kindly pre-processed by Dr Ildem Akerman. Human adipocyte data was acquired from the published work of Fagerberg et al. (348) [ArrayExpress accession: E-MTAB-1733] and Chhibber et al. (209) [GEO accession: GSE70503]. Human hepatocytes data was obtained from the published work of Fagerberg et al. (348) [ArrayExpress accession: E-MTAB-1733] and Chhibber et al. (209) [GEO accession: GSE70503]. Human islets data was obtained from the published work of Colli et al. (349) [GEO accession: GSE133219] and Marselli et al. (350) [GEO accession: GSE159984]. Data for the EndoC-βH1 cell line was acquired from the published work of Colli et al. (349) [GEO accession: GSE148058] and Diedsheim et al. (343) [GEO accession: GSE103383].

3.2.1.2 Experimental considerations for pre-published data obtained from ex-vivo human tissue and the human-derived EndoC-βH1 cell line

As outlined in section 3.1.3, it was essential that RNA-seq experiments analysed within this study considered the experimental methods used within each study, in order to obtain high quality data and to maximise reproducibility. Therefore, within this study, only RNA-seq data with paired-end sequencing, a high number of technical replicates (read depth), the same RNA-seq method (bulk RNA-seq) and studies that reported a high RNA integrity number was analysed (Table 3.1). Further, we aimed to analyse RNA-seq data with a high number of biological replicates; in this study, any further analysis to establish candidate LC-FFA transporter expression was conducted using RNA-seq data from a total of 33 human adipose tissue samples, 30 human liver tissue samples, 56 human pancreatic islet samples and 47 EndoC-βH1 samples.

Table 3.1 Experimental considerations for data obtained from ex-vivo human tissue and the human-derived EndoC-βH1 cell line. RNA-seq: RNA-sequencing; PGRN: The Pharmacogenomics Global Research Network; bp: base pairs. Data presented in this table was compiled in collaboration with Dr Patricia Thomas.

Publication	**Cell type**	**Obtained from**	**Sequencing platform**	**RNA integrity number (RIN)**	**Single vs. Paired end sequencing**	**RNA-seq method**	**Read depth**	**Read length**
Fagerberg et al. (348)	Adipocytes	The Uppsala Biobank	Illumina HiSeq 2000 and 2500 machines	≥7.5	Paired	Bulk	45–171 million	100bp
	Hepatocytes	The Uppsala Biobank	Illumina HiSeq 2000 and 2500 machines	≥7.5	Paired	Bulk	45–171 million	100bp
Chhibber et al. (209)	Adipocytes	The Pharmacogenomics and Risk of Cardiovascular Disease (PGRN)	Illumina HiSeq 2000	≥6.5	Paired	Bulk	18 million	100bp
	Hepatocytes	The Pharmacogenomics of Anticancer Agents Research in Children (PGRN)	Illumina HiSeq 2000	≥6.5	Paired	Bulk	18 million	100bp

Marselli et al.* *(350)	Pancreatic islets	The University of Pisa	Illumina Genome Analyzer II	≥7.5	Paired	Bulk	170 million	100bp
Colli et al.* *(349)	Pancreatic islets	The University of Paris	Illumina HiSeq 2500	>9	Paired	Bulk	>200 million	Not stated
	EndoC-βH1 cell line	Scharfmann et al.	Illumina HiSeq 2500	>9	Paired	Bulk	>200 million	Not stated
Diedisheim et al.* *(343)	EndoC-βH1 cell line	Scharfmann et al.	Illumina NextSeq 500	Evaluated but no number given	Paired	Bulk	Not stated	75bp

3.2.2 Pre-published data and experimental considerations for the rat-derived INS-1 cell line

In this study, data for the analysis of the rat-derived INS-1 cell line was obtained from the published work of Kong et al. (351) [GEO accession: GSE124833]. Due to the lack of available RNA-seq data for the INS-1 cell line, subsequent evaluation of candidate LC-FFA transporter gene expression was achieved using data from a total of 3 INS-1 samples in this study. It is acknowledged that this small sample size is a limitation in this study. As detailed, bulk RNA-seq was performed, and sequencing was performed on an Illumina HiSeq 2500. RNA integrity was determined but no value was provided and read depth was not stated. Raw reads were downloaded from SRA explorer, using the accession number provided [SRA accession: SRP176764].

3.2.2.1 Analysing raw sequencing data for the INS-1 cell line using FastQC

Basic quality control (QC) metrics were visualised using the *FastQC* software version 0.11.9 (352), using the Linux operating system. This software provides a modular set of analyses for raw high-throughput sequencing data (i.e., data obtained from NGS technologies). To examine the raw RNA-seq data, several important metrics were supplied by *FastQC*, including Phred quality scores, per base sequence content, per sequence GC content, and sequence duplication levels.

3.2.2.2 Phred quality scores

Phred quality scores are used to assess the base quality in DNA sequencing. One of the principal *FastQC* modules to consider is the "per base sequence quality". Figure 3.2 illustrates a FastQC 'per base sequence quality' plot for read 2 of sample 3 the INS-1 data. This plot gives an overview of the distribution of quality values throughout all bases at each position in the read. To provide an estimate of base calling accuracy, a *Phred* quality score (Q) is assigned to each base called (Table 3.2).

Table 3.2 Phred quality Scores and base calling accuracy

***Phred* Quality Score**	**Probability of incorrect base call**
Q10	1 in 10
Q20	1 in 100
Q30	1 in 1000
Q40	1 in 10,000

According to the Illumina sequencing pipeline (353), Q30 is considered the standard for quality in NGS, as nearly all reads with this score will be perfect, with no errors or ambiguities. A score of Q20 or above is thought to be acceptable (352). In this module, the most common explanation for warnings and failures is that the quality of the calls degrades as the run progresses (352). An example of the distribution of *Phred* scores obtained for read 2 of sample 3 of the INS-1 data is shown in Figure 3.3. The plot displays a peak at around Q39, indicating that most reads are of very high quality.

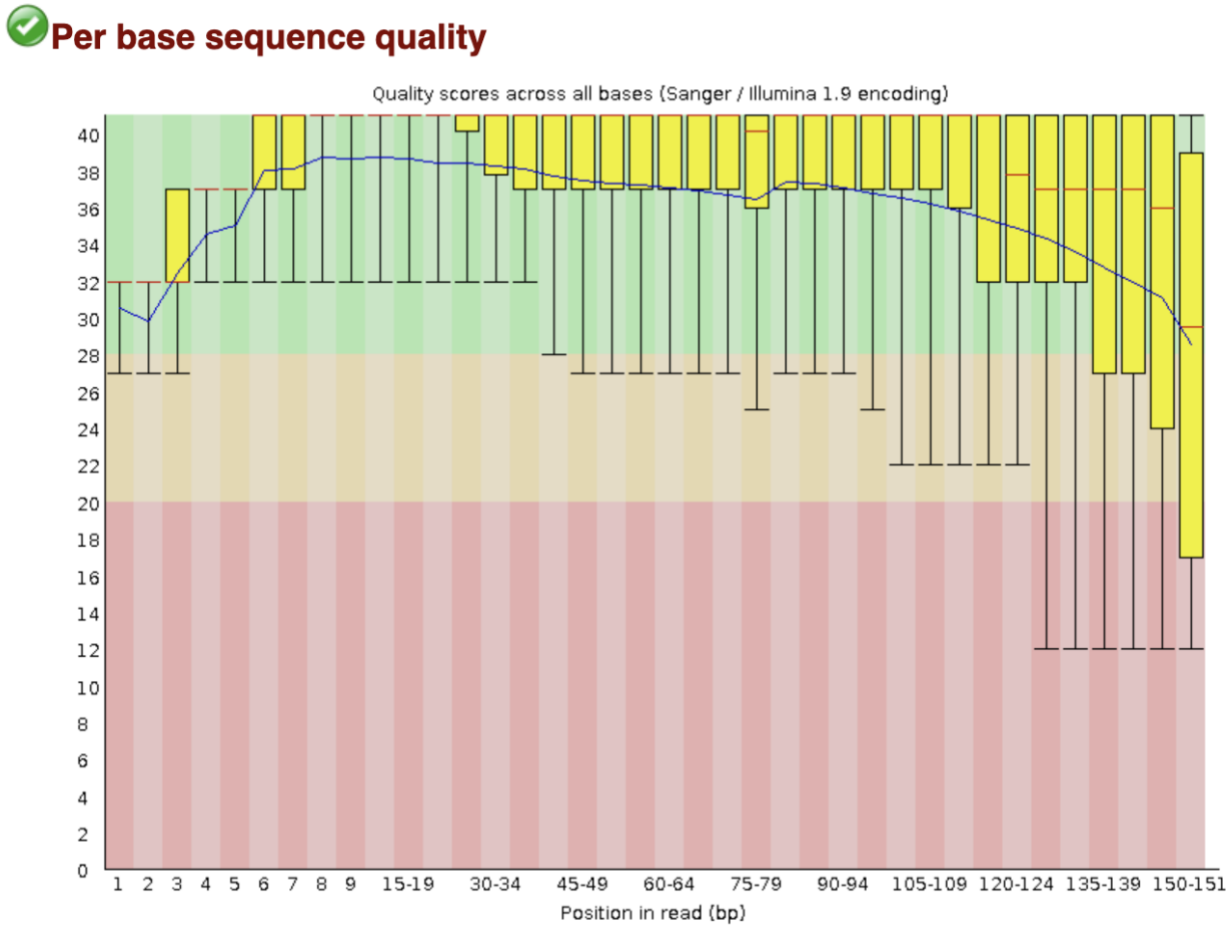

Figure 3.2 Example of the 'per sequence quality' output provided by FastQC. This plot was taken from read 2, sample 3 of the INS-1 data. The x-axis shows the position in the read. The y-axis indicates the Phred score. The yellow boxes illustrate the inter-quartile range (25-75%), the red line in the centre of each box represents the median value, the upper and lower whiskers depict the 10% and 90% points, respectively, and the blue line portrays the mean quality of the reads.

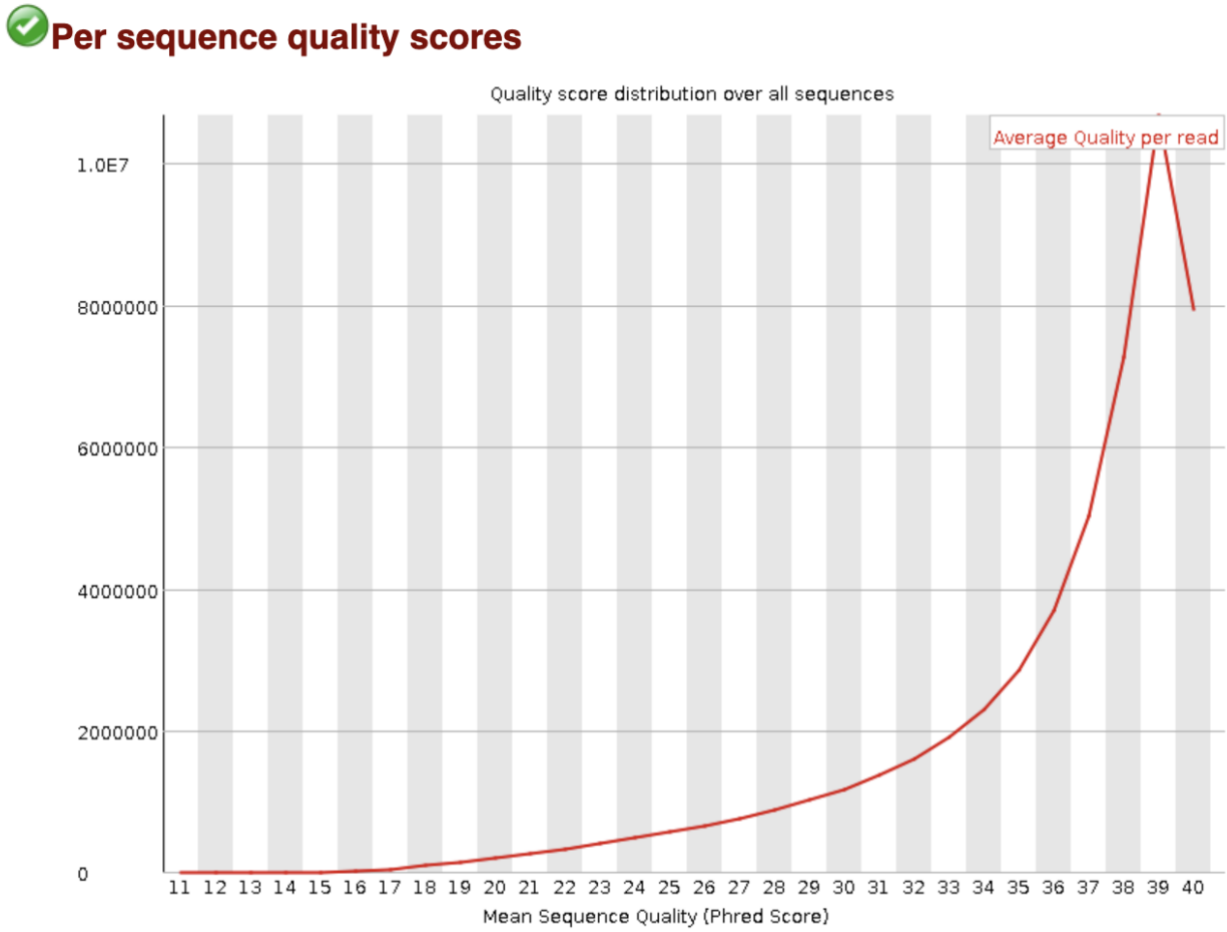

Figure 3.3 Example of a 'per sequence quality' output provided by FastQC. This plot was taken from read 2, sample 3 of the INS-1 data. The x-axis shows the mean Phred Score. The y-axis displays the number of reads.

3.2.2.3 Per base sequence content and per sequence GC content

The 'per base sequence content' plot (Figure 3.4) displays the four normal DNA bases (A, C, G and T) and their position in the read. Preferably, there should be little to no variation between each base of a sequence run, such that the lines (blue, red, green, and black) would be expected to run in parallel with one another. However, it should be noted that RNA-seq data generated by Illumina technology usually produces variation of the base call at the start of the read due to the use of hexamer priming (354). Hexamer primers are used to prime the reverse transcription of RNA into double stranded

complementary DNA (cDNA) (354). However, 'random' hexamer priming can introduce bias in nucleotide composition at the beginning of the read, as hexamer primers anneal better to sequences at the 5'-end of the read (354). Therefore, to prevent the variation between bases having an impact on downstream analysis, this effect is removed following trimming of the sequences (see section 3.2.2.5).

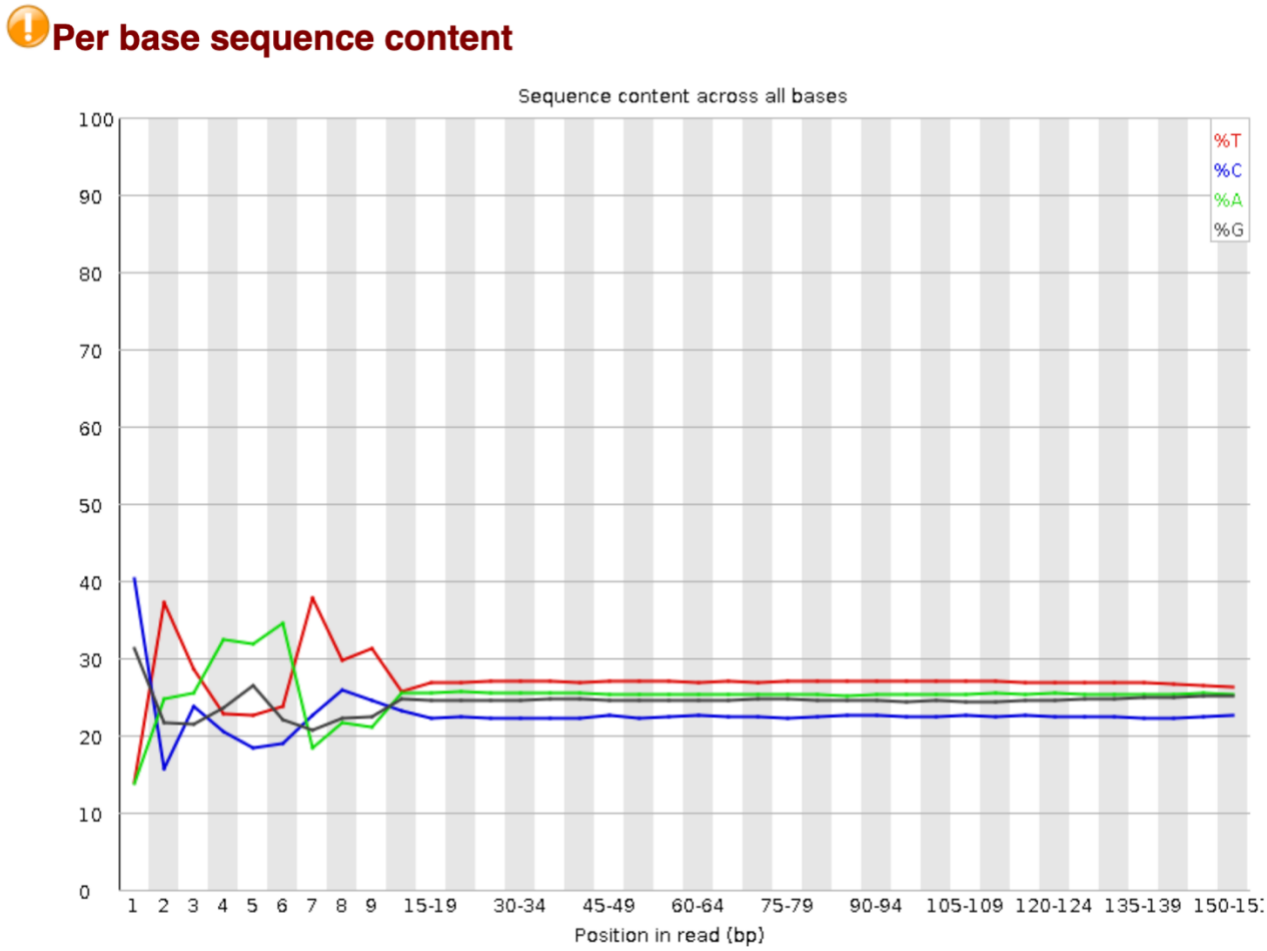

Figure 3.4 Example of a 'per base sequence content' output provided by FastQC. The plot shown was taken from read 2 of sample 3 from the INS-1 data. The x-axis indicates the position in the read. The y-axis displays the base call content.

The ‘per sequence GC content’ plot (Figure 3.5) illustrates the GC content throughout the entire length of the sequence in the file. In a normal sample, the data (red line) is expected to roughly follow a normal distribution (blue line). An unusually shaped distribution, e.g., if the curve is shifted to the right, is usually an indication of a contaminated RNA library. This might include a specific contaminant, such as adapter dimers, or RNA contamination from another species (352). Most of the samples analysed in this study roughly followed the theoretical normal distribution.

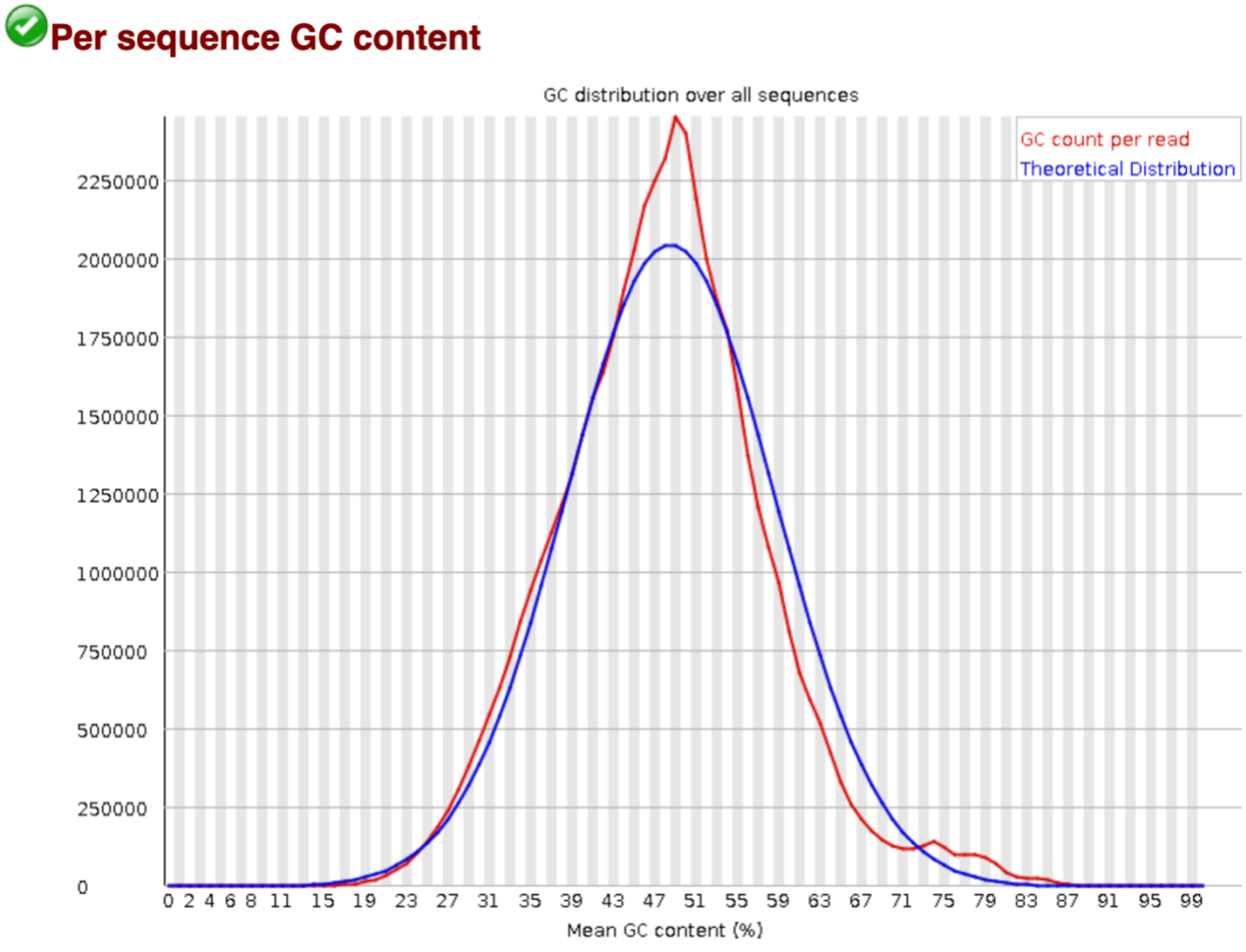

Figure 3.5 Example of a ‘per sequence GC’ output provided by FastQC. A density plot is shown for read 2 of sample 3 from the INS-1 data. The x-axis displays the mean GC content (%). The y-axis shows the number of reads. The red line illustrates the GC count per read, and the blue line shows the theoretical distribution.

3.2.2.4 Sequence duplication levels

The ‘sequence duplication levels’ plot (Figure 3.6) displays the proportion of sequences with different degrees of duplication for all sequences in a read. The blue line illustrates how duplication levels are distributed in the full sequence set, while the red line shows the proportion of sequences that are de-duplicated which originate from different duplication levels in the read. In a diverse RNA library (i.e., a library that exhibits uniform genome coverage), most sequences should only appear once in the final read (352). A high level of duplication usually signifies enrichment of mRNA (e.g., due to polymerase chain reaction (PCR) over-amplification) (352). However, genes that are highly expressed in an RNA-seq experiment will have a very high level of coverage, so a higher duplication level is expected (355).

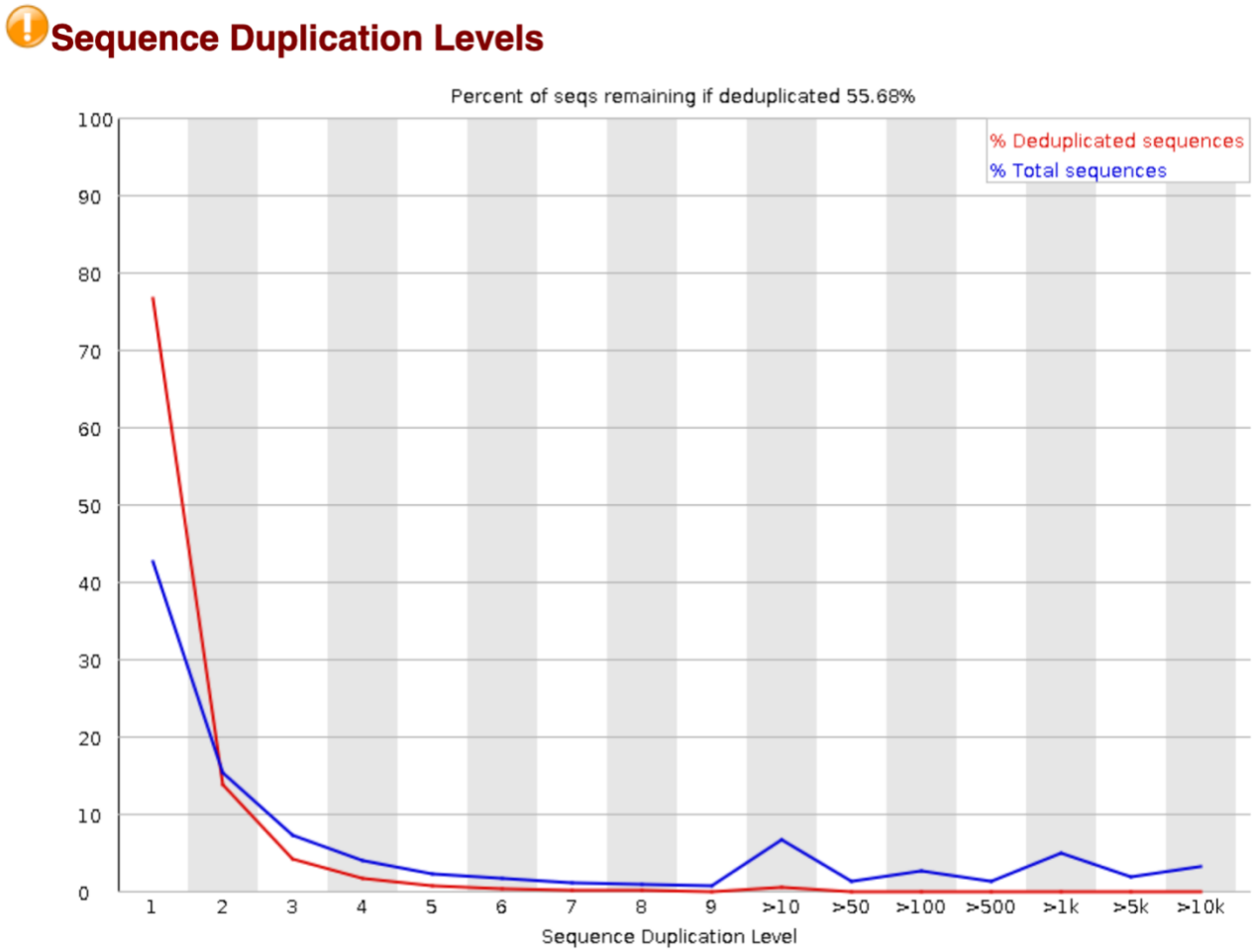

Figure 3.6 Example of a 'sequence duplication levels' output provided by FastQC. The plot shown is for read 2 of sample 3 from the INS-1 data. The x-axis displays the different duplication level bins. The y-axis shows the percentage of duplicated reads. The blue line represents the distribution of duplication levels for the entire sequence set. The red line depicts the distribution of deduplicated sequences.

3.2.2.5 Trimming of raw sequencing data using Trimmomatic

To pre-process the raw reads, *Trimmomatic* version 0.39 (356) was utilised within the Linux operating system. *Trimmomatic* uses a set of algorithms to trim and filter poor-quality reads based on quality metrics, in addition to removing any adapter sequences (356). Table 3.3 displays the commands used in *Trimmomatic* in this study.

Table 3.3 Commands used to pre-process the raw RNA-seq data in *Trimmomatic.*

Command	Description
ILLUMINACLIP	Remove adapter and other illumina-specific sequences from each read
LEADING	Remove bases from the beginning of the read, if beneath a threshold quality
TRAILING	Remove bases from the end of the read, if beneath a threshold quality
SLIDINGWINDOW	Execute sliding window trimming, which involves starting at the 5' end and clipping the read when the average quality within the window declines below threshold
MINLEN	Exclude the entire read if it is less than a defined length

Paired-end reads were processed in *Trimmomatic* (356), which involved the input of 2 files (forward and reverse reads) from each sample and 4 output files (paired forward, paired reverse, unpaired forward, unpaired reverse). 'Paired' output files contained reads that survived the processing, where both files survived, whereas the corresponding 'unpaired' output files contained orphan reads, where one or neither of the reads survived the processing. The 'unpaired' files were discarded and the 'paired' output files were used for subsequent analysis. Quality metrics for the trimmed 'paired' output files for each sample were then re-analysed in *FastQC* and compared with the *FastQC* analysis of the raw reads to confirm that reads were of high-quality.

3.2.2.6 Pseudoalignment of reads to the rat reference transcriptome and quantifying gene expression

To quantify gene expression levels, pseudoalignment was carried out on pre-processed reads using *Kallisto* version 0.46.1 (357). Unlike normal read alignment, which involves identifying where in the genome each sequence is from by mapping reads to a reference genome (i.e., how the nucleotides in the read align with those in the target sequence) (358), *Kallisto* uses pseudoalignment (357), which focuses on detecting transcripts from which the reads might have originated. Pseudoalignment involves processing a transcriptome file (in this case, the rat transcriptome) to generate a 'transcriptome index'. In this study, the rat transcriptome index version 96 was downloaded from the *Kallisto* transcriptome indices site (357). Transcripts were then quantified and transformed into one counts file per sample, in transcripts per million (TPM), using *Kallisto* (357). TPM is a method of normalisation for RNA-seq, which estimates the proportion of transcripts in the sample made up by a given gene or isoform and multiplies this by 10^6 (359). Normalisation using TPM is often used to enable comparisons to be drawn between RNA transcript expression within a single sample (359). To achieve pseudoalignment of the reads and quantification of the transcripts, the following *Kallisto* commands were used:

- **Obtaining the transcriptome index**

`wget` - This command is used to download the transcriptome index.

- **Quantifying gene expression**

`Quant` – To run the quantification algorithm.

`-i` - Filename for the *Kallisto* index to be used for pseudoalignment.

3.2.2.7 Selecting transcripts for analysis of candidate LC-FFA transporter expression

Transcripts for candidate LC-FFA transporters were selected from Ensembl genome browser version 107 (360) for inclusion in plots to visualise their expression (see section 3.2.5). Initially, transcripts were selected that were annotated as the 'principal isoform', 'most highly expressed' or 'most conserved' version of the gene, in accordance with the recommendations by Morales et al. (361). However, transcripts with these labels were not always identified in the counts data generated, whereas 'alternative' isoforms were present. Moreover, transcripts that were labelled as 'alternative' isoforms of the gene were occasionally found to be expressed where principal isoforms were not. Therefore, transcripts were ultimately selected based on their expression in the counts table (i.e., any transcript for a particular gene that was expressed was included). For genes that showed no expression for any of their transcripts, a transcript was included at random.

3.2.3 Data normalisation and gene distribution

Prior to differential expression analysis and data visualisation, separate counts files (i.e., those generated from different samples) produced by *HTSeq* (for the human data) (362) or *Kallisto* (for the rat INS-1 data) (357) were merged according to cell type in *RStudio*, to produce one data frame for each cell type. Data normalisation of *HTSeq* counts data was kindly carried out by Dr Patricia Thomas using the *rlog* function in *DESeq2* version 4.1.1 (363), which converts the counts data to the log2

scale. Normalised counts files were used for any subsequent analysis. To examine gene expression values and their frequency, the distribution of the gene counts was assessed (Appendix B - Supplementary Figure 1). Both human and rodent counts data showed a negative binomial distribution, which provides a good approximation for data where the mean is less than the variance. A negative binomial distribution was particularly useful for differential expression analysis (section 3.2.4), which requires the data to fit a negative binomial distribution to prevent overdispersion (i.e., where the variance of the response is greater than assumed by the model, resulting in greater chance of rejecting the null hypothesis when it is true (type-I error)) (364).

3.2.4 Differential expression analysis

To identify whether the genes for our candidate LC-FFA transporters were differentially expressed in ex-vivo pancreatic islets compared to other metabolically active human tissue types (i.e., hepatocytes and adipocytes) and the immortal EndoC- βH1 cell line, a differential expression analysis was kindly performed by Dr Patricia Thomas using the *DESeq2* package (363) in *RStudio* version 4.1.1. This involved generating a *DESeqDataSet* object, using the *DESeqDataSetFromMatrix* function, which is used for read counts matrices prepared from an alternative source. The data was then pre-filtered to remove genes with a total of <10 reads. Prefiltering is useful to improve data visualisation, as genes with no information for differential gene expression are not plotted. Then, the reference gene expression levels to compare against was specified using the *factor* function. Gene expression was compared in islets vs. EndoC- βH1, islets vs. adipocytes and islets vs. hepatocytes. Differential gene expression analysis was carried out using the *DESeq* function, which assumes a negative binomial distribution (of counts for a particular gene across all samples) to model RNA-seq counts using the following equation:

$$K_{ij} \sim NB(s_{ij}q_{ij}, \alpha_i)$$

where counts Kij indicates the gene (i) and the sample (j), which are modelled using a fitted mean ($s_{ij}q_{ij}$) which signifies the mean acquired as normalised counts and scaled by a normalisation factor, and a gene-specific dispersion parameter (α_i) which measures the extent that a sample fluctuates around the mean value. The coefficients then give an estimate of the log2 fold changes (LFC) for each gene in each sample group. Next, a null hypothesis was generated for each gene, such that LFC=0, where there was "no differential expression between groups". For hypothesis testing, a Wald statistical test was performed. The Wald test extracts the LFC and divides it by the standard error to form a z-statistic. The z-statistic is then compared to a normal distribution and a p-value is calculated. The p-value reports the probability that the data occurred under the null hypothesis (i.e., the likelihood that the z-statistic is what the observed statistic would be if selected randomly). Differentially expressed genes had p-value<0.05. However, due to the large quantity of genes tested in this analysis, there is a greater probability of false positive results, owing to the "multiple testing problem". To correct for the multiple testing problem, we also used a Bonferroni correction, to adjust the p-values for analysis. In this thesis, adjusted p-values were used to determine statistically significant differential gene expression (adjusted p-value<0.05).

3.2.5 Data visualisation

All data visualisation was conducted using the *R statistical language* version 4.1.1. Visualisation of candidate LC-FFA transporter gene expression was performed and the expression for each gene family (e.g., the FATP family) was summarised graphically, using box plots generated using the *ggplot2* data visualisation package (365). Histograms were generated using the hist () function to show gene distribution. MA plots were generated using the *DESeq2* package to illustrate differential gene expression. Heatmaps were produced by Dr Patricia Thomas using the *pheatmap* package to display hierarchical clustering of human cell types (Appendix B – Supplementary Figure 2). As

counts files were generated according to Ensembl gene ID, gene symbols for each gene of interest were determined using the Ensembl genome browser with the corresponding gene ID.

3.3 Results

3.3.1 The gene expression profile of candidate LC-FFA transporters in ex-vivo adipocytes, hepatocytes, and pancreatic islets, and the immortal EndoC-βH1 cell line

To identify whether the candidate LC-FFA transporters identified in chapter 2 (and their isoforms) are cell type-specific, gene expression profiles were constructed for each candidate LC-FFA transporter family (ACSL (Figure 3.7), CAV (Figure 3.8), FATP (Figure 3.9), FABP (Figure 3.10), TBC1D1/TBC1D4 (Figure 3.11) and CD36 (Figure 3.12)) in ex-vivo adipocytes, hepatocytes, pancreatic islets and the immortal EndoC-βH1 cell line. A heat map was also constructed to produce an overview of similarities and differences regarding candidate LC-FFA transporter expression between pancreatic islets, adipocytes, hepatocytes and the EndoC-βH1 cell line (Appendix B – Supplementary Figure 2).

In adipocytes and hepatocytes, ACSL1 exhibited very high expression, while ACSL3, ACSL4 and ACSL5 showed moderate expression and ACSL6 displayed very low expression (Figure 3.7A and 3.7B). In ex-vivo pancreatic islets and the immortal EndoC-βH1 cell line (Figure 3.7C and 3.7D), ACSL1, 3 and 4 showed high expression, whereas ACSL5 and 6 showed low expression. In adipocytes, CAV1 and CAV2 were highly expressed and CAV3 was not expressed (Figure 3.8A). In hepatocytes, there was low expression of CAV1 and CAV2, while CAV3 showed no expression at all (Figure 3.8B). In both pancreatic islets and the EndoC-βH1 cell line, there was low expression of CAV1 and no expression of CAV3 (Figure 3.8C and 3.8D). However, there was moderate expression of CAV2 in pancreatic islets (Figure 3.8C) whereas there was low expression in EndoC-βH1 (Figure 3.8D). In adipocytes, there was a low expression of all FATP family members (Figure 3.9A). In hepatocytes, FATP2 and FATP5 were highly expressed, but the other FATP family members showed

little to no expression (Figure 3.9B). In both pancreatic islets and the EndoC-βH1, FATP4 was identified as highly expressed, while other FATP isoforms exhibited moderate expression (Figure 3.9C and 3.9D). In adipocytes, FABP4 was found to be highly expressed, with little to no expression of the other FABP family members (Figure 3.10A). In hepatocytes, FABP1 was highly expressed, with little to no expression of the other FABP family members (Figure 3.10B). There was little to no expression of any of the FABP family members in both pancreatic islets and the EndoC-βH1 cell line (Figure 3.10C and 3.10D). TBC1D1 and TBC1D4 were found to be moderately expressed in adipocytes and hepatocytes (Figure 3.11A and 3.11B). However, TBC1D1 and TBC1D4 were highly expressed in pancreatic islets and the EndoC-βH1 cell line (Figure 3.11C and 3.11D). The expression of CD36 was found to be extremely high in adipocytes (Figure 3.12). However, there was moderate expression of CD36 in hepatocytes, pancreatic islets and the EndoC-βH1 cell line (Figure 3.12).

Overall, these results illustrate that ex-vivo islets and the immortal EndoC-βH1 cell line exhibit a similar pattern of gene expression for all candidate LC-FFA transporters analysed. In contrast, the expression pattern of candidate LC-FFA transporters is largely different in ex-vivo adipocytes and hepatocytes when compared to pancreatic islets. Highly expressed genes in both islets and EndoC-βH1 include ACSL1, ACSL3, ACSL4, FATP4, TBC1D1 and TBC1D4.

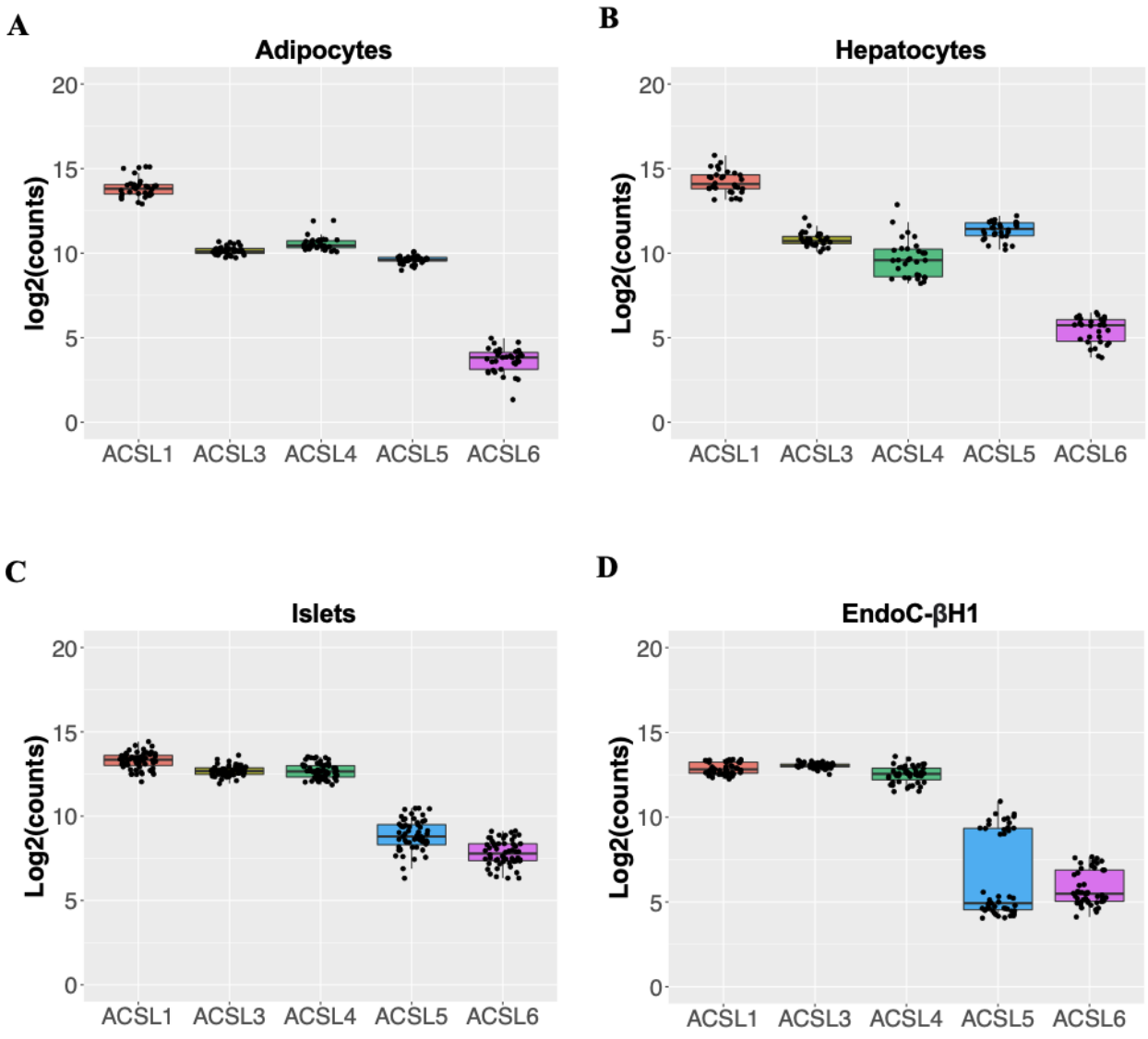

Figure 3.7 The expression profile of the long-chain acyl-CoA synthetase (ACSL) family in human adipocytes, hepatocytes, islets and EndoC-βH1 cells. Distribution of transcript expression levels of ACSL family members in adipocytes (A), hepatocytes (B), islets (C) and EndoC-βH1 cells (D), obtained from combined published bulk RNA-sequencing (RNA-seq) datasets (209, 343, 348, 349, 350). Each data point shows the expression level of each individual sample. This included a total of 33 human adipose tissue, 30 human liver tissue, 56 human pancreatic islets from non-diabetic donors and 47 EndoC-βH1 samples. The central line of each box and whisker plot represents the median gene expression level, the whiskers represent the minimum and maximum gene expression level, and the ends of the boxes represent the upper and lower quartiles. Data was normalised to the log2 scale by Dr Patricia Thomas using the DESeq2 package.

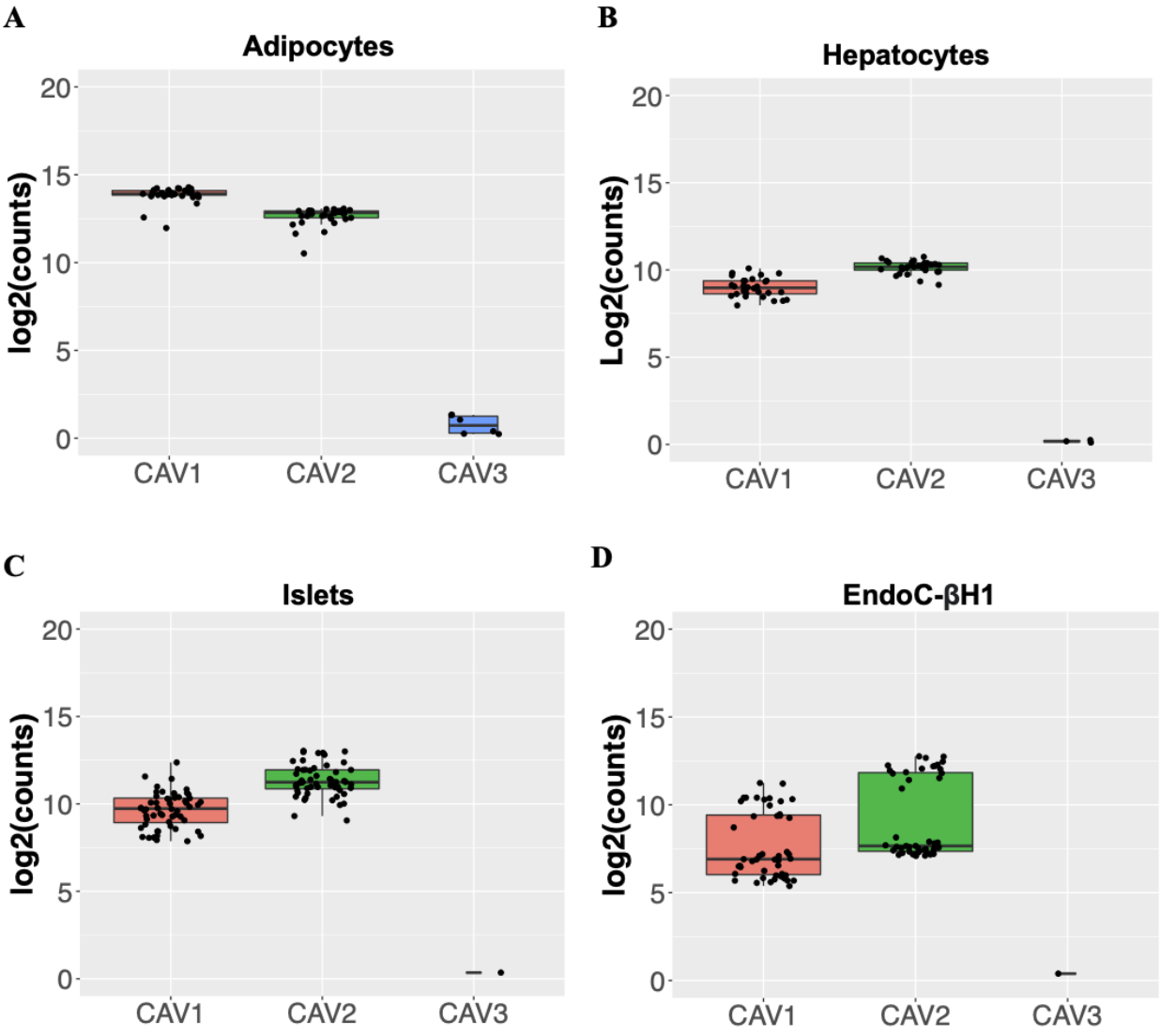

Figure 3.8 The expression profile of the caveolin (CAV) family in human adipocytes, hepatocytes, islets and EndoC-βH1 cells. Box and whisker plots display the distribution of transcript expression levels of CAV family members in adipocytes (A), hepatocytes (B), islets (C) and EndoC-βH1 cells (D), obtained from combined published bulk RNA-sequencing (RNA-seq) datasets (209, 343, 348, 349, 350). Each data point shows the expression level of each individual sample. This included a total of 33 human adipose tissue, 30 human liver tissue, 56 human pancreatic islets from non-diabetic donors and 47 EndoC-βH1 samples. The central line of each box and whisker plot represents the median gene expression level, the whiskers represent the minimum and maximum gene expression level, and the ends of the boxes represent the upper and lower quartiles. Data was normalised to the log2 scale by Dr Patricia Thomas using the DESeq2 package.

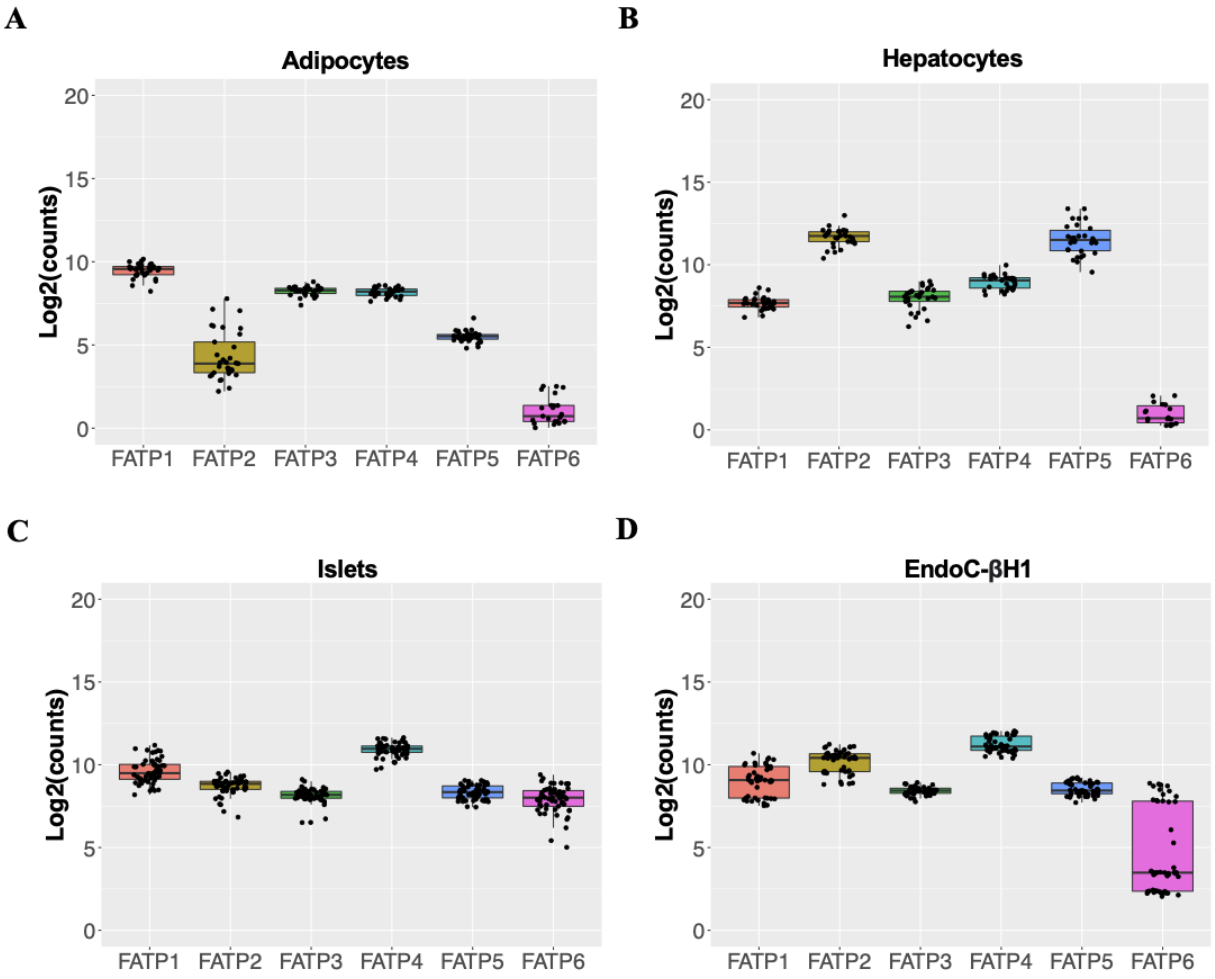

Figure 3.9 The expression profile of the fatty acid transport protein (FATP) family in human adipocytes, hepatocytes, islets and EndoC-βH1 cells. Box and whisker plots display the distribution of transcript expression levels of FATP family members in adipocytes (A), hepatocytes (B), islets (C) and EndoC-βH1 cells (D), obtained from combined published bulk RNA-sequencing (RNA-seq) datasets (209, 343, 348, 349, 350). Each data point shows the expression level of each individual sample. This included a total of 33 human adipose tissue, 30 human liver tissue, 56 human pancreatic islets from non-diabetic donors and 47 EndoC-βH1 samples. The central line of each box and whisker plot represents the median gene expression level, the whiskers represent the minimum and maximum gene expression level, and the ends of the boxes represent the upper and lower quartiles. Data was normalised to the log2 scale by Dr Patricia Thomas using the DESeq2 package.

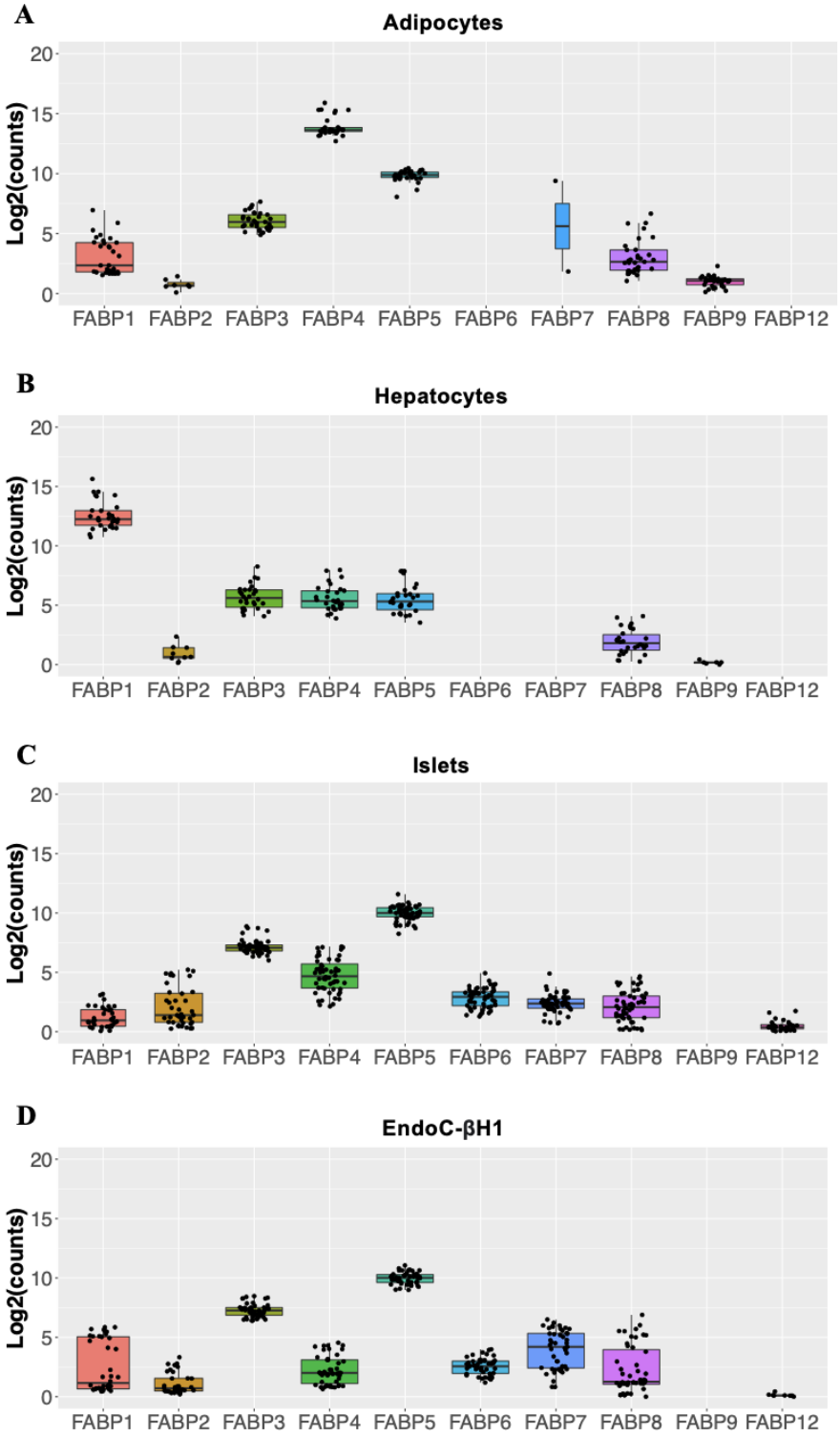

Figure 3.10 The expression profile of the fatty acid binding protein (FABP) family in human adipocytes, hepatocytes, islets and EndoC-βH1 cells. Box and whisker plots display the distribution of transcript expression levels of FABP family members in adipocytes (A), hepatocytes (B), islets (C) and EndoC-βH1 cells (D), obtained from combined published bulk RNA-sequencing (RNA-seq) datasets (209, 343, 348, 349, 350). Each data point shows the expression level of each individual sample. This included a total of 33 human adipose tissue, 30 human liver tissue, 56 human pancreatic

islets from non-diabetic donors and 47 EndoC-βH1 samples. The central line of each box and whisker plot represents the median gene expression level, the whiskers represent the minimum and maximum gene expression level, and the ends of the boxes represent the upper and lower quartiles. Data was normalised to the log2 scale by Dr Patricia Thomas using the DESeq2 package.

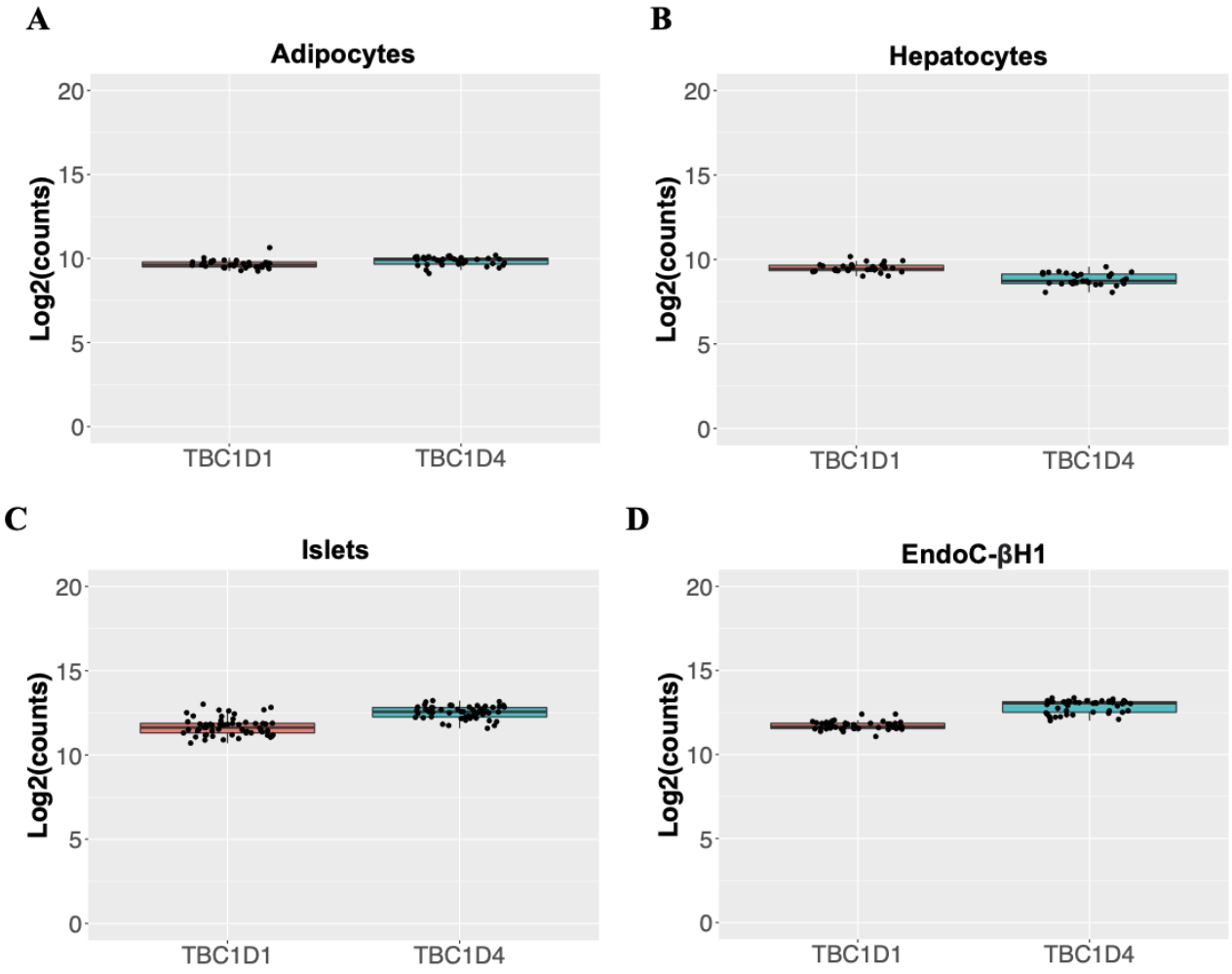

Figure 3.11 The expression profile of TBC1 Domain Family Member 1 (TBC1D1) and 4 (TBC1D4) in human adipocytes, hepatocytes, islets and EndoC-βH1 cells. Box and whisker plots display the distribution of transcript expression levels of ACSL family members in adipocytes (A), hepatocytes (B), islets (C) and EndoC-βH1 cells (D), obtained from combined published bulk RNA-sequencing (RNA-seq) datasets (209, 343, 348, 349, 350). Each data point shows the expression level of each individual sample. This included a total of 33 human adipose tissue, 30 human liver tissue, 56 human pancreatic islets from non-diabetic donors and 47 EndoC-βH1 samples. The central line of each box and whisker plot represents the median gene expression level, the whiskers represent the minimum and maximum gene expression level, and the ends of the boxes represent the upper and lower quartiles. Data was normalised to the log2 scale by Dr Patricia Thomas using the DESeq2 package.

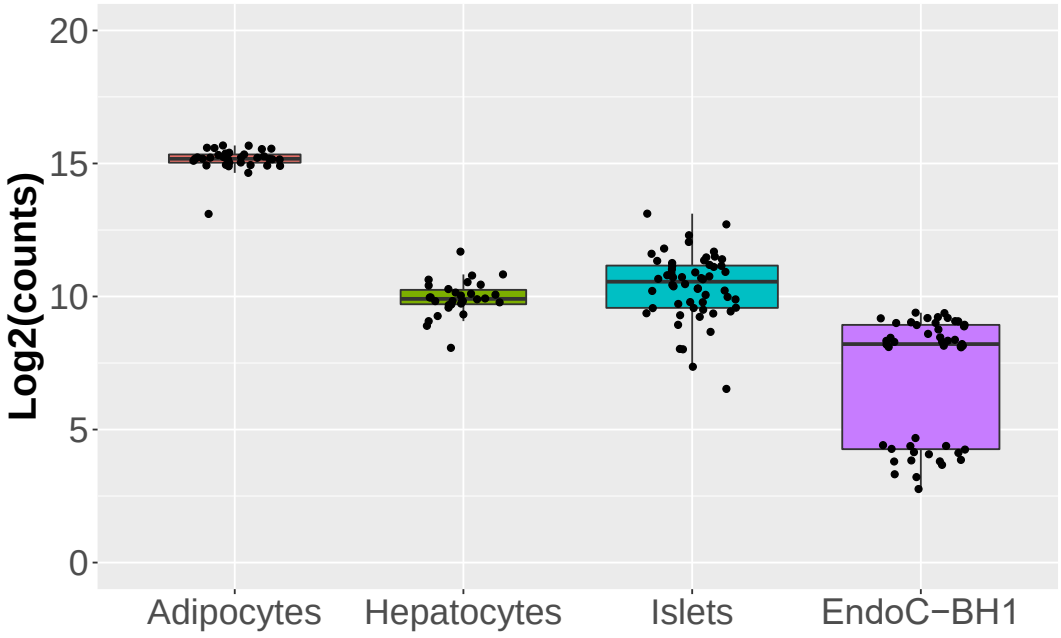

Figure 3.12 The expression profile of cluster of differentiation 36 (CD36) in human adipocytes, hepatocytes, islets and EndoC-βH1 cells. Box and whisker plots displaying the distribution of transcript expression levels of CD36 in adipocytes, hepatocytes, islets and EndoC-βH1 cells, obtained from combined published bulk RNA-sequencing (RNA-seq) datasets (209, 343, 348, 349, 350). Each data point shows the expression level of each individual sample. This included a total of 33 human adipose tissue, 30 human liver tissue, 56 human pancreatic islets from non-diabetic donors and 47 EndoC-βH1 samples. The central line represents the median gene expression level, the whiskers represent the minimum and maximum gene expression level, the ends of the boxes represent the upper and lower quartiles, and the points show the expression level of each individual sample. Data was normalised to the log2 scale by Dr Patricia Thomas using DESeq2 and represents a total of 33 human adipose tissue samples, 30 human liver tissue samples, 56 human pancreatic islet samples and 47 EndoC-βH1 samples.

3.3.2 Gene expression profile of candidate LC-FFA transporters in the INS-1 cell line

Constructing the gene expression profile of candidate LC-FFA transporters in the rat INS-1 cell line allows the identification of expressed genes. Here, several of the candidate LC-FFA transporters were found to be expressed at the RNA level in the immortal INS-1 pancreatic β-cell line (Figure 3.13)**.** ACSL1, 3 and 4, showed high expression, while ACSL5 showed low expression and ACSL6 was found not to be expressed (Figure 3.13A). Remarkably, no members of the CAV family showed expression in this cell line (Figure 3.13B). FATP1, 4 and 5 were expressed at a low level and all other members of the FATP family showed no expression (Figure 3.13C). Both TBC1D1 and TBC1D4 showed little to no expression (Figure 3.13D). No members of the FABP family were found to be expressed in this cell line (Figure 3.13E) and, interestingly, CD36 showed low expression (Figure 3.13F).

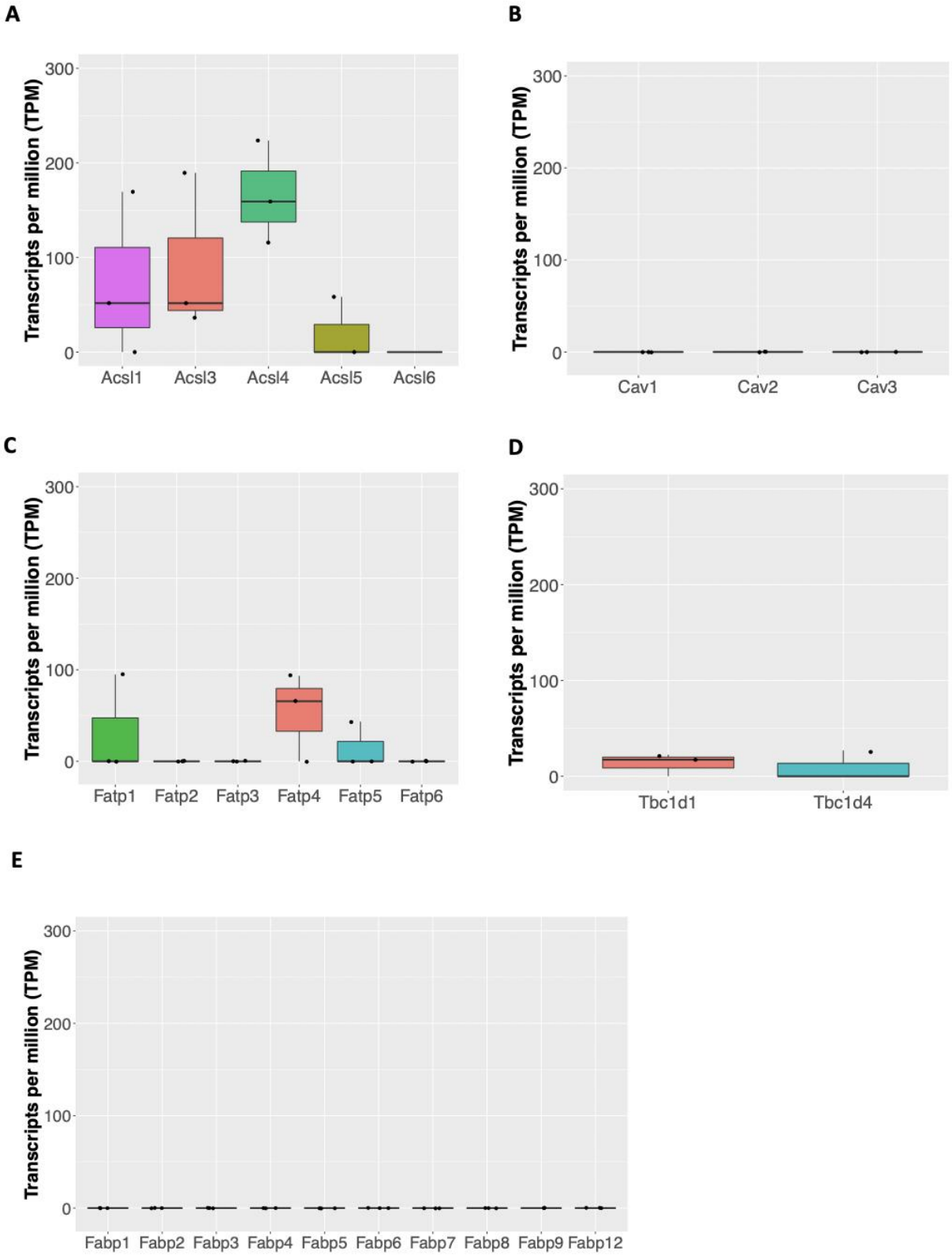
A
Transcripts per million (TPM)
300
200
100
0
Acsl1
Acsl3
Acsl4
Acsl5
Acsl6
B
Transcripts per million (TPM)
300
200
100
0
Cav1
Cav2
Cav3
C
Transcripts per million (TPM)
300
200
100
0
Fatp1
Fatp2
Fatp3
Fatp4
Fatp5
Fatp6
D
Transcripts per million (TPM)
300
200
100
0
Tbc1d1
Tbc1d4
E
Transcripts per million (TPM)
300
200
100
0
Fabp1
Fabp2
Fabp3
Fabp4
Fabp5
Fabp6
Fabp7
Fabp8
Fabp9
Fabp12

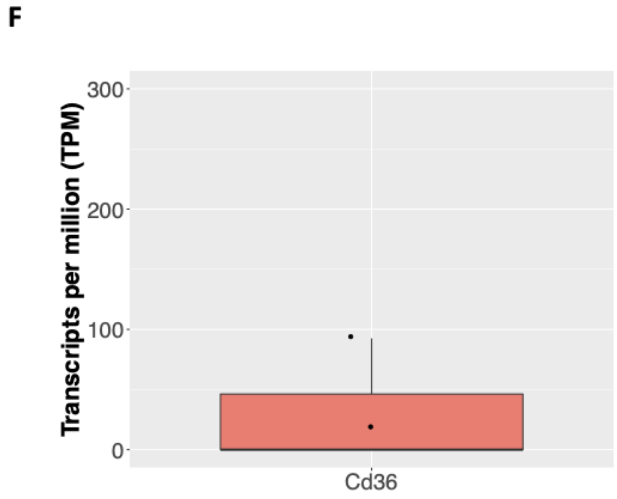

Figure 3.13 The expression profile of long-chain acyl-CoA synthetase (ACSL), caveolin (CAV), fatty acid binding protein (FABP) and fatty acid transport protein (FATP) family members, as well as TBC1 Domain Family Member 1 (TBC1D1) and 4 (TBC1D4), and cluster of differentiation 36 (CD36) in the INS-1 cell line. Box and whisker plots display the distribution of transcript expression levels of ACSL (A), CAV (B), FATP (C), TBC1D1 and TBC1D4 (D), FABP (E) and CD36 (F), obtained from a pre-published RNA-sequencing (RNA-seq) dataset (351). The central line represents the median gene expression level, the whiskers represent the minimum and maximum gene expression level, the ends of the boxes represent the upper and lower quartiles, and the points show the expression level of each individual sample. The x-axis shows the candidate LC-FFA transporter. The y-axis shows the level of gene expression in transcripts per million (TPM). Data was obtained from a total of 3 INS-1 samples.

3.3.3 Differentially expressed candidate LC-FFA transporter genes between islets vs. the immortal EndoC-βH1 cell line, ex-vivo adipocytes and hepatocytes

Differential expression analysis was conducted to validate EndoC-βH1 cells as a suitable model of human islets to study candidate LC-FFA transporters in future experimental work, by establishing which candidate LC-FFA transporter genes were significantly differentially expressed, as well as which genes displayed significantly greater or lower expression in EndoC-βH1 cells, adipocytes and hepatocytes when compared to pancreatic islets (Table 3.4). MA plots were generated for a visual representation of differentially expressed candidate LC-FFA transporters in human pancreatic islets

compared with the human-derived EndoC-βH1 cell line (Figure 3.14), as well as ex-vivo human adipocytes (Figure 3.15) and hepatocytes (Figure 3.16).

The expression pattern of candidate LC-FFA transporters was found to be most similar between human islets and the EndoC-βH1 cell line than human islets and adipocytes or human islets and hepatocytes. However, there was also a significant difference in expression between a selection of highly expressed candidate LC-FFA transporters in human islets and the EndoC-βH1 cell line, including ACSL1, ACSL3, FATP4 and TBC1D4 (all adjusted p-values<0.001) (Table 3.4). ACSL4 and TBC1D1 were not differentially expressed between human islets and EndoC-βH1 (adjusted p-values>0.05). Moreover, CD36 was not differentially expressed between human islets and EndoC-βH1 (adjusted p-value>0.05). Ultimately, it is determined here that differential gene expression analysis supports EndoC-βH1 cells as a suitable model of human islets to study several candidate transport proteins, including ACSL4, TBC1D1 and CD36.

Table 3.4 Significantly expressed candidate LC-FFA transporters in EndoC-βH1 cells, adipocytes and hepatocytes compared to pancreatic islets.

	Greater expression	**Lower expression**	**No significant difference**
EndoC-βH1	ACSL3, FATP2, FATP3, FATP4, FABP1, FABP7, FABP8 and TBC1D4	ACSL1, ACSL6, CAV1, CAV2, FATP1, FATP6, FABP2, FABP4 and FABP12	ACSL4, ACSL5, CAV3, FABP3, FABP5, FABP6, FABP9, FATP5, TBC1D1 and CD36
Adipocytes	ACSL1, ACSL4, ACSL5, CAV1, CAV2, CAV3, FATP1, FATP3, FABP1, FABP3, FABP4, FABP5, FABP8, FABP9, TBC1D1 and CD36	ACSL6, FATP2, FATP5, FATP6, FABP2 and FABP6	ACSL3, FABP4, FABP12 and TBC1D4
Hepatocytes	ACSL1, ACSL3, ACSL5, CAV1, CAV2, CAV3, FATP3, FATP4, FATP5, FABP3, FABP4, FABP8 and CD36	FATP6, FABP5, FABP6, FABP7 and TBC1D4	ACSL4, ACSL6, FABP1, FABP2, FABP9, FABP12, FATP1, FATP2 and TBC1D1

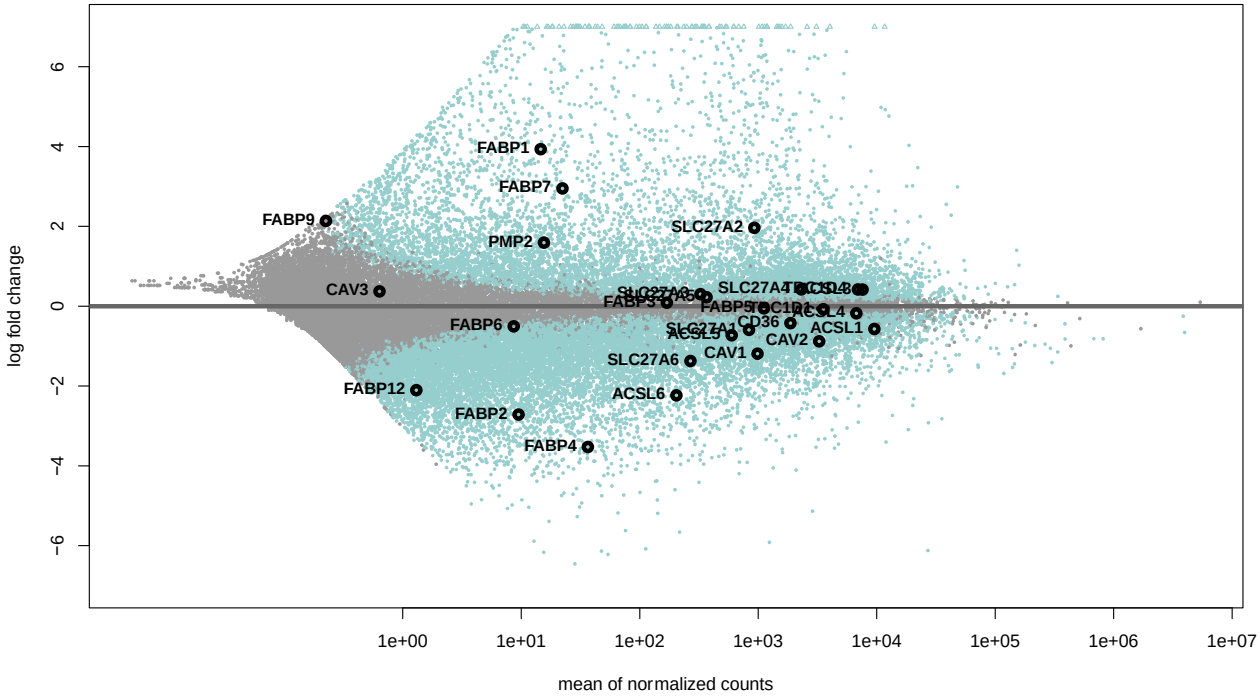

Figure 3.14 Comparison of candidate LC-FFA transporter gene expression in pancreatic islets vs the immortal EndoC-BH1 cell line. MA plot, where the x-axis shows the mean expression of normalised counts, representative of a total of 56 human pancreatic islet samples from non-diabetic donors and 47 EndoC-βH1 samples, and the y-axis represents the log fold change in expression. The grey circles represent genes with no significant difference in expression and blue circles represent genes that were significantly differentially expressed (adjusted p-values ≤ 0.05) Gene symbols were taken from the HUGO Gene Nomenclature Committee (HGNC); PMP2 = FABP8; SLC27A = FATP.

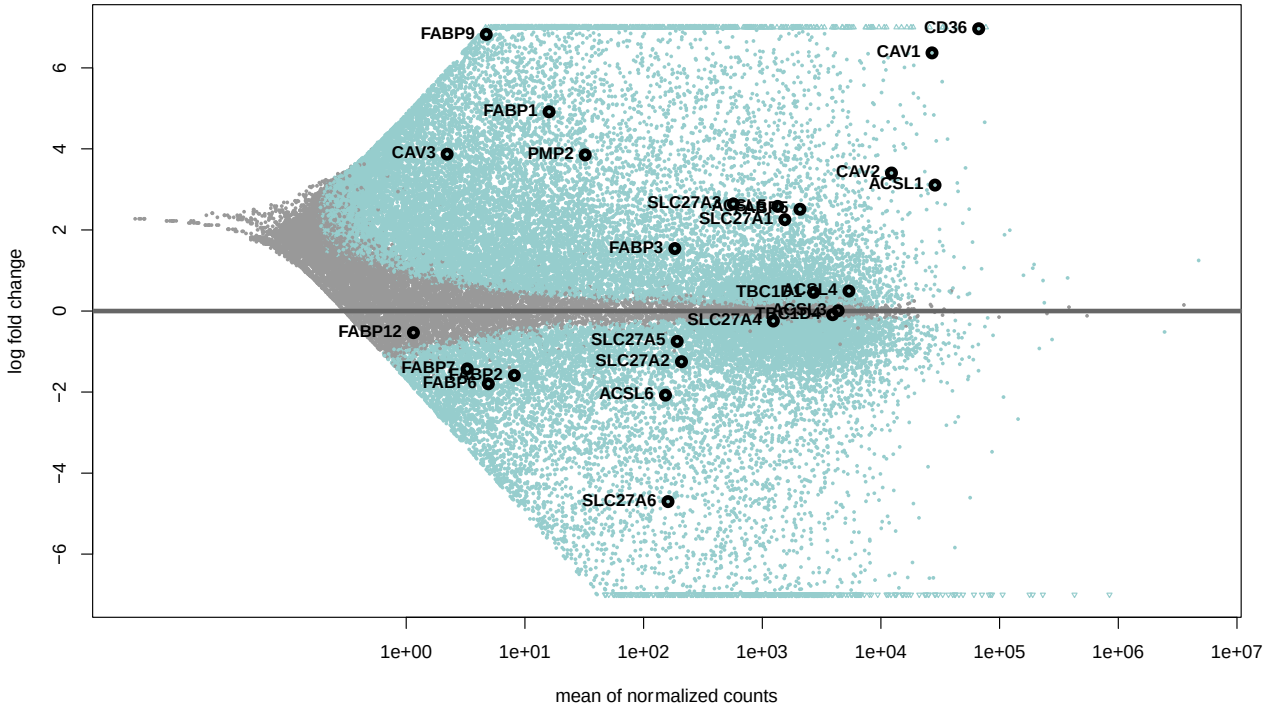

Figure 3.15 Comparison of candidate LC-FFA transporter gene expression in ex-vivo pancreatic islets vs adipocytes. MA plot, where the x axis shows mean expression of normalised counts, representative of a total of 33 human adipose tissue and 56 human pancreatic islet samples from non-diabetic donors, and the y axis represents the log fold change in expression. The grey circles represent genes with no significant difference in expression and blue circles represent genes that were significantly differentially expressed (adjusted p-values ≤ 0.05). Gene symbols were taken from the HUGO Gene Nomenclature Committee (HGNC); PMP2 = FABP8; SLC27A = FATP.

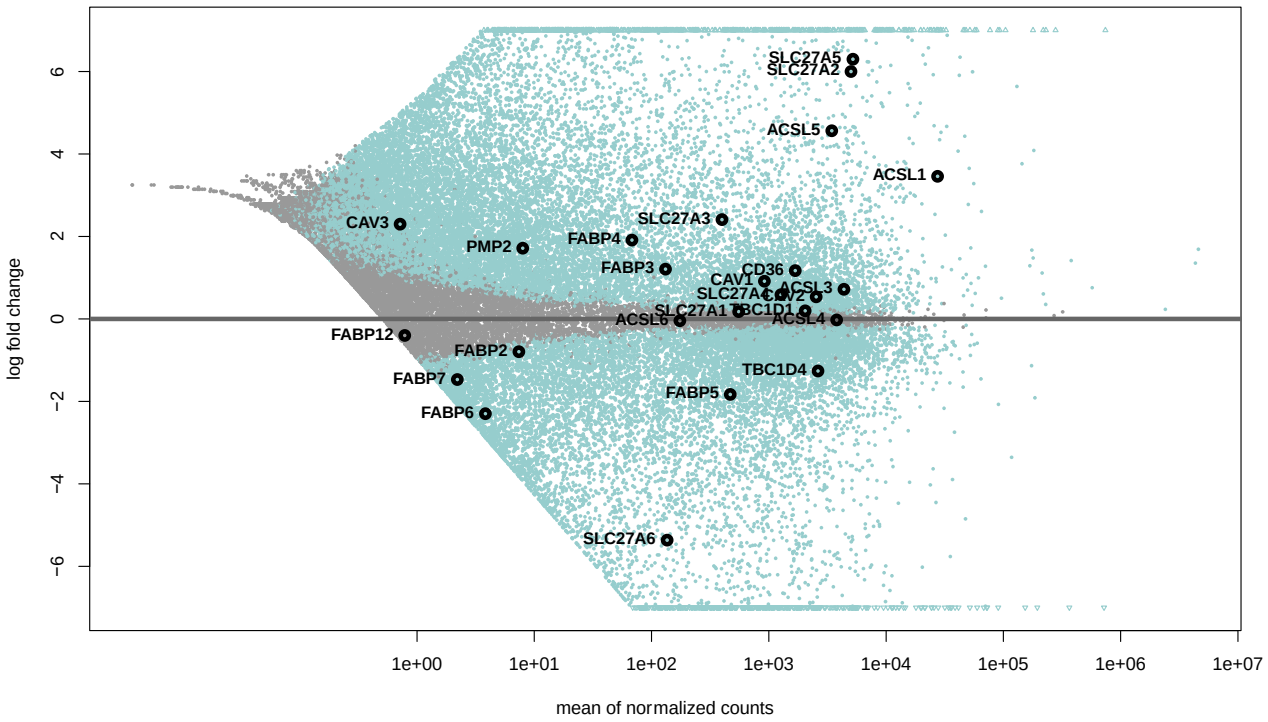

Figure 3.16 Comparison of candidate LC-FFA transporter gene expression in ex-vivo pancreatic islets vs hepatocytes. MA plot, where the x axis shows mean expression of normalised counts, representative of a total of 30 human liver tissue and 56 human pancreatic islet samples from non-diabetic donors, and the y axis represents the log fold change in expression. The grey circles represent genes with no significant difference in expression and blue circles represent genes that were significantly differentially expressed (adjusted p-values ≤ 0.05). Gene symbols were taken from the HUGO Gene Nomenclature Committee (HGNC); PMP2 = FABP8; SLC27A = FATP.

3.4 Discussion

The primary goal of this chapter was to determine the gene expression levels and which isoforms of LC-FFA candidate transport proteins were expressed in human pancreatic β-cells. Next, the expression of candidate LC-FFA transporters in different metabolically active mammalian cell types was examined. Alongside this, we determined whether the EndoC-βH1 cell line, an immortal human-derived pancreatic β-cell line, is an appropriate model to study LC-FFA uptake in human β-cells. To establish this, the expression of the candidate LC-FFA transport proteins identified in chapter 2 within human ex-vivo hepatocytes and adipocytes, as well as the human-derived EndoC-βH1 cell line was analysed, then compared with expression in human ex-vivo pancreatic islets. Further, the gene expression profile of candidate LC-FFA transporters in the rat INS-1 pancreatic β-cell line was constructed.

3.4.1 Overview of results

This work has shown that the EndoC-βH1 cell line and human islets exhibit an extremely similar gene expression pattern of our candidate LC-FFA transport proteins. Moreover, the gene expression pattern of these candidate LC-FFA transport proteins were found to be dissimilar in different human tissue types when compared to pancreatic islets. Taken together, these findings suggest that the EndoC-βH1 cell line is a valid model for LC-FFA uptake in human pancreatic β-cells. These results may also partially explain the conflicting results investigating LC-FFA transport proteins within previous literature. Further, several candidate LC-FFA transporters were found to be expressed in the INS-1 cell line.

3.4.2 Candidate LC-FFA transporters in pancreatic β-cells

To the best of my knowledge, as highlighted in Chapter 2, little is known about LC-FFA candidate transport proteins in pancreatic β-cells. Thus, the main aim of this study was to identify which candidate LC-FFA transporters are expressed in pancreatic β-cells, as well as which specific

isoform(s). Next, this study sought to determine whether data regarding candidate LC-FFA transporters from other (more well-characterised) cell types could be extrapolated to pancreatic β-cells.

In this work, several highly expressed genes were identified in both pancreatic islets and the EndoC-βH1 pancreatic β-cell line, including ACSL1, ACSL3, ACSL4, FATP4, TBC1D1 and TBC1D4. These genes were also expressed in the rat-derived INS-1 pancreatic β-cell line. The expression profile in human adipocytes and hepatocytes were markedly different to human islets.

3.4.2.1 ACSL1, ACSL3 and ACSL4 are highly expressed in pancreatic β-cells

Members of the ACSL family have been suggested to contribute towards LC-FFA uptake, possibly via vectorial acylation (202). Vectorial acylation involves the conversion of LC-FFA to a plasma membrane-impermeable form, through the intrinsic enzymatic activity of ACSLs, to trap the LC-FFAs within the cell (202, 212). In the study conducted here, high expression of several ACSL isoforms was identified in human ex-vivo pancreatic islets. Analogous to these findings, Ansari et al. (366) recently identified ACSL3 and ACSL4 mRNA and protein expression in pancreatic islets and the INS-1 832/13 cell line. Moreover, elevated ACSL1 mRNA expression has previously been identified in pancreatic islets (350) and INS-1 832/13 (366), a subclone of the INS-1 cell line, and has recently been reported to be significantly upregulated in response to treatment with C16:0 (a LC-SFA) in pancreatic islets (350). In summary, a high expression of several ACSL isoforms was observed in human pancreatic islets, which agrees with previous reports. Future research should investigate the expression of the role of the isoforms in LC-FFA transport in human β-cells.

Conversely, it was discovered here that only ACSL1 is highly expressed in both ex-vivo adipocytes and hepatocytes, whereas other family members show low to moderate expression. These results are consistent with previous reports that have identified high ACSL1 protein expression in adipocytes

(202, 367) and high ACSL1 mRNA expression in hepatocytes (368). Collectively, these results indicate that ACSL1 is highly expressed across a range of human cell types, including pancreatic islets, adipocytes, and hepatocytes, suggesting that this gene is an important component of metabolically active cell types. Further, this study has shown that ACSL isoforms show cell-type specificity, which is consistent with previous reports (369). The substrate specificity of ACSL isoforms has been reported to vary in different cell types, for example, many reports (366, 370, 371, 372, 373) have suggested that ACSL3 and ACSL4 demonstrate a preference for unsaturated fatty acids as substrates, while isoforms ACSL1, ACSL5 and ACSL6 prefer saturated fatty acids as substrates. Thus, if ACSL isoforms contribute towards LC-FFA uptake via vectorial acylation, this mechanism may facilitate the transport of different types of LC-FFAs (i.e., saturated vs unsaturated) in different cell types. As such, the results of studies investigating the role of the ACSL family members in LC-FFA uptake in other metabolically active cell types cannot be used to deduce the function of ACSL isoforms in pancreatic β-cells.

3.4.2.2 FATP4 is highly expressed in pancreatic β-cells

As discussed in section 2.4.2, members of the FATP family have been suggested to transport LC-FFA across the plasma membrane via a direct transport mechanism, or their intrinsic enzymatic activity (i.e., vectorial acylation). In the study conducted within this chapter, a high level of expression of FATP4 was identified in pancreatic islets and the human pancreatic β-cell line EndoC-βH1. Moreover, in the rat INS-1 pancreatic β-cell line, Fatp4 was highly expressed in comparison to other Fatp family members. Fitscher et al. (374) have also demonstrated that FATP4 is expressed in the human pancreas, which supports these results. However, very little research has investigated the expression nor function of FATP4 in pancreatic β-cells.

Previous studies have shown FATP2 to be primarily expressed in the liver and kidneys (307), while FATP5 is thought to be expressed exclusively in the liver (307, 375). Observations made here also

found a high level of expression of FATP5 and FATP2 in ex-vivo hepatocytes, which is consistent with these studies.

Surprisingly, in adipocytes, no FATP family members were expressed at a high level. This was particularly unexpected considering the number of publications identified within this thesis (chapter 2) that support the role of FATP1 in LC-FFA uptake in adipocytes. There are several possible explanations for this observation. First, it has been reported that the expression levels of FATP1 might be affected by insulin levels in adipocytes. FATP1 is reported to contain an insulin response sequence, and insulin has been shown to reduce FATP1 transcript levels in white adipose tissue (376, 377). In this study, the retrieved pre-published data for adipocytes (Appendix – Supplementary Table 2) did not provide a history of diabetes or the diabetes status (haemoglobin A1c (HbA1c) test) for the donors; high levels of insulin in a patient with diabetes could possibly result in the reduced expression level of FATP1. Secondly, nutrient depletion has been reported to upregulate FATP1 levels in murine 3T3-L1 adipocytes (377), which is the model primarily used to study LC-FFA uptake in adipocytes (Appendix A – Supplementary Table 1). Pre-published data collected here for adipocytes did not provide the BMI of all donors (Appendix B – Supplementary Table 2); if the donors were obese, they would have had nutrient overload and subsequently a potential downregulation of FATP1. Remarkably, Man et al. (377) reported that, in 3T3-L1 adipocytes, FATP1 mRNA increases 11-fold above control level following a 48h fast, then declines to control level after refeeding for 72h. Therefore, nutrient control should be considered when investigating the expression of isoforms of the FATP family and their role in LC-FFA uptake. Moreover, disparities in these results could be due to the model used, as the 3T3-L1 cell line is a mouse cell line, whereas the results found here are in ex-vivo human adipocytes. Collectively, these results imply that the role of the FATP isoforms cannot be directly extrapolated from different cell types to pancreatic β-cells.

3.4.2.3 TBC1D1 and TBC1D4 are highly expressed in pancreatic β-cells

Previous reports have suggested that TBC1D1 and TBC1D4 may act as negative regulators of LC-FFA uptake, potentially via inhibiting the translocation of FATP4 or CD36 to the plasma membrane (238, 241). Here, it was established that both TBC1D1 and TBC1D4 are highly expressed in pancreatic islets and the EndoC-βH1 pancreatic β-cell line. Both TBC1D1 and TBC1D4 were also expressed in the rat INS-1 pancreatic β-cell line. This is consistent with previous reports that TBC1D1 and TBC1D4 are expressed at the mRNA level in human pancreatic β-cells (378, 379). On the other hand, we identified low to moderate expression of TBC1D1 and TBC1D4 in adipocytes and hepatocytes. Previous publications (380, 381, 382) have reported that TBC1D1 is expressed at low levels in adipocytes and hepatocytes, consistent with the results observed here. Moreover, Moltke et al. (383) reported that TBC1D4 is expressed in human liver tissue, to a lower degree than in pancreatic islets, which agrees with the results in this study. However, the same study identified a higher level of expression of TBC1D4 in human adipose tissue when compared to pancreatic islets, which is not observed here. This could be due to several factors, including heterogeneity between sample populations, biases introduced during construction of the cDNA library and sequence alignment (e.g., heterogeneity between sample populations or differences in experimental procedures), or different read depths (i.e., the number of times each nucleotide base was sequenced) (384). Taken together, these results imply that the role of TBC1D1 and TBC1D4 is cell-type specific, therefore, investigations into the function of TBC1D1 and TBC1D4 in LC-FFA uptake should account for this.

3.4.2.4 CD36 is moderately expressed in pancreatic β-cells

To date, a wealth of literature supports CD36 as a candidate LC-FFA transport protein. The work conducted here has identified a high expression of CD36 in adipocytes, which parallels the results found in previous studies, where this protein was found to facilitate LC-FFA uptake in all almost all studies using this cell type (section 2.3.2). Comparatively, a moderate expression of CD36 is observed

in the study conducted here in hepatocytes. This coincides with the observations of a case control study (284), which compared LC-FFA uptake in a range of cells from individuals with sufficient and deficient levels of CD36. Hames et al. (284) reported that CD36 facilitates transport in adipocytes, myocytes and cardiomyocytes, but that it does not facilitate LC-FFA uptake in hepatocytes, which suggests that the role of CD36 is cell-type specific. Intriguingly, CD36 showed moderate expression in human islets and the EndoC-βH1 cell line. However, it should be noted that the expression of CD36 in pancreatic β-cells was evidently less than in adipocytes. Taken together, these findings suggest that the role of CD36 in other cell types should not be directly extrapolated to pancreatic β-cells. Due to the vast amount of literature supporting CD36 as a candidate LC-FFA transporter (as outlined in chapter 2), further research should investigate the expression of CD36 at protein level in pancreatic β-cells to gain additional insight into the role of CD36 in this cell type, specifically.

As outlined in chapter 2 of this thesis, many studies investigating the role of CD36 in LC-FFA uptake use rat models. The rat ortholog of CD36 was initially discovered as a fatty acid translocase (FAT) (230) and shows 75% amino acid identity with human CD36 (385). Here, gene expression of Cd36 was identified in the INS-1 cell line, a rat insulinoma cell line. Intriguingly, the transcript for Cd36 flagged as 'Ensembl Canonical', a label given to the most conserved and highly expressed transcript, did not show expression in the transcript counts table generated here. Rather, an alternative transcript (ENSRNOT00000008319) was used at this was the only transcript available for Cd36 which showed expression. These different transcripts for Cd36 arise through alternative splicing events (386). As such, the transcript for Cd36 identified here does not have a great deal of evidence of functional potential in comparison to the transcript flagged as 'Ensembl Canonical'. Thus, although this study has identified the expression of a Cd36 transcript in rodent INS-1 cells, the resultant protein may function differently, and therefore may have a different effect on LC-FFA transport when compared

to the protein that arises from the most highly conserved transcript. These results should be considered in functional studies for Cd36 in the rodent INS-1 cell line.

3.4.3 The immortal EndoC-βH1 cell line appears to be a suitable cell line to study candidate LC-FFA transporters

One of the main obstacles this study aimed to overcome is the difficulty in obtaining samples of ex-vivo pancreatic β-cells, by finding a suitable in vitro model for LC-FFA uptake that would mimic the physiological process. We chose to assess the EndoC-βH1 cell line, a human cell line, as previous findings (387) support it as a valid model of human β-cells.

To identify whether highly expressed candidate LC-FFA transporter RNA, as well as CD36 (which was expressed at a moderate level), in pancreatic islets was statistically similar to EndoC-βH1, a differential gene expression analysis was used. Albeit highly expressed in both human islets and EndoC-βH1 cells, four of the candidate LC-FFA transporters were differentially expressed (ACSL1, ACSL3, FATP4 and TBC1D4). Ryaboshapkina et al (388) suggest that discrepancies in transcript expression between EndoC-βH1 cells and adult human β-cells are due to the greater proliferation rate of EndoC-βH1 cells, which may explain the differential expression of candidate LC-FFA transporters observed here. Future work should investigate candidate LC-FFA transporter expression in the conditionally immortalised pancreatic β-cell lines, EndoC-βH2 or EndoC-βH3, which proliferate at a much lower rate than EndoC-βH1 cells and are, therefore, more similar to human β-cells in-vivo (389, 390). Further, the difference in expression between EndoC-βH1 cells and pancreatic islets should be taken into consideration in future experimental work. The remainder of these highly expressed candidate LC-FFA transporters (along with CD36) showed a statistically similar level of expression between human islets and EndoC-βH1 cells. In summary, the results of this study imply that the EndoC-βH1 cell line may be a suitable model to study candidate LC-FFA transporters, however, further investigations are required to consolidate these findings.

This study is not the first to demonstrate that EndoC-βH1 cells are a physiologically relevant cell line for human β-cells. Tsonkova et al. (387) transplanted two million EndoC-βH1 cells into diabetic mice to validate in-vivo functionality of the cell line. Six weeks post-transplantation, the cells were able to produce sufficient insulin to restore glucose levels to normal, which provides good evidence that the EndoC-βH1 cell line is functional. In support of this, other studies have shown similar results in terms of the analogy of the cell line to human islets, including comparable electrophysiological properties, such as voltage-gated ion channels (391), and similar responses to glucose (193). It has also been noted that, at the transcriptional level, the EndoC-βH1 cell line is more akin to adult than to foetal human β-cells (391), which is where EndoC-βH1 cells are derived from (193). However, EndoC-βH1 cells have been reported to display a different response to cytokines than human islets (392), so perhaps not all physiological processes can be recapitulated in this cell line. Seemingly, this work is the first to report that the EndoC-βH1 cell line may be a valid model of LC-FFA uptake in human pancreatic β-cells.

In summary, EndoC-βH1 cells may be a suitable model to study the role of candidate LC-FFA transporters. However, future studies investigating ACSL1, ACSL3, FATP4 and TBC1D4 in EndoC-βH1 cells should consider that these genes were differentially expressed.

3.4.4 Limitations

Limitations of this study are associated with the restricted information obtained from analysing gene expression (as opposed to protein expression), the use of bulk RNA-seq rather than scRNA-seq, differentially expressed genes between pancreatic islets and the EndoC- βH1 cell line, and the difficulties associated with interspecies gene expression analysis.

First, genome-wide association between mRNA and protein expression levels are infamously poor, with only around 40% explanatory power, typically due to additional levels of regulation between

transcript and protein product (357). Thus, this analysis only gives an indication of the potential candidate LC-FFA transport protein expression. Additionally, this study uses pre-published bulk RNA-seq data to analyse gene expression in human islets, which prevents differentiation between the specific cell types which make up the islet (α-cells, δ-cells, PP-cells, and β-cells). Despite this limitation of bulk RNA-seq, this technique was utilised in the present study because, to the best of our knowledge, there is no published scRNA-seq data using the EndoC-βH1 cell line. Moreover, it would be challenging to compare scRNA-seq data of human β-cells to bulk RNA-seq data using the EndoC-βH1 cell line due to the differences in the amplification process of genes; there is a large gene amplification in bulk RNA-seq and a comparatively lower signal for scRNA-seq (393). While this presents a flaw in the study design, the majority (~70%) of islets is composed of β-cells (394), which suggests that the gene expression observed in whole-islet samples is likely to be observed in β-cells alone.

This study used differential gene expression analysis to establish whether the genes for our candidate LC-FFA transporters were expressed at different levels in ex-vivo pancreatic islets compared to other metabolically active human tissue types (i.e., hepatocytes and adipocytes) and the immortal EndoC-βH1 cell line. Using this analysis, many of the highly expressed candidate LC-FFA transporters (ACSL1, ACSL3, FATP4, and TBC1D4) were shown to be differentially expressed between pancreatic islets and the EndoC-βH1 cell line. This study analysed the expression of 47 different EndoC-βH1 samples, taken from two different publications (343, 349). Recently, Ben-David et al. (395) reported that cancer cell lines, which are generally considered to be clonal, exhibit a high degree of genetic heterogeneity. This heterogeneity may result from the presence of new genetic variants or changes in the abundance of pre-existing subclones, possibly due to selection of genes by specific conditions (e.g., growth medium) (395). Therefore, as the EndoC-βH1 cell line expresses the oncoprotein, SV40LT (396), genomic evolution may result in a high magnitude of variation across

cell line strains, which might account for differentially expressed genes in human islets and EndoC-βH1 cells. However, owing to the observation made here that several candidate LC-FFA transporters (ACSL1, ACSL3, ACSL4, FATP4, TBC1D1 and TBC1D4) are highly expressed in both human pancreatic islets and EndoC-βH1 cells (section 3.3.1), it can be determined here that the EndoC-βH1 cell line may be a suitable model to study LC-FFA uptake.

As previously discussed in section 2.1.4, rodent pancreatic β-cells have differences when compared to human β-cells, including islet composition, glucose transporters, expression of genes for insulin and the routing of LC-SFA. This raises questions as to whether rodent β-cells provide a suitable model for studying LC-FFA uptake. The rat INS-1 cell line, is considered an appropriate model for glucose-stimulated insulin secretion (397, 398), which is the primary function of pancreatic β-cells (399). However, to the best of our knowledge, no studies have investigated whether the INS-1 cell line is a physiologically relevant model to study LC-FFA uptake. Comparing the expression levels of candidate LC-FFA transport proteins between the rat INS-1 cell line and human cell types might provide further insight into this. However, it was not possible to conduct such an experiment due to the challenges associated with interspecies comparisons of gene expression. These challenges include differences in the genome, and thus differences in the transcriptomes between the human and rat (400). For example, although genes from different species might have a shared common ancestry (orthologs), they might not be entirely analogous, since gene duplications following speciation may have resulted in the development of one or more extra gene copies (in-paralogs) (400). Therefore, data from all genes, including orthologs and paralogues, must be considered for interspecies comparisons of gene expression. Future studies might consider using a method by Kristiansson et al. (400) to analyse differentially expressed candidate LC-FFA transporter genes between rat and human, as this technique was devised to overcome the limitations of interspecies gene expression analysis.

This might provide further insight into the suitability of the rat INS-1 cell line as a model for LC-FFA uptake in pancreatic β-cells.

3.4.5 Summary

In summary, ACSL1, ACSL3, ACSL4, FATP4, TBC1D1 and TBC1D4 were identified as the most highly expressed candidate LC-FFA transporters in human β-cells and islets. We have also determined here that the EndoC-βH1 cell line may be a suitable model for human islets when investigating LC-FFA candidate transport proteins. Moreover, the gene expression of LC-FFA candidate transport proteins varies between adipocytes and hepatocytes when compared to pancreatic islets. Future work should aim to validate these findings at protein level, which can be achieved using immunocytochemistry to detect and visualise candidate LC-FFA transporters in human pancreatic β-cells.

Chapter 4

Using experimental techniques to investigate long-chain fatty acid transport in the rat INS-1 832/13 and the human EndoC-βH1 cell lines

4.1 Introduction

As discussed in chapter 2, there is a wealth of evidence supporting a role for proteins in LC-FFA uptake. However, there is very little evidence for a role for these proteins in pancreatic β-cells, specifically. In chapter 3, the gene expression of several candidate LC-FFA transporters was identified in pancreatic islets and the human-derived EndoC-βH1 pancreatic β-cell line. Moreover, it was also shown that EndoC-βH1 may a suitable model to study LC-FFA uptake in-vivo (chapter 3). As outlined in section 1.7, there is evidence to suggest that an increased circulating concentration of LC-SFAs, particularly the LC-SFA C16:0, is associated with the death and dysfunction of pancreatic β-cells, via a process known as lipotoxicity (38, 123). Characterising the mechanism of LC-SFA uptake in β-cells will enable the production of therapeutics to control their entry, thereby possibly decelerating or inhibiting the progression of T2D. Thus, the next aim of this study was to investigate protein-mediated LC-SFA uptake in the EndoC-βH1 pancreatic β-cell line, to model LC-SFA uptake into in-vivo pancreatic β-cells. A recent study by Hao et al. (219) suggests that LC-FFA uptake is facilitated by CD36-mediated caveolar endocytosis in adipocytes. To investigate this theory in pancreatic β-cells, a potent dynamin inhibitor (Dyngo-4a) was applied to EndoC-βH1 cells, to inhibit dynamin-dependent endocytosis (including caveolae-mediated endocytosis) (218, 401). In this way, it could be identified whether the uptake of C16:0 into β-cells is mediated by dynamin-dependent endocytosis.

In addition to the evidence supporting a role for a protein-mediated mechanism in the cellular uptake of LC-FFA, there is also evidence to support a role for passive diffusion that should not be overlooked. In the passive diffusion model of LC-FFA uptake, it is thought that LC-FFAs can cross the plasma membrane without the support of proteins (184). Evidence to support a passive diffusion mechanism for the uptake of LC-FFAs includes 1) physics-based models (i.e., the Meyer-Overton rule) (186), 2) the ionisation properties of LC-FFAs (187) and 3) LC-SFA can enter giant unilamellar

vesicles (GUVs) via simple diffusion (unpublished data from Thomas et al. (402)). GUVs are simple model membranes that are of a similar size to human cells (approximately 1-100μm in diameter) and contain no proteins (403). Indeed, the composition of the plasma membrane of GUVs is not akin to the complexity of the pancreatic β-cell membrane. Therefore, it is important to validate this mechanism of simple diffusion of LC-SFA in pancreatic β-cells, to gain a better understanding of the mechanism of LC-FFA uptake in-vivo. However, it would be technically challenging to remove all proteins from the β-cell membrane and the cell would not survive. Instead, we suggest that the most appropriate solution to investigate the role of passive diffusion in LC-SFA uptake is to manipulate the lipid order of the plasma membrane. Seemingly, there are three main lipid phases of the plasma membrane: 1) solid gel (L_β), 2) liquid ordered (L_o) and 3) liquid disordered (L_d) (404). Thus, this chapter also aimed to modify the overall lipid phase of the membrane of human pancreatic β-cells to determine whether this will change the acute uptake of LC-SFA. This will provide further insight into the mechanism of LC-SFA uptake by pancreatic β-cells. For instance, this study may offer additional evidence for passive diffusion, or it might imply that candidate LC-FFA transport proteins are involved in uptake, and that the lipid order of the membrane is an important factor that influences protein interactions for facilitating LC-FFA uptake.

4.1.1 Finding the rate of LC-FFA uptake

Finding the initial rate of uptake of the LC-FFA is seemingly the main model used to discriminate between simple diffusion and facilitated transport (207). This model is used in accordance with Fick's law of simple diffusion, which implies that the rate of diffusion increases linearly as the concentration of the substance (i.e., LC-FFA) increases (405). Further, this model is used in agreement with Michaelis-Menten saturation kinetics (207, 406), which suggests that proteins become saturated at high concentrations of a substance and diffusion will taper off in facilitated transport. Over 40 years ago, Abumrad et al. (207) determined that the initial rate of uptake of the LC-MUFA, C18:1, into

adipocytes is a protein-facilitated process when the concentrations of C18:1 are low, although at high concentrations of C18:1, uptake is seemingly via passive diffusion. Saturable uptake has also been reported for the LC-SFA, C16:0, in giant sarcolemmal vesicles (204), suggesting that both saturated and unsaturated LC-FFAs are transported across the plasma membrane via facilitated diffusion. However, as outlined in chapters 2 and 3, it is likely that the mechanism of LC-FFA uptake is different in different cell types. Therefore, it is important to determine the rate of LC-FFA uptake in pancreatic β-cells, specifically, as this will provide further insight into whether LC-FFA transport across the membrane of these cells using simple diffusion or a protein-mediated mechanism.

4.1.2 Phases of the lipid membrane

The role of passive diffusion in LC-SFA uptake can be investigated by manipulating the lipid order of the plasma membrane. Figure 4.1 illustrates the three main lipid phases of the membrane. In the L_β phase, fatty acid chains of phospholipids are tightly packed, resulting in their low lateral mobility (404, 407). The L_o phase is like the L_β phase in that the fatty acyl chains in the membrane are extended and ordered (i.e., tightly packed together), however, the two can be distinguished by a greater lateral mobility of the lipids in the L_o phase (407). Moreover, in the L_o phase, the hydroxy groups of cholesterol molecules associate with the polar head groups of phospholipid molecules, resulting in a reduced lateral mobility (404). On the other hand, in the L_d phase, the fatty acid chains of phospholipids are fluid and disordered (i.e., not tightly packed together) (404, 408). Additionally, in the L_d phase, the headgroup region of the phospholipids in the membrane are more hydrated than in the L_o phase (408), which means that there are a greater number of water molecules associated with the headgroup region of phospholipids in the L_d phase. Several factors can influence the lipid phase of the membrane, including temperature (409), cholesterol content (410), as well as the type of FFA and/or ratio of different FFAs in the membrane (411). It is out of the scope of this thesis to discuss all these factors; instead, this work focuses on the influence of FFAs on membrane fluidity. Moreover,

different lipid phases of the membrane may regulate the permeability of the membrane to certain substances (412).

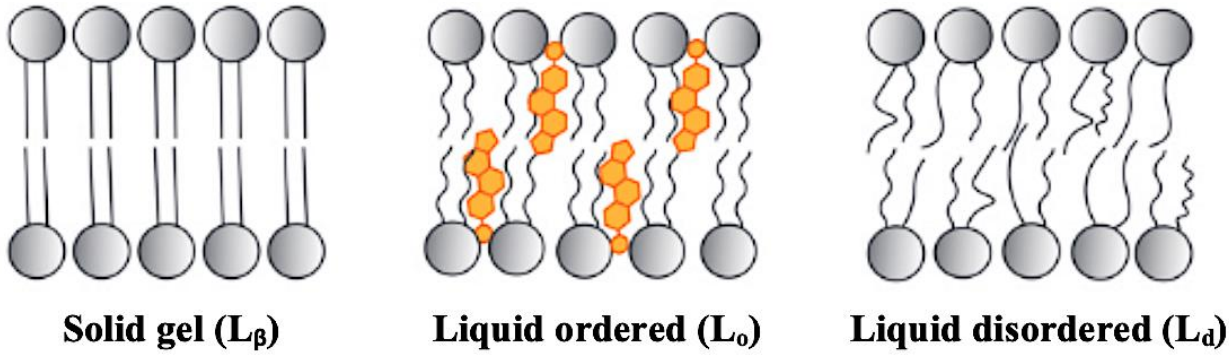

Figure 4.1 The main lipid phases of the membrane are solid gel (L_β), liquid ordered (L_o) and liquid disordered (L_d) (404). Figure adapted from Barba-Bon et al (413) .

4.1.2.1 The effect of FFAs on membrane fluidity

The lipid composition of the plasma membrane is thought to regulate its physicochemical properties, including structure, fluidity and permeability (414). Further, such properties of the plasma membrane seemingly regulate protein functions, including protein-membrane interactions, enzyme activity and receptor binding (414, 415, 416). Fatty acids are constituents of the lipids within the cell membrane (417), mainly constituting phospholipids and cholesterol esters (414), although a small fraction (approximately 0.3-10% of total membrane lipids) are present in their free (non-esterified) form (411, 414). Phospholipids, which are components of the phospholipid bilayer, consist of two chains fatty acids (either saturated or unsaturated or both) which are linked to the phosphatidyl group (411), whereas cholesterol esters consist of cholesterol joined by an ester bond to a fatty acid (418). There is evidence (417, 419) to suggest that fatty acids, in their free form or following their incorporation into phospholipids or cholesterol esters, influence the physical properties of the plasma membrane. Several factors have been named to influence the order of the plasma membrane (i.e., how fluid or

rigid it is), including the degree of saturation of FFAs and the ratio of FFAs in the membrane (411). Fatty acid chain length has also been suggested to influence membrane order; however, most studies (420, 421) have used bacterial membranes to investigate this, so the impact of fatty acid chain length will not be discussed further in this thesis.

The degree of saturation of the FFA is thought to alter membrane fluidity, such that saturated FFAs make the membrane more rigid (i.e., towards the L_o phase) whereas unsaturated FFAs increase membrane fluidity (i.e., towards the L_d phase) (411). Thus, the ratio of saturated to unsaturated FFA in the membrane can be said to influence membrane fluidity. For example, the incorporation of the LC-MUFA, C18:1, or the unsaturated fatty acid, α-linolenic acid, to the membrane have been reported to increase the membrane fluidity, whereas the addition of the LC-SFA, C18:0, results in reduced fluidity in model cholesterol/phospholipid membranes (411). Moreover, the work of Koike et al. (422) has demonstrated that an increased ratio of saturated to unsaturated fatty acids is associated with reduced membrane fluidity in human and mouse fibroblasts. The differing effects of saturated vs unsaturated FFA on membrane order is supposedly due to the geometry of these molecules, where an increase in the number of double bonds (in the *cis* configuration) results in a more "bent" hydrocarbon chain, whereas a completely saturated FFA (e.g., C18:0 or C16:0) has a fully extended chain that resembles a rod (411). The bent shape of unsaturated hydrocarbons (e.g., C18:1) results in an increased distance between FFAs in the membrane, preventing them from packing tightly together, thereby increasing membrane fluidity (411). Taken together, it can be inferred that saturated and unsaturated FFA exert opposing effects on the fluidity of the phospholipid membrane. Hence, modification of the lipid phase of the phospholipid membrane could be achieved by varying the ratio of saturated to unsaturated FFA that cells are exposed to.

It is important to determine membrane fluidity because a change in membrane fluidity can affect the physicochemical properties of the cell and thus could influence LC-FFA uptake. An increase in

rigidity (increase in order) of the membrane is thought to result in reduced flexibility and increased fragility of the membrane (411), however, an increase in fluidity (increase in disorder) of the membrane can render the cells more vulnerable to osmotic lysis (423). Moreover, there is the potential that a change in lipid order might regulate membrane permeability to certain substances (as discussed in section 4.1.2.2), which could include LC-FFAs. Therefore, it is vital that the cell maintains a desirable membrane order (e.g., via regulating the quantity of saturated and unsaturated fatty acid chains in the membrane) in order to efficiently regulate the physicochemical properties of the membrane (411).

4.1.2.2 The impact of membrane fluidity on membrane permeability

It has been proposed that the fluidity of the membrane can influence the permeability of the membrane. The fluidity of the membrane might alter the uptake of substances by passive diffusion (412) or influence membrane protein dynamics (424), thereby disrupting the function of proteins involved in the transport of substances across the plasma membrane. As such, the uptake of LC-FFAs into pancreatic β-cells, should this process be via passive diffusion and/or facilitated by proteins, could be altered by a change in membrane fluidity.

Previous studies (412, 425) have determined that membrane fluidity regulates the passive diffusion of substances, including water, oxygen, methanoic acid and glycerol. It is generally thought that the permeability of the membrane is reduced for various molecules in the L_o phase (more rigid), when compared to the L_d phase (more fluid) (412). For instance, simulation-based research (i.e., research that uses an artificial membrane to mimic the lipid membrane) has suggested that the permeabilities of oxygen and water are 3- and 7-fold lower, respectively, in the L_o phase when compared to the L_d phase (412). Recently, one simulation-based study reported that the transition from the L_d phase to the L_β phase dramatically reduces membrane permeability of water (by 200-fold) and for both methanoic acid and glycerol (by 2000-fold) (425). Collectively, this evidence raises questions as to

whether a change in the overall lipid phase of the membrane might alter the uptake, by passive diffusion, of other substances (e.g., LC-FFAs) into cells.

The function of membrane proteins (e.g., ion channels, receptors and transporters) may also be influenced by membrane fluidity (424). Thus, any process that depends on the function of such proteins, including transmembrane transport, may be affected by membrane fluidity (424). The recent work of Stieger et al. (426) suggests that membrane lipids regulate the activity of transport proteins within the membrane in two ways: 1) lipids are tightly bound to protein transporters, and 2) via the overall lipid composition within the membrane. For example, membrane lipids might interact with clefts found on the surface of the protein transporter, either between transmembrane helices or on hydrophobic surfaces of the protein (426). Alternatively, lipids might interact with protein transporters from a distance, which can be observed as an altered ratio of lipids to proteins within the membrane (427). A change in membrane lipid composition is also expected to change the fluidity of the membrane (as outlined in section 4.1.2), therefore, a change in membrane fluidity could alter these lipid-protein interactions and affect the function of membrane transporter proteins. Taken together, this evidence could imply that a change in membrane fluidity could interfere with the function of candidate LC-FFA transport proteins, and thus alter LC-FFA uptake.

4.1.3 Aims and objectives

There is a wealth of evidence implicating a role for passive diffusion (section 1.8.1), as well as a role for proteins (section 1.8.2) in LC-SFA uptake. Thus, it was hypothesised here that LC-SFA uptake into human pancreatic β-cells may involve both passive diffusion and a protein-mediated process. The aims and objectives of this chapter were, therefore:

Aims:

1) To examine whether acute LC-SFA uptake into human pancreatic β-cells is a passive and/or protein-facilitated process
2) To investigate the role of dynamin-mediated endocytosis in acute LC-SFA uptake
3) To investigate the role of the lipid phase of the membrane in acute LC-SFA uptake

Objectives:

A. Determine the rate of acute uptake of LC-SFA by INS-1 832/13 and EndoC-βH1 cells (aim #1)
B. Establish the rate of acute LC-SFA uptake in INS-1 832/13 and EndoC-βH1 cells in the presence of an inhibitor of dynamin (aim #2)
C. Establish the lipid phase of INS-1 832/13 and EndoC-βH1 cells with no LC-FFA treatment (aim #3)
D. Culture INS-1 832/13 and EndoC-βH1 cells in varying LC-SFA:LC-MUFA ratios and determine the lipid phase of the membrane (aim #3)
E. Measure the rate of acute LC-SFA uptake in EndoC-βH1 cells cultured in varying LC-SFA:LC-MUFA ratios (aim #3)

4.2 Materials and methods

4.2.1 Source of reagents

The sources of all reagents are listed in Table 4.1

Table 4.1 Sources of reagents

Processes	Reagent with manufacturer
Cell culture	Foetal Bovine serum (FBS) (Life Technologies); L-glutamine (Life Technologies); Penicillin-streptomycin (Gibco); HEPES (Merck); Sodium pyruvate (Gibco); β-mercaptoethanol (Sigma-Alderich); Low glucose Dulbecco's Modified Eagles Medium (DMEM) (Gibco); Extracellular matrix (ECM) (Merck); Fibronectin (Merck); Bovine serum albumin fraction V (BSA) (Merck); Phosphate buffered saline (PBS) (Gibco); RPMI-1640 (Life Technologies); Nicotinamide (VWR); Transferrin (Sigma-Alderich); Sodium selenite (Sigma-Alderich); 0.05% Trypsin (v/v) 0.53mM EDTA (Life Technologies)
Fatty acids	All fatty acids were purchased from Sigma-Alderich

pHrodo assay	pHrodo Green AM Intracellular pH Indicator (ThermoFisher Scientific) pHrodo Red AM Intracellular pH Indicator (ThermoFisher Scientific)
Laurdan assay	Laurdan dye (Cambridge BioScience)

4.2.2 Cell lines

Two different immortalised clonal β-cell lines were used in this study: the rat INS-1 832/13 and the human-derived EndoC-βH1. The rat pancreatic β-cell line, INS-1, was originally established from cells that were derived from an x-ray-induced rat insulinoma (399). The continuous growth of this cell line requires β-mercaptoethanol (399). Hohmeier et al. (398) introduced a human proinsulin gene into the INS-1 cell line to amplify the responsiveness of the cells to glucose, thus producing the INS-1 832/13 cell line. The human-derived pancreatic β-cell line, EndoC-βH1, was generated using targeted oncogenesis of human foetal tissue (396). Briefly, this involved the transduction of human foetal pancreatic buds with a lentiviral vector encoding large T antigen of simian virus 40 (SV40LT), which is an oncoprotein (396). The transduced pancreatic buds were then grafted (implanted) into mice to enable their development into mature pancreatic tissue. As the expression of the oncoprotein, SV40LT, was controlled by the insulin promoter, this promoted the proliferation of the human β-cells, forming insulinomas. Subsequently, the β-cells were transfected with human telomerase reverse transcriptase (hTERT), to generate an immortalised cell line, then expanded in vitro (396). The INS-1 and EndoC-βH1 cell lines have both been reported to secrete insulin, as demonstrated by Thomas et al. (428), and express β-cell specific markers, including PDX1 and NKX6-1 (429, 430).

4.2.2.1 Cell culture conditions

The INS-1 832/13 cell line was cultured in RPMI-1640 medium containing 11mM glucose, which was supplemented with 10% (v/v) foetal bovine serum, 2mM L-glutamine, 100ug/ml streptomycin, 100U/ml penicillin, 10mM HEPES, 1mM sodium pyruvate and 50 mM/L β-mercaptoethanol. Supplemental reagents were added to facilitate growth. Cells were cultured in complete medium (which was pre-heated to 37°C) and grown in 75cm^2 flasks, in a 37°C incubator containing a 5% CO_2 humidified atmosphere. Cells were passaged twice weekly.

EndoC-βH1 cells were cultured on 25cm^2 flasks that were coated 1h before seeding to facilitate cellular adherence. Coating medium consisted of DMEM (25mM glucose) supplemented with 1% (v/v) extracellular matrix (ECM), 2μg/ml fibronectin and 1% (v/v) penicillin/streptomycin (P/S) and was maintained at 4°C while coating the flasks, then at 37°C for the 1h incubation period prior to cell seeding. The EndoC-βH1 cell line was cultured in DMEM containing 5.6mM glucose, which was supplemented with 2% (w/v) bovine serum albumin fraction V (BSA), 10mM nicotinamide, 5.5ug/ml transferrin, 2.7nM sodium selenite, 100ug/ml streptomycin and 100U/ml penicillin, and 50M/L β-mercaptoethanol. Cells were grown in a 37°C incubator containing a 5% CO_2 humidified atmosphere. Culture medium was replaced twice weekly.

4.2.2.2 Cell passage

Both the INS-1 832/13 and EndoC-βH1 cell lines were subcultured when cells had grown to a confluency of approximately 80%.

INS-1 832/13 cells were lifted from flasks by incubating (37°C) with 0.05% trypsin-0.53mM EDTA for 5 min. Trypsin was neutralised with the aid of culture medium containing 10% (v/v) FBS, then cells were centrifuged at 89g for 5 min. INS-1 832/13 cells were seeded into a new flask at 1/10th of the original population.

To detach EndoC-βH1 cells from flasks, cells were washed twice in PBS, then incubated (37°C) in 0.05% (v/v) trypsin-0.53mM EDTA for 3min. To neutralise the trypsin, 20% FBS/ 80% (v/v) PBS was added. Cells were then centrifuged at 89g for 3 min. To sustain the cell line, EndoC-βH1 cells were seeded into a new flask at $2.5x10^6$ cells/flask.

4.2.2.3 Cell seeding

Cells were seeded in a monolayer at the seeding densities listed in Table 4.2 for subsequent use in experiments.

Table 4.2 Cell seeding densities

Cell line	Plate size	Seeding density (per well)
INS-1 832/13	6-well plate	$1x10^6$
INS-1 832/13	12-well plate	$0.2x10^6$
EndoC-βH1	6-well plate	$1x10^6$
EndoC-βH1	12-well plate	$0.2x10^6$

In experiments using fixed or live cell imaging, glass coverslips were sterilised in 95% (v/v) ethanol (EtOH) for 30 min, repeated 3 times, prior to cell seeding.

4.2.3 Preparing fatty acids and treatment of cells

The fatty acids used in this study were C18:1 and C16:0. Both fatty acids (C18:1 and C16:0) were suspended in 50% (v/v) EtOH. To dissolve the fatty acids in EtOH, they were heated at 70°C for 10 min. Fatty acids dissolved in EtOH were then conjugated to albumin by adding the fatty acids to a

10% (w/v) bovine fatty acid-free albumin solution (BSA) at a 1:10 dilution, then incubating for 1h at 37°C. Fatty acids conjugated to albumin were then added to serum-free media (i.e., without BSA for EndoC-βH1 cells or without FBS for INS-1 832/13 cells) at 1:10 dilution. This yielded a final concentration of 0.5% (v/v) EtOH and 1% (w/v) BSA. Cells were seeded (Table 4.2) 24h prior to treatment with fatty acid-BSA complexes. Vehicle control (VC) samples received vehicle only (i.e., no fatty acids), which comprised of a final concentration of 0.5% (v/v) EtOH and 1% (w/v) BSA. Media control (MC) samples received EtOH alone in serum-free media, which consisted of a final concentration of 0.5% (v/v) EtOH in serum-free media and no fatty acids.

4.2.4 Determining the rate of acute long-chain saturated fatty acid uptake

4.2.4.1 pHrodo AM intracellular pH indicator

The pHrodo AM intracellular pH indicators are modified with acetoxymethyl (AM) ester groups (431). These groups are added to yield an uncharged molecule, so that it can permeate the cell membrane (431). Once the probe has entered the cell, these AM groups are cleaved by nonspecific esterases, which traps the compound within the intracellular environment and selectively labels the cytosol (432). This generates a pH probe which emits a greater fluorescence as the pH of the intracellular environment drops (that is, as the intracellular environment becomes more acidic) (433). Thus, due to the acidic nature of LC-FFAs, it should be expected that fluorescence intensity will increase as LC-FFAs are taken into the cell.

4.2.4.2 pHrodo assay

INS-1 832/13 and EndoC-βH1 cells were seeded in a 6-well plate (Table 4.2) 24h before the experiment. On the day of imaging, live cell imaging media (LCIM) was made up using HEPES-bicarbonate buffer, comprising (in mmol/L) 5 HEPES, 120 NaCl, 24 $NaHCO_3$, 4.8 KCl, 0.5 Na_2HPO_4, 2.5 $CaCl_2$ and 1.2 $MgCl_2$, then a gas mixture (95% O_2, 5% CO_2) was applied for 10 min to dissolve the $CaCl_2$ and incubated at 37°C in a water bath. Treatments (i.e., the MC, VC, and 0.5mM

C16:0) were prepared and incubated at 37°C for 1h to allow conjugation of the fatty acid to the vehicle. To prepare the dye, the pHrodo probe was added to powerload concentrate (1:10 dilution), then diluted further in LCIM (1:10). To prepare slides for imaging, the culture medium was removed, and cells were washed once in LCIM. The cells were then incubated in the dye for 30 min at 37°C, 5% CO_2. After a 30 min incubation period, the dye was removed, and cells were washed in LCIM.

Cells were subsequently imaged in LCIM at 37°C using a Nikon Ti Eclipse spinning disk confocal microscope (20x objective) and Metamorph imaging software. Excitation/emission was set to 470/533 nm (green probe) or 555/580 nm (red probe). A timelapse of the cells was acquired, where 1 image was captured every 4 sec for 20 min, providing a total of 301 time points. At the 26^{th} time point, the MC, VC or C16:0 was slowly injected (at 1:10 dilution) onto the cells. The same process was completed for each well, with the only disparity being the injected treatment (MC/VC/C16:0). All experiments were performed on three separate occasions using two replicate wells (for EndoC-βH1 cells) or either one or three replicate wells (for INS-1 832/13 cells) per each experimental condition. Quantitative analysis was carried out as described in section 4.2.4.3.

4.2.4.3 Quantitative analysis

Intracellular pHrodo dye fluorescence was quantified using *ImageJ* (version 1.53k) (434). Using *ImageJ*, a region of interest (ROI) was drawn around 20 cellular membranes to isolate each cell. The multi-measure function was used to measure the mean grey value (the sum of the grey values in the ROI divided by the number of pixels) in each ROI in all 301 time points. Using freehand selections in *ImageJ*, 20 circles were drawn to select the background, avoiding the cells. Again, the mean grey value was calculated in *ImageJ*. The average background for each time point was then calculated in excel. To obtain a more accurate measure of fluorescence intensity of the cells, the average background for each time point was subtracted from each ROI (each cell) in that time point. Then, the average fluorescence intensity was calculated for each time point (without background).

For comparisons of the INS-1 832/13 and the EndoC-βH1 data, min-max normalisation was used to quantify intracellular pHrodo dye fluorescence, where the minimum fluorescence intensity was assigned "0" and the maximum fluorescence intensity was assigned "1". The following equation was applied:

$$\frac{(\text{average fluorescence intensity} - \text{minimum fluorescence intensity})}{(\text{maximum fluorescence intensity} - \text{minimum fluorescence intensity})}$$

For the EndoC-βH1 data, the average fluorescence intensity for cells treated with VC/C16:0 was also normalised to the average fluorescence intensity for cells treated with serum-free media only. This method of normalisation involved taking the average fluorescence intensity of cells treated with VC/C16:0 at each time point and dividing this value by the average fluorescence intensity of cells treated with serum-free media only at each time point. A global average for each treatment was then calculated and visualised using line charts.

To further quantify uptake of the VC/C16:0, the mean fold change from basal fluorescence intensity to maximum intensity was calculated. To determine the rate of uptake, the time taken to reach maximum intensity was also calculated (time at maximum fluorescence intensity – time at the point of acute injection).

4.2.4.4 Optimisation of quantitative analysis

Initially, min-max normalisation was used to quantify intracellular pHrodo dye fluorescence. Ultimately, the average fluorescence intensity for cells treated with VC/C16:0 to treated with serum-free media only was selected as the normalisation method, as this technique was found to retain more information. However, both methods of normalisation are viable.

4.2.5 Inhibiting dynamin-mediated endocytosis

EndoC-βH1 cells were seeded in a 6-well plate (Table 4.2) 24h before the experiment. On the day of imaging, LCIM and treatments were prepared as described previously (section 4.2.4.2).

The pHrodo dye was prepared as outlined previously (section 4.2.4.2), but with the inclusion of dimethyl sulfoxide (DMSO) (control) or Dyngo-4a (a dynamin inhibitor (Figure 4.2)). This yielded a final concentration of 0.001% (v/v) for DMSO or 50μM Dyngo-4a. The dye mixtures were then incubated at 37°C. Cells were then exposed to pHrodo dye/LCIM +/- Dyngo-4a for 30 min, following the same procedure described in section 4.2.4.2. When imaging, the VC or C16:0 was slowly injected (at 1:10 dilution) at the 26th time point.

The results obtained from this assay were provided by Dr Patricia Thomas. Experiments were performed on two separate occasions using 3 replicate wells for each experimental condition. I carried out a third repetition (Appendix B – Supplementary Figure 3), however, this result could not be included in the results section of this thesis due to an issue with the microscope when using the pHrodo red probe, resulting in large fluctuations in fluorescence intensity.

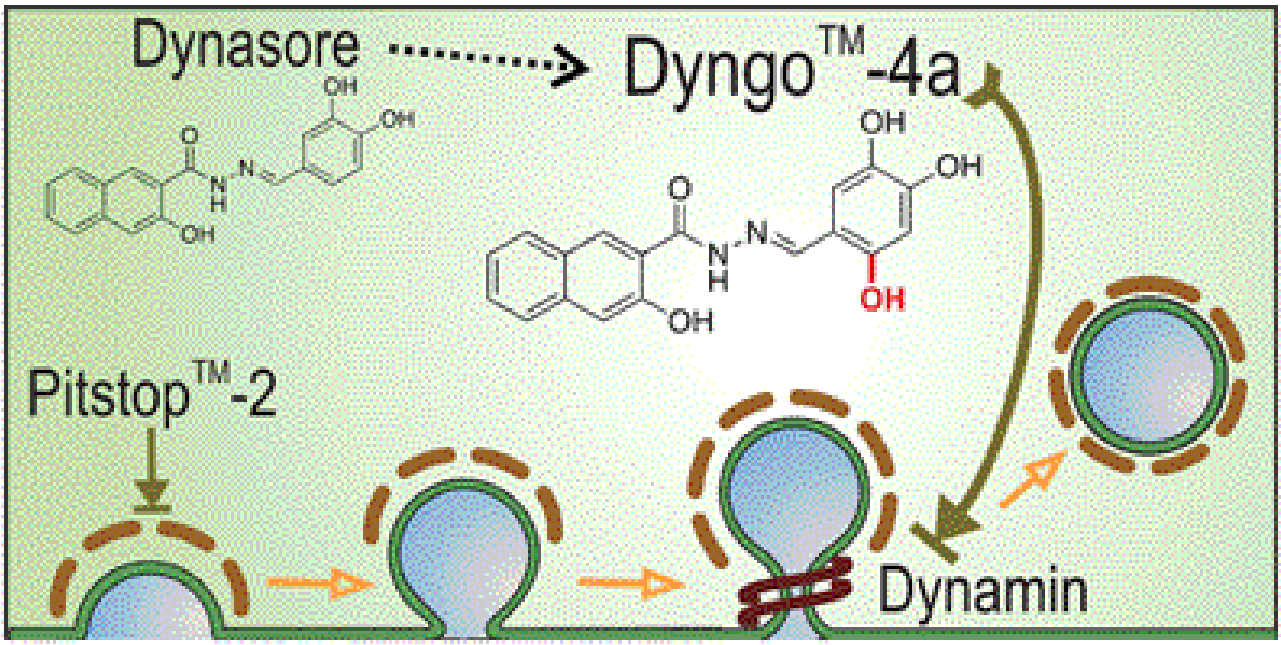

Figure 4.2 Dyngo-4a inhibits dynamin I and dynamin-mediated endocytosis. Dyngo-4a is an analogue of dynasore (a dynamin inhibitor). Dynamin is a GTPase, that is essential for several types of endocytosis including clathrin- and caveolae-mediated endocytosis (218). Figure taken from McCluskey et al (401).

4.2.5.1 Quantitative analysis

Min-max normalisation was used to quantify the intracellular pHrodo dye fluorescence, as outlined in section *4.2.4.3.*

4.2.6 Determining the lipid phase of the membrane

4.2.6.1 Laurdan

The fluorescent probe 2-Dimethylamino-6-lauroylnaphthalene (Laurdan) has been used in many membrane studies (435, 436, 437) to distinguish the lipid phase of the membrane. This dye is incorporated into the plasma membrane, where it is evenly distributed (438). The function of this probe is attributed to its sensitivity to the polarity of its environment, such that variations in the water content in the membrane causes shifts in the emission spectrum (439). This is because water is a polar molecule, due to the uneven distribution of electrons between oxygen and hydrogen atoms that it is

composed of (440). In this way, the difference in polarity detected by Laurdan is thought to be a consequence of the changes in number and/or mobility of these water particles present at the glycerol backbones of the phospholipids in the membrane (439). Laurdan fluoresces more intensely at blue wavelengths (when the membrane is in the gel/liquid ordered phase), where the emission maximum is read at 430~470nm according to the work of Pilkington et al. (441). Conversely, the emission maximum shifts to green wavelengths when the membrane is in the liquid disordered phase, read at 480~550nm (441). Then, to quantify the order of the membrane, the spectral properties of this probe can be analysed using the generalised polarisation (GP) value (435).

4.2.6.2 Laurdan assay

INS-1 832/13 and EndoC-βH1 cells were seeded on coverslips in a 12-well plate (please refer to Table 4.2 for seeding density), 24h before the experiment. Cells were then exposed to one of the following treatments: 1) VC, 2) 375μM C16:0 and 125μM C18:1, 3) 125μM C16:0 and 375μM C18:1, and 4) 250μM C16:0 and 250μM C18:1.

Treatments were added to cells at 1:10 dilution in serum-free media. Cells were then incubated for 1, 3 or 5 days before fixing. For 5-day treatments, cells were replenished with nutrients on the 3rd (ideally) or 4th day.

After the specified incubation period (1 day, 3 days or 5 days), media was removed from the cells 3 wells at a time, to prevent dehydration of the cells. The cells were then washed once in LCIM (made up as described in section 4.2.4.2) and Laurdan (4mM suspended in DMSO) was added to each well (12.5μl dye + 988μl LCIM). Cells were then incubated with the dye for 30 min at 37°C, in a 5% CO_2 atmosphere, then washed once in LCIM. An equal ratio of LCIM and 4% (w/v) paraformaldehyde (PFA) was added to each well and cells were incubated at room temperature for 15 min. Fixed cells were then washed twice in phosphate-buffered saline (PBS) and coverslips were mounted onto slides,

using a fluorescence mounting medium (Dako, Agilent). Slides were stored for at least 48h to ensure the mounting media had solidified. Imaging was carried out using a Nikon eclipse Ti2 equipped with a spinning disk and N-SIM units (100x oil immersion objective), using NIS-Elements software. Excitation was set to 405nm, and emissions were read at 430-470nm for the gel/liquid ordered phase (blue) and at 480-550nm for the liquid disordered phase (green). All experiments were performed on 4 separate occasions.

4.2.6.3 Experimental optimisation of the Laurdan assay

Cells were originally seeded at 0.5 x 10^6 cells/ml (1 ml/well), but this returned a high confluency (~75%). To optimise, cells were seeded at 0.2 x 10^6 cells/ml (~50% confluency).

4.2.6.4 Quantitative analysis

Quantitative analysis of membrane order for rat INS-1 832/123 and human EndoC-βH1 cells was kindly undertaken by Luca Panconi. Briefly, cell membranes were identified using CellPose segmentation software version 1.0 in Python version 3.8 (442) by locating cells with a mean diameter of 10μm (the approximate size of a pancreatic β-cell) (Figure 4.3) (265). Whole-cell outlines were obtained, and their corresponding GP values were computed (I_1-I_2/ I_1+I_2 where I_1 refers to the ordered channels and I_2 the disordered) to determine the average membrane GP values for each cell. Outward-facing cell membranes, from cell clusters, were then detected using the TOBLERONE cell segmentation package version 1.0.0 (443) in the R programming language version 4.2.1 (Figure 4.3). The difference between the whole-cell membranes and outward-facing membranes was calculated to determine the inward-facing membranes (i.e., intercell membranes) (Figure 4.3) and GP values were obtained from both outlines. Statistical analyses were undertaken in RStudio Desktop version 2022.07.1.554.

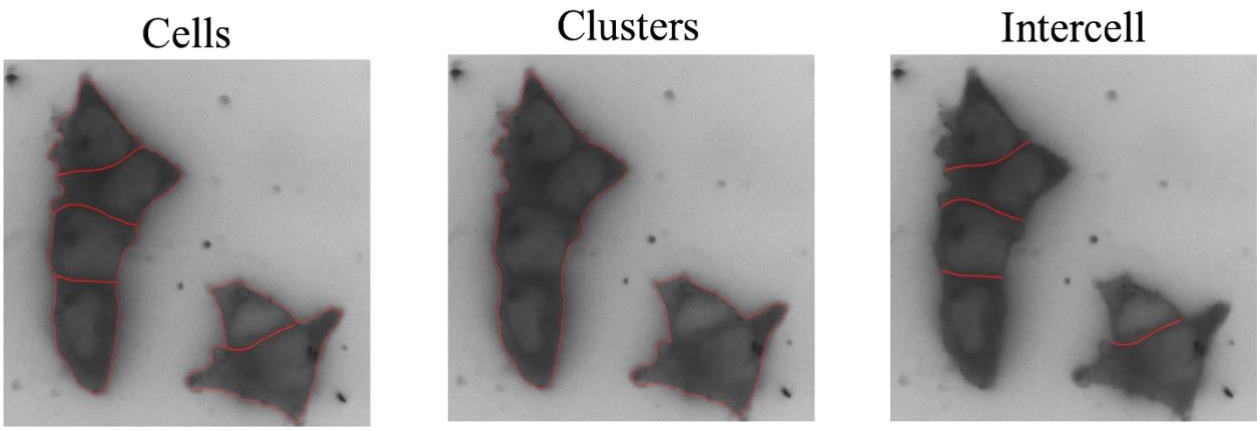

Figure 4.3 Determination of cell membrane borders. CellPose is used to determine individual cell segmentation (i.e., the whole-cell membrane) (left). TOBLERONE is used to determine cell segmentation of the outward-facing membranes of cell clusters (middle) and the segmentation of cell membranes that are connecting with other membranes (intercell membranes) (right). The images presented here were kindly provided by Luca Panconi.

4.2.6.5 Optimisation of quantitative analysis

Initially, GP analysis was conducted using a plugin in *ImageJ* (version 1.53k) (434), using an in-house script kindly provided by Dr Meurig Gallagher, adapted from Owen et al. (444). Ultimately, however, using the CellPose segmentation software and TOBLERONE software for analysis (section 4.2.6.4) was ideal for this experiment as it enabled confirmation of the membrane localisation of Laurdan, as well as the examination of membrane domains (outward- and inward-facing membranes, as well as whole cell membranes).

4.3 Results

4.3.1 The rate of LC-SFA uptake in human and rodent pancreatic β-cells

The rate of LC-FFA uptake can be used to determine whether transport is via simple diffusion or a protein-mediated process. According to Fick's law of diffusion and Michaelis-Menten saturation kinetics, passive diffusion displays a linear relationship (uptake vs. time) (405), whereas protein-

mediated uptake is a saturable process (i.e., transport reaches a maximum when all solute binding sites are occupied) (207, 406).

To gain insight into whether acute C16:0 uptake into EndoC-βH1 and INS-1 832/13 cells is via simple-diffusion or a protein-mediated process, the rate of acute C16:0 uptake into EndoC-βH1 and INS-1 832/13 cells was measured. It was observed here that the time taken to reach maximum fluorescence intensity (i.e., for the maximum increase in pH) was rapid following C16:0 injection in EndoC-βH1 (80 seconds) and INS-1 832/13 cells (108 seconds), suggesting that the uptake of C16:0 is rapid in these cell types (Table 4.3). Interestingly, the mean fold change in fluorescence intensity was markedly smaller following the acute injection of C16:0 to EndoC-βH1 cells when compared to the acute injection of BSA to EndoC-βH1 cells, or BSA/C16:0 to INS-1 832/13 cells, which could imply that the uptake of C16:0 into EndoC-βH1 cells is restricted (Table 4.3). Remarkably, the VC also appeared to be rapidly taken up in both EndoC-βH1 and INS-1 832/13 cells, with an extremely similar time taken to reach maximum fluorescence intensity in both cell lines (Table 4.3). Overall, following acute injection of 0.5mM C16:0, uptake was rapid but modest in both EndoC-βH1 and INS-1 832/13 cells (Figure 4.4) and, intriguingly, a similar pattern was observed following the injection of the vehicle in both cell lines (Figure 4.4). Moreover, a similar pattern of VC and C16:0 uptake is shown in EndoC-βH1 cells using a different normalisation method (Figure 4.5).

Taken together, this evidence suggests that the acute uptake of C16:0 and BSA is a saturable process in both EndoC-βH1 and INS-1 832/13 cells.

Table 4.3 Mean fold change in fluorescence intensity and the time taken to reach maximum intensity following the injection of palmitate (C16:0) or the vehicle (VC). Data is included from three independent experiments using min-max normalisation.

Cell line	Acute injection	Mean fold change in fluorescence intensity	Time taken to reach maximum fluorescence intensity (seconds)
EndoC-βH1	VC	2.1	152
	C16:0	1.2	80
INS-1 832/13	VC	2.4	156
	C16:0	2.3	108

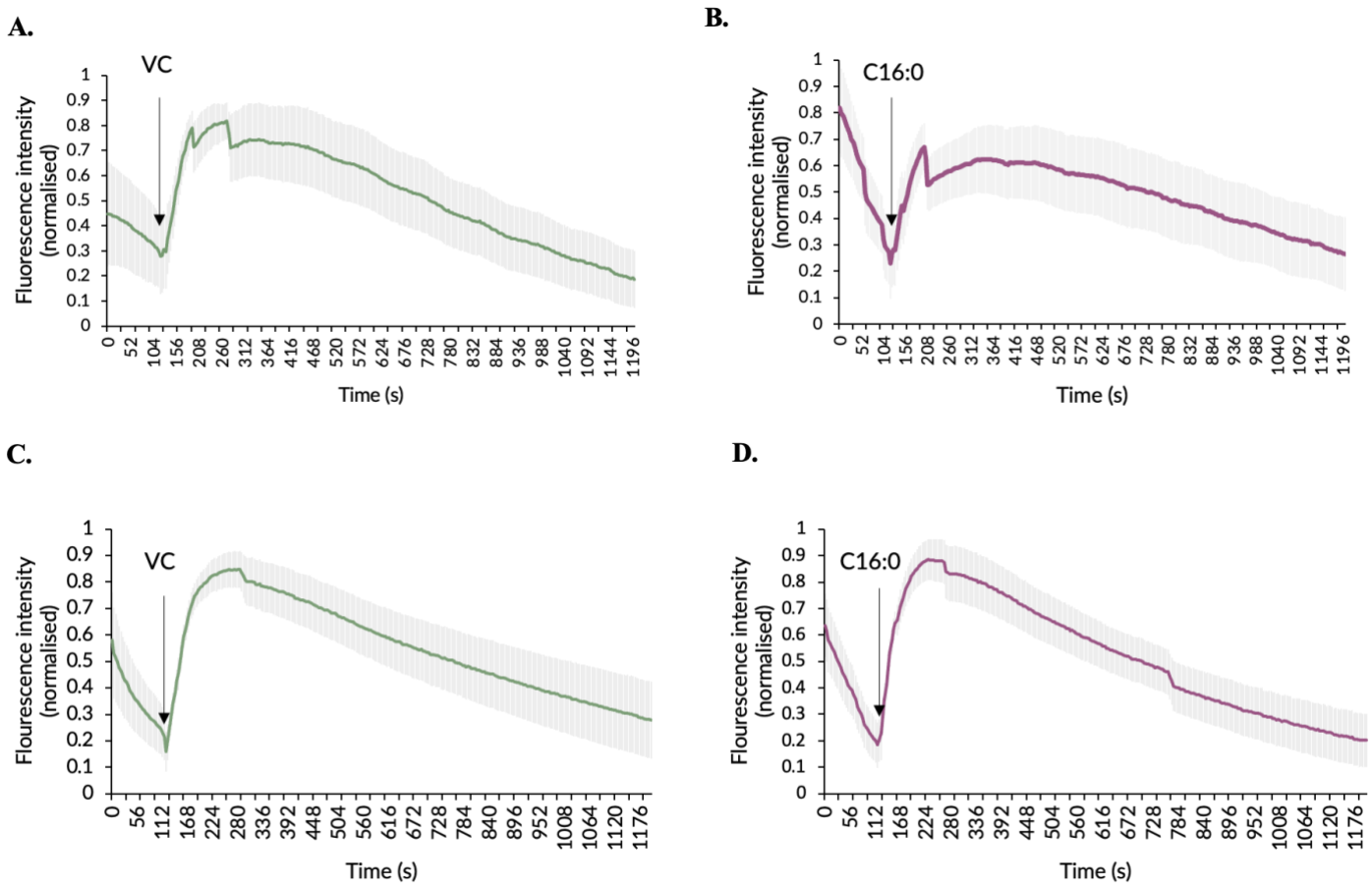

Figure 4.4 Acute uptake of palmitate and the vehicle in human-derived EndoC-βH1 cells and rat-derived INS-1 832/13 cells. EndoC-βH1 and INS-1 832/13 cells were incubated with pHrodo Green AM intracellular pH indicator for 30 min. After 30 min, the pH indicator was removed, and cells were imaged in live cell imaging media. Basal intracellular pH (fluorescence intensity) was measured for 104 s. After 104 s, EndoC-βH1 **(A and B)** and INS-1 832/13 **(C and D)** cells were injected with the vehicle control (VC) **(A and C)** or 0.5mM C16:0 **(B and D)**; intracellular pH was measured every 4 s for a total of 20 min. Imaging was conducted on a Nikon Ti Eclipse spinning disk confocal using an excitation/emission of 470/533 nm. To quantify changes in intracellular pH, the fluorescence intensity of time series images was analysed using ImageJ. All data was normalised using min-max normalisation. Results are displayed as the mean ± S.E.M, representative of three independent experiments.

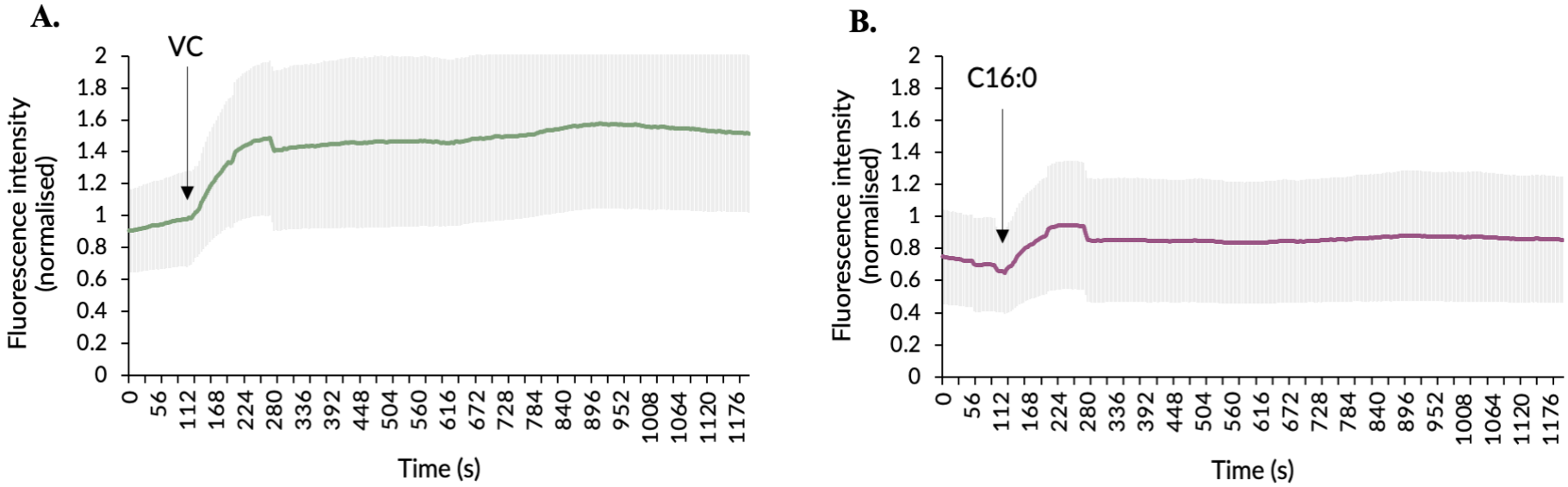

Figure 4.5 Acute uptake of palmitate and the vehicle in human-derived EndoC-βH1 cells. EndoC-βH1 cells were incubated with pHrodo Green AM intracellular pH indicator for 30 min. After 30 min, the pH indicator was removed, and cells were imaged in live cell imaging media. Basal intracellular pH (fluorescence intensity) was measured for 104 s. After 104 s, EndoC-βH1 cells were injected with the vehicle control (VC) **(A)** or 0.5mM C16:0 **(B)**; intracellular pH was measured every 4 s for a total of 20 min. Imaging was conducted on a Nikon Ti Eclipse spinning disk confocal using an excitation/emission of 470/533 nm. To quantify changes in intracellular pH, the fluorescence intensity of time series images was analysed using ImageJ. Data was normalised using the rate of uptake of serum-free media only into cells. Results are displayed as the mean ± S.E.M, representative of three independent experiments.

4.3.2 Effects of inhibition of dynamin-mediated endocytosis on LC-SFA uptake in human pancreatic β-cells

Hao et al. (219) have recently proposed a model of LC-FFA uptake in adipocytes that involves an endocytosis-mediated process. However, to the best of our knowledge, this has not yet been investigated in pancreatic β-cells. Thus, in the present study, we sought to examine the role of dynamin-mediated endocytosis in the uptake of the LC-SFA, C16:0, in the human pancreatic β-cell line, EndoC-βH1. To establish whether dynamin-mediated endocytosis is involved in the uptake of C16:0 across the plasma membrane of β-cells, we have determined the acute uptake of C16:0 and the vehicle (BSA) in the presence and absence of a potent dynamin inhibitor (Dyngo-4a) (Figure 4.6). Strikingly, the uptake of both the vehicle and C16:0 was prevented in the presence of Dyngo-4a, which is shown by a steep reduction in intracellular fluorescence (i.e., a considerable increase in intracellular pH). A similar trend was also observed using a third repetition (Appendix B - Supplementary Figure 3), however, the results were not included in the results section of this chapter due to an issue with the microscope light source. Due to these issues, we accept that this is a limitation of this thesis as, without a third repeat, we are unable to determine the significance of the results shown here. Given the trend, these results indicate that C16:0 may be taken into pancreatic β-cells via a dynamin-mediated process, which supports the role of proteins in LC-SFA uptake. However, further repeats are necessary, along with further experiments, to eliminate the possibility of off-target effects. Moreover, as the observations made here were carried out using qualitative data, additional repeats should be carried out to quantify specific differences in response (i.e., to compare the mean fold change in fluorescence intensity, following injection of VC or C16:0, between control (DMSO) and Dyngo-4a treated cells).

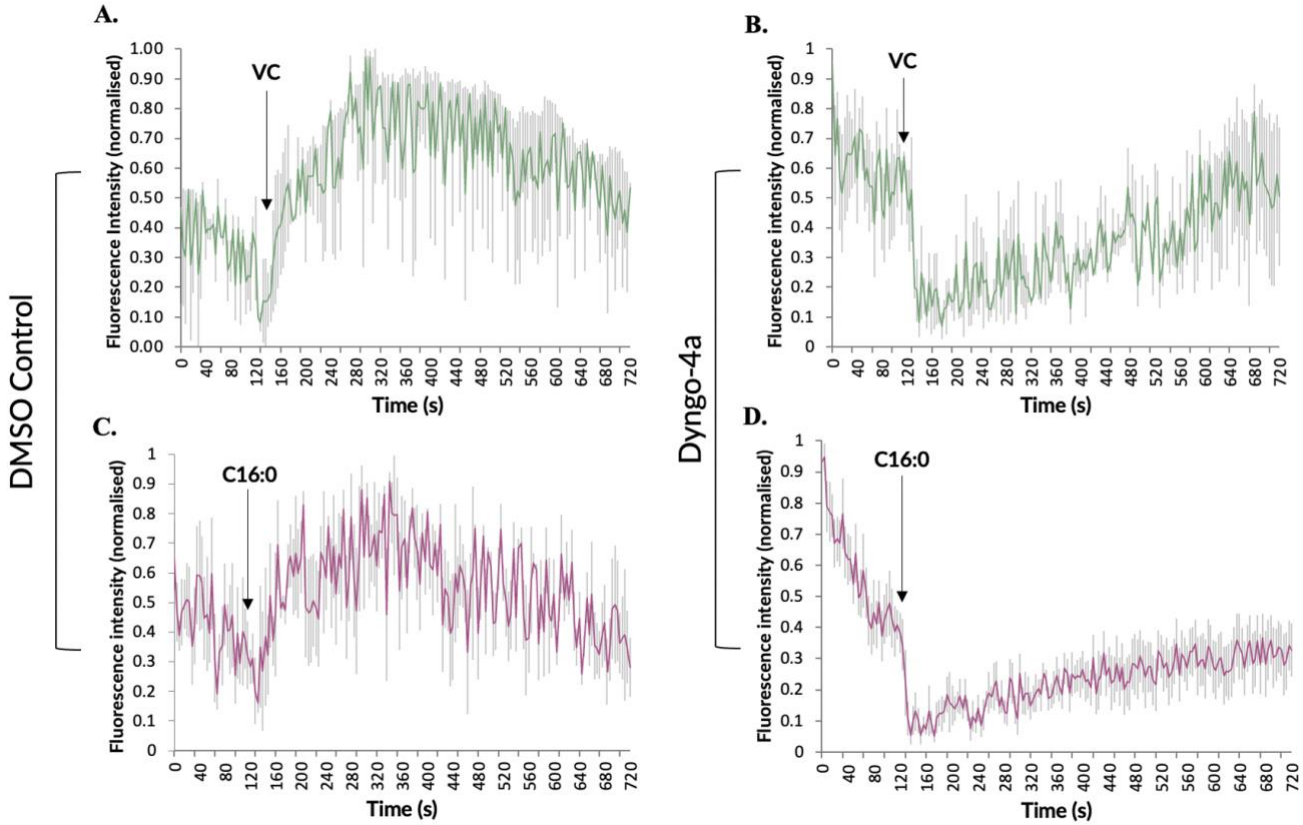

Figure 4.6 Acute uptake of palmitate (C16:0) and the vehicle in EndoC-βH1 cells is prevented in the presence of an inhibitor of dynamin-mediated endocytosis (Dyngo-4a). EndoC-βH1 cells were pretreated with either 0.001% (v/v) DMSO control **(A and C)** or 50μM Dyngo-4a suspended in 0.001% (v/v) DMSO **(B and D)** and incubated with pHrodo Red AM intracellular pH indicator for 30 min. After 30 min, Dyngo-4a/DMSO and the pH indicator were removed, and cells were imaged in live cell imaging media. Basal intracellular pH (fluorescence intensity) was measured for 104 s. After 104 s, EndoC-βH1 cells were injected with the BSA vehicle control (VC) **(A and B)** or 0.5mM palmitate (C16:0) **(C and D)**; intracellular pH was measured every 4 s for a total of 20 min. Imaging was conducted on a Nikon Ti Eclipse spinning disk confocal using an excitation/emission of 555/580 nm. To quantify changes in intracellular pH, the fluorescence intensity of time series images was analysed using ImageJ. Results are displayed as the mean ± S.E.M, representative of two independent experiments. The graphs presented here were derived from the work of Dr Patricia Thomas.

4.3.3 The lipid phase of the plasma membrane in human and rodent pancreatic β-cells

After investigating of the involvement of protein-mediated processes in LC-SFA uptake, this study next sought to explore the role of passive diffusion in LC-SFA uptake. As outlined in section 4.1.2.2, Ghysels et al. (412) have previously suggested that the lipid composition of the plasma membrane could regulate the uptake of substances by passive diffusion. Further, Bastiaanse et al. (424) and Stieger et al. (426) have proposed that the lipid composition of the membrane might influence membrane protein dynamics, thereby disrupting the function of proteins that regulate transport of substances across the plasma membrane. Due to their ease of culture, this experiment was first optimised in the rat-derived INS-1 832/13 cell line, by exploring the composition of the cell membrane in INS-1 832/13 cells prior to experiments using EndoC-βH1 cells. The lipid phase of the membrane was explored in INS-1 832/13 cells and human pancreatic β-cells, following culture for 1, 3 and 5 days in varying ratios of the LC-SFA, C16:0, and the LC-MUFA, C18:1, including: 1) VC only, 2) 250μM C16:0 and 250μM C18:1, 3) 125μM C16:0 and 375μM C18:1, or 4) 375μM C16:0 and 125μM C18:1.

On account of the importance of the findings detailed below, results are displayed following 3-day incubation (Figure 4.7). Similar results were also obtained following 1 and 5-day culture, however this data was omitted due to the length of this thesis (data available upon request).

Differences in GP values between human and rodent β-cells were averaged for cells cultured in each treatment for 3 days (Figure 4.7). Strikingly, there was a considerable difference in GP values between the human-derived EndoC-βH1 cells and rat-derived INS-1 832/13 groups (EndoC-βH1 cells averaged at around -0.8 whereas INS-1 832/13 averaged at around 0.80), which suggests that the membrane of INS-1 832/13 cells is much more ordered than the membrane of EndoC-βH1 cells. Intriguingly, there was a significant difference between INS-1 832/13 and EndoC-βH1 cells treated with the VC only, which suggests that the membrane order is different in rat pancreatic β-cells when

compared to human, even without the presence of LC-FFAs. To the best of our knowledge, this is the first study to report that the order of the lipid membrane is markedly different in rat pancreatic β-cells when compared to human pancreatic β-cells.

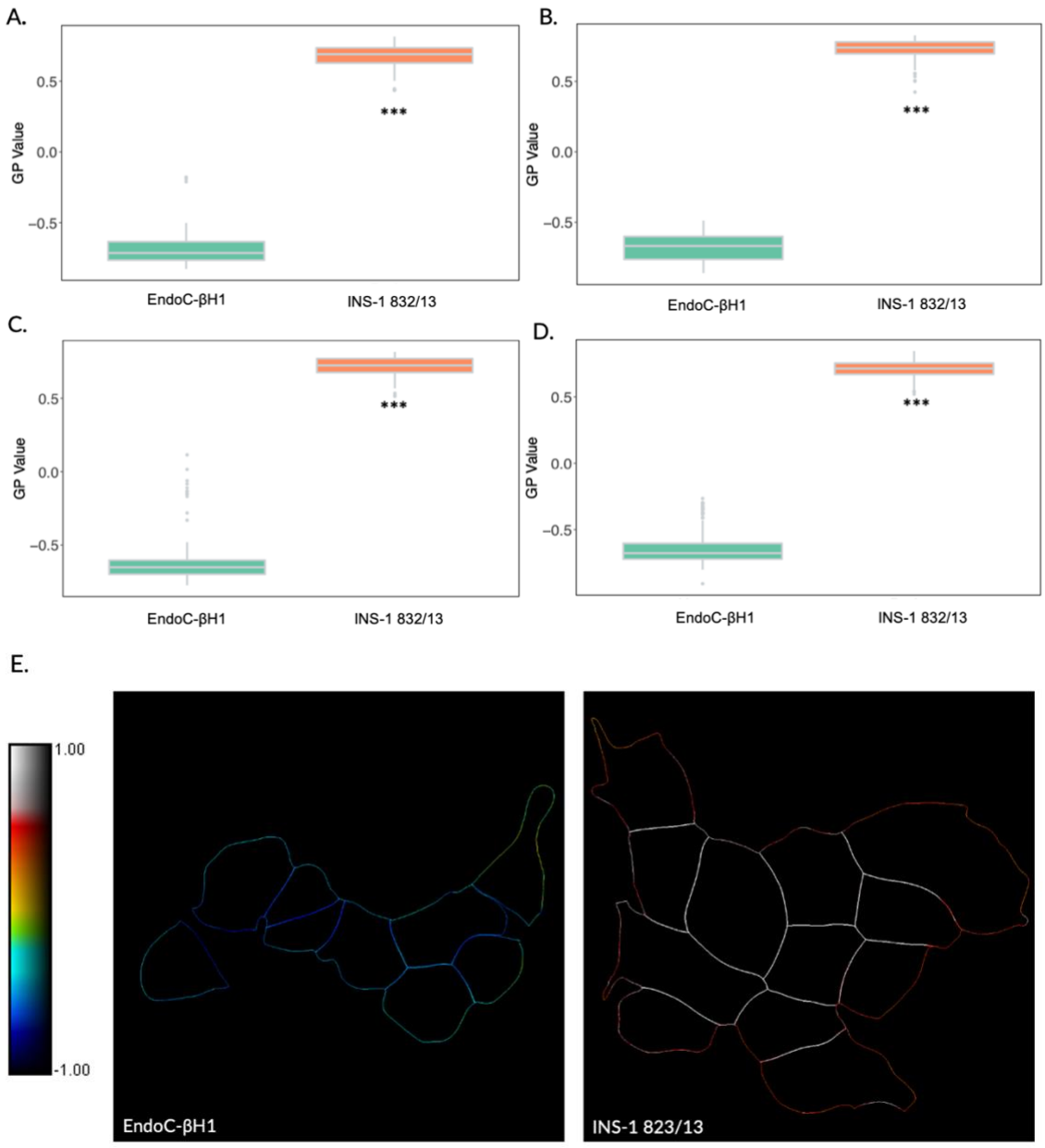

Figure 4.7 The lipid phase of the membrane is different between human and rodent pancreatic β-cells. EndoC-βH1 and INS-1 832/13 cells were cultured for 3 days in either vehicle control only (A), 250µM C16:0 and 250µM C18:1 (B), 125µM C16:0 and 375µM C18:1 (C), or 375µM C16:0 and 125µM C18:1 (D). Box and whisker plots display the distribution of the generalised polarisation (GP) values, where the central line represents the median GP value, the whiskers represent the minimum and maximum GP value, and the ends of the boxes represent the upper and lower quartiles. P-values are relative to the mean GP value of EndoC-βH1 cells, where *** denotes $p<0.001$.

Pseudocoloured images depict the GP values of a cluster of EndoC-βH1 and INS-1 832/13 cells treated for 3 days with vehicle control only are shown (E), where blue illustrates the liquid disordered phase and red illustrates the gel/liquid ordered phase. Data included from 2-3 individual experiments. Graphs and pseudocoloured images presented here were kindly provided by Luca Panconi.

4.3.4 The lipid phase of the plasma membrane in human-derived EndoC-βH1 cells following 1-, 3-, and 5-day culture in varying ratios of LC-SFA:LC-MUFA

The ratio of saturated to unsaturated FFA in the membrane is thought to alter membrane fluidity, such that saturated FFAs make the membrane more rigid (i.e., towards the L_o phase) whereas unsaturated FFAs increase membrane fluidity (i.e., towards the L_d phase) (see section 4.1.2.1) (411). As such, the lipid phase of the membrane was examined in human pancreatic β-cells (Figure 4.8), following culture for 1, 3 and 5 days in varying levels of the LC-SFA, C16:0, and the LC-MUFA, C18:1, including: 1) VC only, 2) 250μM C16:0 and 250μM C18:1, 3) 125μM C16:0 and 375μM C18:1, or 4) 375μM C16:0 and 125μM C18:1.

Cells cultured for 1, 3 or 5 days in VC alone (BSA), or in 250μM C16:0 and 250μM C18:1, did not show any significant difference in membrane order. On the other hand, the whole-cell membranes of EndoC-βH1 cells cultured in 375μM C16:0 and 125μM C18:1 showed a significant increase in membrane order at 3 days ($p<0.05$), which was in line with the expected hypothesis. Surprisingly, however, the whole-cell membranes of EndoC-βH1 cells cultured in 125μM C16:0 and 375μM C18:1 also showed significantly increased membrane order at 1 day ($p<0.01$) and 3 days ($p<0.05$). Taken together, these results suggest that a high level of either the LC-SFA, C16:0, or the LC-MUFA, C18:1, can alter the composition of the β-cell plasma membrane by reducing membrane fluidity.

No significant difference in GP value was observed for inward-facing cell membranes nor outward-facing cell membranes following culture in any of the treatments, which could indicate that the culture

of pancreatic β-cells in varying ratios of LC-SFA:LC-MUFA does not impact the membrane order of outward-facing and inward-facing cell membranes, or it could imply an experimental error.

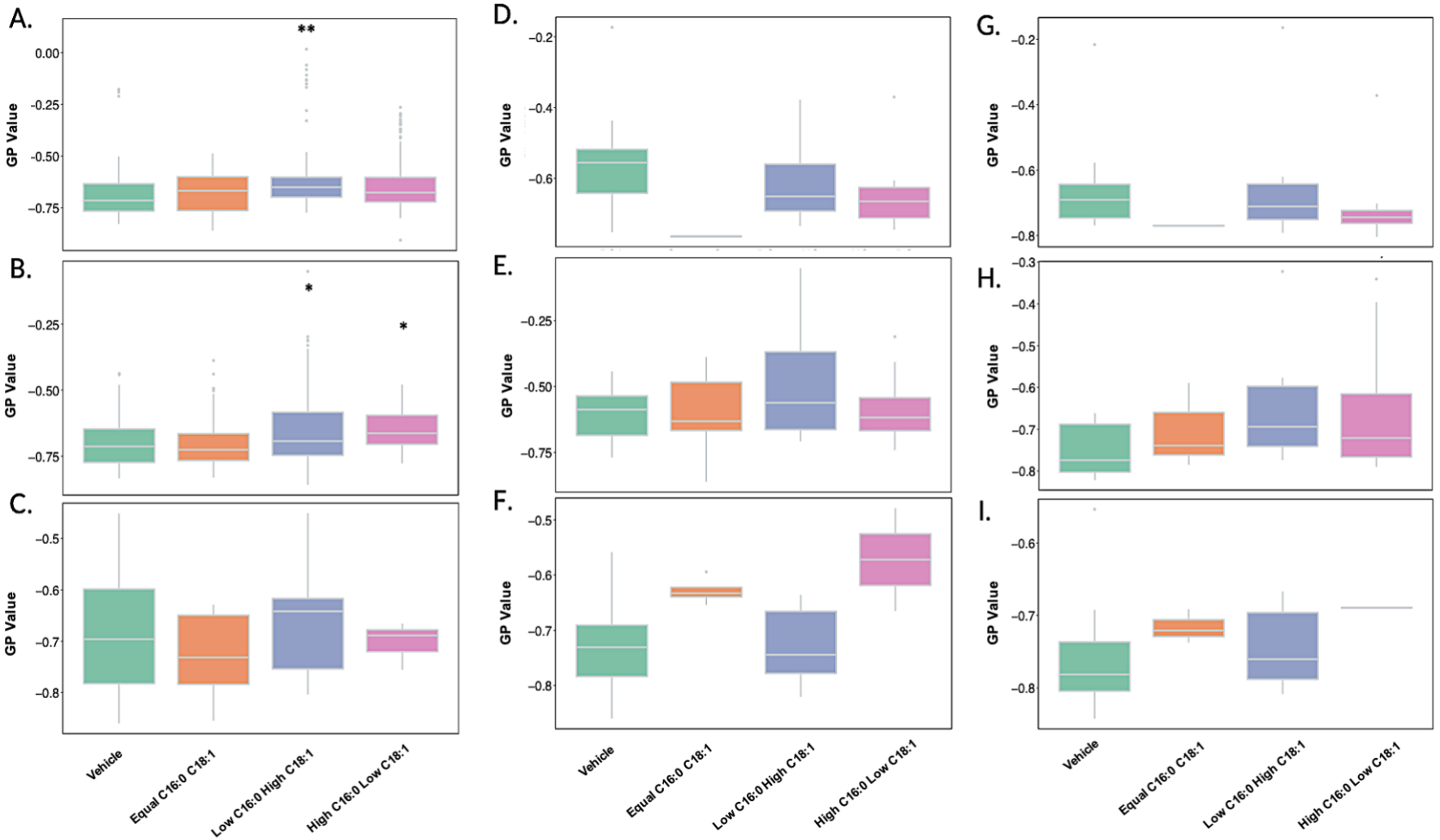

Figure 4.8 The lipid phase of the membrane in human pancreatic β-cells following 1-, 3-, and 5-day culture in varying ratios of LC-SFA:LC-MUFA. EndoC-βH1 cells were cultured for 1 **(A, D, G)**, 3 **(B, E, H)** and 5 **(C, F, I)** days in either the vehicle (BSA/EtOH), 250μM C16:0 and 250μM C18:1 (Equal C16:0 C18:1), 125μM C16:0 and 375μM C18:1 (Low C16:0 High C18:1), or 375μM C16:0 and 125μM C18:1 (High C16:0 Low C18:1) before cell membranes were labelled with the fluorescent probe Laurdan for 30 min. Cells were then fixed

in paraformaldehyde. Imaging was conducted on a Nikon eclipse Ti2 using an excitation of 405nm, and emissions of 430-470nm for the gel/liquid ordered phase (blue) and 480-550nm for the liquid disordered phase (green). Confocal images were analysed using CellPose and TOBLERONE segmentation softwares to quantify generalised polarisation (GP) values. Box and whisker plots display the distribution of the GP values of whole-cell membranes **(A-C)**, outward-facing membranes **(D-F)** and inward-facing membranes **(G-I)**. The central line of each box and whisker plot represents the median GP value, the whiskers represent the minimum and maximum GP value, and the ends of the boxes represent the upper and lower quartiles. * $p<0.05$ and ** $p<0.01$ relative to the vehicle. Results are representative of three independent experiments. All graphs presented here were kindly provided by Luca Panconi.

4.3.5 The rate of LC-SFA uptake in human pancreatic β-cells following 3-day culture in varying ratios of LC-SFA:LC-MUFA

Alongside investigations of the lipid phase of the plasma membrane following culture in varying ratios of LC-SFA:LC-MUFA, this study investigated whether culturing cells in varying ratios of LC-SFA:LC-MUFA for 3 days could influence the rate of C16:0 or VC uptake.

It was observed here that in EndoC-βH1 cells cultured for 3 days in the VC only (BSA), the acute uptake of the VC is inhibited, whereas the uptake of C16:0 is rapidly elevated (nearly 6-fold in 132 seconds) (Table 4.4) (Figure 4.9). In 250μM C16:0 + 250μM C18:1, however, acute uptake of C16:0 into cells was inhibited, whereas the VC increased (2.2-fold) in a slow, linear fashion (1064 seconds) (Table 4.4) (Figure 4.10). Taken together, these results imply that the order of the plasma membrane of human β-cells does not play a role in LC-SFA uptake.

As stated above, EndoC-βH1 cells cultured for 3 days in 125μM C16:0 + 375μM C18:1 or 375μM C16:0 + 125μM C18:1 show an increase in membrane order when compared to cells cultured in BSA alone. Interestingly, for cells cultured in 125μM C16:0 + 375μM C18:1, the uptake of C16:0 and the VC was slow and modest (Table 4.4) (Figure 4.11). In cells cultured in 375μM C16:0 + 125μM C18:1 for 3 days, however, acute uptake of the VC was 4.8-fold compared to baseline, whereas uptake of C16:0 was seemingly prevented (Table 4.4) (Figure 4.12). Collectively, these results suggest that the treatment of EndoC-βH1 cells in varying ratios of LC-SFA:LC-MUFA can influence LC-SFA uptake rate. Further, the uptake of BSA seemingly occurs via a different mechanism to C16:0 uptake.

In section 4.3.1, it was shown that BSA is taken up into EndoC-βH1 cells following the culture of cells in 2% (w/v) BSA. Remarkably, however, culturing cells in a lower % BSA (1% (w/v)) and no LC-FFA appears to inhibit BSA uptake but promote C16:0 uptake (Figure 4.9). Taken together, these

results suggest that the culture of EndoC-βH1 cells in 1% (w/v) BSA and no LC-FFA could be a more appropriate model to study LC-FFA uptake.

Collectively, these results suggest that the order of the plasma membrane of human β-cells does not mediate LC-SFA uptake. Moreover, the uptake of BSA seemingly occurs via a different mechanism to C16:0 uptake. Finally, the culture of EndoC-βH1 cells in 1% (w/v) BSA and no LC-FFA could be a suitable model to study LC-FFA uptake, as LC-FFA uptake is promoted while the VC is not taken into the cell (i.e., the VC remains a control).

Table 4.4 Mean fold change in fluorescence intensity and the time taken to reach maximum intensity following the injection of palmitate (C16:0) or the vehicle (VC) after 3-day treatment of EndoC-βH1 cells in varying ratios of LC-SFA:LC-MUFA. Data is included from two or three independent experiments using min-max normalisation.

Treatment	**Acute injection**	**Mean fold change in fluorescence intensity**	**Time taken to reach maximum fluorescence intensity (seconds)**
VC	VC	1.0	1080
	C16:0	5.9	132
250uM C16:0 + 250uM C18:1	VC	2.2	1064
	C16:0	1.4	1048
125uM C16:0 + 375uM C18:1	VC	1.6	312
	C16:0	1.4	340
375uM C16:0 + 125uM C18:1	VC	4.8	160
	C16:0	1.5	1080

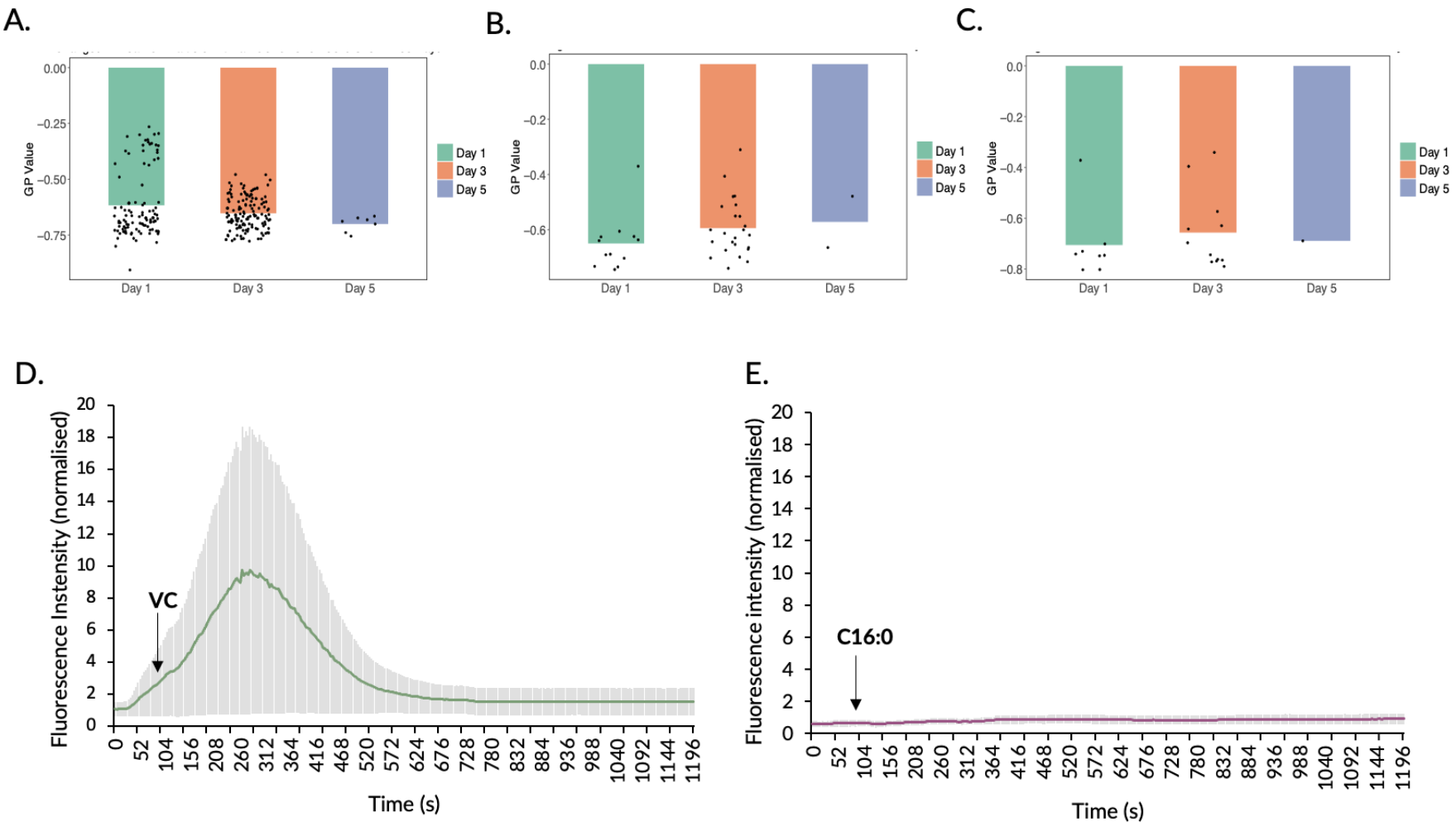

Figure 4.9 Acute uptake of palmitate and the vehicle in human-derived EndoC-βH1 cells following 3-day culture in the vehicle control only (BSA). (A-C) EndoC-βH1 cells cultured for 1, 3 or 5 days in the vehicle control (VC) only. The mean generalised polarisation (GP) values are displayed in bar charts for whole-cell membranes **(A)**, outward facing membranes **(B)** and intercell membranes **(C)**. Cell membranes labelled with the fluorescent probe Laurdan for 30 min. Cells were then fixed in paraformaldehyde. Imaging was conducted on a Nikon eclipse Ti2 using an excitation of 405nm, and emissions of 430-470nm for the gel/liquid ordered phase (blue) and 480-550nm for

the liquid disordered phase (green). Confocal images were analysed using CellPose and TOBLERONE segmentation softwares to quantify GP values. Each bar chart represents the mean GP value with independent data points. Graphs **A-C** provided by Luca Panconi. **(D and E)** EndoC-βH1 cells cultured for 3 days in VC only (BSA). Cells were incubated with pHrodo Green AM intracellular pH indicator for 30 min. After 30 min, the pH indicator was removed, and cells imaged in live cell imaging media. Basal intracellular pH (fluorescence intensity) was measured for 104 s. After 104 s, cells were injected with the VC **(D)** or 0.5mM palmitate (C16:0) **(E)**; intracellular pH was measured every 4 s for a total of 20 min. Imaging was conducted on a Nikon Ti Eclipse spinning disk confocal using an excitation/emission of 470/533 nm. To quantify changes in intracellular pH, the fluorescence intensity of time series images was analysed using ImageJ. Data was normalised to media. All results are representative of two or three independent experiments.

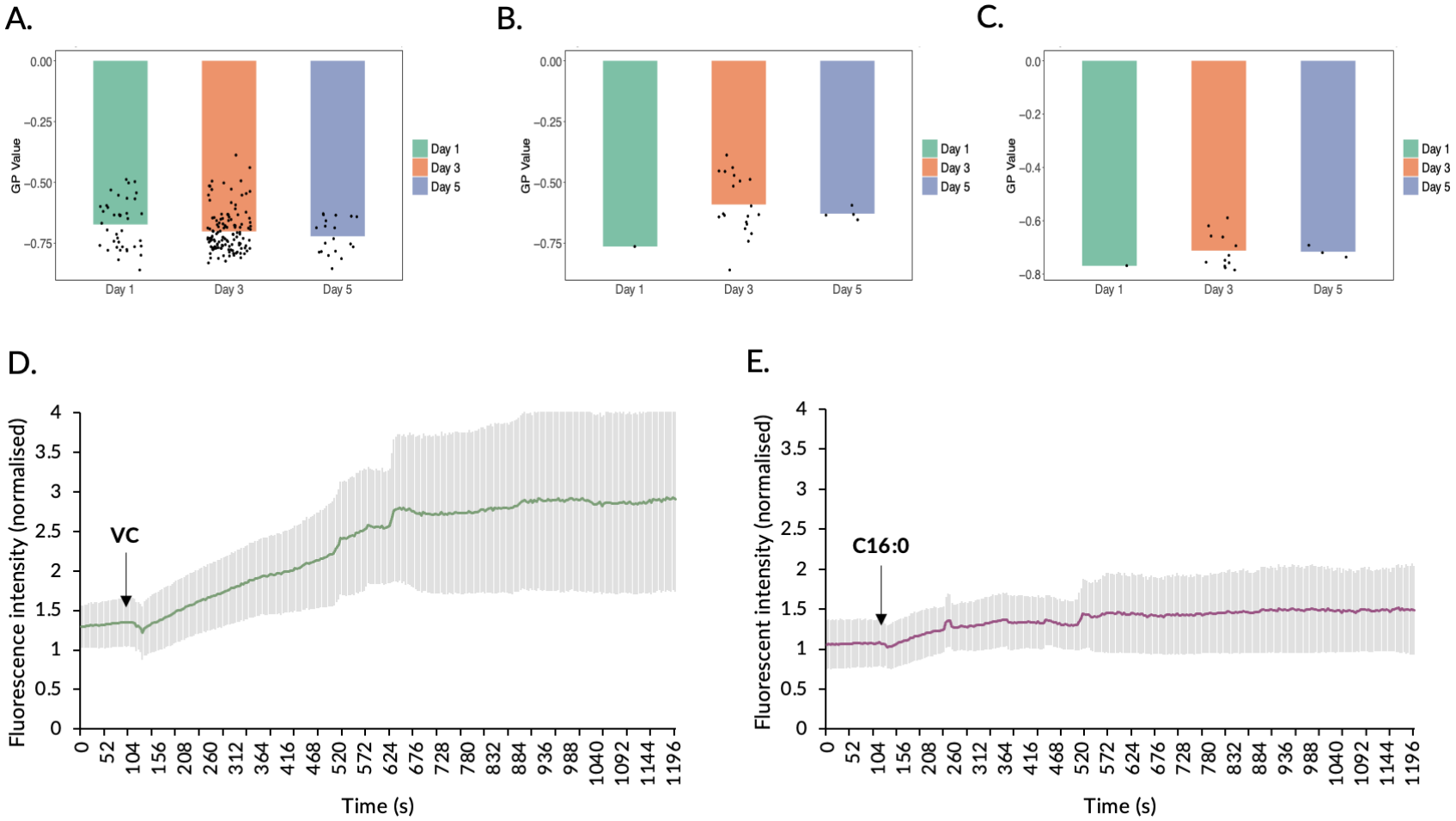

Figure 4.10 Acute uptake of palmitate and the vehicle in human-derived EndoC-βH1 cells following 3-day culture in 250µM C16:0 and 250µM C18:1. (A-C) EndoC-βH1 cells cultured for 1, 3 or 5 days in the culture in 250µM C16:0 and 250µM C18:1. The mean generalised polarisation (GP) values are displayed in bar charts for whole-cell membranes **(A)**, outward facing membranes **(B)** and intercell membranes **(C)**. Cell membranes labelled with the fluorescent probe Laurdan for 30 min. Cells were then fixed in paraformaldehyde. Imaging was conducted on a Nikon eclipse Ti2 using an excitation of 405nm, and emissions of 430-470nm for the gel/liquid ordered phase (blue) and 480-550nm for the liquid disordered phase (green). Confocal images were analysed using CellPose and TOBLERONE segmentation

softwares to quantify GP values. Each bar chart represents the mean GP value with independent data points. Graphs **A-C** provided by Luca Panconi. **(D and E)** EndoC-βH1 cells cultured for 3 days in VC only (BSA). Cells were incubated with pHrodo Green AM intracellular pH indicator for 30 min. After 30 min, the pH indicator was removed, and cells imaged in live cell imaging media. Basal intracellular pH (fluorescence intensity) was measured for 104 s. After 104 s, cells were injected with the VC **(D)** or 0.5mM palmitate (C16:0) **(E)**; intracellular pH was measured every 4 s for a total of 20 min. Imaging was conducted on a Nikon Ti Eclipse spinning disk confocal using an excitation/emission of 470/533 nm. To quantify changes in intracellular pH, the fluorescence intensity of time series images was analysed using ImageJ. Data was normalised to media. All results are representative of two or three independent experiments.

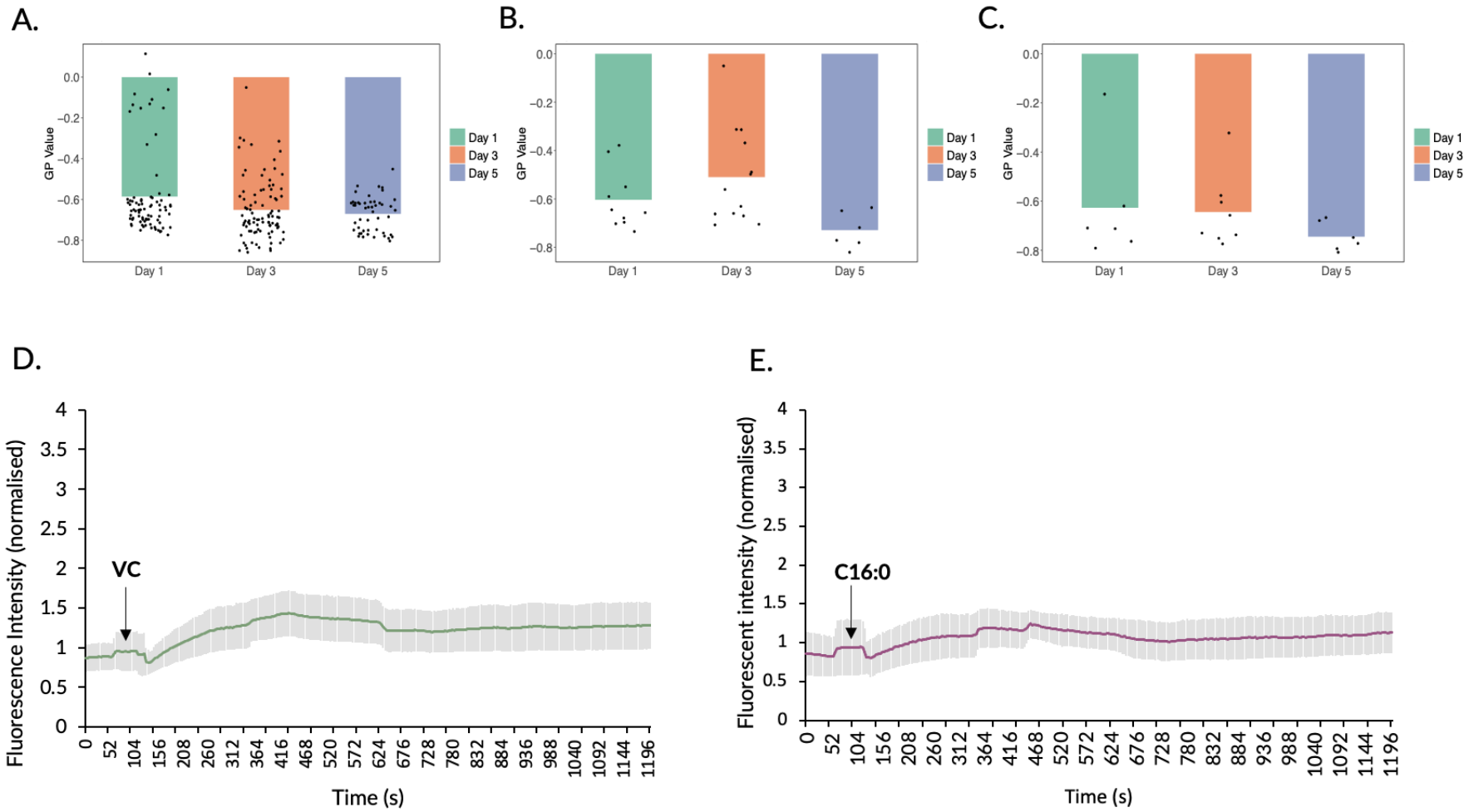

Figure 4.11 Acute uptake of palmitate and the vehicle in human-derived EndoC-βH1 cells following 3-day culture in 125µM C16:0 and 375µM C18:1. (A-C) EndoC-βH1 cells cultured for 1, 3 or 5 days in the culture in 125µM C16:0 and 375µM C18:1. The mean generalised polarisation (GP) values are displayed in bar charts for whole-cell membranes **(A)**, outward facing membranes **(B)** and intercell membranes **(C)**. Cell membranes labelled with the fluorescent probe Laurdan for 30 min. Cells were then fixed in paraformaldehyde. Imaging

was conducted on a Nikon eclipse Ti2 using an excitation of 405nm, and emissions of 430-470nm for the gel/liquid ordered phase (blue) and 480-550nm for the liquid disordered phase (green). Confocal images were analysed using CellPose and TOBLERONE segmentation softwares to quantify GP values. Each bar chart represents the mean GP value with independent data points. Graphs **A-C** provided by Luca Panconi. **(D and E)** EndoC-βH1 cells cultured for 3 days in VC only (BSA). Cells were incubated with pHrodo Green AM intracellular pH indicator for 30 min. After 30 min, the pH indicator was removed, and cells imaged in live cell imaging media. Basal intracellular pH (fluorescence intensity) was measured for 104 s. After 104 s, cells were injected with the VC **(D)** or 0.5mM palmitate (C16:0) **(E)**; intracellular pH was measured every 4 s for a total of 20 min. Imaging was conducted on a Nikon Ti Eclipse spinning disk confocal using an excitation/emission of 470/533 nm. To quantify changes in intracellular pH, the fluorescence intensity of time series images was analysed using ImageJ. Data was normalised to media. All results are representative of two or three independent experiments.

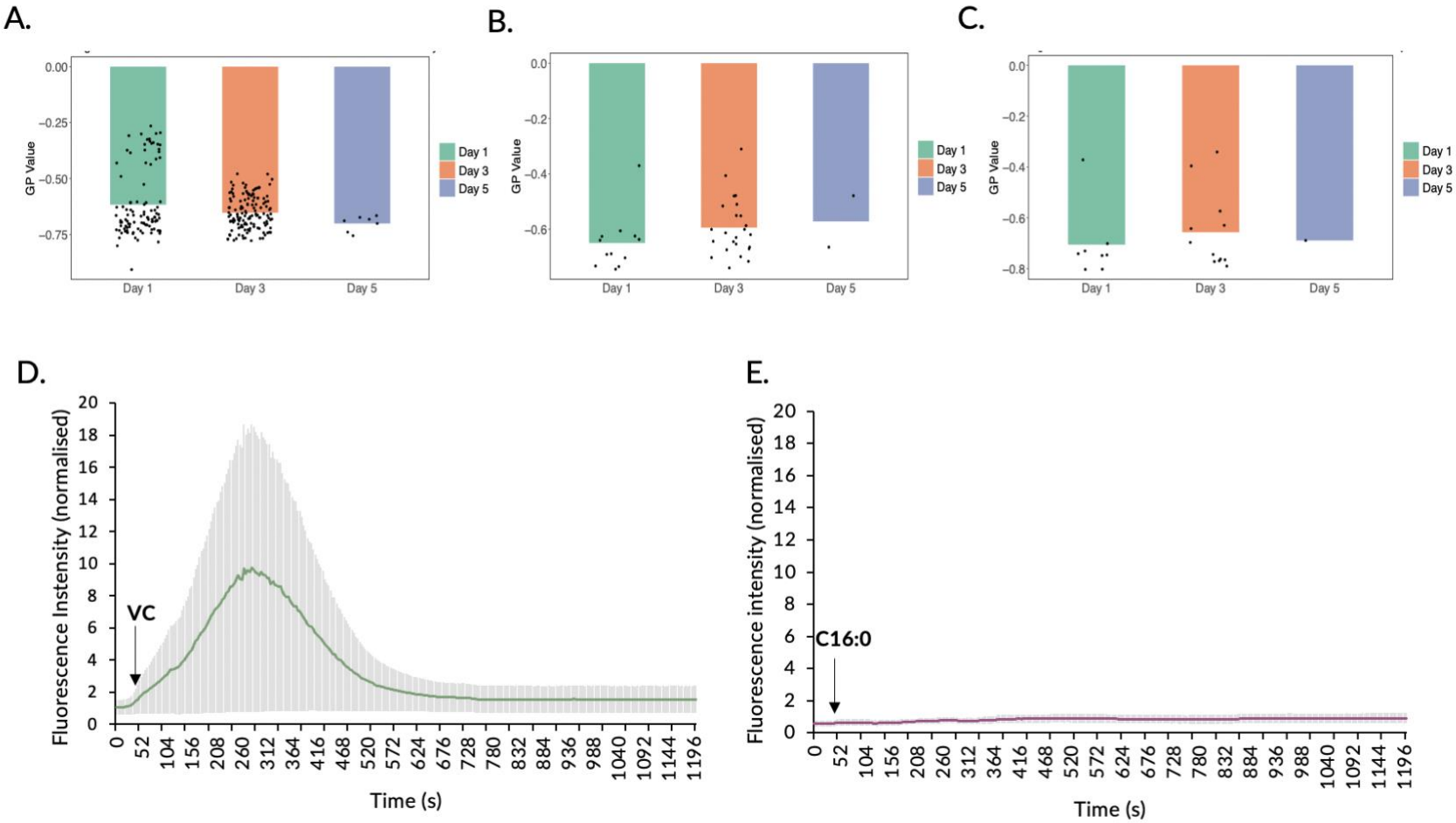

Figure 4.12 Acute uptake of palmitate and the vehicle in human-derived EndoC-βH1 cells following 3-day culture in 375µM C16:0 and 125µM C18:1. (A-C) EndoC-βH1 cells cultured for 1, 3 or 5 days in the culture in 375µM C16:0 and 125µM C18:1. The mean generalised polarisation (GP) values are displayed in bar charts for whole-cell membranes **(A)**, outward facing membranes **(B)** and intercell membranes **(C)**. Cell membranes labelled with the fluorescent probe Laurdan for 30 min. Cells were then fixed in paraformaldehyde. Imaging was conducted on a Nikon eclipse Ti2 using an excitation of 405nm, and emissions of 430-470nm for the gel/liquid ordered phase (blue) and

480-550nm for the liquid disordered phase (green). Confocal images were analysed using CellPose and TOBLERONE segmentation softwares to quantify GP values. Each bar chart represents the mean GP value with independent data points. Graphs **A-C** provided by Luca Panconi. **(D and E)** EndoC-βH1 cells cultured for 3 days in VC only (BSA). Cells were incubated with pHrodo Green AM intracellular pH indicator for 30 min. After 30 min, the pH indicator was removed, and cells imaged in live cell imaging media. Basal intracellular pH (fluorescence intensity) was measured for 104 s. After 104 s, cells were injected with the VC **(D)** or 0.5mM palmitate (C16:0) **(E)**; intracellular pH was measured every 4 s for a total of 20 min. Imaging was conducted on a Nikon Ti Eclipse spinning disk confocal using an excitation/emission of 470/533 nm. To quantify changes in intracellular pH, the fluorescence intensity of time series images was analysed using ImageJ. Data was normalised to media. All results are representative of two or three independent experiments.

4.4 Discussion

The main aims of this chapter were to investigate 1) whether LC-SFA uptake involves a passive and/or protein-facilitated process, 2) the role of dynamin-mediated endocytosis in LC-SFA uptake, and 3) the role of the lipid phase of the membrane in LC-SFA uptake.

4.4.1 Overview of results

This work has shown that the acute uptake of LC-SFA is a saturable process in rat-derived INS-1 832/13 cells and human-derived EndoC-βH1 cells which, in accordance with Michaelis-Menten saturation kinetics, could indicate that LC-SFA uptake is protein-mediated in pancreatic β-cells. Further, this work has shown that the uptake LC-SFA could potentially occur via a dynamin-mediated process. Strikingly, BSA (the VC) was also shown to be taken up into INS-1 832/13 and EndoC-βH1 cells. Another remarkable observation made in this study is that there is a significant difference in the membrane order between INS-1 832/13 cells vs. EndoC-βH1 cells. Moreover, a high level of LC-FFA, regardless of the degree of saturation, was shown here to increase the membrane order (i.e., reduce membrane fluidity) of EndoC-βH1 cells. Interestingly, the rate of acute C16:0 uptake into EndoC-βH1 cells was different following culture in different ratios of LC-SFA:LC-MUFA, although this did not appear to be a consequence of a change in membrane order. Following culture of EndoC-βH1 cells in 1% (w/v) BSA, LC-SFA uptake was promoted, whereas uptake of BSA was inhibited, which could indicate that culture in 1% (w/v) BSA is a more appropriate model to study LC-FFA uptake in comparison to 2% (w/v) BSA. Finally, BSA appears to be taken up into EndoC-βH1 cells via a different mechanism to C16:0 when cultured in different ratios of LC-SFA:LC-MUFA, suggesting that BSA is not a suitable control when studying LC-FFA uptake.

4.4.2 Acute uptake of LC-SFA is saturable in human and rodent pancreatic β-cells

This is seemingly the first study to examine the acute uptake of LC-SFA into pancreatic β-cells. This work is not the first to observe saturable uptake of C16:0, however. Comparable to our findings,

Bonen et al. (445) have shown similar transport kinetics of C16:0 in giant sarcolemmal vesicles taken from red and white rat hindlimb muscles, and Turcotte et al. (231) have discovered that C16:0 uptake is saturable in ex-vivo rodent skeletal muscle. In addition, Abumrad et al. (207) have shown that acute uptake of the LC-MUFA, C18:1, into rodent adipocytes is also a saturable process, which suggests that the mechanism of LC-SFA uptake could be similar to LC-MUFA. It is important to note, however, that the acute uptake of C16:0 into EndoC-βH1 cells was lower when compared to the uptake of BSA to EndoC-βH1 cells, or BSA/C16:0 to INS-1 832/13 cells. This could indicate that the acute uptake of C16:0 into EndoC-βH1 cells is restricted, which could be due to the regulation of LC-SFA uptake by proteins. Such proteins could include TBC1D1 and/or TBC1D4, which have been previously reported to be negative regulators of LC-FFA uptake (as discussed in section 3.4.3.3) (238, 241). The negative regulation of LC-FFA uptake into pancreatic β-cells via TBC1D1 and TBC1D4 is a particularly attractive theory, as it was shown in chapter 3 that these proteins are highly expressed in EndoC-βH1 cells, as well as ex-vivo human pancreatic islets. In summary, these findings suggest that the acute uptake of LC-SFA could be a protein-mediated process in human pancreatic β-cells, which supports previous reports in other cell types (231, 445). It is acknowledged here, however, that BSA exerts a strong effect on intracellular pH levels. Therefore, further experiments are needed to clearly separate the results for C16:0 and BSA. Such experiments could include culturing cells in different concentrations of BSA, or changing the molar ratio of C16:0:BSA. Limitations regarding the use of BSA as a vehicle control are discussed further in section 4.4.7. Future work should also repeat the pHrodo assay for a longer duration than conducted here (i.e., more than 20 min), to assess whether the uptake of C16:0 occurs over a greater period of time. In addition, future experiments could assess the role of TBC1D1 and TBC1D4 in the regulation of LC-FFA uptake in EndoC-βH1 cells (e.g., using a knockdown or knockout approach).

One might argue that the saturation kinetics observed here for C16:0 are due to the desorption of C16:0 from albumin, which is thought to be the main protein carrier for LC-FFA in the blood (446), via catalysis by another protein. Indeed, studies of C18:1 uptake into perfused liver (447) prompted the idea that an albumin receptor on the plasma membrane is responsible for the apparent saturable component of LC-FFA uptake. Weisiger et al. (447) discovered that uptake of C18:1 increases linearly as the quantity of C18:1 available increases, while albumin concentrations are fixed, which may suggest the presence of an albumin receptor. However, in the present study, it was shown that BSA is taken into EndoC-βH1 cells and INS-1 832/13 alongside C16:0, which implies that a protein catalyst is not required for the desorption of C16:0 from albumin. This finding was particularly surprising, as it is widely believed (191, 448) that LC-FFAs are cleaved from BSA prior to entry into the cell. To the best of our knowledge, however, no studies to date have suggested that BSA is taken up into the cell alongside LC-FFAs. Moreover, as BSA is a large globular protein (66 kDa) (449), the observation that BSA is taken up into β-cells led us to believe that the uptake of C16:0 and BSA could be via an endocytosis-mediated process. Endocytosis is a common method of transport for large molecules (180), and has been shown previously (450) to facilitate the uptake of BSA into cells. Taken together, these observations imply that BSA is taken into the cell alongside C16:0, which could indicate that the uptake of LC-SFA is mediated by endocytosis. Further investigations regarding the role of endocytosis in LC-SFA uptake are discussed below (section 4.4.3).

4.4.3 Acute uptake of LC-SFA seemingly occurs via a dynamin-mediated process

Here, we have shown that the inhibition of dynamin, a protein that is essential for the regulation of several types of endocytosis (e.g., clathrin-mediated and caveolae-mediated endocytosis) (218), seemingly prevents the uptake of C16:0, as well as BSA (the VC). As detailed in the results section of this chapter (section 4.3.2), the acute uptake of C16:0 into human-derived EndoC-βH1 cells is shown by a reduction in intracellular pH. Following the inhibition of dynamin, however, we have

observed a large increase in intracellular pH after the acute treatment of cells with C16:0. Surprisingly, the results of this experiment do not align with previous reports, which have suggested that a reduced intracellular pH inhibits endocytosis (451, 452, 453) and the binding of dynamin to adaptin (which may be necessary for the regulation of clathrin-mediated endocytosis) (454). Further, the work of Sakai et al. (455) has shown that an increase in intracellular pH facilitates endocytosis in rodent osteoclasts and microglia.

There are several possible explanations for the results observed in this study, including 1) the action of cell survival pathways, 2) dynamin involvement in a different cellular uptake process (other than endocytosis), and 3) off-target effects of Dyngo-4a. First, it is possible that the uptake of BSA, in the presence of a dynamin inhibitor, could trigger a cellular stress response within EndoC-βH1 cells which, in turn, could promote the activation of cell survival pathways, resulting in an increase in intracellular pH (456). Kazyken et al. (456) have shown that an elevated intracellular pH in mouse embryonic fibroblasts can occur due to the extracellular addition of amino acids. The increase in intracellular pH was then shown to activate energetic stress sensors (e.g., AMPK) and attenuate apoptosis, thereby promoting cell survival (456). As such, the uptake of BSA, a protein which is comprised of 583 amino acids (457), could be eliciting the same response in EndoC-βH1 cells. Further, as EndoC-βH1 cells are a cell line that have been generated using targeted oncogenesis (396), which promotes proliferation and cell survival, the results observed here could be a feature of the cell line. Another possible explanation for the results observed in this study is that dynamin is facilitating LC-SFA uptake into EndoC-βH1 cells via a mechanism other than endocytosis, which may be associated with their well-known role in membrane remodelling (458). Aside from its localisation to sites of endocytosis, dynamin is also found within actin structures, such as membrane ruffles, podosomes, and invadopodia (as reviewed by Ferguson et al. (459)). Alternatively, the results observed here might be due to off-target effects of the dynamin inhibitor used within this study

(Dyngo-4a). Dyngo-4a has been reported to have off-target effects, for example, the inhibition of actin remodelling beneath the plasma membrane (as reviewed by Preta et al. (458)) which could, in turn, affect LC-SFA transport. As such, future studies might consider using a knockout approach to prevent dynamin function when assessing LC-SFA uptake, to reduce the possibility of off-target effects. Knockout of dynamin can be conducted using a triple-knockout approach (of all 3 dynamin genes), as described in previous reports using β-cells (460).

Collectively, these results suggest that the acute uptake of LC-SFA by human-derived EndoC-βH1 cells is seemingly via a dynamin-dependent process. This mechanism may not necessarily involve endocytosis, however. Further research is required to elucidate the potential mechanisms relating the involvement of dynamin in LC-SFA uptake.

4.4.4 The lipid order of the plasma membrane is dissimilar in human-derived vs. rodent-derived β-cells

Remarkably, it has been shown in this study that the lipid order of the membrane is different in rodent vs. human pancreatic β-cells. Rodent pancreatic β-cells are often used to study the function of pancreatic β-cells (398, 461, 462). Moreover, rat models have been used in many studies to investigate LC-FFA uptake (as outlined in chapter 2). It is becoming increasingly apparent, however, that rodent pancreatic β-cell models may not be physiologically relevant to investigate all β-cell functions. As discussed in section 2.1.4, rodent β-cells have been shown to have numerous differences when compared to human β-cells, including glucose transporters (273), expression of genes for insulin (274) and islet composition (275). Further, the work of Thomas et al. (278) has recently shown that there is a difference in the way that pancreatic β-cells route LC-SFA in rodent vs. human cells. Collectively, the results obtained here suggest that rodent-derived INS-1 832/13 cell line is not an appropriate model to study the role of the plasma membrane composition in LC-FFA uptake, as it is not reflective of the human situation.

4.4.5 Effects of cell culture in varying LC-SFA:LC-MUFA ratios on membrane fluidity in human-derived β-cells

Interestingly, the results of this study imply that a high level of LC-FFA, regardless of the degree of saturation, can alter the composition of the β-cell plasma membrane by increasing membrane order (i.e., reducing membrane fluidity). Strikingly, however, these results do not agree with previous findings (411), which suggest that a high ratio of LC-MUFA:LC-SFA should reduce membrane order. One plausible explanation for these observations is that EndoC-βH1 cells cultured for 3 days in a high ratio of LC-SFA:LC-MUFA or a high ratio of LC-MUFA:LC-SFA may be apoptotic. For example, the work of Bailey et al. (463) reports that an increased membrane order can be associated with the late stages of apoptosis (i.e., membrane blebbing and fragmentation). The morphology of the cells imaged here did not indicate membrane blebbing at day 3, however, future work should aim to examine cell viability to ensure that the observations made here are not a result of apoptosis. These investigations can be carried out using flow cytometry (464, 465). Due to time restrictions, a viability assay was not carried out here.

Intriguingly, no significant difference in membrane order was observed between any of the treatments for outward-facing membranes of EndoC-βH1 cells alone, nor in the connecting membranes of the cells. This finding was particularly surprising, considering the clear difference and small variability in GP values between treatments (e.g., outward-facing membranes cultured for 1 day in BSA alone vs. 250μM C16:0 and 250μM C18:1). At present, it is unclear why the membrane order is different in whole cell membranes but not in outward- or inward-facing cell membranes. The lack of significant difference in membrane order could be due to an experimental error or an alternative mechanism in the cell that is yet to be determined. As such, further repeats should be carried out to clarify these results.

In summary, a high level of LC-FFA can increase membrane order, despite the degree of saturation. Further investigations should be carried out to ensure cell viability and additional repeats should be conducted for more robust results.

4.4.6 Effects of cell culture in varying LC-SFA:LC-MUFA ratios on LC-SFA uptake in human-derived β-cells

The results of this study could indicate that C16:0 uptake is not mediated by membrane order. Instead, the acute C16:0 uptake could be mediated by the metabolic requirements of the β-cell. Previous studies (466) have discovered that LC-FFAs can activate different G-protein coupled receptors in the plasma membrane, collectively known as FFARs. Specifically, LC-FFAs are thought to activate the specific FFAR isoforms FFAR1 (GPR40) and FFAR4 (GPR120) (466). The activation of these receptors has been shown to influence key physiological processes including the regulation of whole-body homeostasis and cell metabolism in adipose, intestinal and immune tissue, as well as pancreatic β-cells (as reviewed by Al Mahri et al. (467), Ichimura et al. (468), and Nolan et al. (469)). Intriguingly, a recent study (470) has also reported that the activation of these FFARs may regulate LC-FFA uptake. Using an in-vivo mouse model, Schilperoort et al. (470) have shown that the activation of FFAR4, due to binding of a potent selective agonist (TUG-891), can enhance C18:1 uptake into brown adipose tissue. It has been suggested that the increase in C18:1 uptake is due to an increase in metabolic activity, by increasing fatty acid oxidation, resulting in a greater fuel requirement of the cell (470). Taken together, this evidence could imply that culturing EndoC-βH1 cells in varying ratios of LC-SFA:LC-MUFA results in different metabolic requirements which, in turn, could regulate LC-FFA uptake. Further research is required to elucidate the potential role of β-cell metabolism in LC-SFA uptake. For example, the role of FFAR activation in LC-FFA uptake in pancreatic β-cells could be explored in future work.

Collectively, the results obtained in this study suggest that membrane order is not involved in regulating LC-SFA uptake. Moreover, observations made here, together with evidence collated from previous studies, could suggest that LC-SFA uptake is coupled to the metabolic requirements of the cell.

4.4.7 BSA is seemingly an unsuitable control for studying LC-SFA uptake

The observations made here could suggest that the culture of EndoC-βH1 cells in a lower concentration of BSA (1% (w/v)) (0.147mM) and no fatty acids could be the ideal model to study LC-FFA uptake. Moreover, BSA appears to be taken up into EndoC-βH1 cells via a different mechanism to C16:0 when cultured in different ratios of LC-SFA:LC-MUFA, suggesting that BSA is not a suitable control when studying LC-FFA uptake.

In accordance with the work in this study, many previous studies (387, 471, 472) have used 2% (w/v) BSA (0.294mM) for the culture of EndoC-βH1 cells, although whether this concentration is physiologically relevant remains to be fully established. The normal physiological concentration of albumin in the circulation of healthy adults has been reported to be 0.6 mM by Raoufinia et al. (473), however, there is no evidence to suggest the concentration of albumin in the interstitial space of pancreatic tissue, specifically, in-vivo.

As discussed in section 4.4.2, it is widely believed (191, 448) that LC-FFAs are cleaved from BSA prior to their entry into the cell. Culture of human-derived EndoC-βH1 cells in 1% (w/v) BSA and no fatty acids support these observations, whereas culture in 2% (w/v) or the addition of LC-FFA do not. These observations could imply that a much lower concentration of BSA (when compared to the overall concentration of circulating albumin in the human plasma) is required for the culture of EndoC-βH1 cells in-vitro to obtain a more physiologically relevant model of LC-FFA uptake into β-cells in-vivo. In support of this, it seems that many in-vitro experiments culture EndoC-βH1 cells in

much lower concentrations of BSA (e.g., 0.2% (w/v)) to examine GSIS (391, 396, 474), the key function of β-cells that has been previously shown (105, 106, 107, 110) to be influenced by FFAs (as discussed in chapter 1). Taken together, this evidence could indicate that the culture of EndoC-βH1 cells in 1% (w/v) BSA is the ideal model to study LC-FFA uptake. Under physiological conditions, however, pancreatic β-cells are also exposed to a range of fatty acids; indeed, the recent work of Kokotou et al. (66) has identified 74 different FFAs in the plasma of healthy individuals. In keeping with the results of this study, which have shown that different combinations of LC-SFA:LC-MUFA can alter the acute uptake of LC-SFA, it is important that future work also examines the role of different combinations of LC-FFA in culture on LC-FFA uptake.

It is possible that the metabolic requirements of the cell could account for the differences in BSA uptake when EndoC-βH1 cells are exposed to lower concentrations of BSA or different ratios of LC-SFA:LC-MUFA. Not only does BSA function as a carrier protein (e.g., for FFA, hormones, amino acids and peptides) (475), it could also have a nutritional function, to provide a source of amino acids following its hydrolysis within the cell (as suggested by Biggers et al. (476)). Very little research exists regarding the intracellular fate of albumin. Interestingly, however, the work of Andersson et al. (477) has shown that albumin is taken up at low levels in normal lysosomal tissue and high levels in the lysosomes of tumour tissue due to differences in their metabolic rate. Taken together, this evidence implies that the acute uptake of BSA into EndoC-βH1 cells could, in part, be dependent on the metabolic demands of the cell. Overall, these observations have shown that BSA is not a suitable control to examine LC-FFA uptake in β-cells.

In summary, the culture of EndoC-βH1 cell in 1% (w/v) BSA and no fatty acids could be ideal to study LC-FFA uptake, although the physiological relevance of this model is yet to be determined. Ultimately, however, BSA appears to be an inappropriate control to study LC-FFA uptake in pancreatic β-cells.

4.4.8 Limitations

The key limitations associated with this study include 1) the control used, and 2) the cell lines that we have chosen to investigate LC-SFA uptake.

One of the main limitations of this study is that BSA, which we have used as a vehicle control, is seemingly unsuitable for studying LC-SFA uptake into EndoC-βH1 cells (as discussed in section 4.4.7). Moreover, as previously mentioned in section 4.2.2, the INS-1 832/13 cell line was originally established from cells that were derived from a rat insulinoma (399) and the EndoC-βH1 cell line was generated using targeted oncogenesis of human foetal tissue (396). This means that both INS-1 832/13 and EndoC-βH1 cells can proliferate indefinitely (478), which is not the case in in-vivo β-cells. During cellular stress, such as growing tumour tissue, albumin has been shown to be taken into cells as a source of energy (479). Moreover, experiments (479) have reported that albumin is transported into tumour tissue by endocytosis and directed to lysosomes, where it is degraded. This brings into question whether the uptake of BSA into β-cells, as observed here, is a feature of the cell lines used, or whether BSA is also taken into human β-cells in-vivo. Investigations are currently being undertaken by Dr Patricia Thomas to determine whether these results can be repeated in human-derived EndoC-βH3 cells, which are de-immortalised by the removal of SV40LT (389). These experiments should provide further insight into the human situation in-vivo. Should the results of experiments using EndoC-βH3 cells be similar to those observed in EndoC-βH1 cells, future studies should consider using CellLight Early Endosomes-GFP, BacMam 2.0, which labels early endosomes with green fluorescent protein, to examine early-stage endocytosis (480, 481). Alternatively, should the results of experiments using EndoC-βH3 cells be different to those observed in EndoC-βH1 cells, future work should aim to investigate the role of candidate LC-FFA transporters that we have identified as highly expressed in both EndoC-βH1 cells and pancreatic islets (see chapter 3).

4.4.9 Summary

In summary, the acute uptake of LC-SFA into EndoC-βH1 cells appears to be protein-mediated and potentially involves a dynamin-dependent process. This mechanism may not necessarily involve endocytosis, however. It was also discovered here that the rodent-derived INS-1 832/13 cell line is not an appropriate model to study the role of the lipid phase of the plasma membrane in LC-FFA uptake. Surprisingly, a high concentration of LC-FFA could increase membrane order in EndoC-βH1 cells, regardless of the degree of saturation. Further research is required to determine whether the lipid phase of the plasma membrane influences LC-SFA uptake into EndoC-βH1 cells. Finally, BSA appears to be an unsuitable control for studying LC-SFA uptake.

Chapter 5.

Discussion

5.1 Overall summary

The overall aim of this thesis was to elucidate the mechanisms of LC-FFA uptake in pancreatic β-cells. The main objectives or this study included 1) to identify candidate transporters for LC-FFA with the most evidence to support uptake in mammalian cells, 2) to determine which of these candidate LC-FFA transport proteins are expressed in human pancreatic β-cells, 3) to investigate the role of endocytosis in LC-FFA transport across the plasma membrane of human β-cells and 4) to investigate the role of the lipid phase of the plasma membrane in LC-FFA uptake in human pancreatic β-cells.

Using a scoping review methodology, CD36 and isoforms of the FATP family were identified here to have the greatest evidence to support a role in facilitating LC-FFA uptake in humans. The FABP, ACSL and CAV family members, along with TBC1D1 and TBC1D4, were also reported to facilitate LC-FFA uptake, but additional evidence is required to underpin their role in transport. However, no studies were identified to examine LC-FFA uptake in pancreatic β-cells.

Using a bioinformatic approach, ACSL1, ACSL3, ACSL4, FATP4, TBC1D1 and TBC1D4 were discovered here to be the most highly expressed candidate LC-FFA transporters in both human-derived EndoC-βH1 pancreatic β-cells and human pancreatic islets. Strikingly, the expression of CD36, a protein which we have identified to have the most evidence to support LC-FFA uptake in nearly 30 years of literature (as discussed in chapter 1), is expressed at only a moderate level in EndoC-βH1 cells and human islets. Moreover, the gene expression of LC-FFA candidate transporters were found to vary between adipocytes and hepatocytes when compared to human islets, which raises questions as to whether information regarding LC-FFA uptake into other metabolically active cell types can be extrapolated to pancreatic β-cells.

Experimental work conducted in this project supports the role of proteins in LC-FFA transport into β-cells, as it was shown that the uptake of the LC-SFA, C16:0, into both human-derived EndoC-βH1 and rodent-derived INS-1 832/13 pancreatic β-cells displays saturable kinetics. Moreover, the work conducted here has revealed that the acute uptake of LC-SFA into EndoC-βH1 cells appears to involve a dynamin-dependent process. However, further investigations are required to elucidate the role of endocytosis in LC-FFA uptake.

Surprisingly, it was also shown here that the rodent-derived INS-1 832/13 cell line appears to be an inappropriate model to study the role of the plasma membrane composition in LC-FFA uptake, due to the significant differences in membrane order between EndoC-βH1 and INS-1 832/13 cells. This study has also discovered that chronic exposure of EndoC-βH1 cells to an elevated concentration of LC-SFA or LC-MUFA increases membrane order, regardless of the degree of saturation. The composition of the membrane, however, does not appear to have an effect on LC-SFA uptake into EndoC-βH1 cells. Finally, BSA, appears to be an unsuitable vehicle control for studying LC-SFA uptake.

In summary, the mechanism of LC-FFA uptake into human β-cells seemingly involves protein-mediated transport, although the exact mechanism of uptake remains unclear.

5.2 Limitations

One key limitation was the rate of proliferation of the EndoC-βH1 cell line. The work of Andersson et al. (193) has reported that the time taken for EndoC-βH1 cells to double is roughly 174 h for β-cells, which is considerably slower than INS-1 832/13 cells (approximately 44 h). The replication rate of EndoC-βH1 cells made it challenging to obtain results as it often took several weeks to grow an adequate number of cells to carry out a suitable number of replicates. Despite these challenges,

however, the results recorded here were largely consistent, and included data taken from at least two or three replicates.

5.3 Future work

Key future work should focus on investigating the role of candidate LC-FFA transporters identified here in human pancreatic β-cells, to provide greater insight to the role of proteins in LC-FFA uptake into β-cells. As identified in chapter 2 of this thesis, no studies have investigated the role of candidate LC-FFA transporters in β-cells, specifically. This is important because information regarding candidate LC-FFA transporters in other cell types seemingly cannot be extrapolated to β-cells, as we have illustrated in section 3.4. Consequently, functional studies should be carried out (i.e., loss-of-function or gain-of-function) to determine the role of candidate LC-FFA transport proteins in LC-FFA uptake into β-cells.

5.4 Conclusion

The mechanism of LC-FFA uptake into human β-cells seemingly involves protein-mediated transport, although the exact mechanism of uptake is still unclear. Thus, future work should investigate the function of candidate LC-FFA transporters in pancreatic β-cells.

Bibliography

1. International Diabetes Federation. Diabetes around the world in 2021 2021 [9 September,2022]. Available from: https://diabetesatlas.org.
2. Diabetes.co.uk. Type 2 Diabetes 2022 [11 September, 2022]. Available from: https://www.diabetes.co.uk/type2-diabetes.html.
3. World Health Organisation. World Health Day 2016: WHO calls for global action to halt rise in and improve care for people with diabetes 2016 11 September, 2022]. Available from: https://www.who.int/news/item/06-04-2016-world-health-day-2016-who-calls-for-global-action-to-halt-rise-in-and-improve-care-for-people-with-diabetes.
4. World Health Organisation. Diabetes 2021 [11 September, 2022]. Available from: https://www.who.int/news-room/fact-sheets/detail/diabetes.
5. Kotronen A, Juurinen L, Tiikkainen M, Vehkavaara S, Yki-Järvinen H. Increased liver fat, impaired insulin clearance, and hepatic and adipose tissue insulin resistance in type 2 diabetes. Gastroenterology. 2008;135(1):122-30.
6. Petersen KF, Shulman GI. Pathogenesis of skeletal muscle insulin resistance in type 2 diabetes mellitus. Am J Cardiol. 2002;90(5A):11G-8G.
7. Swisa A, Glaser B, Dor Y. Metabolic Stress and Compromised Identity of Pancreatic Beta Cells. Front Genet. 2017;8:21.
8. Agiostratidou G, Anhalt H, Ball D, Blonde L, Gourgari E, Harriman KN, et al. Standardizing Clinically Meaningful Outcome Measures Beyond HbA. Diabetes Care. 2017;40(12):1622-30.
9. Nauck MA, Wefers J, Meier JJ. Treatment of type 2 diabetes: challenges, hopes, and anticipated successes. Lancet Diabetes Endocrinol. 2021;9(8):525-44.
10. Marín-Peñalver JJ, Martín-Timón I, Sevillano-Collantes C, Del Cañizo-Gómez FJ. Update on the treatment of type 2 diabetes mellitus. World J Diabetes. 2016;7(17):354-95.
11. Lean ME, Leslie WS, Barnes AC, Brosnahan N, Thom G, McCombie L, et al. Primary care-led weight management for remission of type 2 diabetes (DiRECT): an open-label, cluster-randomised trial. Lancet. 2018;391(10120):541-51.
12. Bailey CJ. Metformin: historical overview. Diabetologia. 2017;60(9):1566-76.
13. Swinnen SG, Hoekstra JB, DeVries JH. Insulin therapy for type 2 diabetes. Diabetes Care. 2009;32 Suppl 2:S253-9.
14. Bi Y, Wang T, Xu M, Xu Y, Li M, Lu J, et al. Advanced research on risk factors of type 2 diabetes. Diabetes Metab Res Rev. 2012;28 Suppl 2:32-9.
15. Kyrou I, Tsigos C, Mavrogianni C, Cardon G, Van Stappen V, Latomme J, et al. Sociodemographic and lifestyle-related risk factors for identifying vulnerable groups for type 2 diabetes: a narrative review with emphasis on data from Europe. BMC Endocrine Disorders. 2020;20(S1).
16. Bellary S, Kyrou I, Brown JE, Bailey CJ. Type 2 diabetes mellitus in older adults: clinical considerations and management. Nat Rev Endocrinol. 2021;17(9):534-48.
17. Agardh E, Allebeck P, Hallqvist J, Moradi T, Sidorchuk A. Type 2 diabetes incidence and socio-economic position: a systematic review and meta-analysis. Int J Epidemiol. 2011;40(3):804-18.
18. Meeks KA, Freitas-Da-Silva D, Adeyemo A, Beune EJ, Modesti PA, Stronks K, et al. Disparities in type 2 diabetes prevalence among ethnic minority groups resident in Europe: a systematic review and meta-analysis. Intern Emerg Med. 2016;11(3):327-40.
19. Barnett AH, Dixon AN, Bellary S, Hanif MW, O'hare JP, Raymond NT, et al. Type 2 diabetes and cardiovascular risk in the UK south Asian community. Diabetologia. 2006;49(10):2234-46.

20. Bennet L, Groop L, Lindblad U, Agardh CD, Franks PW. Ethnicity is an independent risk indicator when estimating diabetes risk with FINDRISC scores: a cross sectional study comparing immigrants from the Middle East and native Swedes. Prim Care Diabetes. 2014;8(3):231-8.
21. Jenum AK, Diep LM, Holmboe-Ottesen G, Holme IM, Kumar BN, Birkeland KI. Diabetes susceptibility in ethnic minority groups from Turkey, Vietnam, Sri Lanka and Pakistan compared with Norwegians - the association with adiposity is strongest for ethnic minority women. BMC Public Health. 2012;12:150.
22. Bonnefond A, Froguel P. Rare and common genetic events in type 2 diabetes: what should biologists know? Cell Metab. 2015;21(3):357-68.
23. Xue A, Wu Y, Zhu Z, Zhang F, Kemper KE, Zheng Z, et al. Genome-wide association analyses identify 143 risk variants and putative regulatory mechanisms for type 2 diabetes. Nat Commun. 2018;9(1):2941.
24. Ali O. Genetics of type 2 diabetes. World J Diabetes. 2013;4(4):114-23.
25. Tillil H, Köbberling J. Age-corrected empirical genetic risk estimates for first-degree relatives of IDDM patients. Diabetes. 1987;36(1):93-9.
26. Mambiya M, Shang M, Wang Y, Li Q, Liu S, Yang L, et al. The Play of Genes and Non-genetic Factors on Type 2 Diabetes. Front Public Health. 2019;7:349.
27. Neuenschwander M, Ballon A, Weber KS, Norat T, Aune D, Schwingshackl L, et al. Role of diet in type 2 diabetes incidence: umbrella review of meta-analyses of prospective observational studies. BMJ. 2019;366:l2368.
28. Abdullah A, Peeters A, de Courten M, Stoelwinder J. The magnitude of association between overweight and obesity and the risk of diabetes: a meta-analysis of prospective cohort studies. Diabetes Res Clin Pract. 2010;89(3):309-19.
29. World Health Organisation. Obesity and overweight 2021 [11 September, 2022]. Available from: https://www.who.int/news-room/fact-sheets/detail/obesity-and-overweight.
30. World Obesity Federation. World Obesity Atlas 2022 2022 [11 September, 2022]. Available from: https://www.worldobesityday.org/assets/downloads/World_Obesity_Atlas_2022_WEB.pdf.
31. Gatineau M, Hancock C, Holman N, Outhwaite H, Oldridge L, Christie A, et al. Adult obesity and type 2 diabetes. Oxford: Public Health England; 2014.
32. Hill JO, Wyatt HR, Peters JC. Energy balance and obesity. Circulation. 2012;126(1):126-32.
33. Romieu I, Dossus L, Barquera S, Blottière HM, Franks PW, Gunter M, et al. Energy balance and obesity: what are the main drivers? Cancer Causes Control. 2017;28(3):247-58.
34. Kahn BB, Flier JS. Obesity and insulin resistance. Journal of Clinical Investigation. 2000;106(4):473-81.
35. Eckel RH, Kahn SE, Ferrannini E, Goldfine AB, Nathan DM, Schwartz MW, et al. Obesity and type 2 diabetes: what can be unified and what needs to be individualized? J Clin Endocrinol Metab. 2011;96(6):1654-63.
36. Olaogun I, Farag M, Hamid P. The Pathophysiology of Type 2 Diabetes Mellitus in Non-obese Individuals: An Overview of the Current Understanding. Cureus. 2020;12(4):e7614.
37. Snel M, Jonker JT, Schoones J, Lamb H, de Roos A, Pijl H, et al. Ectopic fat and insulin resistance: pathophysiology and effect of diet and lifestyle interventions. Int J Endocrinol. 2012;2012:983814.
38. Sergi D, Williams LM. Potential relationship between dietary long-chain saturated fatty acids and hypothalamic dysfunction in obesity. Nutr Rev. 2020;78(4):261-77.
39. White MG, Shaw JA, Taylor R. Type 2 Diabetes: The Pathologic Basis of Reversible β-Cell Dysfunction. Diabetes Care. 2016;39(11):2080-8.

40. Heilbronn L, Smith SR, Ravussin E. Failure of fat cell proliferation, mitochondrial function and fat oxidation results in ectopic fat storage, insulin resistance and type II diabetes mellitus. Int J Obes Relat Metab Disord. 2004;28 Suppl 4:S12-21.
41. Kershaw EE, Flier JS. Adipose tissue as an endocrine organ. J Clin Endocrinol Metab. 2004;89(6):2548-56.
42. Biondi G, Marrano N, Borrelli A, Rella M, Palma G, Calderoni I, et al. Adipose Tissue Secretion Pattern Influences β-Cell Wellness in the Transition from Obesity to Type 2 Diabetes. Int J Mol Sci. 2022;23(10).
43. Dunmore SJ, Brown JE. The role of adipokines in β-cell failure of type 2 diabetes. J Endocrinol. 2013;216(1):T37-45.
44. Donath MY, Böni-Schnetzler M, Ellingsgaard H, Halban PA, Ehses JA. Cytokine production by islets in health and diabetes: cellular origin, regulation and function. Trends Endocrinol Metab. 2010;21(5):261-7.
45. Levelt E, Pavlides M, Banerjee R, Mahmod M, Kelly C, Sellwood J, et al. Ectopic and Visceral Fat Deposition in Lean and Obese Patients With Type 2 Diabetes. J Am Coll Cardiol. 2016;68(1):53-63.
46. Lee Y, Lingvay I, Szczepaniak LS, Ravazzola M, Orci L, Unger RH. Pancreatic steatosis: harbinger of type 2 diabetes in obese rodents. Int J Obes (Lond). 2010;34(2):396-400.
47. Lim EL, Hollingsworth KG, Aribisala BS, Chen MJ, Mathers JC, Taylor R. Reversal of type 2 diabetes: normalisation of beta cell function in association with decreased pancreas and liver triacylglycerol. Diabetologia. 2011;54(10):2506-14.
48. Miljkovic I, Kuipers AL, Cvejkus RK, Carr JJ, Terry JG, Thyagarajan B, et al. Hepatic and Skeletal Muscle Adiposity Are Associated with Diabetes Independent of Visceral Adiposity in Nonobese African-Caribbean Men. Metab Syndr Relat Disord. 2020;18(6):275-83.
49. Strable MS, Ntambi JM. Genetic control of de novo lipogenesis: role in diet-induced obesity. Crit Rev Biochem Mol Biol. 2010;45(3):199-214.
50. Rustan AC, Drevon CA. Fatty Acids: Structures and Properties. The Encyclopedia of Life 2005.
51. Calder PC. Functional Roles of Fatty Acids and Their Effects on Human Health. JPEN J Parenter Enteral Nutr. 2015;39(1 Suppl):18S-32S.
52. Huber AH, Kleinfeld AM. Unbound free fatty acid profiles in human plasma and the unexpected absence of unbound palmitoleate. J Lipid Res. 2017;58(3):578-85.
53. Goldberg IJ. Clinical review 124: Diabetic dyslipidemia: causes and consequences. J Clin Endocrinol Metab. 2001;86(3):965-71.
54. Klop B, Elte JW, Cabezas MC. Dyslipidemia in obesity: mechanisms and potential targets. Nutrients. 2013;5(4):1218-40.
55. I S Sobczak A, A Blindauer C, J Stewart A. Changes in Plasma Free Fatty Acids Associated with Type-2 Diabetes. Nutrients. 2019;11(9).
56. Dictionary of Toxicology. 3rd ed: Academic Press; 2015. A; p. 1-46.
57. Kimura I, Ichimura A, Ohue-Kitano R, Igarashi M. Free Fatty Acid Receptors in Health and Disease. Physiol Rev. 2020;100(1):171-210.
58. Albuquerque TG, Nunes MA, Bessada SMF, Costa HS, Oliveira MBPP. Biologically active and health promoting food components of nuts, oilseeds, fruits, vegetables, cereals, and legumes. Chemical Analysis of Food. 2nd ed: Academic Press; 2020. p. 609-56.
59. Thomas P, Leslie KA, Welters HJ, Morgan NG. Long-chain saturated fatty acid species are not toxic to human pancreatic β-cells and may offer protection against pro-inflammatory cytokine induced β-cell death. Nutr Metab (Lond). 2021;18(1):9.

60. Sieber J, Jehle AW. Free Fatty acids and their metabolism affect function and survival of podocytes. Front Endocrinol (Lausanne). 2014;5:186.
61. Quehenberger O, Armando AM, Brown AH, Milne SB, Myers DS, Merrill AH, et al. Lipidomics reveals a remarkable diversity of lipids in human plasma. J Lipid Res. 2010;51(11):3299-305.
62. Spiller S, Blüher M, Hoffmann R. Plasma levels of free fatty acids correlate with type 2 diabetes mellitus. Diabetes Obes Metab. 2018;20(11):2661-9.
63. Henderson GC. Plasma Free Fatty Acid Concentration as a Modifiable Risk Factor for Metabolic Disease. Nutrients. 2021;13(8).
64. Boden G. Obesity and free fatty acids. Endocrinol Metab Clin North Am. 2008;37(3):635-46, viii-ix.
65. Lewis GF, Carpentier A, Adeli K, Giacca A. Disordered fat storage and mobilization in the pathogenesis of insulin resistance and type 2 diabetes. Endocr Rev. 2002;23(2):201-29.
66. Kokotou MG, Mantzourani C, Batsika CS, Mountanea OG, Eleftheriadou I, Kosta O, et al. Lipidomics Analysis of Free Fatty Acids in Human Plasma of Healthy and Diabetic Subjects by Liquid Chromatography-High Resolution Mass Spectrometry (LC-HRMS). Biomedicines. 2022;10(5).
67. Sansone A, Tolika E, Louka M, Sunda V, Deplano S, Melchiorre M, et al. Hexadecenoic Fatty Acid Isomers in Human Blood Lipids and Their Relevance for the Interpretation of Lipidomic Profiles. PLoS One. 2016;11(4):e0152378.
68. Carta G, Murru E, Banni S, Manca C. Palmitic Acid: Physiological Role, Metabolism and Nutritional Implications. Front Physiol. 2017;8:902.
69. Song X, Huang Y, Neuhouser ML, Tinker LF, Vitolins MZ, Prentice RL, et al. Dietary long-chain fatty acids and carbohydrate biomarker evaluation in a controlled feeding study in participants from the Women's Health Initiative cohort. Am J Clin Nutr. 2017;105(6):1272-82.
70. Tak I-U-R, Ali F, Dar JS, Magray AR, Ganai BA, Chishti MZ. Posttranslational Modifications of Proteins and Their Role in Biological Processes and Associated Diseases. Protein Modificomics: From Modifications to Clinical Perspectives Academic Press; 2019. p. 1-35.
71. Donnelly KL, Smith CI, Schwarzenberg SJ, Jessurun J, Boldt MD, Parks EJ. Sources of fatty acids stored in liver and secreted via lipoproteins in patients with nonalcoholic fatty liver disease. J Clin Invest. 2005;115(5):1343-51.
72. Goldstein BJ. Insulin resistance as the core defect in type 2 diabetes mellitus. Am J Cardiol. 2002;90(5A):3G-10G.
73. Corcoran MP, Lamon-Fava S, Fielding RA. Skeletal muscle lipid deposition and insulin resistance: effect of dietary fatty acids and exercise. Am J Clin Nutr. 2007;85(3):662-77.
74. Fryk E, Olausson J, Mossberg K, Strindberg L, Schmelz M, Brogren H, et al. Hyperinsulinemia and insulin resistance in the obese may develop as part of a homeostatic response to elevated free fatty acids: A mechanistic case-control and a population-based cohort study. EBioMedicine. 2021;65:103264.
75. Barzilai N, Ferrucci L. Insulin resistance and aging: a cause or a protective response? J Gerontol A Biol Sci Med Sci. 2012;67(12):1329-31.
76. Stefanovski D, Punjabi NM, Boston RC, Watanabe RM. Insulin Action, Glucose Homeostasis and Free Fatty Acid Metabolism: Insights From a Novel Model. Front Endocrinol (Lausanne). 2021;12:625701.
77. Schinner S, Scherbaum WA, Bornstein SR, Barthel A. Molecular mechanisms of insulin resistance. Diabet Med. 2005;22(6):674-82.
78. Shanik MH, Xu Y, Skrha J, Dankner R, Zick Y, Roth J. Insulin resistance and hyperinsulinemia: is hyperinsulinemia the cart or the horse? Diabetes Care. 2008;31 Suppl 2:S262-8.

79. Sears B, Perry M. The role of fatty acids in insulin resistance. Lipids Health Dis. 2015;14:121.
80. Sadur CN, Eckel RH. Insulin stimulation of adipose tissue lipoprotein lipase. Use of the euglycemic clamp technique. J Clin Invest. 1982;69(5):1119-25.
81. Kumari A, Kristensen KK, Ploug M, Winther AL. The Importance of Lipoprotein Lipase Regulation in Atherosclerosis. Biomedicines. 2021;9(7).
82. Kumari S, Mg S, Mayor S. Endocytosis unplugged: multiple ways to enter the cell. Cell Res. 2010;20(3):256-75.
83. Pavlic M, Valéro R, Duez H, Xiao C, Szeto L, Patterson BW, et al. Triglyceride-rich lipoprotein-associated apolipoprotein C-III production is stimulated by plasma free fatty acids in humans. Arterioscler Thromb Vasc Biol. 2008;28(9):1660-5.
84. Jennings RE, Berry AA, Strutt JP, Gerrard DT, Hanley NA. Human pancreas development. Development. 2015;142(18):3126-37.
85. Ferrannini E, Mari A. β-Cell function in type 2 diabetes. Metabolism. 2014;63(10):1217-27.
86. Rahman MS, Hossain KS, Das S, Kundu S, Adegoke EO, Rahman MA, et al. Role of Insulin in Health and Disease: An Update. Int J Mol Sci. 2021;22(12).
87. Gerber KM, Whitticar NB, Rochester DR, Corbin KL, Koch WJ, Nunemaker CS. The Capacity to Secrete Insulin Is Dose-Dependent to Extremely High Glucose Concentrations: A Key Role for Adenylyl Cyclase. Metabolites. 2021;11(6).
88. Gilon P. The Role of α-Cells in Islet Function and Glucose Homeostasis in Health and Type 2 Diabetes. J Mol Biol. 2020;432(5):1367-94.
89. Seyed Ahmadi S, Westman K, Pivodic A, Ólafsdóttir AF, Dahlqvist S, Hirsch IB, et al. The Association Between HbA. Diabetes Care. 2020;43(9):2017-24.
90. Wendt A, Eliasson L. Pancreatic α-cells - The unsung heroes in islet function. Semin Cell Dev Biol. 2020;103:41-50.
91. Svendsen B, Larsen O, Gabe MBN, Christiansen CB, Rosenkilde MM, Drucker DJ, et al. Insulin Secretion Depends on Intra-islet Glucagon Signaling. Cell Rep. 2018;25(5):1127-34.e2.
92. Capozzi ME, Svendsen B, Encisco SE, Lewandowski SL, Martin MD, Lin H, et al. β Cell tone is defined by proglucagon peptides through cAMP signaling. JCI Insight. 2019;4(5).
93. de Souza AH, Tang J, Yadev AK, Saghafi ST, Kibbe CR, Linnemann AK, et al. Intra-islet GLP-1, but not CCK, is necessary for β-cell function in mouse and human islets. Sci Rep. 2020;10(1):2823.
94. Arrojo E Drigo R, Jacob S, García-Prieto CF, Zheng X, Fukuda M, Nhu HTT, et al. Structural basis for delta cell paracrine regulation in pancreatic islets. Nat Commun. 2019;10(1):3700.
95. Röder PV, Wu B, Liu Y, Han W. Pancreatic regulation of glucose homeostasis. Exp Mol Med. 2016;48(3):e219.
96. Hauge-Evans AC, King AJ, Carmignac D, Richardson CC, Robinson IC, Low MJ, et al. Somatostatin secreted by islet delta-cells fulfills multiple roles as a paracrine regulator of islet function. Diabetes. 2009;58(2):403-11.
97. Sakata N, Yoshimatsu G, Kodama S. Development and Characteristics of Pancreatic Epsilon Cells. Int J Mol Sci. 2019;20(8).
98. Zhao Y, Zhou Y, Xiao M, Huang Y, Qi M, Kong Z, et al. Impaired glucose tolerance is associated with enhanced postprandial pancreatic polypeptide secretion. J Diabetes. 2022;14(5):334-44.
99. Khan D, Vasu S, Moffett RC, Irwin N, Flatt PR. Islet distribution of Peptide YY and its regulatory role in primary mouse islets and immortalised rodent and human beta-cell function and survival. Mol Cell Endocrinol. 2016;436:102-13.
100. Association AD. Postprandial blood glucose. American Diabetes Association. Diabetes Care. 2001;24(4):775-8.

101. Campbell JE, Newgard CB. Mechanisms controlling pancreatic islet cell function in insulin secretion. Nat Rev Mol Cell Biol. 2021;22(2):142-58.
102. Rorsman P, Renström E. Insulin granule dynamics in pancreatic beta cells. Diabetologia. 2003;46(8):1029-45.
103. Kalwat MA, Cobb MH. Mechanisms of the amplifying pathway of insulin secretion in the β cell. Pharmacol Ther. 2017;179:17-30.
104. Jensen MV, Joseph JW, Ronnebaum SM, Burgess SC, Sherry AD, Newgard CB. Metabolic cycling in control of glucose-stimulated insulin secretion. Am J Physiol Endocrinol Metab. 2008;295(6):E1287-97.
105. Yaney GC, Corkey BE. Fatty acid metabolism and insulin secretion in pancreatic beta cells. Diabetologia. 2003;46(10):1297-312.
106. Itoh Y, Kawamata Y, Harada M, Kobayashi M, Fujii R, Fukusumi S, et al. Free fatty acids regulate insulin secretion from pancreatic beta cells through GPR40. Nature. 2003;422(6928):173-6.
107. Haber EP, Ximenes HM, Procópio J, Carvalho CR, Curi R, Carpinelli AR. Pleiotropic effects of fatty acids on pancreatic beta-cells. J Cell Physiol. 2003;194(1):1-12.
108. Chueire VB, Muscelli E. Effect of free fatty acids on insulin secretion, insulin sensitivity and incretin effect - a narrative review. Arch Endocrinol Metab. 2021;65(1):24-31.
109. Larsson O, Deeney JT, Bränström R, Berggren PO, Corkey BE. Activation of the ATP-sensitive K+ channel by long chain acyl-CoA. A role in modulation of pancreatic beta-cell glucose sensitivity. J Biol Chem. 1996;271(18):10623-6.
110. Poitout V. Fatty Acids and Insulin Secretion: From FFAR and Near? Diabetes. 2018;67(10):1932-4.
111. Casares D, Escribá PV, Rosselló CA. Membrane Lipid Composition: Effect on Membrane and Organelle Structure, Function and Compartmentalization and Therapeutic Avenues. Int J Mol Sci. 2019;20(9).
112. Weijers RN. Lipid composition of cell membranes and its relevance in type 2 diabetes mellitus. Curr Diabetes Rev. 2012;8(5):390-400.
113. Singer SJ, Nicolson GL. The fluid mosaic model of the structure of cell membranes. Science. 1972;175(4023):720-31.
114. Nicolson GL. The Fluid-Mosaic Model of Membrane Structure: still relevant to understanding the structure, function and dynamics of biological membranes after more than 40 years. Biochim Biophys Acta. 2014;1838(6):1451-66.
115. Escribá PV, González-Ros JM, Goñi FM, Kinnunen PK, Vigh L, Sánchez-Magraner L, et al. Membranes: a meeting point for lipids, proteins and therapies. J Cell Mol Med. 2008;12(3):829-75.
116. Desai AJ, Miller LJ. Changes in the plasma membrane in metabolic disease: impact of the membrane environment on G protein-coupled receptor structure and function. Br J Pharmacol. 2018;175(21):4009-25.
117. Perona JS. Membrane lipid alterations in the metabolic syndrome and the role of dietary oils. Biochim Biophys Acta Biomembr. 2017;1859(9 Pt B):1690-703.
118. Oh YS, Bae GD, Baek DJ, Park EY, Jun HS. Fatty Acid-Induced Lipotoxicity in Pancreatic Beta-Cells During Development of Type 2 Diabetes. Front Endocrinol (Lausanne). 2018;9:384.
119. Cerf ME. Beta cell dysfunction and insulin resistance. Front Endocrinol (Lausanne). 2013;4:37.
120. Kristinsson H, Smith DM, Bergsten P, Sargsyan E. FFAR1 is involved in both the acute and chronic effects of palmitate on insulin secretion. Endocrinology. 2013;154(11):4078-88.
121. Goberna R, Tamarit J, Osorio J, Fussgänger R, Pfeiffer EF. Action of B-hydroxy butyrate, acetoacetate and palmitate on the insulin release in the perfused isolated rat pancreas. Horm Metab Res. 1974;6(4):256-60.

122. Roomp K, Kristinsson H, Schvartz D, Ubhayasekera K, Sargsyan E, Manukyan L, et al. Combined lipidomic and proteomic analysis of isolated human islets exposed to palmitate reveals time-dependent changes in insulin secretion and lipid metabolism. PLoS One. 2017;12(4):e0176391.
123. Unger RH, Zhou YT. Lipotoxicity of beta-cells in obesity and in other causes of fatty acid spillover. Diabetes. 2001;50 Suppl 1:S118-21.
124. Newsholme P, Keane D, Welters HJ, Morgan NG. Life and death decisions of the pancreatic beta-cell: the role of fatty acids. Clin Sci (Lond). 2007;112(1):27-42.
125. Moffitt JH, Fielding BA, Evershed R, Berstan R, Currie JM, Clark A. Adverse physicochemical properties of tripalmitin in beta cells lead to morphological changes and lipotoxicity in vitro. Diabetologia. 2005;48(9):1819-29.
126. Maedler K, Spinas GA, Dyntar D, Moritz W, Kaiser N, Donath MY. Distinct effects of saturated and monounsaturated fatty acids on beta-cell turnover and function. Diabetes. 2001;50(1):69-76.
127. Cnop M, Hannaert JC, Hoorens A, Eizirik DL, Pipeleers DG. Inverse relationship between cytotoxicity of free fatty acids in pancreatic islet cells and cellular triglyceride accumulation. Diabetes. 2001;50(8):1771-7.
128. Eitel K, Staiger H, Brendel MD, Brandhorst D, Bretzel RG, Häring HU, et al. Different role of saturated and unsaturated fatty acids in beta-cell apoptosis. Biochem Biophys Res Commun. 2002;299(5):853-6.
129. Maedler K, Oberholzer J, Bucher P, Spinas GA, Donath MY. Monounsaturated fatty acids prevent the deleterious effects of palmitate and high glucose on human pancreatic beta-cell turnover and function. Diabetes. 2003;52(3):726-33.
130. Gehrmann W, Würdemann W, Plötz T, Jörns A, Lenzen S, Elsner M. Antagonism Between Saturated and Unsaturated Fatty Acids in ROS Mediated Lipotoxicity in Rat Insulin-Producing Cells. Cell Physiol Biochem. 2015;36(3):852-65.
131. Kharroubi I, Ladrière L, Cardozo AK, Dogusan Z, Cnop M, Eizirik DL. Free fatty acids and cytokines induce pancreatic beta-cell apoptosis by different mechanisms: role of nuclear factor-kappaB and endoplasmic reticulum stress. Endocrinology. 2004;145(11):5087-96.
132. Bachar E, Ariav Y, Ketzinel-Gilad M, Cerasi E, Kaiser N, Leibowitz G. Glucose amplifies fatty acid-induced endoplasmic reticulum stress in pancreatic beta-cells via activation of mTORC1. PLoS One. 2009;4(3):e4954.
133. Maris M, Waelkens E, Cnop M, D'Hertog W, Cunha DA, Korf H, et al. Oleate-induced beta cell dysfunction and apoptosis: a proteomic approach to glucolipotoxicity by an unsaturated fatty acid. J Proteome Res. 2011;10(8):3372-85.
134. El-Assaad W, Buteau J, Peyot ML, Nolan C, Roduit R, Hardy S, et al. Saturated fatty acids synergize with elevated glucose to cause pancreatic beta-cell death. Endocrinology. 2003;144(9):4154-63.
135. Vilas-Boas EA, Almeida DC, Roma LP, Ortis F, Carpinelli AR. Lipotoxicity and β-Cell Failure in Type 2 Diabetes: Oxidative Stress Linked to NADPH Oxidase and ER Stress. Cells. 2021;10(12).
136. Lenzen S. Oxidative stress: the vulnerable beta-cell. Biochem Soc Trans. 2008;36(Pt 3):343-7.
137. Payet LA, Pineau L, Snyder EC, Colas J, Moussa A, Vannier B, et al. Saturated fatty acids alter the late secretory pathway by modulating membrane properties. Traffic. 2013;14(12):1228-41.
138. Lytrivi M, Castell AL, Poitout V, Cnop M. Recent Insights Into Mechanisms of β-Cell Lipo- and Glucolipotoxicity in Type 2 Diabetes. J Mol Biol. 2020;432(5):1514-34.
139. Thomas P. Fat: friend or foe? Understanding the role of fat in health and disease: unpublished teaching slides. 2022.

140. Elmendorf JS. Fluidity of insulin action. Mol Biotechnol. 2004;27(2):127-38.
141. Dobrzyn P, Jazurek M, Dobrzyn A. Stearoyl-CoA desaturase and insulin signaling--what is the molecular switch? Biochim Biophys Acta. 2010;1797(6-7):1189-94.
142. Murphy MG. Dietary fatty acids and membrane protein function. J Nutr Biochem. 1990;1(2):68-79.
143. Véret J, Bellini L, Giussani P, Ng C, Magnan C, Le Stunff H. Roles of Sphingolipid Metabolism in Pancreatic β Cell Dysfunction Induced by Lipotoxicity. J Clin Med. 2014;3(2):646-62.
144. Cha HJ, He C, Zhao H, Dong Y, An IS, An S. Intercellular and intracellular functions of ceramides and their metabolites in skin (Review). Int J Mol Med. 2016;38(1):16-22.
145. Boslem E, MacIntosh G, Preston AM, Bartley C, Busch AK, Fuller M, et al. A lipidomic screen of palmitate-treated MIN6 β-cells links sphingolipid metabolites with endoplasmic reticulum (ER) stress and impaired protein trafficking. Biochem J. 2011;435(1):267-76.
146. Bandet CL, Tan-Chen S, Bourron O, Le Stunff H, Hajduch E. Sphingolipid Metabolism: New Insight into Ceramide-Induced Lipotoxicity in Muscle Cells. Int J Mol Sci. 2019;20(3).
147. Sui J, He M, Wang Y, Zhao X, He Y, Shi B. Sphingolipid metabolism in type 2 diabetes and associated cardiovascular complications. Exp Ther Med. 2019;18(5):3603-14.
148. Boon J, Hoy AJ, Stark R, Brown RD, Meex RC, Henstridge DC, et al. Ceramides contained in LDL are elevated in type 2 diabetes and promote inflammation and skeletal muscle insulin resistance. Diabetes. 2013;62(2):401-10.
149. Kolak M, Westerbacka J, Velagapudi VR, Wågsäter D, Yetukuri L, Makkonen J, et al. Adipose tissue inflammation and increased ceramide content characterize subjects with high liver fat content independent of obesity. Diabetes. 2007;56(8):1960-8.
150. Summers SA. Ceramides in insulin resistance and lipotoxicity. Prog Lipid Res. 2006;45(1):42-72.
151. Gulbins E, Kolesnick R. Raft ceramide in molecular medicine. Oncogene. 2003;22(45):7070-7.
152. Legler DF, Micheau O, Doucey MA, Tschopp J, Bron C. Recruitment of TNF receptor 1 to lipid rafts is essential for TNFalpha-mediated NF-kappaB activation. Immunity. 2003;18(5):655-64.
153. Shah J, Atienza JM, Rawlings AV, Shipley GG. Physical properties of ceramides: effect of fatty acid hydroxylation. J Lipid Res. 1995;36(9):1945-55.
154. Megha, Sawatzki P, Kolter T, Bittman R, London E. Effect of ceramide N-acyl chain and polar headgroup structure on the properties of ordered lipid domains (lipid rafts). Biochim Biophys Acta. 2007;1768(9):2205-12.
155. Salvesen GS, Dixit VM. Caspase activation: the induced-proximity model. Proc Natl Acad Sci U S A. 1999;96(20):10964-7.
156. Grassme H, Jekle A, Riehle A, Schwarz H, Berger J, Sandhoff K, et al. CD95 signaling via ceramide-rich membrane rafts. J Biol Chem. 2001;276(23):20589-96.
157. Cremesti A, Paris F, Grassmé H, Holler N, Tschopp J, Fuks Z, et al. Ceramide enables fas to cap and kill. J Biol Chem. 2001;276(26):23954-61.
158. Lipke K, Kubis-Kubiak A, Piwowar A. Molecular Mechanism of Lipotoxicity as an Interesting Aspect in the Development of Pathological States-Current View of Knowledge. Cells. 2022;11(5).
159. Phaniendra A, Jestadi DB, Periyasamy L. Free radicals: properties, sources, targets, and their implication in various diseases. Indian J Clin Biochem. 2015;30(1):11-26.
160. Hauck AK, Bernlohr DA. Oxidative stress and lipotoxicity. J Lipid Res. 2016;57(11):1976-86.

161. Al-Aubaidy HA, Jelinek HF. Oxidative DNA damage and obesity in type 2 diabetes mellitus. Eur J Endocrinol. 2011;164(6):899-904.
162. Sakuraba H, Mizukami H, Yagihashi N, Wada R, Hanyu C, Yagihashi S. Reduced beta-cell mass and expression of oxidative stress-related DNA damage in the islet of Japanese Type II diabetic patients. Diabetologia. 2002;45(1):85-96.
163. Leenders F, Groen N, de Graaf N, Engelse MA, Rabelink TJ, de Koning EJP, et al. Oxidative Stress Leads to β-Cell Dysfunction Through Loss of β-Cell Identity. Front Immunol. 2021;12:690379.
164. Miki A, Ricordi C, Sakuma Y, Yamamoto T, Misawa R, Mita A, et al. Divergent antioxidant capacity of human islet cell subsets: A potential cause of beta-cell vulnerability in diabetes and islet transplantation. PLoS One. 2018;13(5):e0196570.
165. Eguchi N, Vaziri ND, Dafoe DC, Ichii H. The Role of Oxidative Stress in Pancreatic β Cell Dysfunction in Diabetes. Int J Mol Sci. 2021;22(4).
166. Cohen G, Riahi Y, Shamni O, Guichardant M, Chatgilialoglu C, Ferreri C, et al. Role of lipid peroxidation and PPAR-δ in amplifying glucose-stimulated insulin secretion. Diabetes. 2011;60(11):2830-42.
167. Yadav DK, Kumar S, Choi EH, Chaudhary S, Kim MH. Molecular dynamic simulations of oxidized skin lipid bilayer and permeability of reactive oxygen species. Sci Rep. 2019;9(1):4496.
168. Cohen G, Shamni O, Avrahami Y, Cohen O, Broner EC, Filippov-Levy N, et al. Beta cell response to nutrient overload involves phospholipid remodelling and lipid peroxidation. Diabetologia. 2015;58(6):1333-43.
169. Gu F, Crump CM, Thomas G. Trans-Golgi network sorting. Cell Mol Life Sci. 2001;58(8):1067-84.
170. Tsuchiya Y, Hatakeyama H, Emoto N, Wagatsuma F, Matsushita S, Kanzaki M. Palmitate-induced down-regulation of sortilin and impaired GLUT4 trafficking in C2C12 myotubes. J Biol Chem. 2010;285(45):34371-81.
171. Plötz T, Krümmel B, Laporte A, Pingitore A, Persaud SJ, Jörns A, et al. The monounsaturated fatty acid oleate is the major physiological toxic free fatty acid for human beta cells. Nutr Diabetes. 2017;7(12):305.
172. Welters HJ, Tadayyon M, Scarpello JH, Smith SA, Morgan NG. Mono-unsaturated fatty acids protect against beta-cell apoptosis induced by saturated fatty acids, serum withdrawal or cytokine exposure. FEBS Lett. 2004;560(1-3):103-8.
173. Nolan CJ, Larter CZ. Lipotoxicity: why do saturated fatty acids cause and monounsaturates protect against it? J Gastroenterol Hepatol. 2009;24(5):703-6.
174. Morgan NG, Dhayal S, Diakogiannaki E, Welters HJ. The cytoprotective actions of long-chain mono-unsaturated fatty acids in pancreatic beta-cells. Biochem Soc Trans. 2008;36(Pt 5):905-8.
175. Morgan NG, Dhayal S. Unsaturated fatty acids as cytoprotective agents in the pancreatic beta-cell. Prostaglandins Leukot Essent Fatty Acids. 2010;82(4-6):231-6.
176. Listenberger LL, Han X, Lewis SE, Cases S, Farese RV, Ory DS, et al. Triglyceride accumulation protects against fatty acid-induced lipotoxicity. Proc Natl Acad Sci U S A. 2003;100(6):3077-82.
177. Leekumjorn S, Cho HJ, Wu Y, Wright NT, Sum AK, Chan C. The role of fatty acid unsaturation in minimizing biophysical changes on the structure and local effects of bilayer membranes. Biochim Biophys Acta. 2009;1788(7):1508-16.
178. Cheng V, Kimball DR, Conboy DJC. Determination of the Rate-Limiting Step in Fatty Acid Transport. J Phys Chem B. 2019;123(33):7157-68.

179. Füllekrug J, Ehehalt R, Poppelreuther M. Outlook: membrane junctions enable the metabolic trapping of fatty acids by intracellular acyl-CoA synthetases. Front Physiol. 2012;3:401.
180. Cooper GM. Transport of Small Molecules. The Cell: A Molecular Approach. 2nd ed. Sunderland (MA): Sinauer Associates; 2000.
181. Sahoo S, Aurich MK, Jonsson JJ, Thiele I. Membrane transporters in a human genome-scale metabolic knowledgebase and their implications for disease. Front Physiol. 2014;5:91.
182. Krupka RM. Coupling mechanisms in active transport. Biochim Biophys Acta. 1993;1183(1):105-13.
183. Doherty GJ, McMahon HT. Mechanisms of endocytosis. Annu Rev Biochem. 2009;78:857-902.
184. Jay AG, Simard JR, Huang N, Hamilton JA. SSO and other putative inhibitors of FA transport across membranes by CD36 disrupt intracellular metabolism, but do not affect FA translocation. J Lipid Res. 2020;61(5):790-807.
185. Barta E. Mathematical Models Suggest Facilitated Fatty Acids Crossing of the Luminal Membrane in the Cardiac Muscle. J Membr Biol. 2017;250(1):103-14.
186. Barta E. Transport of Free Fatty Acids from Plasma to the Endothelium of Cardiac Muscle: A Theoretical Study. J Membr Biol. 2015;248(4):783-93.
187. Kamp F, Hamilton JA. pH gradients across phospholipid membranes caused by fast flip-flop of un-ionized fatty acids. Proc Natl Acad Sci U S A. 1992;89(23):11367-70.
188. Hamilton JA, Brunaldi K. A model for fatty acid transport into the brain. J Mol Neurosci. 2007;33(1):12-7.
189. Missner A, Pohl P. 110 years of the Meyer-Overton rule: predicting membrane permeability of gases and other small compounds. Chemphyschem. 2009;10(9-10):1405-14.
190. Grime JM, Edwards MA, Rudd NC, Unwin PR. Quantitative visualization of passive transport across bilayer lipid membranes. Proc Natl Acad Sci U S A. 2008;105(38):14277-82.
191. Hamilton JA. Fatty acid transport: difficult or easy? J Lipid Res. 1998;39(3):467-81.
192. Madshus IH. Regulation of intracellular pH in eukaryotic cells. Biochem J. 1988;250(1):1-8.
193. Andersson LE, Valtat B, Bagge A, Sharoyko VV, Nicholls DG, Ravassard P, et al. Characterization of stimulus-secretion coupling in the human pancreatic EndoC-βH1 beta cell line. PLoS One. 2015;10(3):e0120879.
194. Kamp F, Zakim D, Zhang F, Noy N, Hamilton JA. Fatty acid flip-flop in phospholipid bilayers is extremely fast. Biochemistry. 1995;34(37):11928-37.
195. Pohl EE, Peterson U, Sun J, Pohl P. Changes of intrinsic membrane potentials induced by flip-flop of long-chain fatty acids. Biochemistry. 2000;39(7):1834-9.
196. Kamp F, Guo W, Souto R, Pilch PF, Corkey BE, Hamilton JA. Rapid flip-flop of oleic acid across the plasma membrane of adipocytes. J Biol Chem. 2003;278(10):7988-95.
197. Wu ML, Chan CC, Su MJ. Possible mechanism(s) of arachidonic acid-induced intracellular acidosis in rat cardiac myocytes. Circ Res. 2000;86(3):E55-62.
198. Meshulam T, Simard JR, Wharton J, Hamilton JA, Pilch PF. Role of caveolin-1 and cholesterol in transmembrane fatty acid movement. Biochemistry. 2006;45(9):2882-93.
199. Tong F, Black PN, Coleman RA, DiRusso CC. Fatty acid transport by vectorial acylation in mammals: roles played by different isoforms of rat long-chain acyl-CoA synthetases. Arch Biochem Biophys. 2006;447(1):46-52.
200. Zhan T, Poppelreuther M, Ehehalt R, Füllekrug J. Overexpressed FATP1, ACSVL4/FATP4 and ACSL1 increase the cellular fatty acid uptake of 3T3-L1 adipocytes but are localized on intracellular membranes. PLoS One. 2012;7(9):e45087.
201. Ellis JM, Bowman CE, Wolfgang MJ. Metabolic and tissue-specific regulation of acyl-CoA metabolism. PLoS One. 2015;10(3):e0116587.

202. Gargiulo CE, Stuhlsatz-Krouper SM, Schaffer JE. Localization of adipocyte long-chain fatty acyl-CoA synthetase at the plasma membrane. J Lipid Res. 1999;40(5):881-92.
203. Pohl J, Ring A, Ehehalt R, Schulze-Bergkamen H, Schad A, Verkade P, et al. Long-chain fatty acid uptake into adipocytes depends on lipid raft function. Biochemistry. 2004;43(14):4179-87.
204. Abumrad N, Harmon C, Ibrahimi A. Membrane transport of long-chain fatty acids: evidence for a facilitated process. J Lipid Res. 1998;39(12):2309-18.
205. Kobayashi H, Mitsui T, Nomura S, Ohno Y, Kadomatsu K, Muramatsu T, et al. Expression of glucose transporter 4 in the human pancreatic islet of Langerhans. Biochem Biophys Res Commun. 2004;314(4):1121-5.
206. Poulsen SB, Fenton RA, Rieg T. Sodium-glucose cotransport. Curr Opin Nephrol Hypertens. 2015;24(5):463-9.
207. Abumrad NA, Perkins RC, Park JH, Park CR. Mechanism of long chain fatty acid permeation in the isolated adipocyte. J Biol Chem. 1981;256(17):9183-91.
208. Schwenk RW, Holloway GP, Luiken JJ, Bonen A, Glatz JF. Fatty acid transport across the cell membrane: regulation by fatty acid transporters. Prostaglandins Leukot Essent Fatty Acids. 2010;82(4-6):149-54.
209. Chhibber A, French CE, Yee SW, Gamazon ER, Theusch E, Qin X, et al. Transcriptomic variation of pharmacogenes in multiple human tissues and lymphoblastoid cell lines. Pharmacogenomics J. 2017;17(2):137-45.
210. Kazantzis M, Stahl A. Fatty acid transport proteins, implications in physiology and disease. Biochim Biophys Acta. 2012;1821(5):852-7.
211. Sharom FJ. Flipping and flopping--lipids on the move. IUBMB Life. 2011;63(9):736-46.
212. Longo N, Frigeni M, Pasquali M. Carnitine transport and fatty acid oxidation. Biochim Biophys Acta. 2016;1863(10):2422-35.
213. Knottnerus SJG, Bleeker JC, Wüst RCI, Ferdinandusse S, IJlst L, Wijburg FA, et al. Disorders of mitochondrial long-chain fatty acid oxidation and the carnitine shuttle. Rev Endocr Metab Disord. 2018;19(1):93-106.
214. El-Gharbawy A, Vockley J. Inborn Errors of Metabolism with Myopathy: Defects of Fatty Acid Oxidation and the Carnitine Shuttle System. Pediatr Clin North Am. 2018;65(2):317-35.
215. SJOESTRAND FS. A COMPARISON OF PLASMA MEMBRANE, CYTOMEMBRANES, AND MITOCHONDRIAL MEMBRANE ELEMENTS WITH RESPECT TO ULTRASTRUCTURAL FEATURES. J Ultrastruct Res. 1963;52:561-80.
216. Schenkel LC, Bakovic M. Formation and regulation of mitochondrial membranes. Int J Cell Biol. 2014;2014:709828.
217. Antonescu CN, Foti M, Sauvonnet N, Klip A. Ready, set, internalize: mechanisms and regulation of GLUT4 endocytosis. Biosci Rep. 2009;29(1):1-11.
218. Mayor S, Parton RG, Donaldson JG. Clathrin-independent pathways of endocytosis. Cold Spring Harb Perspect Biol. 2014;6(6).
219. Hao JW, Wang J, Guo H, Zhao YY, Sun HH, Li YF, et al. CD36 facilitates fatty acid uptake by dynamic palmitoylation-regulated endocytosis. Nat Commun. 2020;11(1):4765.
220. Daquinag AC, Gao Z, Fussell C, Immaraj L, Pasqualini R, Arap W, et al. Fatty acid mobilization from adipose tissue is mediated by CD36 posttranslational modifications and intracellular trafficking. JCI Insight. 2021;6(17).
221. Pohl J, Ring A, Stremmel W. Uptake of long-chain fatty acids in HepG2 cells involves caveolae: analysis of a novel pathway. J Lipid Res. 2002;43(9):1390-9.
222. Pohl J, Ring A, Korkmaz U, Ehehalt R, Stremmel W. FAT/CD36-mediated long-chain fatty acid uptake in adipocytes requires plasma membrane rafts. Mol Biol Cell. 2005;16(1):24-31.

223. Pownall HJ. Commentary on SSO and other putative inhibitors of FA transport across membranes by CD36 disrupt intracellular metabolism, but do not affect fatty acid translocation. J Lipid Res. 2020;61(5):595-7.
224. Housden BE, Muhar M, Gemberling M, Gersbach CA, Stainier DY, Seydoux G, et al. Loss-of-function genetic tools for animal models: cross-species and cross-platform differences. Nat Rev Genet. 2017;18(1):24-40.
225. Febbraio M, Abumrad NA, Hajjar DP, Sharma K, Cheng W, Pearce SF, et al. A null mutation in murine CD36 reveals an important role in fatty acid and lipoprotein metabolism. J Biol Chem. 1999;274(27):19055-62.
226. Newberry EP, Xie Y, Kennedy S, Han X, Buhman KK, Luo J, et al. Decreased hepatic triglyceride accumulation and altered fatty acid uptake in mice with deletion of the liver fatty acid-binding protein gene. J Biol Chem. 2003;278(51):51664-72.
227. Zhou SL, Stump D, Sorrentino D, Potter BJ, Berk PD. Adipocyte differentiation of 3T3-L1 cells involves augmented expression of a 43-kDa plasma membrane fatty acid-binding protein. J Biol Chem. 1992;267(20):14456-61.
228. Angin Y, Steinbusch LK, Simons PJ, Greulich S, Hoebers NT, Douma K, et al. CD36 inhibition prevents lipid accumulation and contractile dysfunction in rat cardiomyocytes. Biochem J. 2012;448(1):43-53.
229. Steinbusch LK, Wijnen W, Schwenk RW, Coumans WA, Hoebers NT, Ouwens DM, et al. Differential regulation of cardiac glucose and fatty acid uptake by endosomal pH and actin filaments. Am J Physiol Cell Physiol. 2010;298(6):C1549-59.
230. Harmon CM, Luce P, Beth AH, Abumrad NA. Labeling of adipocyte membranes by sulfo-N-succinimidyl derivatives of long-chain fatty acids: inhibition of fatty acid transport. J Membr Biol. 1991;121(3):261-8.
231. Turcotte LP, Swenberger JR, Tucker MZ, Yee AJ, Trump G, Luiken JJ, et al. Muscle palmitate uptake and binding are saturable and inhibited by antibodies to FABP(PM). Mol Cell Biochem. 2000;210(1-2):53-63.
232. Luiken JJFP, Turcotte LP, Bonen A. Protein-mediated palmitate uptake and expression of fatty acid transport proteins in heart giant vesicles. Journal of Lipid Research. 1999;40(6):1007-16.
233. Stremmel W. Uptake of fatty acids by jejunal mucosal cells is mediated by a fatty acid binding membrane protein. J Clin Invest. 1988;82(6):2001-10.
234. Bantounas I, Phylactou LA, Uney JB. RNA interference and the use of small interfering RNA to study gene function in mammalian systems. J Mol Endocrinol. 2004;33(3):545-57.
235. Lam JK, Chow MY, Zhang Y, Leung SW. siRNA Versus miRNA as Therapeutics for Gene Silencing. Mol Ther Nucleic Acids. 2015;4:e252.
236. Rao DD, Senzer N, Cleary MA, Nemunaitis J. Comparative assessment of siRNA and shRNA off target effects: what is slowing clinical development. Cancer Gene Ther. 2009;16(11):807-9.
237. Wang Q, Wei L, Guan X, Wu Y, Zou Q, Ji Z. Briefing in family characteristics of microRNAs and their applications in cancer research. Biochim Biophys Acta. 2014;1844(1 Pt B):191-7.
238. Benninghoff T, Espelage L, Eickelschulte S, Zeinert I, Sinowenka I, Müller F, et al. The RabGAPs TBC1D1 and TBC1D4 Control Uptake of Long-Chain Fatty Acids Into Skeletal Muscle via Fatty Acid Transporter SLC27A4/FATP4. Diabetes. 2020;69(11):2281-93.
239. Lobo S, Wiczer BM, Smith AJ, Hall AM, Bernlohr DA. Fatty acid metabolism in adipocytes: functional analysis of fatty acid transport proteins 1 and 4. J Lipid Res. 2007;48(3):609-20.
240. Lobo S, Wiczer BM, Bernlohr DA. Functional analysis of long-chain acyl-CoA synthetase 1 in 3T3-L1 adipocytes. J Biol Chem. 2009;284(27):18347-56.
241. Mikłosz A, Łukaszuk B, Supruniuk E, Grubczak K, Moniuszko M, Choromańska B, et al. Does TBC1D4 (AS160) or TBC1D1 Deficiency Affect the Expression of Fatty Acid Handling

Proteins in the Adipocytes Differentiated from Human Adipose-Derived Mesenchymal Stem Cells (ADMSCs) Obtained from Subcutaneous and Visceral Fat Depots? Cells. 2021;10(6).
242. Dance A. The shifting sands of 'gain-of-function' research. Nature. 2021;598(7882):554-7.
243. Schaffer JE, Lodish HF. Expression cloning and characterization of a novel adipocyte long chain fatty acid transport protein. Cell. 1994;79(3):427-36.
244. Douglas KL. Toward development of artificial viruses for gene therapy: a comparative evaluation of viral and non-viral transfection. Biotechnol Prog. 2008;24(4):871-83.
245. Even DY, Kedmi A, Basch-Barzilay S, Ideses D, Tikotzki R, Shir-Shapira H, et al. Engineered Promoters for Potent Transient Overexpression. PLoS One. 2016;11(2):e0148918.
246. Howarth JL, Lee YB, Uney JB. Using viral vectors as gene transfer tools (Cell Biology and Toxicology Special Issue: ETCS-UK 1 day meeting on genetic manipulation of cells). Cell Biol Toxicol. 2010;26(1):1-20.
247. Patil S, Gao YG, Lin X, Li Y, Dang K, Tian Y, et al. The Development of Functional Non-Viral Vectors for Gene Delivery. Int J Mol Sci. 2019;20(21).
248. Ehehalt R, Sparla R, Kulaksiz H, Herrmann T, Füllekrug J, Stremmel W. Uptake of long chain fatty acids is regulated by dynamic interaction of FAT/CD36 with cholesterol/sphingolipid enriched microdomains (lipid rafts). BMC Cell Biol. 2008;9:45.
249. Ibrahimi A, Sfeir Z, Magharaie H, Amri EZ, Grimaldi P, Abumrad NA. Expression of the CD36 homolog (FAT) in fibroblast cells: effects on fatty acid transport. Proc Natl Acad Sci U S A. 1996;93(7):2646-51.
250. Stahl A, Hirsch DJ, Gimeno RE, Punreddy S, Ge P, Watson N, et al. Identification of the major intestinal fatty acid transport protein. Mol Cell. 1999;4(3):299-308.
251. Felgner PL, Gadek TR, Holm M, Roman R, Chan HW, Wenz M, et al. Lipofection: a highly efficient, lipid-mediated DNA-transfection procedure. Proc Natl Acad Sci U S A. 1987;84(21):7413-7.
252. Holloway GP, Chou CJ, Lally J, Stellingwerff T, Maher AC, Gavrilova O, et al. Increasing skeletal muscle fatty acid transport protein 1 (FATP1) targets fatty acids to oxidation and does not predispose mice to diet-induced insulin resistance. Diabetologia. 2011;54(6):1457-67.
253. Rols MP. Electropermeabilization, a physical method for the delivery of therapeutic molecules into cells. Biochim Biophys Acta. 2006;1758(3):423-8.
254. van der Donk LEH, van der Spek J, van Duivenvoorde T, Ten Brink MS, Geijtenbeek TBH, Kuijl CP, et al. An optimized retroviral toolbox for overexpression and genetic perturbation of primary lymphocytes. Biol Open. 2022;11(2).
255. Schneider H, Staudacher S, Poppelreuther M, Stremmel W, Ehehalt R, Füllekrug J. Protein mediated fatty acid uptake: synergy between CD36/FAT-facilitated transport and acyl-CoA synthetase-driven metabolism. Arch Biochem Biophys. 2014;546:8-18.
256. García-Martínez C, Marotta M, Moore-Carrasco R, Guitart M, Camps M, Busquets S, et al. Impact on fatty acid metabolism and differential localization of FATP1 and FAT/CD36 proteins delivered in cultured human muscle cells. Am J Physiol Cell Physiol. 2005;288(6):C1264-72.
257. Salameh A, Daquinag AC, Staquicini DI, An Z, Hajjar KA, Pasqualini R, et al. Prohibitin/annexin 2 interaction regulates fatty acid transport in adipose tissue. JCI Insight. 2016;1(10).
258. Sandy P, Ventura A, Jacks T. Mammalian RNAi: a practical guide. Biotechniques. 2005;39(2):215-24.
259. Stoebel DM, Dean AM, Dykhuizen DE. The cost of expression of Escherichia coli lac operon proteins is in the process, not in the products. Genetics. 2008;178(3):1653-60.
260. Moriya H. Quantitative nature of overexpression experiments. Mol Biol Cell. 2015;26(22):3932-9.

261. Carley AN, Kleinfeld AM. Fatty acid (FFA) transport in cardiomyocytes revealed by imaging unbound FFA is mediated by an FFA pump modulated by the CD36 protein. J Biol Chem. 2011;286(6):4589-97.
262. Chabowski A, Górski J, Glatz JF, P Luiken JJ, Bonen A. Protein-mediated Fatty Acid Uptake in the Heart. Curr Cardiol Rev. 2008;4(1):12-21.
263. Turpeinen AK, Takala TO, Nuutila P, Axelin T, Luotolahti M, Haaparanta M, et al. Impaired free fatty acid uptake in skeletal muscle but not in myocardium in patients with impaired glucose tolerance: studies with PET and 14(R,S)-[18F]fluoro-6-thia-heptadecanoic acid. Diabetes. 1999;48(6):1245-50.
264. Choe SS, Huh JY, Hwang IJ, Kim JI, Kim JB. Adipose Tissue Remodeling: Its Role in Energy Metabolism and Metabolic Disorders. Front Endocrinol (Lausanne). 2016;7:30.
265. Marchetti P, Bugliani M, De Tata V, Suleiman M, Marselli L. Pancreatic Beta Cell Identity in Humans and the Role of Type 2 Diabetes. Front Cell Dev Biol. 2017;5:55.
266. Walker CA, Spinale FG. The structure and function of the cardiac myocyte: a review of fundamental concepts. J Thorac Cardiovasc Surg. 1999;118(2):375-82.
267. Fritzen AM, Lundsgaard AM, Kiens B. Tuning fatty acid oxidation in skeletal muscle with dietary fat and exercise. Nat Rev Endocrinol. 2020;16(12):683-96.
268. Alves-Bezerra M, Cohen DE. Triglyceride Metabolism in the Liver. Compr Physiol. 2017;8(1):1-8.
269. Laffel L. Ketone bodies: a review of physiology, pathophysiology and application of monitoring to diabetes. Diabetes Metab Res Rev. 1999;15(6):412-26.
270. Resnik DB. Limits on risks for healthy volunteers in biomedical research. Theor Med Bioeth. 2012;33(2):137-49.
271. Linnemann AK, Baan M, Davis DB. Pancreatic β-cell proliferation in obesity. Adv Nutr. 2014;5(3):278-88.
272. Morgan NG, Richardson SJ. Fifty years of pancreatic islet pathology in human type 1 diabetes: insights gained and progress made. Diabetologia. 2018;61(12):2499-506.
273. De Vos A, Heimberg H, Quartier E, Huypens P, Bouwens L, Pipeleers D, et al. Human and rat beta cells differ in glucose transporter but not in glucokinase gene expression. J Clin Invest. 1995;96(5):2489-95.
274. Shiao MS, Liao BY, Long M, Yu HT. Adaptive evolution of the insulin two-gene system in mouse. Genetics. 2008;178(3):1683-91.
275. Brissova M, Fowler MJ, Nicholson WE, Chu A, Hirshberg B, Harlan DM, et al. Assessment of human pancreatic islet architecture and composition by laser scanning confocal microscopy. J Histochem Cytochem. 2005;53(9):1087-97.
276. Olson EM, Lin NU, Krop IE, Winer EP. The ethical use of mandatory research biopsies. Nat Rev Clin Oncol. 2011;8(10):620-5.
277. Mishima T, Miner JH, Morizane M, Stahl A, Sadovsky Y. The expression and function of fatty acid transport protein-2 and -4 in the murine placenta. PLoS One. 2011;6(10):e25865.
278. Thomas P, Arden C, Corcoran J, Hacker C, Welters HJ, Morgan NG. Differential routing and disposition of the long-chain saturated fatty acid palmitate in rodent vs human beta-cells. Nutr Diabetes. 2022;12(1):22.
279. Tricco AC, Lillie E, Zarin W, O'Brien KK, Colquhoun H, Levac D, et al. PRISMA Extension for Scoping Reviews (PRISMA-ScR): Checklist and Explanation. Ann Intern Med. 2018;169(7):467-73.
280. Scanlan JN, Novak T. Sensory approaches in mental health: A scoping review. Aust Occup Ther J. 2015;62(5):277-85.

281. Bosco L, Lorello GR, Flexman AM, Hastie MJ. Women in anaesthesia: a scoping review. Br J Anaesth. 2020;124(3):e134-e47.
282. Park D, Kim E, Lee H, Shin EA, Lee JW. Tetraspanin TM4SF5 in hepatocytes negatively modulates SLC27A transporters during acute fatty acid supply. Arch Biochem Biophys. 2021;710:109004.
283. Wang J, Hao JW, Wang X, Guo H, Sun HH, Lai XY, et al. DHHC4 and DHHC5 Facilitate Fatty Acid Uptake by Palmitoylating and Targeting CD36 to the Plasma Membrane. Cell Rep. 2019;26(1):209-21.e5.
284. Hames KC, Vella A, Kemp BJ, Jensen MD. Free fatty acid uptake in humans with CD36 deficiency. Diabetes. 2014;63(11):3606-14.
285. Luiken JJ, Willems J, van der Vusse GJ, Glatz JF. Electrostimulation enhances FAT/CD36-mediated long-chain fatty acid uptake by isolated rat cardiac myocytes. Am J Physiol Endocrinol Metab. 2001;281(4):E704-12.
286. Momken I, Chabowski A, Dirkx E, Nabben M, Jain SS, Mcfarlan JT, et al. A new leptin-mediated mechanism for stimulating fatty acid oxidation: a pivotal role for sarcolemmal FAT/CD36. Biochemical Journal. 2017;474(1):149-62.
287. Chabowski A, Coort SL, Calles-Escandon J, Tandon NN, Glatz JF, Luiken JJ, et al. The subcellular compartmentation of fatty acid transporters is regulated differently by insulin and by AICAR. FEBS Lett. 2005;579(11):2428-32.
288. Luiken JJ, Koonen DP, Willems J, Zorzano A, Becker C, Fischer Y, et al. Insulin stimulates long-chain fatty acid utilization by rat cardiac myocytes through cellular redistribution of FAT/CD36. Diabetes. 2002;51(10):3113-9.
289. Bonen A, Luiken JJ, Arumugam Y, Glatz JF, Tandon NN. Acute regulation of fatty acid uptake involves the cellular redistribution of fatty acid translocase. J Biol Chem. 2000;275(19):14501-8.
290. Wiczer BM, Bernlohr DA. A novel role for fatty acid transport protein 1 in the regulation of tricarboxylic acid cycle and mitochondrial function in 3T3-L1 adipocytes. J Lipid Res. 2009;50(12):2502-13.
291. Wu Q, Ortegon AM, Tsang B, Doege H, Feingold KR, Stahl A. FATP1 Is an Insulin-Sensitive Fatty Acid Transporter Involved in Diet-Induced Obesity. Molecular and Cellular Biology. 2006;26(9):3455-67.
292. Lynes M, Narisawa S, Millán JL, Widmaier EP. Interactions between CD36 and global intestinal alkaline phosphatase in mouse small intestine and effects of high-fat diet. Am J Physiol Regul Integr Comp Physiol. 2011;301(6):R1738-47.
293. Chabowski A, Żendzian-Piotrowska M, Konstantynowicz K, Pankiewicz W, Mikłosz A, Łukaszuk B, et al. Fatty acid transporters involved in the palmitate and oleate induced insulin resistance in primary rat hepatocytes. Acta Physiol (Oxf). 2013;207(2):346-57.
294. Guthmann F, Haupt R, Looman AC, Spener F, Rüstow B. Fatty acid translocase/CD36 mediates the uptake of palmitate by type II pneumocytes. Am J Physiol. 1999;277(1):L191-6.
295. Mitchell RW, On NH, Del Bigio MR, Miller DW, Hatch GM. Fatty acid transport protein expression in human brain and potential role in fatty acid transport across human brain microvessel endothelial cells. Journal of Neurochemistry. 2011:no-no.
296. Gimeno RE, Ortegon AM, Patel S, Punreddy S, Ge P, Sun Y, et al. Characterization of a heart-specific fatty acid transport protein. J Biol Chem. 2003;278(18):16039-44.
297. Sorrentino D, Stump D, Potter BJ, Robinson RB, White R, Kiang CL, et al. Oleate uptake by cardiac myocytes is carrier mediated and involves a 40-kD plasma membrane fatty acid binding protein similar to that in liver, adipose tissue, and gut. J Clin Invest. 1988;82(3):928-35.

298. Xu S, Jay A, Brunaldi K, Huang N, Hamilton JA. CD36 enhances fatty acid uptake by increasing the rate of intracellular esterification but not transport across the plasma membrane. Biochemistry. 2013;52(41):7254-61.
299. Siddiqi S, Sheth A, Patel F, Barnes M, Mansbach CM. Intestinal caveolin-1 is important for dietary fatty acid absorption. Biochimica et Biophysica Acta (BBA) - Molecular and Cell Biology of Lipids. 2013;1831(8):1311-21.
300. Glatz JFC, Nabben M, Luiken JJFP. CD36 (SR-B2) as master regulator of cellular fatty acid homeostasis. Curr Opin Lipidol. 2022;33(2):103-11.
301. Glatz JFC, Luiken JJFP. Dynamic role of the transmembrane glycoprotein CD36 (SR-B2) in cellular fatty acid uptake and utilization. J Lipid Res. 2018;59(7):1084-93.
302. Klip A, McGraw TE, James DE. Thirty sweet years of GLUT4. J Biol Chem. 2019;294(30):11369-81.
303. Parton RG, Simons K. The multiple faces of caveolae. Nat Rev Mol Cell Biol. 2007;8(3):185-94.
304. Vistisen B, Roepstorff K, Roepstorff C, Bonen A, van Deurs B, Kiens B. Sarcolemmal FAT/CD36 in human skeletal muscle colocalizes with caveolin-3 and is more abundant in type 1 than in type 2 fibers. J Lipid Res. 2004;45(4):603-9.
305. Coe NR, Smith AJ, Frohnert BI, Watkins PA, Bernlohr DA. The fatty acid transport protein (FATP1) is a very long chain acyl-CoA synthetase. J Biol Chem. 1999;274(51):36300-4.
306. Hall AM, Wiczer BM, Herrmann T, Stremmel W, Bernlohr DA. Enzymatic properties of purified murine fatty acid transport protein 4 and analysis of acyl-CoA synthetase activities in tissues from FATP4 null mice. J Biol Chem. 2005;280(12):11948-54.
307. Anderson CM, Stahl A. SLC27 fatty acid transport proteins. Mol Aspects Med. 2013;34(2-3):516-28.
308. Grevengoed TJ, Klett EL, Coleman RA. Acyl-CoA metabolism and partitioning. Annu Rev Nutr. 2014;34:1-30.
309. Prentki M, Corkey BE. Are the beta-cell signaling molecules malonyl-CoA and cystolic long-chain acyl-CoA implicated in multiple tissue defects of obesity and NIDDM? Diabetes. 1996;45(3):273-83.
310. Hertz R, Magenheim J, Berman I, Bar-Tana J. Fatty acyl-CoA thioesters are ligands of hepatic nuclear factor-4alpha. Nature. 1998;392(6675):512-6.
311. Milger K, Herrmann T, Becker C, Gotthardt D, Zickwolf J, Ehehalt R, et al. Cellular uptake of fatty acids driven by the ER-localized acyl-CoA synthetase FATP4. J Cell Sci. 2006;119(Pt 22):4678-88.
312. Ibrahim A, Yucel N, Kim B, Arany Z. Local Mitochondrial ATP Production Regulates Endothelial Fatty Acid Uptake and Transport. Cell Metab. 2020;32(2):309-19.e7.
313. Krammer J, Digel M, Ehehalt F, Stremmel W, Füllekrug J, Ehehalt R. Overexpression of CD36 and acyl-CoA synthetases FATP2, FATP4 and ACSL1 increases fatty acid uptake in human hepatoma cells. Int J Med Sci. 2011;8(7):599-614.
314. Digel M, Staffer S, Ehehalt F, Stremmel W, Ehehalt R, Füllekrug J. FATP4 contributes as an enzyme to the basal and insulin-mediated fatty acid uptake of C_2C_{12} muscle cells. Am J Physiol Endocrinol Metab. 2011;301(5):E785-96.
315. Tao C, Sifuentes A, Holland WL. Regulation of glucose and lipid homeostasis by adiponectin: effects on hepatocytes, pancreatic β cells and adipocytes. Best Pract Res Clin Endocrinol Metab. 2014;28(1):43-58.
316. Thompson BR, Lobo S, Bernlohr DA. Fatty acid flux in adipocytes: the in's and out's of fat cell lipid trafficking. Mol Cell Endocrinol. 2010;318(1-2):24-33.

317. Malaisse WJ, Best L, Kawazu S, Malaisse-Lagae F, Sener A. The stimulus-secretion coupling of glucose-induced insulin release: fuel metabolism in islets deprived of exogenous nutrient. Arch Biochem Biophys. 1983;224(1):102-10.
318. Luo L, Liu M. Adipose tissue in control of metabolism. J Endocrinol. 2016;231(3):R77-R99.
319. Mashek DG, Li LO, Coleman RA. Long-chain acyl-CoA synthetases and fatty acid channeling. Future Lipidol. 2007;2(4):465-76.
320. Holloway G, Schwenk R, Luiken J, Glatz J, Bonen A. Fatty acid transport in skeletal muscle: role in energy provision and insulin resistance. Clinical Lipidology; 2017.
321. Stremmel W, Pohl L, Ring A, Herrmann T. A new concept of cellular uptake and intracellular trafficking of long-chain fatty acids. Lipids. 2001;36(9):981-9.
322. Hirasawa A, Tsumaya K, Awaji T, Katsuma S, Adachi T, Yamada M, et al. Free fatty acids regulate gut incretin glucagon-like peptide-1 secretion through GPR120. Nat Med. 2005;11(1):90-4.
323. Pham MT, Rajić A, Greig JD, Sargeant JM, Papadopoulos A, McEwen SA. A scoping review of scoping reviews: advancing the approach and enhancing the consistency. Res Synth Methods. 2014;5(4):371-85.
324. Brien SE, Lorenzetti DL, Lewis S, Kennedy J, Ghali WA. Overview of a formal scoping review on health system report cards. Implement Sci. 2010;5:2.
325. Garner P, Hopewell S, Chandler J, MacLehose H, Schünemann HJ, Akl EA, et al. When and how to update systematic reviews: consensus and checklist. BMJ. 2016;354:i3507.
326. Crick F. Central dogma of molecular biology. Nature. 1970;227(5258):561-3.
327. Kukurba KR, Montgomery SB. RNA Sequencing and Analysis. Cold Spring Harb Protoc. 2015;2015(11):951-69.
328. Stark R, Grzelak M, Hadfield J. RNA sequencing: the teenage years. Nat Rev Genet. 2019;20(11):631-56.
329. Wang Z, Gerstein M, Snyder M. RNA-Seq: a revolutionary tool for transcriptomics. Nat Rev Genet. 2009;10(1):57-63.
330. Maxam AM, Gilbert W. A new method for sequencing DNA. Proc Natl Acad Sci U S A. 1977;74(2):560-4.
331. Sanger F, Nicklen S, Coulson AR. DNA sequencing with chain-terminating inhibitors. Proc Natl Acad Sci U S A. 1977;74(12):5463-7.
332. Park ST, Kim J. Trends in Next-Generation Sequencing and a New Era for Whole Genome Sequencing. Int Neurourol J. 2016;20(Suppl 2):S76-83.
333. Head SR, Komori HK, LaMere SA, Whisenant T, Van Nieuwerburgh F, Salomon DR, et al. Library construction for next-generation sequencing: overviews and challenges. Biotechniques. 2014;56(2):61-4, 6, 8, passim.
334. Schurch NJ, Schofield P, Gierliński M, Cole C, Sherstnev A, Singh V, et al. How many biological replicates are needed in an RNA-seq experiment and which differential expression tool should you use? RNA. 2016;22(6):839-51.
335. McIntyre LM, Lopiano KK, Morse AM, Amin V, Oberg AL, Young LJ, et al. RNA-seq: technical variability and sampling. BMC Genomics. 2011;12:293.
336. Corley SM, MacKenzie KL, Beverdam A, Roddam LF, Wilkins MR. Differentially expressed genes from RNA-Seq and functional enrichment results are affected by the choice of single-end versus paired-end reads and stranded versus non-stranded protocols. BMC Genomics. 2017;18(1):399.
337. Freedman AH, Gaspar JM, Sackton TB. Short paired-end reads trump long single-end reads for expression analysis. BMC Bioinformatics. 2020;21(1):149.
338. Gallego Romero I, Pai AA, Tung J, Gilad Y. RNA-seq: impact of RNA degradation on transcript quantification. BMC Biol. 2014;12:42.

339. Li X, Wang CY. From bulk, single-cell to spatial RNA sequencing. Int J Oral Sci. 2021;13(1):36.
340. Thind AS, Monga I, Thakur PK, Kumari P, Dindhoria K, Krzak M, et al. Demystifying emerging bulk RNA-Seq applications: the application and utility of bioinformatic methodology. Brief Bioinform. 2021;22(6).
341. Haque A, Engel J, Teichmann SA, Lönnberg T. A practical guide to single-cell RNA-sequencing for biomedical research and clinical applications. Genome Med. 2017;9(1):75.
342. Hong M, Tao S, Zhang L, Diao LT, Huang X, Huang S, et al. RNA sequencing: new technologies and applications in cancer research. J Hematol Oncol. 2020;13(1):166.
343. Diedisheim M, Oshima M, Albagli O, Huldt CW, Ahlstedt I, Clausen M, et al. Modeling human pancreatic beta cell dedifferentiation. Mol Metab. 2018;10:74-86.
344. Blanchet E, Van de Velde S, Matsumura S, Hao E, LeLay J, Kaestner K, et al. Feedback inhibition of CREB signaling promotes beta cell dysfunction in insulin resistance. Cell Rep. 2015;10(7):1149-57.
345. Muraro MJ, Dharmadhikari G, Grün D, Groen N, Dielen T, Jansen E, et al. A Single-Cell Transcriptome Atlas of the Human Pancreas. Cell Syst. 2016;3(4):385-94.e3.
346. Xin Y, Kim J, Okamoto H, Ni M, Wei Y, Adler C, et al. RNA Sequencing of Single Human Islet Cells Reveals Type 2 Diabetes Genes. Cell Metab. 2016;24(4):608-15.
347. Weir GC, Gaglia J, Bonner-Weir S. Inadequate β-cell mass is essential for the pathogenesis of type 2 diabetes. Lancet Diabetes Endocrinol. 2020;8(3):249-56.
348. Fagerberg L, Hallström BM, Oksvold P, Kampf C, Djureinovic D, Odeberg J, et al. Analysis of the human tissue-specific expression by genome-wide integration of transcriptomics and antibody-based proteomics. Mol Cell Proteomics. 2014;13(2):397-406.
349. Colli ML, Ramos-Rodríguez M, Nakayasu ES, Alvelos MI, Lopes M, Hill JLE, et al. An integrated multi-omics approach identifies the landscape of interferon-α-mediated responses of human pancreatic beta cells. Nat Commun. 2020;11(1):2584.
350. Marselli L, Piron A, Suleiman M, Colli ML, Yi X, Khamis A, et al. Persistent or Transient Human β Cell Dysfunction Induced by Metabolic Stress: Specific Signatures and Shared Gene Expression with Type 2 Diabetes. Cell Rep. 2020;33(9):108466.
351. Kong X, Liu CX, Wang GD, Yang H, Yao XM, Hua Q, et al. LncRNA LEGLTBC Functions as a ceRNA to Antagonize the Effects of miR-34a on the Downregulation of SIRT1 in Glucolipotoxicity-Induced INS-1 Beta Cell Oxidative Stress and Apoptosis. Oxid Med Cell Longev. 2019;2019:4010764.
352. Andrews S. FastQC: A Quality Control Tool for High Throughput Sequence Data 2010 [13 September, 2022]. Available from: https://www.bioinformatics.babraham.ac.uk/projects/fastqc/.
353. Illumina. Quality Scores for Next-Generation Sequencing: assessing sequencing accuracy using Phred quality scoring 2011 [13 September, 2022]. Available from: https://www.illumina.com/documents/products/technotes/technote_Q-Scores.pdf.
354. Hansen KD, Brenner SE, Dudoit S. Biases in Illumina transcriptome sequencing caused by random hexamer priming. Nucleic Acids Res. 2010;38(12):e131.
355. Bansal V. A computational method for estimating the PCR duplication rate in DNA and RNA-seq experiments. BMC Bioinformatics. 2017;18(Suppl 3):43.
356. Bolger AM, Lohse M, Usadel B. Trimmomatic: a flexible trimmer for Illumina sequence data. Bioinformatics. 2014;30(15):2114-20.
357. Bray NL, Pimentel H, Melsted P, Pachter L. Near-optimal probabilistic RNA-seq quantification. Nat Biotechnol. 2016;34(5):525-7.
358. Alser M, Rotman J, Deshpande D, Taraszka K, Shi H, Baykal PI, et al. Technology dictates algorithms: recent developments in read alignment. Genome Biol. 2021;22(1):249.

359. Zhao Y, Li MC, Konaté MM, Chen L, Das B, Karlovich C, et al. TPM, FPKM, or Normalized Counts? A Comparative Study of Quantification Measures for the Analysis of RNA-seq Data from the NCI Patient-Derived Models Repository. J Transl Med. 2021;19(1):269.
360. Cunningham F, Allen JE, Allen J, Alvarez-Jarreta J, Amode R, M, Armean M, Irina, et al. Ensembl 2022. Nucleic Acids Research. 2022;50(D1):D988-D95.
361. Morales J, Pujar S, Loveland JE, Astashyn A, Bennett R, Berry A, et al. A joint NCBI and EMBL-EBI transcript set for clinical genomics and research. Nature. 2022;604(7905):310-5.
362. Putri GH, Anders S, Pyl PT, Pimanda JE, Zanini F. Analysing high-throughput sequencing data in Python with HTSeq 2.0. Bioinformatics. 2022;38(10):2943-5.
363. Love MI, Huber W, Anders S. Moderated estimation of fold change and dispersion for RNA-seq data with DESeq2. Genome Biology. 2014;15(12).
364. Payne EH, Gebregziabher M, Hardin JW, Ramakrishnan V, Egede LE. An empirical approach to determine a threshold for assessing overdispersion in Poisson and negative binomial models for count data. Communications in Statistics - Simulation and Computation. 2018;47(6):1722-38.
365. Wickham H. ggplot2: Elegant Graphics for Data Analysis: Springer-Verlag New York; 2016.
366. Ansari IH, Longacre MJ, Stoker SW, Kendrick MA, O'Neill LM, Zitur LJ, et al. Characterization of Acyl-CoA synthetase isoforms in pancreatic beta cells: Gene silencing shows participation of ACSL3 and ACSL4 in insulin secretion. Arch Biochem Biophys. 2017;618:32-43.
367. Wang YL, Guo W, Zang Y, Yaney GC, Vallega G, Getty-Kaushik L, et al. Acyl coenzyme a synthetase regulation: putative role in long-chain acyl coenzyme a partitioning. Obes Res. 2004;12(11):1781-8.
368. Lewin TM, Kim JH, Granger DA, Vance JE, Coleman RA. Acyl-CoA synthetase isoforms 1, 4, and 5 are present in different subcellular membranes in rat liver and can be inhibited independently. J Biol Chem. 2001;276(27):24674-9.
369. Cooper DE, Young PA, Klett EL, Coleman RA. Physiological Consequences of Compartmentalized Acyl-CoA Metabolism. J Biol Chem. 2015;290(33):20023-31.
370. Soupene E, Kuypers FA. Mammalian long-chain acyl-CoA synthetases. Exp Biol Med (Maywood). 2008;233(5):507-21.
371. Kang MJ, Fujino T, Sasano H, Minekura H, Yabuki N, Nagura H, et al. A novel arachidonate-preferring acyl-CoA synthetase is present in steroidogenic cells of the rat adrenal, ovary, and testis. Proc Natl Acad Sci U S A. 1997;94(7):2880-4.
372. Oikawa E, Iijima H, Suzuki T, Sasano H, Sato H, Kamataki A, et al. A novel acyl-CoA synthetase, ACS5, expressed in intestinal epithelial cells and proliferating preadipocytes. J Biochem. 1998;124(3):679-85.
373. Iijima H, Fujino T, Minekura H, Suzuki H, Kang MJ, Yamamoto T. Biochemical studies of two rat acyl-CoA synthetases, ACS1 and ACS2. Eur J Biochem. 1996;242(2):186-90.
374. Fitscher BA, Riedel HD, Young KC, Stremmel W. Tissue distribution and cDNA cloning of a human fatty acid transport protein (hsFATP4). Biochim Biophys Acta. 1998;1443(3):381-5.
375. Doege H, Baillie RA, Ortegon AM, Tsang B, Wu Q, Punreddy S, et al. Targeted deletion of FATP5 reveals multiple functions in liver metabolism: alterations in hepatic lipid homeostasis. Gastroenterology. 2006;130(4):1245-58.
376. Hui TY, Frohnert BI, Smith AJ, Schaffer JE, Bernlohr DA. Characterization of the murine fatty acid transport protein gene and its insulin response sequence. J Biol Chem. 1998;273(42):27420-9.
377. Man MZ, Hui TY, Schaffer JE, Lodish HF, Bernlohr DA. Regulation of the murine adipocyte fatty acid transporter gene by insulin. Mol Endocrinol. 1996;10(8):1021-8.

378. Rütti S, Arous C, Nica AC, Kanzaki M, Halban PA, Bouzakri K. Expression, phosphorylation and function of the Rab-GTPase activating protein TBC1D1 in pancreatic beta-cells. FEBS Lett. 2014;588(1):15-20.
379. Bouzakri K, Ribaux P, Tomas A, Parnaud G, Rickenbach K, Halban PA. Rab GTPase-activating protein AS160 is a major downstream effector of protein kinase B/Akt signaling in pancreatic beta-cells. Diabetes. 2008;57(5):1195-204.
380. Chadt A, Leicht K, Deshmukh A, Jiang LQ, Scherneck S, Bernhardt U, et al. Tbc1d1 mutation in lean mouse strain confers leanness and protects from diet-induced obesity. Nat Genet. 2008;40(11):1354-9.
381. Taylor EB, An D, Kramer HF, Yu H, Fujii NL, Roeckl KS, et al. Discovery of TBC1D1 as an insulin-, AICAR-, and contraction-stimulated signaling nexus in mouse skeletal muscle. J Biol Chem. 2008;283(15):9787-96.
382. Chavez JA, Roach WG, Keller SR, Lane WS, Lienhard GE. Inhibition of GLUT4 translocation by Tbc1d1, a Rab GTPase-activating protein abundant in skeletal muscle, is partially relieved by AMP-activated protein kinase activation. J Biol Chem. 2008;283(14):9187-95.
383. Moltke I, Grarup N, Jørgensen ME, Bjerregaard P, Treebak JT, Fumagalli M, et al. A common Greenlandic TBC1D4 variant confers muscle insulin resistance and type 2 diabetes. Nature. 2014;512(7513):190-3.
384. Whitley SK, Horne WT, Kolls JK. Research Techniques Made Simple: Methodology and Clinical Applications of RNA Sequencing. J Invest Dermatol. 2016;136(8):e77-e82.
385. Abumrad NA, el-Maghrabi MR, Amri EZ, Lopez E, Grimaldi PA. Cloning of a rat adipocyte membrane protein implicated in binding or transport of long-chain fatty acids that is induced during preadipocyte differentiation. Homology with human CD36. J Biol Chem. 1993;268(24):17665-8.
386. Jacobs A, Elmer KR. Alternative splicing and gene expression play contrasting roles in the parallel phenotypic evolution of a salmonid fish. Mol Ecol. 2021;30(20):4955-69.
387. Tsonkova VG, Sand FW, Wolf XA, Grunnet LG, Kirstine Ringgaard A, Ingvorsen C, et al. The EndoC-βH1 cell line is a valid model of human beta cells and applicable for screenings to identify novel drug target candidates. Mol Metab. 2018;8:144-57.
388. Ryaboshapkina M, Saitoski K, Hamza GM, Jarnuczak AF, Pechberty S, Berthault C, et al. Characterization of the Secretome, Transcriptome, and Proteome of Human β Cell Line EndoC-βH1. Mol Cell Proteomics. 2022;21(5):100229.
389. Benazra M, Lecomte MJ, Colace C, Müller A, Machado C, Pechberty S, et al. A human beta cell line with drug inducible excision of immortalizing transgenes. Mol Metab. 2015;4(12):916-25.
390. Scharfmann R, Pechberty S, Hazhouz Y, von Bülow M, Bricout-Neveu E, Grenier-Godard M, et al. Development of a conditionally immortalized human pancreatic β cell line. J Clin Invest. 2014;124(5):2087-98.
391. Hastoy B, Godazgar M, Clark A, Nylander V, Spiliotis I, van de Bunt M, et al. Electrophysiological properties of human beta-cell lines EndoC-βH1 and -βH2 conform with human beta-cells. Sci Rep. 2018;8(1):16994.
392. Oleson BJ, McGraw JA, Broniowska KA, Annamalai M, Chen J, Bushkofsky JR, et al. Distinct differences in the responses of the human pancreatic β-cell line EndoC-βH1 and human islets to proinflammatory cytokines. Am J Physiol Regul Integr Comp Physiol. 2015;309(5):R525-34.
393. Gustafsson J, Held F, Robinson JL, Björnson E, Jörnsten R, Nielsen J. Sources of variation in cell-type RNA-Seq profiles. PLoS One. 2020;15(9):e0239495.
394. Cabrera O, Berman DM, Kenyon NS, Ricordi C, Berggren PO, Caicedo A. The unique cytoarchitecture of human pancreatic islets has implications for islet cell function. Proc Natl Acad Sci U S A. 2006;103(7):2334-9.

395. Ben-David U, Siranosian B, Ha G, Tang H, Oren Y, Hinohara K, et al. Genetic and transcriptional evolution alters cancer cell line drug response. Nature. 2018;560(7718):325-30.
396. Ravassard P, Hazhouz Y, Pechberty S, Bricout-Neveu E, Armanet M, Czernichow P, et al. A genetically engineered human pancreatic β cell line exhibiting glucose-inducible insulin secretion. J Clin Invest. 2011;121(9):3589-97.
397. Hectors TL, Vanparys C, Pereira-Fernandes A, Martens GA, Blust R. Evaluation of the INS-1 832/13 cell line as a beta-cell based screening system to assess pollutant effects on beta-cell function. PLoS One. 2013;8(3):e60030.
398. Hohmeier HE, Mulder H, Chen G, Henkel-Rieger R, Prentki M, Newgard CB. Isolation of INS-1-derived cell lines with robust ATP-sensitive K+ channel-dependent and -independent glucose-stimulated insulin secretion. Diabetes. 2000;49(3):424-30.
399. Asfari M, Janjic D, Meda P, Li G, Halban PA, Wollheim CB. Establishment of 2-mercaptoethanol-dependent differentiated insulin-secreting cell lines. Endocrinology. 1992;130(1):167-78.
400. Kristiansson E, Österlund T, Gunnarsson L, Arne G, Larsson DG, Nerman O. A novel method for cross-species gene expression analysis. BMC Bioinformatics. 2013;14:70.
401. McCluskey A, Daniel JA, Hadzic G, Chau N, Clayton EL, Mariana A, et al. Building a better dynasore: the dyngo compounds potently inhibit dynamin and endocytosis. Traffic. 2013;14(12):1272-89.
402. Thomas P. Finding needles in a transporter haystack: investigations into how long-chain fatty acids translocate the plasma membrane of pancreatic beta cells: unpublished work. 2022.
403. Bhatia T, Husen P, Brewer J, Bagatolli LA, Hansen PL, Ipsen JH, et al. Preparing giant unilamellar vesicles (GUVs) of complex lipid mixtures on demand: Mixing small unilamellar vesicles of compositionally heterogeneous mixtures. Biochim Biophys Acta. 2015;1848(12):3175-80.
404. Crane JM, Tamm LK. Role of cholesterol in the formation and nature of lipid rafts in planar and spherical model membranes. Biophys J. 2004;86(5):2965-79.
405. Stewart JM, Driedzic WR, Berkelaar JA. Fatty-acid-binding protein facilitates the diffusion of oleate in a model cytosol system. Biochem J. 1991;275 (Pt 3):569-73.
406. Schultz SG. Membrane Transport | Membrane Transport, General Concepts. Encyclopedia of Biological Chemistry III. 2. 3rd ed2013. p. 876-9.
407. Brown DA, London E. Structure and origin of ordered lipid domains in biological membranes. J Membr Biol. 1998;164(2):103-14.
408. M'Baye G, Mély Y, Duportail G, Klymchenko AS. Liquid ordered and gel phases of lipid bilayers: fluorescent probes reveal close fluidity but different hydration. Biophys J. 2008;95(3):1217-25.
409. Los DA, Murata N. Membrane fluidity and its roles in the perception of environmental signals. Biochim Biophys Acta. 2004;1666(1-2):142-57.
410. Zhang X, Barraza KM, Beauchamp JL. Cholesterol provides nonsacrificial protection of membrane lipids from chemical damage at air-water interface. Proc Natl Acad Sci U S A. 2018;115(13):3255-60.
411. Hac-Wydro K, Wydro P. The influence of fatty acids on model cholesterol/phospholipid membranes. Chem Phys Lipids. 2007;150(1):66-81.
412. Ghysels A, Krämer A, Venable RM, Teague WE, Lyman E, Gawrisch K, et al. Permeability of membranes in the liquid ordered and liquid disordered phases. Nat Commun. 2019;10(1):5616.
413. Barba-Bon A, Nilam M, Hennig A. Supramolecular Chemistry in the Biomembrane. Chembiochem. 2020;21(7):886-910.

414. Funari SS, Barceló F, Escribá PV. Effects of oleic acid and its congeners, elaidic and stearic acids, on the structural properties of phosphatidylethanolamine membranes. J Lipid Res. 2003;44(3):567-75.
415. Escribá PV, Sastre M, García-Sevilla JA. Disruption of cellular signaling pathways by daunomycin through destabilization of nonlamellar membrane structures. Proc Natl Acad Sci U S A. 1995;92(16):7595-9.
416. Giorgione J, Epand RM, Buda C, Farkas T. Role of phospholipids containing docosahexaenoyl chains in modulating the activity of protein kinase C. Proc Natl Acad Sci U S A. 1995;92(21):9767-70.
417. Epand RM, Epand RF, Ahmed N, Chen R. Promotion of hexagonal phase formation and lipid mixing by fatty acids with varying degrees of unsaturation. Chem Phys Lipids. 1991;57(1):75-80.
418. Gonen A, Miller YI. From Inert Storage to Biological Activity-In Search of Identity for Oxidized Cholesteryl Esters. Front Endocrinol (Lausanne). 2020;11:602252.
419. Naito M. Effects of Cholesterol and Cholesterol Esters on Cell Function II. The Effects of Various Cholesterol Esters on the Cell Membrane and Related Functions. Cell Structure and Function. 1978;3(3):219-26.
420. Hazel JR, Williams EE. The role of alterations in membrane lipid composition in enabling physiological adaptation of organisms to their physical environment. Prog Lipid Res. 1990;29(3):167-227.
421. Suutari M, Laakso S. Microbial fatty acids and thermal adaptation. Crit Rev Microbiol. 1994;20(4):285-328.
422. Koike T, Ishida G, Taniguchi M, Higaki K, Ayaki Y, Saito M, et al. Decreased membrane fluidity and unsaturated fatty acids in Niemann–Pick disease type C fibroblasts 1998;1406(3):327–35.
423. Ammendolia DA, Bement WM, Brumell JH. Plasma membrane integrity: implications for health and disease. BMC Biol. 2021;19(1):71.
424. Bastiaanse E. The effect of membrane cholesterol content on ion transport processes in plasma membranes. Cardiovascular Research. 1997;33(2):272-83.
425. Frallicciardi J, Melcr J, Siginou P, Marrink SJ, Poolman B. Membrane thickness, lipid phase and sterol type are determining factors in the permeability of membranes to small solutes. Nature Communications. 2022;13(1):1605.
426. Stieger B, Steiger J, Locher KP. Membrane lipids and transporter function. Biochim Biophys Acta Mol Basis Dis. 2021;1867(5):166079.
427. Brown MF. Soft Matter in Lipid–Protein Interactions. The Annual Review of Biophysics. 2017;46:379–410.
428. Thomas P. An investigation into the mechanisms of lipotoxicity in rodent and human-derived β-cell lines [PhD Thesis]. Exeter: University of Exeter; 2019.
429. Lawlor N, Márquez EJ, Orchard P, Narisu N, Shamim MS, Thibodeau A, et al. Multiomic Profiling Identifies cis-Regulatory Networks Underlying Human Pancreatic β Cell Identity and Function. Cell Rep. 2019;26(3):788-801.e6.
430. Koltes JE, Arora I, Gupta R, Nguyen DC, Schaid M, Kim JA, et al. A gene expression network analysis of the pancreatic islets from lean and obese mice identifies complement 1q like-3 secreted protein as a regulator of β-cell function. Sci Rep. 2019;9(1):10119.
431. Han J, Burgess K. Fluorescent indicators for intracellular pH. Chem Rev. 2010;110(5):2709-28.
432. Jobsis PD, Rothstein EC, Balaban RS. Limited utility of acetoxymethyl (AM)-based intracellular delivery systems, in vivo: interference by extracellular esterases. J Microsc. 2007;226(Pt 1):74-81.

433. Stijlemans B, Cnops J, Naniima P, Vaast A, Bockstal V, De Baetselier P, et al. Development of a pHrodo-based assay for the assessment of in vitro and in vivo erythrophagocytosis during experimental trypanosomosis. PLoS Negl Trop Dis. 2015;9(3):e0003561.
434. Schneider CA, Rasband WS, Eliceiri KW. NIH Image to ImageJ: 25 years of image analysis. Nat Methods. 2012;9(7):671-5.
435. Parasassi T, Gratton E. Membrane lipid domains and dynamics as detected by Laurdan fluorescence. J Fluoresc. 1995;5(1):59-69.
436. Golfetto O, Hinde E, Gratton E. Laurdan fluorescence lifetime discriminates cholesterol content from changes in fluidity in living cell membranes. Biophys J. 2013;104(6):1238-47.
437. Sameni S, Malacrida L, Tan Z, Digman MA. Alteration in Fluidity of Cell Plasma Membrane in Huntington Disease Revealed by Spectral Phasor Analysis. Sci Rep. 2018;8(1):734.
438. Wheeler G, Tyler KM. Widefield microscopy for live imaging of lipid domains and membrane dynamics. Biochim Biophys Acta. 2011;1808(3):634-41.
439. Harris FM, Best KB, Bell JD. Use of laurdan fluorescence intensity and polarization to distinguish between changes in membrane fluidity and phospholipid order. Biochim Biophys Acta. 2002;1565(1):123-8.
440. Campbell I. Organization of the Body: Control of the Internal Environment. Anaesthesia & Intensive Care Medicine. 2003;4(10):345-8.
441. Pilkington EH, Gurzov EN, Kakinen A, Litwak SA, Stanley WJ, Davis TP, et al. Pancreatic β-Cell Membrane Fluidity and Toxicity Induced by Human Islet Amyloid Polypeptide Species. Sci Rep. 2016;6:21274.
442. Stringer C, Wang T, Michaelos M, Pachitariu M. Cellpose: a generalist algorithm for cellular segmentation. Nat Methods. 2021;18(1):100-6.
443. Panconi L, Makarova M, Lambert ER, May RC, Owen DM. Topology-based fluorescence image analysis for automated cell identification and segmentation. 2022.
444. Owen DM, Rentero C, Magenau A, Abu-Siniyeh A, Gaus K. Quantitative imaging of membrane lipid order in cells and organisms. Nat Protoc. 2011;7(1):24-35.
445. Bonen A, Luiken JJ, Liu S, Dyck DJ, Kiens B, Kristiansen S, et al. Palmitate transport and fatty acid transporters in red and white muscles. Am J Physiol. 1998;275(3):E471-8.
446. van der Vusse GJ. Albumin as fatty acid transporter. Drug Metab Pharmacokinet. 2009;24(4):300-7.
447. Weisiger R, Gollan J, Ockner R. Receptor for albumin on the liver cell surface may mediate uptake of fatty acids and other albumin-bound substances. Science. 1981;211(4486):1048-51.
448. Daniels C, Noy N, Zakim D. Rates of hydration of fatty acids bound to unilamellar vesicles of phosphatidylcholine or to albumin. Biochemistry. 1985;24(13):3286-92.
449. Charalel RA, Engberg K, Noolandi J, Cochran JR, Frank C, Ta CN. Diffusion of protein through the human cornea. Ophthalmic Res. 2012;48(1):50-5.
450. Li HH, Li J, Wasserloos KJ, Wallace C, Sullivan MG, Bauer PM, et al. Caveolae-dependent and -independent uptake of albumin in cultured rodent pulmonary endothelial cells. PLoS One. 2013;8(11):e81903.
451. Davoust J, Gruenberg J, Howell KE. Two threshold values of low pH block endocytosis at different stages. EMBO J. 1987;6(12):3601-9.
452. Cosson P, de Curtis I, Pouysségur J, Griffiths G, Davoust J. Low cytoplasmic pH inhibits endocytosis and transport from the trans-Golgi network to the cell surface. J Cell Biol. 1989;108(2):377-87.
453. Sandvig K, Olsnes S, Petersen OW, van Deurs B. Acidification of the cytosol inhibits endocytosis from coated pits. J Cell Biol. 1987;105(2):679-89.

454. Wang LH, Südhof TC, Anderson RG. The appendage domain of alpha-adaptin is a high affinity binding site for dynamin. J Biol Chem. 1995;270(17):10079-83.
455. Sakai H, Li G, Hino Y, Moriura Y, Kawawaki J, Sawada M, et al. Increases in intracellular pH facilitate endocytosis and decrease availability of voltage-gated proton channels in osteoclasts and microglia. J Physiol. 2013;591(23):5851-66.
456. Kazyken D, Lentz SI, Fingar DC. Alkaline intracellular pH (pHi) activates AMPK-mTORC2 signaling to promote cell survival during growth factor limitation. J Biol Chem. 2021;297(4):101100.
457. Topală T, Bodoki A, Oprean L, Oprean R. Bovine Serum Albumin Interactions with Metal Complexes. Clujul Med. 2014;87(4):215-9.
458. Preta G, Cronin JG, Sheldon IM. Dynasore - not just a dynamin inhibitor. Cell Commun Signal. 2015;13:24.
459. Ferguson SM, De Camilli P. Dynamin, a membrane-remodelling GTPase. Nat Rev Mol Cell Biol. 2012;13(2):75-88.
460. Fan F, Wu Y, Hara M, Rizk A, Ji C, Nerad D, et al. Dynamin deficiency causes insulin secretion failure and hyperglycemia. Proc Natl Acad Sci U S A. 2021;118(32).
461. Haythorne E, Rohm M, van de Bunt M, Brereton MF, Tarasov AI, Blacker TS, et al. Diabetes causes marked inhibition of mitochondrial metabolism in pancreatic β-cells. Nat Commun. 2019;10(1):2474.
462. Lamontagne J, Al-Mass A, Nolan CJ, Corkey BE, Madiraju SRM, Joly E, et al. Identification of the signals for glucose-induced insulin secretion in INS1 (832/13) β-cells using metformin-induced metabolic deceleration as a model. J Biol Chem. 2017;292(47):19458-68.
463. Bailey RW, Nguyen T, Robertson L, Gibbons E, Nelson J, Christensen RE, et al. Sequence of physical changes to the cell membrane during glucocorticoid-induced apoptosis in S49 lymphoma cells. Biophys J. 2009;96(7):2709-18.
464. Kummrow A, Frankowski M, Bock N, Werner C, Dziekan T, Neukammer J. Quantitative assessment of cell viability based on flow cytometry and microscopy. Cytometry Part A. 2013;83A(2):197-204.
465. Adan A, Alizada G, Kiraz Y, Baran Y, Nalbant A. Flow cytometry: basic principles and applications. Critical Reviews in Biotechnology. 2017;37(2):163-76.
466. Hara T, Kimura I, Inoue D, Ichimura A, Hirasawa A. Free fatty acid receptors and their role in regulation of energy metabolism. Rev Physiol Biochem Pharmacol. 2013;164:77-116.
467. Al Mahri S, Malik SS, Al Ibrahim M, Haji E, Dairi G, Mohammad S. Free Fatty Acid Receptors (FFARs) in Adipose: Physiological Role and Therapeutic Outlook. Cells. 2022;11(4).
468. Ichimura A, Hasegawa S, Kasubuchi M, Kimura I. Free fatty acid receptors as therapeutic targets for the treatment of diabetes. Front Pharmacol. 2014;5:236.
469. Nolan CJ, Madiraju MS, Delghingaro-Augusto V, Peyot ML, Prentki M. Fatty acid signaling in the beta-cell and insulin secretion. Diabetes. 2006;55 Suppl 2:S16-23.
470. Schilperoort M, van Dam AD, Hoeke G, Shabalina IG, Okolo A, Hanyaloglu AC, et al. The GPR120 agonist TUG-891 promotes metabolic health by stimulating mitochondrial respiration in brown fat. EMBO Mol Med. 2018;10(3).
471. Krizhanovskii C, Kristinsson H, Elksnis A, Wang X, Gavali H, Bergsten P, et al. EndoC-βH1 cells display increased sensitivity to sodium palmitate when cultured in DMEM/F12 medium. Islets. 2017;9(3):e1296995.
472. Fignani D, Licata G, Brusco N, Nigi L, Grieco GE, Marselli L, et al. SARS-CoV-2 Receptor Angiotensin I-Converting Enzyme Type 2 (ACE2) Is Expressed in Human Pancreatic. Front Endocrinol (Lausanne). 2020;11:596898.
473. Raoufinia R, Mota A, Keyhanvar N, Safari F, Shamekhi S, Abdolalizadeh J. Overview of Albumin and Its Purification Methods. Adv Pharm Bull. 2016;6(4):495-507.

474. Krizhanovskii C, Fred RG, Oskarsson ME, Westermark GT, Welsh N. Addition of exogenous sodium palmitate increases the IAPP/insulin mRNA ratio via GPR40 in human EndoC-βH1 cells. Ups J Med Sci. 2017;122(3):149-59.
475. Francis GL. Albumin and mammalian cell culture: implications for biotechnology applications. Cytotechnology. 2010;62(1):1-16.
476. Biggers JD, Summers MC, McGinnis LK. Polyvinyl alcohol and amino acids as substitutes for bovine serum albumin in culture media for mouse preimplantation embryos. Hum Reprod Update. 1997;3(2):125-35.
477. Andersson C, Iresjö BM, Lundholm K. Identification of tissue sites for increased albumin degradation in sarcoma-bearing mice. J Surg Res. 1991;50(2):156-62.
478. Carter M, Shieh J. Cell Culture Techniques. Guide to Research Techniques in Neuroscience. 2nd ed: Academic Press; 2015. p. 295-310.
479. Stehle G, Sinn H, Wunder A, Schrenk HH, Stewart JC, Hartung G, et al. Plasma protein (albumin) catabolism by the tumor itself--implications for tumor metabolism and the genesis of cachexia. Crit Rev Oncol Hematol. 1997;26(2):77-100.
480. Xu S, Edman M, Kothawala MS, Sun G, Chiang L, Mircheff A, et al. A Rab11a-enriched subapical membrane compartment regulates a cytoskeleton-dependent transcytotic pathway in secretory epithelial cells of the lacrimal gland. Journal of Cell Science. 2011;124(20):3503-14.
481. Dolman NJ, Kilgore JA, Davidson MW. A review of reagents for fluorescence microscopy of cellular compartments and structures, part I: BacMam labeling and reagents for vesicular structures. Curr Protoc Cytom. 2013;Chapter 12:Unit 12.30.

Appendix A

Supplementary Tables

Supplementary Table 1: Data extracted from final publications retrieved for review. The data presented here was compiled in collaboration with Dr Patricia Thomas.

	Ref.	Cell type	Model organism	Candidate transport protein(s)	Experimental conditions	LC-FFA transported	Did the protein facilitate LC-FFA transport?
Adipocytes							
	Jay et al. (2020)	Adipocytes	Rat	CD36	Chemical inhibition	Oleate	No
	Febbraio et al.	Adipocytes	Mouse	CD36	Knockout	Oleate	Yes
	Hao et al. (2020)	Adipocytes (3T3-L1)	Mouse	CD36 CAV1	Knockout	Oleate	CD36: Yes CAV1: Yes
	Lobo et al. (2007)	Adipocytes (3T3-L1)	Mouse	FATP1 FATP4	Knockdown (using short hairpin RNA (shRNA))	Palmitate and oleate	FATP1: Yes FATP4: No
	Pohl et al. (2005)	Adipocytes (3T3-L1)	Mouse	CD36	Chemical inhibition	Oleate	Yes

	Gargiulo et al. (1999)	Adipocytes (3T3-L1)	Mouse	ACSL1 FATP1	Overexpressed	Oleate	ACSL1: Yes FATP1: Yes
	Lobo et al. (2009)	Adipocytes (3T3-L1)	Mouse	ACSL1 CD36	Knockdown (using short hairpin RNA (shRNA))	Palmitate	ACSL1: No CD36: Yes
	Wiczer et al. (2009)	Adipocytes (3T3-L1)	Mouse	FATP1	Knockdown (using short hairpin RNA (shRNA))	Palmitate	Yes
	Zhou et al. (1992)	Adipocytes (3T3-L1)	Mouse	FABP1	Chemical inhibition	Oleate	Yes
	Schaffer, E. and Lodish, F. (1994)	Adipocytes (3T3-L1)	Mouse	FATP1	Overexpressed	Palmitate and oleate	Yes
Adipose-Derived Mesenchymal Stem cells							
	Mikłosz et al. (2021)	Adipose-Derived Mesenchymal Stem Cells (ADMSCs)	Human	TBC1D1 TBC1D4	Knockdown (siRNAs)	Palmitate	TBC1D1: No TBC1D4: Yes (knockdown

							increased transport)
Brain micro vessel endothelial cells							
	Mitchell et al. (2011)	Brain microvessel endothelial cells (HBMEC)	Human	FATP1 FATP4 FABP5 CD36	Knockdown (siRNAs)	Oleate and palmitate	FATP1: Yes FATP4: No FABP5: Yes CD36: Yes
Cardiomyocytes							
	Angin et al. (2012)	Cardiomyocytes	Rat	CD36	Chemical inhibition	Palmitate	Yes
	Steinbusch et al. (2010)	Cardiomyocytes	Rat	CD36	Chemical inhibition	Palmitate	Yes
	Luiken et al. (2001)	Cardiomyocytes	Rat	CD36	Chemical inhibition	Palmitate	Yes

	Carley, A. and Kleinfeld, A. (2011)	Cardiomyocytes	Mouse	CD36	Knockout	Oleate	No, except for OA*o* 20 nM (not at 100 nM or 200nM)
Embryonic kidney cells							
	Xu et al. (2013)	Embryonic kidney cells (HEK293T)	Human	CD36	Overexpressed	Oleate	No
	Meshulam et al. (2006)	Embryonic kidney cells (HEK293T)	Human	CAV1	Overexpressed	Palmitate and oleate	Yes
Enterocytes							
	Lynes et al. (2011)	Enterocytes	Mouse	CD36	Chemical inhibition	Palmitate	High fat diet: Yes Normal fat diet: No
Epithelial kidney cells							

	Schneider et al. (2014)	Epithelial kidney cells (MDCK)	Dog	CD36 CAV1	CD36: Overexpressed CAV1: Knockdown (RNAi)	Oleate	CD36: Yes CAV1: No
Fibroblasts							
	Ehehalt et al. (2008)	Fibroblast-like cell line (COS)	Grivet	CD36	Overexpressed	Oleate	Yes
	Gimeno et al. (2003)	Fibroblast-like cell line (COS)	Monkey	FATP6	Overexpressed	Palmitate and oleate	Yes
	Ibrahimi et al. (1996)	Fibroblasts (Obl7PY)	Mouse	CD36	Overexpressed	Palmitate and oleate	Yes
Giant sarcolemmal vesicles							
	Holloway et al. (2011)	Giant sarcolemmal vesicles	Rat	FATP1	Overexpressed	Palmitate	Yes
	Bonen et al. (2000)	Giant sarcolemmal vesicles	Rat	CD36	Chemical inhibition	Palmitate	Yes

	Luiken et al. (1999)	Giant sarcolemmal vesicles (heart and muscle)	Rat	CD36 FABPpm	Chemical inhibition	Palmitate	CD36: Yes FABPpm: Yes
	Turcotte et al. (2000)	Giant sarcolemmal vesicles	Rat	FABPpm	Chemical inhibition	Palmitate	Yes
Hepatocytes							
	Chabowski et al. (2013)	Hepatocytes (primary)	Rat	CD36	Chemical inhibition	Palmitate and oleate	Yes
	Park et al. (2021)	Hepatocytes (primary)	Mouse	TM4SF5	Knockdown (siRNAs) Chemical inhibition Overexpressed	Palmitate	Yes. Knockdown and inhibition increased LCFA transport, over expression reduced LCFA uptake
	Newberry et al. (2003)	Hepatocytes	Mouse	FABP1	Knockout	Oleate	In the fasted state: Yes In the fed state: No

Intestinal brush border cells							
	Siddiqi et al. (2013)	Intestinal brush border	Rat and mouse	CAV1	Knockout	Oleate	Yes
Jejunal mucosal cells							
	Stremmel, W. (1988)	Jejunal mucosal cells	Rat	FABP8	Chemical inhibition	Palmitate and oleate	Yes
Myocytes							
	García-Martínez et al. (2005)	Myocytes	Human	CD36 FATP1	Overexpressed	Palmitate and oleate	CD36: Yes FATP1: Yes
	Benninghoff et al. (2020)	Myocytes	Mouse	TBC1D1 TBC1D4 Rab8a Rab8b Rab10	Knockdown (siRNAs)	Palmitate and oleate	TBC1D1 and TBC1D4: Knockdown increased LCFA transport

				Rab14 Rab28 FATP4 CD36			Rab8a, Rab8b, Rab10 and Rab14: Yes Rab28: No CD36: Yes FATP4: Yes
	Chabowski et al. (2005)	Myocytes	Rat	CD36	Chemical inhibition	Palmitate	Yes
	Luiken et al. (2002)	Myocytes	Rat	CD36	Chemical inhibition	Palmitate	Yes
	Sorrentino et al. (1988)	Myocytes	Rat	FABPpm	Chemical inhibition	Oleate	Yes
Pneumocytes							
	Guthmann et al. (1999)	Pneumocytes (type II)	Rat	CD36	Chemical inhibition	Palmitate	Yes
Multiple cell types							

Hames et al. (2014)	Adipocytes Myocytes (skeletal muscle) Cardiomyocytes Hepatocytes	Human	CD36	Comparison of CD36 sufficient and CD36 deficient patients	Palmitate	In adipocytes, myocytes, and cardiomyocytes: Yes In hepatocytes: No
Pohl et al. (2004)	Adipocytes (3T3-L1) Fibroblasts (3T3-L1)	Mouse	CAV3	Chemical inhibition	Oleate and stearate	Adipocytes: Yes Fibroblasts: No
Wu et al. (2006)	Adipocytes (3T3-L1) Myocytes	Mouse	FATP1	Knockout	Oleate	In unstimulated cells: No In insulin stimulated cells: Yes
Salameh et al. (2016)	Adipocytes (3T3-L1) Endothelial cells derived from brain tissue (bEnd.3)	Mouse	PHB ANX2 CD36	PHB: Knockdown in 3T3-L1 (siRNA), overexpressed in bENd.3 ANX2: Knockout 3T3-L1	Palmitate	PHB: Yes ANX2: Yes CD36: Yes

				ANX2/PHB: Chemical inhibition in 3T3-L1 CD36: Chemical inhibition in 3T3-L1		
Momken et al. (2017)	Cardiomyocytes Skeletal muscle (giant sarcolemmal vesicles)	Mouse	CD36	Chemical inhibition in cardiomyocytes Knockout in skeletal muscle	Palmitate	Yes
Wang et al. (2019)	Embryonic kidney cells (HEK293T) Preadipocytes (3T3-L1)	Human	DHHC4 DHHC5 CD36	DHHC5: Knockdown (shRNA), knockout in 3T3-L1 CD36: Knockdown in HEK293 (shRNA), Overexpressed in 3T3-L1	Oleate	DHHC4: Yes DHHC5: Yes CD36: Yes
Stahl et al. (1999)	Embryonic kidney cells (HEK293T) Enterocytes	HEK293: Human Enterocytes: Mouse	FATP4	Overexpressed in HEK293 Chemical inhibition in enterocytes	Palmitate and oleate	Yes

Supplementary Table 2: Characteristics of human tissue and islet donors included in RNA-seq analysis. The information in the table presented here was kindly collated by Dr Patricia Thomas.

Tissue type	**Study donor ID**	**Ethnicity**	**Age (yrs)**	**Sex**	**History of diabetes (Y/N)**	**BMI (kg/m^2)**	**Time from diagnosis**	**HbA1c**
				Fagerberg et al.				
Adipocytes	Not given	Not given	Not given	Not given	Not given	Not given	Not given	Not given
Hepatocytes	Not given	Not given	Not given	Not given	Not given	Not given	Not given	Not given
				Chhibber et al.				
Hepatocytes	1	Caucasian	75	Female	Not given	Not given	Not given	Not given
Hepatocytes	2	Caucasian	72	Male	Not given	Not given	Not given	Not given
Hepatocytes	3	Caucasian	68	Female	Not given	Not given	Not given	Not given
Hepatocytes	4	Caucasian	62	Male	Not given	Not given	Not given	Not given
Hepatocytes	5	Caucasian	53	Male	Not given	Not given	Not given	Not given
Hepatocytes	6	Caucasian	28	Male	Not given	Not given	Not given	Not given
Hepatocytes	7	Caucasian	45	Male	Not given	Not given	Not given	Not given
Hepatocytes	8	Caucasian	54	Male	Not given	Not given	Not given	Not given

Hepatocytes	9	Caucasian	60	Male	Not given	Not given	Not given	Not given
Hepatocytes	10	Caucasian	60	Male	Not given	Not given	Not given	Not given
Hepatocytes	11	Caucasian	67	Male	Not given	Not given	Not given	Not given
Hepatocytes	12	Caucasian	15	Female	Not given	Not given	Not given	Not given
Hepatocytes	13	Caucasian	66	Female	Not given	Not given	Not given	Not given
Hepatocytes	14	Caucasian	57	Male	Not given	Not given	Not given	Not given
Hepatocytes	15	Caucasian	49	Male	Not given	Not given	Not given	Not given
Hepatocytes	16	Caucasian	68	Male	Not given	Not given	Not given	Not given
Hepatocytes	17	Caucasian	16	Female	Not given	Not given	Not given	Not given
Hepatocytes	18	Caucasian	75	Female	Not given	Not given	Not given	Not given
Hepatocytes	19	Caucasian	30	Female	Not given	Not given	Not given	Not given
Hepatocytes	20	Caucasian	47	Female	Not given	Not given	Not given	Not given
Hepatocytes	21	Caucasian	53	Male	Not given	Not given	Not given	Not given
Hepatocytes	22	Caucasian	56	Male	Not given	Not given	Not given	Not given
Hepatocytes	23	Caucasian	47	Female	Not given	Not given	Not given	Not given

Hepatocytes	24	Caucasian	70	Male	Not given	Not given	Not given	Not given
Adipocytes	1	Caucasian	55	Female	Not given	Not given	Not given	Not given
Adipocytes	2	Caucasian	36	Female	Not given	Not given	Not given	Not given
Adipocytes	3	African-American	47	Male	Not given	Not given	Not given	Not given
Adipocytes	4	African-American	31	Female	Not given	Not given	Not given	Not given
Adipocytes	5	Asian	34	Female	Not given	Not given	Not given	Not given
Adipocytes	6	Caucasian	56	Female	Not given	Not given	Not given	Not given
Adipocytes	7	Caucasian	56	Female	Not given	Not given	Not given	Not given
Adipocytes	8	African-American	23	Female	Not given	Not given	Not given	Not given
Adipocytes	9	Unknown	42	Female	Not given	Not given	Not given	Not given
Adipocytes	10	Unknown	23	Female	Not given	Not given	Not given	Not given
Adipocytes	11	Caucasian	57	Female	Not given	Not given	Not given	Not given
Adipocytes	12	Caucasian	25	Female	Not given	Not given	Not given	Not given

Adipocytes	13	Caucasian	45	Female	Not given	Not given	Not given	Not given
Adipocytes	14	Caucasian	41	Female	Not given	Not given	Not given	Not given
Adipocytes	15	Caucasian	41	Male	Not given	Not given	Not given	Not given
Adipocytes	16	African-American	35	Male	Not given	Not given	Not given	Not given
Adipocytes	17	Asian	24	Female	Not given	Not given	Not given	Not given
Adipocytes	18	Caucasian	28	Female	Not given	Not given	Not given	Not given
Adipocytes	19	Caucasian	52	Male	Not given	Not given	Not given	Not given
Adipocytes	20	Unknown	59	Female	Not given	Not given	Not given	Not given
Adipocytes	21	Unknown	52	Female	Not given	Not given	Not given	Not given
Adipocytes	22	Caucasian	29	Female	Not given	Not given	Not given	Not given
Adipocytes	23	Caucasian	43	Male	Not given	Not given	Not given	Not given
Adipocytes	24	Unknown	30	Female	Not given	Not given	Not given	Not given
Adipocytes	25	Asian	36	Female	Not given	Not given	Not given	Not given

Islets	12/34	Not given	46	Female	No	25.0	N/A	Not given
Islets	12/35	Not given	53	Male	No	Not given	N/A	Not given
Islets	14/46	Not given	40	Male	No	26.2	N/A	Not given
Islets	15/40	Not given	77	Male	No	25.2	N/A	Not given
Islets	16/4	Not given	62	Female	No	24.8	N/A	Not given
Islets	16/34	Not given	59	Male	No	19.4	N/A	Not given
Islets	16/35	Not given	81	Female	No	25.0	N/A	Not given
Islets	17/2	Not given	77	Male	No	24.2	N/A	Not given
Islets	17/4	Not given	76	Male	No	24.2	N/A	Not given
Islets	17/7	Not given	39	Male	No	32.6	N/A	Not given
Islets	17/20	Not given	22	Male	No	19.6	N/A	Not given
Islets	17/22	Not given	78	Male	No	23.9	N/A	Not given
Islets	17/30	Not given	68	Female	No	20.8	N/A	Not given
Islets	17/37	Not given	79	Female	No	27.5	N/A	Not given
Islets	17/41	Not given	56	Female	No	22.5	N/A	Not given

Islets	17/42	Not given	53	Female	No	20.8	N/A	Not given
Islets	17/44	Not given	67	Male	No	24.2	N/A	Not given
Islets	17/53	Not given	56	Male	No	24.7	N/A	Not given
Islets	17/54	Not given	81	Female	No	27.3	N/A	Not given
Islets	17/62	Not given	81	Female	No	25.9	N/A	Not given
Islets	17/65	Not given	72	Female	No	23.9	N/A	Not given
Islets	17/66	Not given	52	Female	No	23.4	N/A	Not given
Islets	17/70	Not given	71	Male	No	25.4	N/A	Not given
Islets	17/75	Not given	53	Female	No	41.9	N/A	Not given
Islets	18/4	Not given	27	Female	No	25.0	N/A	Not given
Islets	18/5	Not given	61	Male	No	32.4	N/A	Not given
Islets	18/8	Not given	80	Female	No	23.4	N/A	Not given
Islets	18/11	Not given	86	Female	No	33.1	N/A	Not given
Islets	18/12	Not given	50	Male	No	22.4	N/A	Not given
Islets	18/17	Not given	50	Female	No	20.2	N/A	Not given

Islets	18/18	Not given	80	Female	No	18.4	N/A	Not given
Islets	18/19	Not given	58	Female	No	24.2	N/A	Not given
Islets	18/20	Not given	83	Male	No	25.9	N/A	Not given
Islets	18/22	Not given	33	Male	No	21.8	N/A	Not given
Islets	18/25	Not given	71	Female	No	29.4	N/A	Not given
Islets	18/31	Not given	66	Male	No	27.8	N/A	Not given
Islets	18/35	Not given	74	Male	No	26.1	N/A	Not given
Islets	18/37	Not given	78	Female	No	25.3	N/A	Not given
Islets	18/42	Not given	51	Male	No	26.2	N/A	Not given
Islets	18/45	Not given	79	Female	No	29.7	N/A	Not given
Islets	18/46	Not given	79	Female	No	25.7	N/A	Not given
Islets	18/50	Not given	53	Male	No	27.8	N/A	Not given
Islets	19/2	Not given	81	Female	No	20.2	N/A	Not given
Islets	19/4	Not given	61	Male	No	24.8	N/A	Not given
Islets	19/8	Not given	67	Female	No	23.9	N/A	Not given

Islets	19/15	Not given	72	Female	No	22.0	N/A	Not given
Islets	19/18	Not given	63	Male	No	26.8	N/A	Not given
Islets	19/26	Not given	28	Female	No	20.2	N/A	Not given
Islets	19/27	Not given	52	Male	No	30.0	N/A	Not given
Islets	19/29	Not given	59	Male	No	27.7	N/A	Not given
Islets	19/34	Not given	76	Female	No	19.5	N/A	Not given
Islets	19/72	Not given	69	Male	No	26.1	N/A	Not given
Islets	20/5	Not given	77	Male	No	24.5	N/A	Not given
Islets	20/8	Not given	82	Male	No	24.5	N/A	Not given
Islets	20/11	Not given	64	Female	No	29.4	N/A	Not given
Islets	20/26	Not given	64	Female	No	21.3	N/A	Not given
Islets	20/82	Not given	79	Male	No	25.3	N/A	Not given
Islets	21/29	Not given	82	Female	No	30.1	N/A	Not given
				Colli et al.				
Islets	Donor 15	Not given	67	Male	Not given	25.7	Not given	Not given

Islets	Donor 16	Not given	87	Female	Not given	23.8	Not given	Not given
Islets	Donor 17	Not given	67	Female	Not given	24.6	Not given	Not given
Islets	Donor 18	Not given	83	Female	Not given	37.1	Not given	Not given
Islets	Donor 19	Not given	84	Female	Not given	24.5	Not given	Not given
Islets	Donor 20	Not given	40	Femlae	Not given	22.5	Not given	Not given

Appendix B

Supplementary Figures

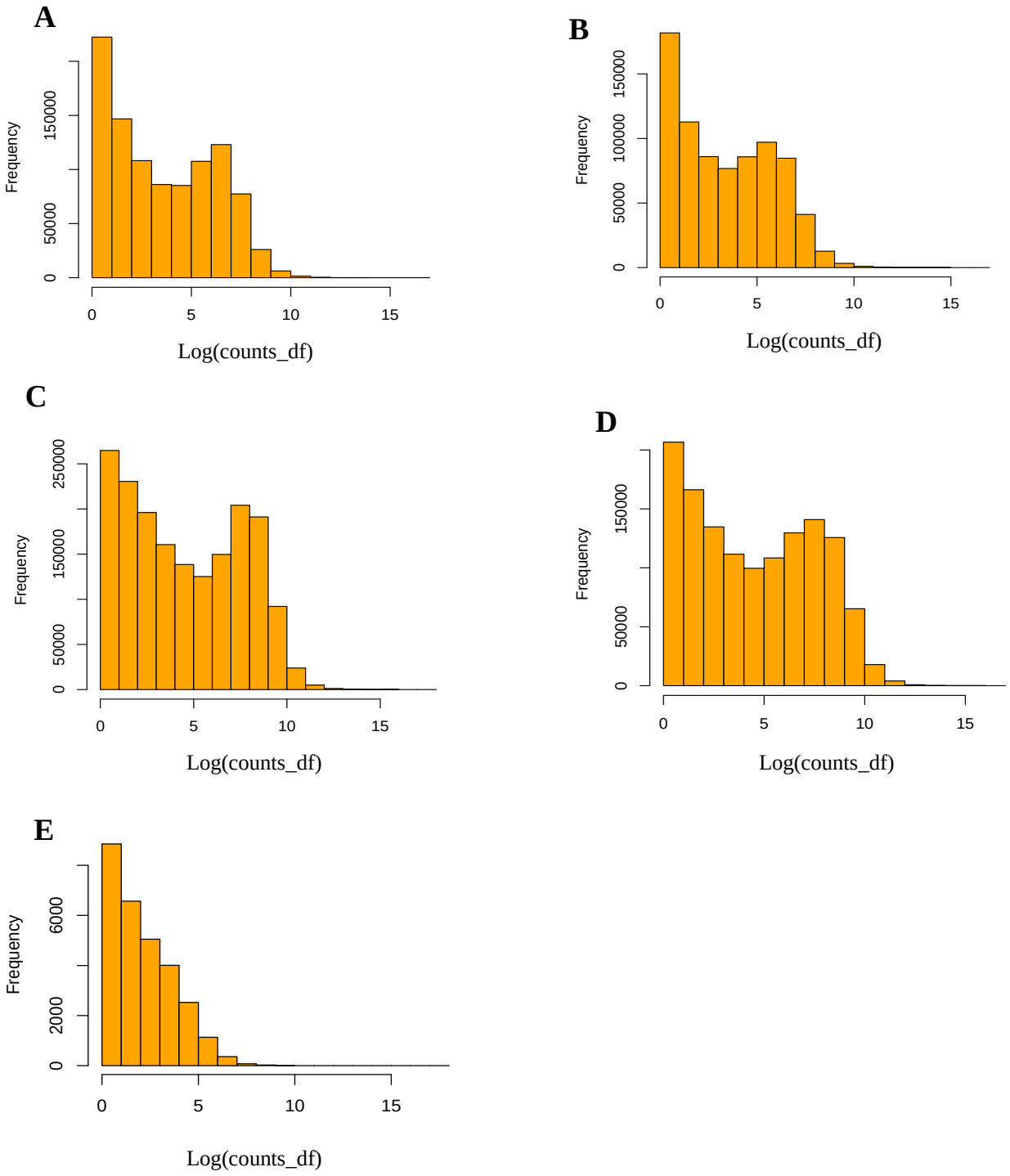

Supplementary Figure 1. The distribution of the gene counts in human adipocytes, hepatocytes, islets and EndoC-βH1 cells, as well as rodent INS-1 832/13 cells. Histograms display a negative binomial distribution of gene counts for human adipocytes (A), hepatocytes (B), islets (C), and EndoC-βH1 cells (D), as well as rodent INS-1 832/13 cells (E). The x-axis illustrates the log-average counts for all genes across all samples obtained for each cell type, and the y-axis represents the frequency of each counts value.

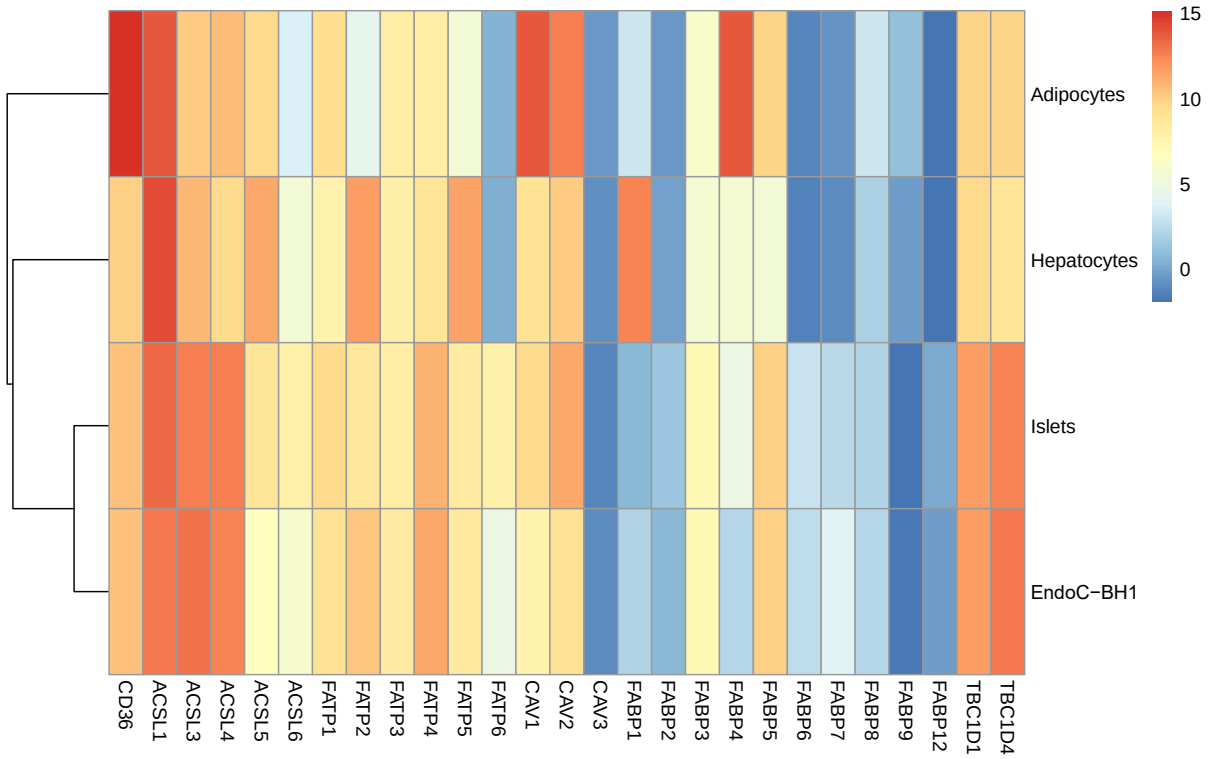

Supplementary Figure 2. Heatmap showing gene expression of candidate LC-FFA transporters. Candidate LC-FFA transporters are displayed on the x-axis and the cell type is displayed on the y-axis. Blue rectangles illustrate low expression, and red rectangles illustrate high expression. Hierarchical clustering is shown on the left side of the diagram. The figure presented here was provided by Dr Patricia Thomas.

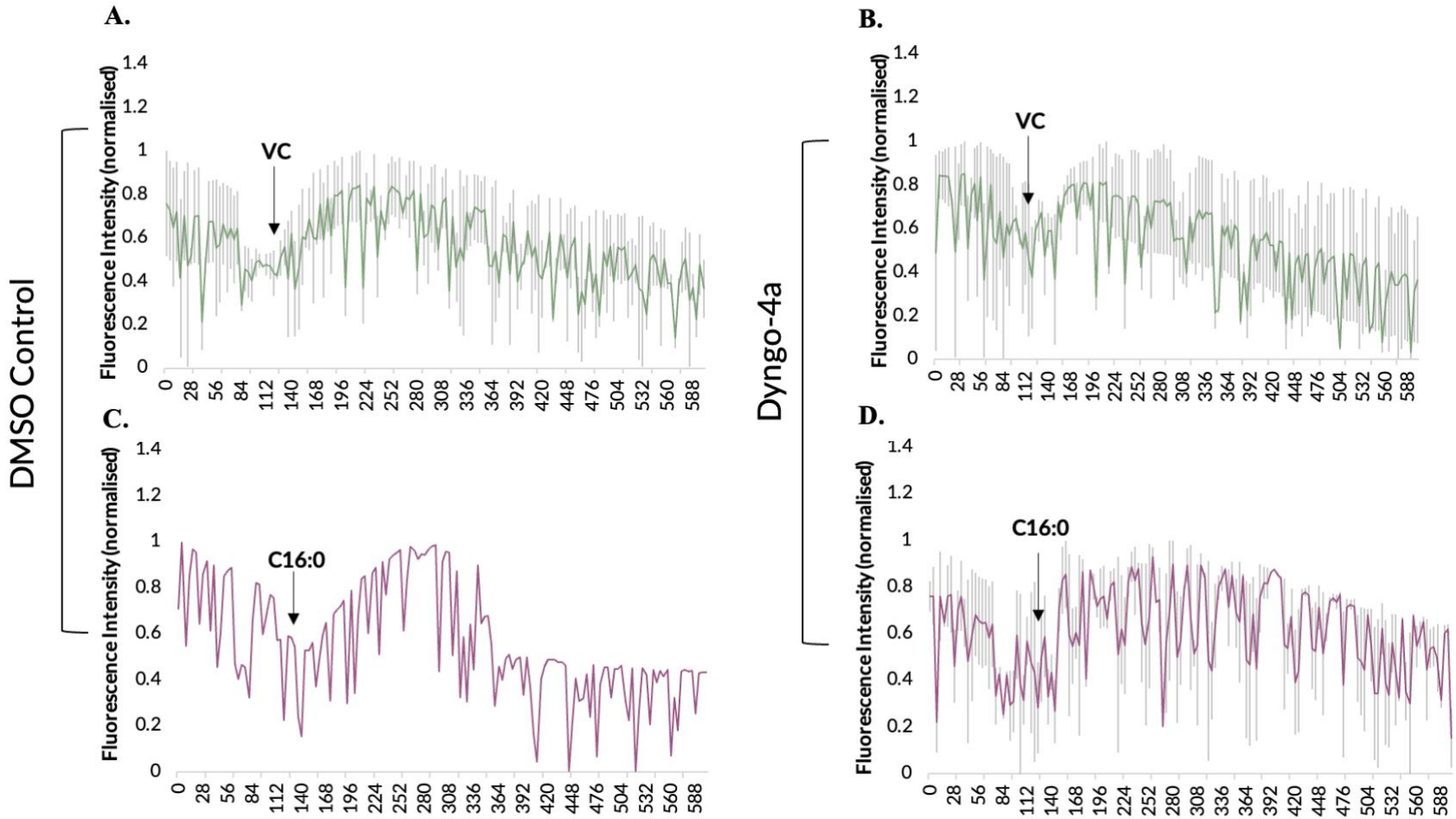

Supplementary Figure 3. Acute uptake of palmitate (C16:0) and the vehicle in EndoC-βH1 cells shows a similar trend using a third repetition in the presence of an inhibitor of dynamin-mediated endocytosis (Dyngo-4a). EndoC-βH1 cells were injected with the vehicle control (VC) in the presence of DMSO (A) or Dyngo-4a (B), and 0.5mM palmitate (C16:0) in the presence of DMSO (C) or Dyngo-4a (D). Results are displayed as the mean ± S.E.M, representative of one independent experiment. No error bars are given for the C16:0 injection in the presence of DMSO as only one slide was imaged.